Volume 15, Number 2, 2024

ISSN 1847-6996

FERIT
FACULTY OF ELECTRICAL ENGINEERING, COMPUTER SCIENCE AND INFORMATION TECHNOLOGY **OSIJEK**

IJECES International Journal of Electrical and Computer Engineering Systems

International Journal of Electrical and Computer Engineering Systems

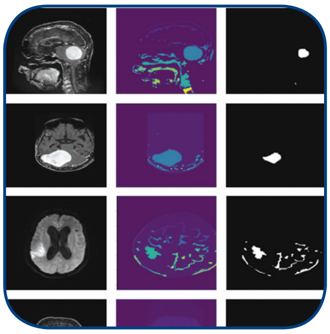

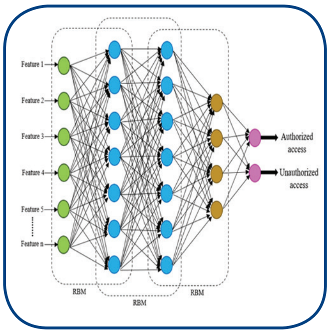

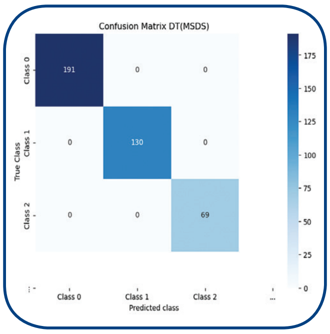

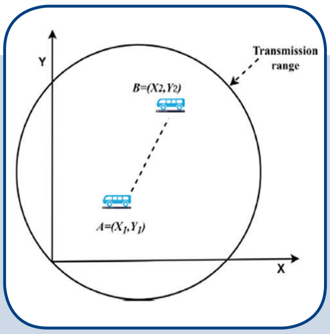

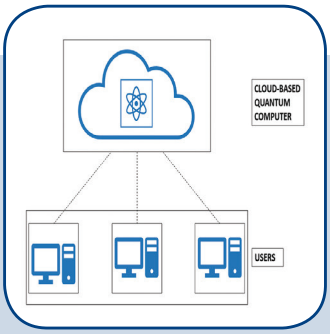

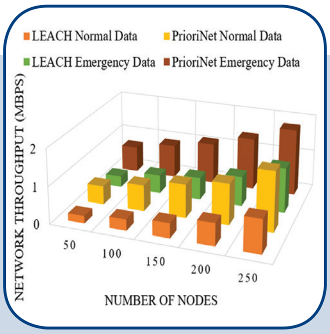

ISSN: 1847-6996

INTERNATIONAL JOURNAL OF ELECTRICAL AND COMPUTER ENGINEERING SYSTEMS

Published by Faculty of Electrical Engineering, Computer Science and Information Technology Osijek, Josip Juraj Strossmayer University of Osijek, Croatia

Osijek, Croatia | Volume 15, Number 2, 2024 | Pages 121 - 214

The International Journal of Electrical and Computer Engineering Systems is published with the financial support of the Ministry of Science and Education of the Republic of Croatia

CONTACT

International Journal of Electrical and Computer Engineering Systems (IJECES)

Faculty of Electrical Engineering, Computer Science and Information Technology Osijek, Josip Juraj Strossmayer University of Osijek, Croatia
Kneza Trpimira 2b, 31000 Osijek, Croatia
Phone: +38531224600, Fax: +38531224605
e-mail: ijeces@ferit.hr

Subscription Information

The annual subscription rate is 50€ for individuals, 25€ for students and 150€ for libraries.
Giro account: 2390001 - 1100016777,
Croatian Postal Bank

Journal is referred in:

- Scopus
- Web of Science Core Collection (Emerging Sources Citation Index - ESCI)
- Google Scholar
- CiteFactor
- Genamics
- Hrčak
- Ulrichweb
- Reaxys
- Embase
- Engineering Village

Bibliographic Information

Commenced in 2010.
ISSN: 1847-6996
e-ISSN: 1847-7003
Published: quarterly
Circulation: 300

IJECES online

https://ijeces.ferit.hr

TABLE OF CONTENTS

Intrusion Detection System based on Chaotic Opposition for IoT Network

Original Scientific Paper

Richa Singh
G.G.S.I.P.U.,
University School of Information, Communication, and Technology
Delhi, India
richa.singh081991@gmail.com

R.L. Ujjwal
G.G.S.I.P.U.,
University School of Information, Communication, and Technology
Delhi, India
ujjwal@ipu.ac.in

Abstract – *The rapid advancement of network technologies and protocols has fueled the widespread endorsement of the Internet of Things (IoT) in numerous domains, including everyday life, healthcare, industries, agriculture, and more. However, this rapid growth has also given rise to numerous security concerns within IoT systems. Consequently, privacy and security have become paramount issues in the IoT framework. Due to the heterogeneous data produced by smart IoT devices, traditional intrusion detection system doesn't work well with IoT system. The massive volume of heterogeneous data has several irrelevant, redundant, and unnecessary features which lead to high computation time and low accuracy of IDS. Therefore, to tackle these challenges, this paper presents a novel metaheuristic-based IDS model for the IoT systems. The chaotic opposition-based Harris Hawk optimization (CO-IHHO) algorithm is used to perform the feature selection of data traffic. The chosen features are subsequently inputted into a machine learning (ML) classifier to detect network traffic intrusions. The performance of the CO-IHHO based IDS model is verified against the BoT-IoT dataset. Experimental findings reveal that CO-IHHO-DT achieves the maximal accuracy of 99.65% for multiclass classification and 100% for binary classification, and minimal computation time of 31.34 sec for multiclass classification and 133.54 sec for binary classification.*

Keywords: *IoT, IDS, feature selection, machine learning, HHO*

1. INTRODUCTION

The Internet of Things (IoT) is a collection of several interconnected embedded devices that can communicate with each other through wireless or wired mediums [1]. Within the IoT system, numerous smart sensors collaborate to create intelligent environments. The advancement in IoT systems makes spectacular development in the everyday utilization of electronic services and appliances [2]. It has a profusion of applications and services in various domains including agriculture, healthcare, industry, military, smart homes, etc. However, the widespread adoption of IoT also makes these systems attractive targets for malicious actors aiming to carry out activities such as physical damage to devices, denial of service (DoS) attacks, and theft of information. Consequently, ensuring the security of IoT devices becomes paramount. [3]. Moreover, staying informed about contemporary vulnerabilities is essential to take appropriate measures for mitigation.

An intrusion detection system provides a security mechanism for protecting the IoT system from several malicious activities by analysing data packets received and generating responses when necessary. An IDS for the IoT system has to deal with rigorous conditions of high-volume data processing, rapid response, memory constraints, and low processing. Therefore, typical IDS are not suitable for IoT systems. The IDS are classified into major categories based on analysis strategy i.e. anomaly, signature [4], and hybrid. Signature IDS detects attack by analysing network traffic and matching attack signatures with signatures already stored in a database, generating an alarm if signatures are matched. While Anomaly-based IDS constructs user profiles by analyzing system usage patterns. Any deviation from established user behavior is treated as a potential intrusion. Hybrid combines the merits of both strategies.

The considerable volume of network traffic generated by IoT devices presents a significant challenge when it comes to ensuring the security of IoT network traffic. Feature selection (FS) can resolve this issue by considering only the relevant and important features instead of all the features. It is an important technique that improves the performance of IDS for the IoT framework. FS [5] is intermediate phase of IDS that choose subset from the original features set without irrelevance, and redundancy. It helps in reducing the volume of training data, improving the classification accuracy, and reducing computation time [6]. FS is typically divided into three primary approaches: filter, wrapper, and hybrid. In the filter approach, statistical measures such as correlation and consistency are utilized for evaluation, and this process is conducted independently of any specific learning algorithm. In contrast, the wrapper approach entails the learning algorithm itself evaluating the feature subset, with the subset's efficiency determined by the error rate. While the wrapper approach is computationally more intensive, it often yields superior results compared to the filter approach because of its continuous interaction with the learning algorithm [7]. The hybrid approach leverages the strengths of both the filter and wrapper approaches.

Metaheuristic algorithms (MHA) are the wrapper approach of FS which gives a magnificent performance because of their global search capability. However, it is necessary to have equitable exploration and exploitation phase of MHA to avoid local optima [8]. Extreme exploitation and inadequate exploration cause premature convergence while extreme exploration and inadequate exploitation cause a slower convergence rate. Exploration refers to generating a candidate solution that leads to wider coverage of search space while exploitation refers to finding a near-optimal solution by focusing on the local area of the search process.

This paper introduces an IDS tailored for the IoT domian, employing a Metaheuristic Algorithm (MHA). The IDS model's feature selection process utilizes the proposed Chaotic Opposition-based Improved Harris Hawk Optimization (CO-IHHO) algorithm on the BoT-IoT dataset. CO-IHHO is employed to identify the most pertinent features, optimizing computational efficiency while upholding the accuracy of the IDS. Following feature selection, binary and multiclass classification tasks are carried out using machine learning (ML) classifiers. Consequently, the primary contributions of this paper encompass the following:

- Improving the population diversity of original HHO by applying opposition-based learning in the beginning of population selection of HHO. This helps in getting the best fitness solution in the early stages and leads to improving convergence speed.
- The chaotic map technique is employed for generating random numbers used in HHO.
- Non-linear target energy escaping form is used to have an equitable exploration and exploitation phase.
- The paper conducts classification tasks utilizing two distinct ML classifiers and subsequently assesses their performance. To address the issue of class imbalance, a sampling technique is employed as a resolution.
- The CEC-06 2019 Benchmark function is employed to evaluate the performance of proposed CO-IHHO.

The effectiveness of CO-IHHO is compared against seven other MHAs for the BoT-IoT dataset. The intrusion detection with CO-IHHO as FS algorithm achieves high accuracy with less computation time, compared to other MHAs used as FS algorithm. Further, the proposed work is also attaining better accuracy compared to other recent work.

The remaining paper unfolds as follows: section 2 describes a contribution summary of the latest IDS for the IoT system followed by a preliminary discussion about the original HHO, OB learning, and chaotic map techniques. Afterward, the proposed IDS model is described in section 3. Section 4 describes the proposed CO-IHHO algorithm in detail. Section 5 is dedicated to the implementation and analysis of results from the proposed work. Section 6 offers the paper's conclusion.

2. LITERATURE REVIEW

Researchers have developed several IDS for the IoT network using learning algorithms in recent years. This section summarizes the recent work done for the FS using MHAs, and other recent IDS for the IoT framework. Afterward, the original HHO, OB learning, and the chaotic map are discussed.

The authors in [9] proposed IoT based IDS using deep learning framework. They use MHA spider monkey optimization (SMO) for optimal FS. Afterwards, they employed stacked-deep polynomial network for the classification of intrusive traffic in IoT system. They used L2 regularization technique to avoid model overfitting. However, the proposed IDS is verified using NSL-KDD, which is an outdated dataset and doesn't include latest attacks. The random forest (RF) based smart IoT-based IDS is proposed in [10]. They combine elements of grey wolf optimization and particle swarm optimization to enhance the FS process for intrusive traffic. Furthermore, RF is used to perform multiclass classification. They performed oversampling to handle imbalanced data. The model is evaluated against outdated datasets including CICIDS-2017, KDDCup99, and NSL–KDD and attains accuracy above 99% for all three datasets. These datasets don't have IoT traces. The work in [11] proposed a hybridized MHA for the IoT system. The study combines the bird swarm algorithm with the gorilla troops optimizer to improve FS. The model's performance is assessed on various datasets, including CICIDS-2017, NSL-KDD, BoT-IoT, and UNSW-NB15, resulting in accuracies of 98.7%, 95.5%, 81.5%, and 81.5%, respectively. Authors in [12] proposed an smart botnet detection method for IoT system. They hybridized salp swarm algorithm with an ant lion optimization algorithm for the FS of the N-BaIoT dataset. This hybrid approach leveraged the global search capabilities of ALO and the local search capabilities of SSA to obtain the optimal solution. The classification is performed using the KNN classifier. In paper [13], a lightweight IDS tailored for IoT systems was presented. This research involved a fusion of the genetic algorithm (GA) and the GWO for the FS. Their model's performance was evaluated against AWID dataset. Authors in [14] proposed MHA-based FS for the IoT system. They proposed three models based on simulated annealing and shuffled shepherd optimization algorithms i.e. SSO, SSO-SA1, and SSO-SA2 to perform FS. In SSA-SA1, SA is merged within SSO and in SSA-SA2, SA is used after SSO. Features obtained from the proposed system are classified using the KNN classifier. Experimental result shows that SSO-SA2 is better in contrast to all other algorithms. Hamed et al. [15] proposed an IDS to protect the edge layer of the IoT system from malware. The optimal feature selection of a dataset with opcodes and bytecodes is performed by using the GWO algorithm. They proposed a multi-kernel SVM approach for the classification of malware. The proposed approach is better than deep-RNN and fuzzy-based IDS. The authors in [16] proposed an IoT-based IDS with a deep neural network (DNN) framework. They used filter-based mutual information for feature selection. Features with a high MI score are selected as optimal features. The IoT traffic is classified as an anomaly or begins using DNN. The proposed system attains an accuracy of 99.01%. The authors in [17] proposed a hybrid IDS designed specifically for IoT framework. Their approach involved the use of an enhanced shuffled frog leaping algorithm as a wrapper for FS. Following this, they employed a Light Convolutional Neural Network with Gated Recurrent Neural Network (LCNNGRNN) for the classification of intrusive network traffic. The performance of their proposed model demonstrated its effectiveness when benchmarked against other methods, especially when evaluated on the NSL-KDD dataset. The work in [18] proposed a NIDS for the medical IoT system. They employed a butterfly optimization algorithm (BOA) to get the best features. Afterward, ANN is used to categorize the network traffic based on optimal features obtained using BOA. The proposed system attains an accuracy of 93.27% over the NSL-KDD dataset. The authors in [19] proposed GA based anomaly detection system for the fog based IoT framework. The FS is performed using wrapper based GA and classification is performed using deep brief network. Proposed system achieves 99.73% accuracy and 0.06% false positive rate for the NSL-KDD dataset. However, existing IDS approaches performed well for the IoT framework still there are certain limitations, which includes:

Mostly datasets like UNSW-NB15, KDDcup99, CICIDS-2017, NSL-KDD, etc. are used for performance evaluation of IDS for IoT framework. However, such datasets become obscure and doesn't have IoT traces.

- Most of the proposed IDS used MHA for FS either incur high computation time or doesn't include any information about computation time. Furthermore, detecting intrusive traffic with less computation time, and high accuracy is important concern.
- The FS using HHO might leads to premature convergence and trapped in local optima.

2.1. HARRIS HAWK ALGORITHM (HHO)

The HHO algorithm is developed in 2019 by authors in [20]. HHO mimics the hunting behavior of Hawk birds required to catch the prey (rabbit). These birds perch in the air, search for prey, and then dive on it collectively. Each group of hawks contains two to seven members. The HHO algorithm includes two phases: exploration, which models hawks preaching behavior, and exploitation, which models different attacking styles of hawks.

Exploration Phase: During this phase, hawks are distributed randomly in the search area, waiting for their prey to arrive. They detect and trace prey with their powerful eyes. These birds can wait for several hours for a prey to arrive. If d≥0.5, hawks use family member position for hunting, while if d<0.5, then hawks use random positions for hunting. Using the value of d, hawks position is updated using following equations:

$$A(k+1) = \begin{cases} A_{rn}(k) - rn1|A_{rn}(k) - 2\, rn2\, A(k)|, & d \geq 0.5 \\ \left(A_{target}(k) - A_{mean}(k)\right) - rn3(LBU + rn4\,(UBU - LBU), & d < 0.5 \end{cases} \tag{1}$$

where, d, $rn1$, $rn2$, $rn3$, and $rn4$ represents random numbers within range 0, and 1. d is used to toggle between two position-updating equations. LBU represents lower limit and UBU represents upper limit of search space. Target position is denoted by $A_{target}(k)$, and A_{rn} denotes the randomly selected hawks. $A(k)$ is the current hawks position, and $A_{mean}(k)$ signifies the average position computed based on the current population of hawks. This average position is determined through the following formula:

$$A_{mean}(k) = \frac{1}{k_{maxite}} \sum_{i=1}^{k_{maxite}} A_i(k) \tag{2}$$

Escaping Energy (En): The shift from exploration to the exploitation phase is contingent upon the energy levels of the prey, and the act of evading often results in a depletion of their energy. The energy is a time-varying variable defined by the equation:

$$En = 2E_{initial} * \left(1 - \frac{k}{k_{maxite}}\right) \tag{3}$$

$$E_{initial} = -1 + 2 \times rand() \tag{4}$$

where $E_{initial}$ denotes initial prey escaping energy. k denotes current iteration. k_{maxite} denotes the maximum iteration number. Depending on the E_n value exploration and exploitation phase happen. If E_n≥1 then the exploration part of HHO is executes while if E_n<1 then the exploitation part of HHO executes.

Exploitation Phase: During this phase, hawks exploit prey using surprise dives. Based on escaping behavior of prey, the hawk selects their attacking strategy. The strategies include hard besiege (HB), hard besiege with progressive dive (HBPD), soft besiege (SB), and soft besiege with progressive dive (SBPD). Progressive dive strategies show the intelligent behavior of hawks. The strategy to be adopted by the hawks depends upon the value of escaping probability (pr), and escaping energy (En). If pr<0.5 then the prey escape successfully and if pr≥0.5 then the prey is unsuccessful in escaping before a surprise attack.

SB: Whenever the prey possesses sufficient energy to escape, the hawks employ a gentle encirclement strategy, which gradually tires out the prey, enabling them to execute surprise attacks effectively. The SB is determined using the following equation:

$$A(k+1) = \Delta A(k) - En\left|J\, A_{target}(k) - A(k)\right| \quad (5)$$

where, $A(k)$ is the current hawks position, En is energy level, $A_{target}(k)$ is target position, J is the jumping strength, which is determined using following equation:

$$J = 2(1 - rn5) \quad (6)$$

where, $rn5$ is the random number. Further, $\Delta A(k)$ refers to the disparity between the current hawks position and its target position. It is determined using following equation:

$$\Delta A(k) = A_{target}(k) - A(k) \quad (7)$$

HB: In this scenario, the prey lacks the necessary energy to escape from the hawks. The hard besiege is mathematically modeled as:

$$A(k+1) = A_{target}(k) - E|\Delta A(k)| \quad (8)$$

SBPD: In this method, the levy flight function (LFF) determines the zigzag maneuver of prey during an escape. The target has enough escaping power. Therefore, hawks try to distract the target so that it changes its path. This process continues until hawks perch their target. The hawk chooses their next favorable move using the equation:

$$B = A_{target}(k) - E\left|J\, A_{target}(k) - A(k)\right| \quad (9)$$

If the hawks find that target is trying to mislead hawks and tries to escape, then LFF function is used to perform dive. The position is determined using following equation:

$$C = B + X \times LFF \quad (10)$$

where, X is random vector of size 1 X DM (Dimension). LFF is determined using the following equation:

$$LFF = \frac{e \times \sigma}{|f|^{\frac{1}{\beta}}}, \text{ where } \sigma = \left(\frac{\Gamma(1+\beta)\times\sin\left(\frac{\pi\beta}{2}\right)}{\Gamma\left(\frac{1+\beta}{2}\right)\times \beta\times 2^{\left(\frac{\beta-1}{2}\right)}}\right)^{\frac{1}{\beta}} \quad (11)$$

where, β is constant with a value 1.5, e and f are random number, lies in interval 0 and 1.

Therefore, in SBPD Hawks positon is determined using the following mathematical equation:

$$A(k+1) = \begin{cases} B \text{ if } FF(B) < FF(A(k)) \\ C \text{ if } FF(C) < FF(A(k)) \end{cases} \quad (12)$$

where, FF is the fitness function obtained using equation 24.

HBPD: In this method, prey has insufficient escaping energy. Hence, hawks strive to minimize the distance between their mean location and the location of their prey, which is determined using the following equation:

$$A(k+1) = \begin{cases} B' \text{ if } FF(B') < FF(A(k)) \\ C' \text{ if } FF(C') < FF(A(k)) \end{cases} \quad (13)$$

where,

$$B' = A_{target}(k) - E\left|J\, A_{target}(k) - A_{mean}(k)\right| \quad (14)$$

$$\text{and } C' = B' + X \times LFF \quad (15)$$

LFF is the levy flight function obtained from equation 11, A_{target} (k) is the target position, and X defines a random vector of size 1× DM (dimension). A_{mean} (k) is determined by equation 2.

The HHO is a population-based MHA that has several advantages and limitations as well. The HHO is popular due to its simpler structure. It requires few parameter settings compared to other MHA [21], and ease of implementation. The HHO is flexible, scalable, and robust. It provides a good convergence speed. However, it doesn't have any theoretical analysis, and also lacks mathematical analysis. Moreover, the existence of random variables in the different phases of HHO reduces its convergence speed and is stuck in local optima. Therefore, chaos theory is used to determine the value of these random variables used in HHO and helps to improve its performance.

2.2. CHAOTIC MAPS

The term chaotic refers to "state of chaos". The CM are functions that mathematically computes random values based on the seed value provided initially. From the last few decades, CM are widely adopted for optimizing MH algorithms due to their dynamic behaviour [22]. Searching search space becomes faster using CM than random number generator. They generate random numbers that lies between certain range. The chaotic map has various characteristic such as randomness, ergodicity, i.e. traverse all states without repetition, and highly sensitive to initial value [23]. These attributes of Chaotic Maps (CM) assist Metaheuristic (MH) algorithms in enhancing convergence speed and steering clear of local optima. The exploration and exploitation phases of HHO involve multiple random numbers, which could potentially lead to HHO becoming trapped in local optima. Therefore, in this paper, these random numbers are determined by using a chaotic map "Chossat-Golubitsky" [24]. The equation of CG-CM is given by:

$$A = a \times (x^2 + y^2) + b \times x \times (x^2 - 3y^2) + c \quad (16)$$

2.3. OPPOSITION BASED LEARNING

The OB learning concept was initially introduced by the authors in [25] and has been applied in various studies, including [26] and [27], to optimize Metaheuristic Algorithms (MHAs). Typically, many MHAs begin with the selection of random numbers as their initial solutions. Therefore, in this paper, the OB learning technique is employed to enhance the population diversity of the original HHO algorithm. Instead of selecting the hawk's population randomly from search space, the OB learning method is used to select random hawk positions i.e. $A_{rn}(k)$. This approach navigates the search space in dual directions, taking into consideration both the original solution and its reverse counterpart. By doing so, it offers a more comprehensive coverage of the search space [28]. The convergence speed of the MHA is slower in most cases. Therefore, OB learning resolves this problem by by taking into account both randomly generated solutions and their opposites [29]. The authors in [30] shows that the opposite solution is more capable to reach global optima compared to the original solution.

Definition: In general, let $x \in [l,u]$ be a real number. The opposite number ($\bar{x}$) is evaluated using the following equation:

$$\bar{x} = (lbu + ubu - x)$$

where lbu is lower bound. ubu is upper bound.

If x is a multi-dimensional vector then, all elements of $\bar{x}$ is defined by:

$\bar{x}=(lbu_w+ubu_w-x_w)$ where, w=1,2,3, 4, ….., d and d is the multi-dimension.

3. PROPOSED SYSTEM

With the growing security concerns surrounding IoT devices, the need for an efficient IDS that can accurately detect intrusions while minimizing processing time becomes crucial. The complete architecture of the suggested system is illustrated in Fig. 1. The IDS is organized into multiple stages, encompassing data collection, data pre-processing, feature selection using the CO-IHHO method, and the classification phase. The proposed IDS is verified using BoT-IoT [31] dataset. The data undergoes pre-processing to eliminate ambiguities and address missing values. Subsequently, CO-IHHO is applied for feature selection on the pre-processed data, followed by binary and multiclass classification of intrusive traffic. The section aims to provide a comprehensive overview of each of these phases within the IDS.

3.1. DATA COLLECTION

During this phase various logging tools are used for used for preparing dataset, created dataset can be used to train model for identifying intrusive traffic. In this paper, publicly available BoT-IoT dataset [31] is used as collected data, described briefly in later section. It is feed as an input to data-processing phase of the IDS model.

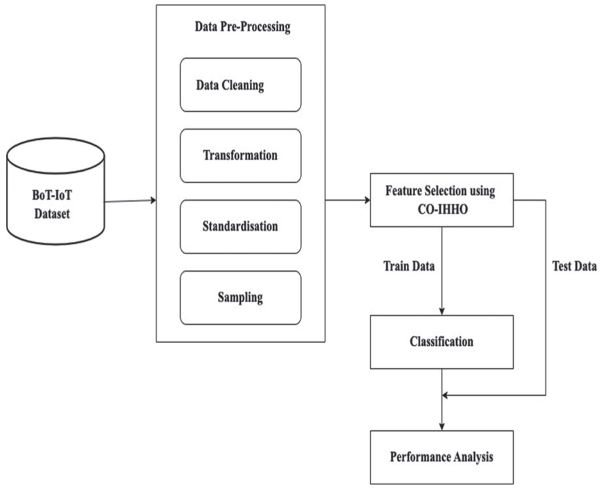

Fig. 1. Proposed System Design

3.2. PRE-PROCESSING

From the review of the literature conducted above, it becomes apparent that the majority of the datasets utilized for performance evaluation exhibit characteristics such as noise, missing values, irrelevant information, and redundancy. Additionally, it's worth noting that the data generated by IoT devices is inherently heterogeneous in nature. Hence, it is necessary to handle these redundant and irrelevant data and further, alter the data into a uniform form. The pre-pressing phase helps in improving data quality and providing effective, and accurate result. The data from the data collection module is provided as an input to the pre-processing phase. The pre-processing task includes, cleaning, transformation, standardization, and sampling.

During cleaning, the quality of the collected data is improved by eliminating undesired, and redundant attributes. Undesired attributes are those whose value doesn't impact the performance of intrusion detection while redundant attributes value can be derived from other attribute value. Furthermore, attributes with missing values are also eliminated. In this paper, redundant, and irrelevant attributes such as 'ltime', 'daddr', 'saddr', 'stime', 'flgs', 'state', 'proto', 'pkSeqID', 'sport', 'dport', and 'seq' are eliminated.

During transformation and standardization, several ML classifiers takes only numerical value as processing input. Consequently, categorical values are converted into numerical values using a method called Label encoding. Furthermore, the data is standardized to ensure that data values fall within the range of [0,1]. Failure to standardize data can impact the performance of the IDS due to varying data value ranges. To achieve this, the Standard Scaler function is employed.

Sampling: The BoT-IoT dataset exhibits imbalanced data with a significantly higher number of intrusive traffic instances compared to normal instances. To address this disparity, sampling techniques are applied to balance the instance counts between these two categories. Imbalanced dataset makes the classifier biased towards majority class (intrusive traffic, in this case) and reduces the possibility to detect minority class (normal instances). In this context, random sampling is utilized to mitigate the imbalanced nature of the BoT-IoT dataset. After preprocessing, the FS is performed using CO-IHHO, described in later section.

3.3. CLASSIFICATION PHASE

During this phase, the task involves identifying intrusive traffic, and it encompasses both binary and multiclass classification. Binary classification distinguishes between normal and intrusive traffic, while multiclass classification goes further by identifying specific attack categories within the intrusive traffic, alongside normal traffic. To carry out these classification tasks, the selected features obtained from the feature selection phase are used as input for two machine learning classifiers: Decision Tree (DT) and K-Nearest Neighbor (KNN). Subsequently, an analysis of their performance is conducted. These ML algorithms offer several benefits, including interpretability, ability to handle mixed data types, resilience to noise and irrelevant features, and ease of implementation. These advantages make them well-suited for tasks involving classification and detection.

4. FEATURE SELECTION USING CO-IHHO

The fine-tuned is provided as an input to the FS phase. FS eliminates unwanted, and irrelevant features from dataset and extracts best features out of it [32]. The random number used in MHA has crucial effect on their performance of determining global and local search capability. HHO structure has several random parameters which prevent them in obtaining global optima. Therefore, CM techniques is embedded in the structure of HHO for determining random numbers. The hawks position in the exploration phase of HHO is determined either by family members or randomly selected population of hawks. Therefore, in this paper, OB learning technique is employed to intensify the population update of hawks instead of random population selection. Furthermore, the sine and cosine function are used to enhance the capability of hawk's exploration. The exploitation phase of HHO is also enhance by introducing dynamic capability using S function, which is inspired by [33] , and introducing random parameters to the advanced dive phase. This helps the hawks to exploit local regions rigorously. Here, CO-IHHO is used for the FS task, which overcomes the drawback of original HHO. The algorithm 1 depicts the pseudocode of proposed CO-IHHO.

Algorithm 1. Chaotic Opposition based Improved HHO (CO-IHHO).

Input: N is population size, and k_{maxite} is maximum iterations
Output: Optimal Feature subset
Assign the population s=1, 2,….,n
While(k<=k_{maxite})
Initialize "Chossat-Golubitsky" chaotic map to identify random numbers using equation 16
Compute population of fittest hawks $A_{OBL}(k)$
Compute hawks mean position using equation (2)
Compute escaping energy using equation 23
if ($|En|$ >=1.5) *Exploration phase
  revise hawks positon using equation 17
else if ($|En|$ <1.5) * Exploitation phase
if ($|En|$ ≥1 and pr ≥ 0.5)
  revise hawks position using equation 18 #SB
if ($|En|$ <1 and pr ≥ 0.5)
  revise hawks position using equation 19 #HB
else if ($|En|$ ≥1 and pr <0.5)
  revise hawks position using equation 20 #SBPD
else if ($|En|$ <1 and pr <0.5)
  revise hawks position using equation 21 #HBPD
end if
return optimal selected features
end while
end

The CO-IHHO is the result of following enhancements made to original HHO-

Chaotic Map: The incorporation of a chaotic map to generate random numbers plays a pivotal role in both the exploration and exploitation phases of the HHO algorithm. This deliberate inclusion serves as a safeguard against HHO becoming ensnared in local optima, leading to a substantial improvement in its convergence speed.

OB Learning: The OB learning is used for enhancing the population diversity of HHO. Instead of selecting hawks population randomly in equation (14), OB learning is used for selecting hawks population. OB Learning with CO-IHHO:

- Hawks position A is initialized as a_s, where s=1,2,3,….,n
- Calculate opposite position of hawks as $\bar{a}_s$, where j=1,2,3,…,n.
- Choose the n fittest hawks from ($a_s \cup \bar{a}_s$) which represent the new initial population of hawks i.e. A_{OBL} (k).

Exploration Phase (En≥1.5): CO-IHHO enhances the exploration capability of HHO by using sine and cosine functions in updating the position of Hawks. Inertia weight (w) is also introduced. The Hawks position is calculated as:

$$A(k+1) = \begin{cases} w \times A_{OBL}(k) - \sin(rd1) \times T \times |A_{rn}(k) - 2\,rd2\,A(k)|, & d \geq 0.5 \\ w \times \left(A_{target}(t) - A_{mean}(k)\right) - \cos(rd3) \times T \times (LBU + rd4\,(UBU - LBU), & d < 0.5 \end{cases} \quad (17)$$

where, $w = \left(1 - \frac{k}{k_{maxite}}\right)^{\sqrt{\frac{k}{k_{maxite}}}}$ and $T = \left(1 - \frac{k^{\frac{1}{p}}}{k_{maxite}^{\frac{1}{p}}}\right)$
where p=6, $rd1$, $rd2$, $rd3$, and $rd4$ are the random vari-

ables computed using CM. UBU is upper search space limit. LBU is the upper search space limit. Harris hawks population mean position i.e. $A_{mean}(k)$ is calculated using equation 2, and $A_{target}(k)$ is target positon. Also, k is current iteration. $rd1$, $rd2$, $rd3$, and $rd4$ are random number determined using CM. k_{maxite} is maximum iteration.

Exploitation Phase **(*En*<1.5):** The CO-IHHO enhances the exploitation capability of HHO by adding dynamic capability using value of S and random number. Depending upon the value of En and p (random number), the hawks position is updated using the following equations:

SB: This phase executes when $|En|$ >=1 and p >= 0.5. The position is determined using

$$A(k+1) = \Delta A(k) \times rd5 - En\left|J\, A_{target}(k) - A(k)\right| + S \quad (18)$$

where, $rd5$ is random number determined using CM. $\Delta A(k)$ is obtained using equation 7. En is escaping energy obtained using equation 23. Jumping strength is obtained using equation 6. $A_{target}(k)$ is target positon. $A(k)$ is current position.

HB: This phase executes when ($|En|$ >=1 and p >= 0.5). The position is determined using:

$$A(k+1) = A_{target}(k) - En|\Delta A(k)| + S \quad (19)$$

where, $\Delta A(k)$ is obtained using equation 7. $A_{target}(k)$ is target position.

SBPD: This phase executes when ($|E_n|$ >=1 and p <0.5). The position is determined using

$$A(k+1) = \begin{cases} B \times rd6 + A(k) \times rd7 + S & if\ FF(B) < FF(A(k)) \\ C \times rd8 + A(k) \times rd9 + S & if\ FF\ (C) < FF(A(k)) \end{cases} \quad (20)$$

where, B and C are obtained using equation 9 and equation 10, respectively. FF is the fitness function. $rd6$, $rd7$, $rd8$, and $rd9$ are random number between 0 and 1, determined using CM. $A(k)$ is current hawks position.

HBPD: This phase executes when (|En| <1 and p <0.5). The position is determined using:

$$A(t+1) = \begin{cases} B' \times rd10 + A(k) \times rd11 + S & if\ FF(Y') < FF(A(k)) \\ C' \times rd12 + A(k) \times rd13 + S & if\ FF(Z') < FF(A(k)) \end{cases} \quad (21)$$

where,

$$S = randInt \times \left[\sin\left(\pi \times \frac{k}{2 \times k_{maxite}}\right) + \cos\left(\pi \times \frac{k}{2 \times k_{maxite}}\right) - 1\right] \quad (22)$$

$rd10$, $rd11$, $rd12$, and $rd13$ are random number determined using CM between [0,1]. FF is fitness function. $A(k)$ is current hawks position. B' and C' are obtained using equation 14 and equation 15 respectively.

Escaping Energy: The CO-IHHO modifies the escaping energy equation, shifting it from a linear to a non-linear form in order to achieve a more balanced exploration and exploitation phase. This transformation is precisely defined by the following equation:

$$En = rd0 \times E_o \times e^{\left[\left(\frac{k_{maxite}-k}{k_{maxite}+k}\right) \times 1.5\right]} \quad (23)$$

where, E_o=0.75, and $rd0$ is random number lying between (0,1).

5. IMPLEMENTATION AND RESULT ANALYSIS

This section describes the experimental setup, and CEC-06 2019 benchmark function to evaluate the performance of proposed CO-IHHO. Furthermore, dataset used for model evaluation, and performance metrics considered for evaluating the model are described. Afterward, a comparison with other MHAs and recent IoT-based IDS is done.

5.1. EXPERIMENTAL SETUP

The experiment conducted in this paper is implemented using Python 3.2 on Mac OS Catalina with 8 GB RAM. For an accurate comparison, each implemented algorithm is given a standard situation. The number of iterations i.e. 50, and the population used by all algorithms is the same. Table 1 presents the parameter setting of each MHA used as FS.

Table 1. Parameter Setting.

S. No.	Method	Parameter Setting
1.	CO-IHHO	Threshold= 0.5 β = 1.5 E_o=0.75
2.	ISSA	Maximum iteration for local search algorithm ($maxLt$) = 10
3.	ISCA	Elites number (Ne) = 10 α= 2
4.	TMGWO	Mutation Probability (Mp) = 0.5
5.	SSA	Threshold = 0.5
6.	GWO	Threshold = 0.5
7.	HHO	Threshold = 0.5 β= 1.5
8.	WOA	b = 1 (constant)
9.	Chossat-Golubitsky	a = -1.0 b = 0.1 c = 1.52 d = -0.8 x = 0.1 y = 0.1

5.2. BENCHMARK CEC-06 2019 EVALUATION

The proposed CO-IHHO algorithm's performance is assessed using the CEC-06 2019 benchmark functions, which consist of 10 single-objective optimization problems [34]. These functions, labeled CEC F01 to CEC F10, present diverse challenges with shifted and rotated configurations for some functions. The dimensions of CEC F1, CEC F2, and CEC F3 are 9, 16, and 18, respectively, while the rest are 10-dimensional. The evaluation involves running all MHAs, including the original HHO, proposed CO-IHHO, SSA, GWO, WOA, and PSO [35], for 100 iterations on each function. Table 2 provides the names and ranges of the CEC-06 benchmark functions, while Table 3 displays the evaluation results for the minimization function.

The effectiveness of exploration and exploitation phases is evaluated using function assessment. The competitive outcomes indicate that CO-IHHO maintains a balanced trade-off between exploitation and exploration, outperforming other algorithms in terms of best value, average value, and standard deviation for CEC F1, CEC F2, CEC F3, CEC F6, CEC F7, CEC F8, and CEC F10. The results reveal that CO-IHHO consistently outperforms other MHAs in various instances. The performance of PSO is better for CEC F4 as compared to other algorithms, and GWO performs better for CEC F5. The original HHO shows superior performance for best value and average value in CEC F9, however, the convergence of CO-IHHO is better compared to original HHO for CEC F9, as shown in Fig. 10. It is noteworthy that PSO achieves zero standard deviation for CEC F9, indicating no further improvement can be made with this algorithm. Fig. 2 demonstrates that CO-IHHO exhibits better convergence compared to the HHO algorithm for CEC F1. Similarly, Fig. 3 demonstrates that CO-IHHO achieves better convergence in comparison to the original HHO for CEC F2. Moreover, Fig. 4, Fig. 5, and Fig. 6 illustrate the convergence behaviour of CO-IHHO and HHO for CEC F3, CEC F4, and CEC F5 benchmark functions, respectively. Notably, Fig. 7, Fig. 8, and Fig. 9, provide evidence that CO-IHHO consistently outperforms HHO for CEC F6, CEC F7, and CEC F8, respectively. In the case of CEC F10, as shown in Fig. 11, the CO-IHHO demonstrates better results compared to the performance of original HHO. These results suggest that CO-IHHO performs well in terms of convergence, best value, average value and standard deviation for most of the tested functions, outperforming the HHO and other MHAs in many cases.

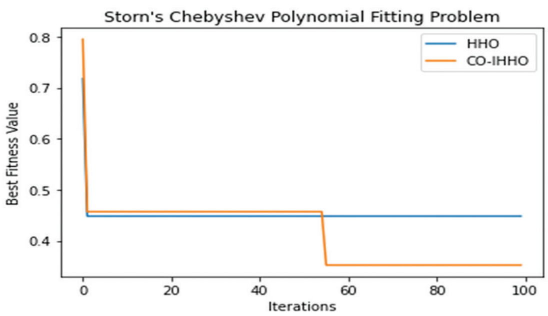

Fig. 2. Convergence curve for CEC F1

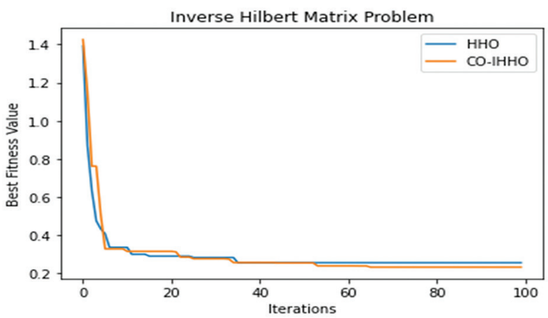

Fig. 3. Convergence curve for CEC F2

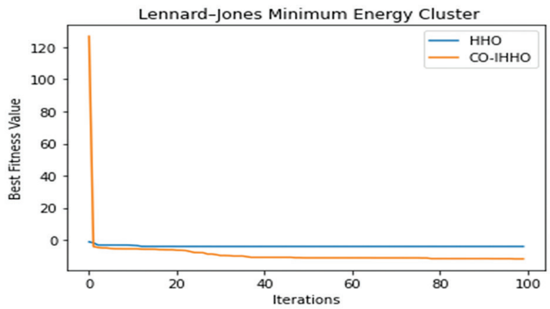

Fig. 4. Convergence curve for CEC F3

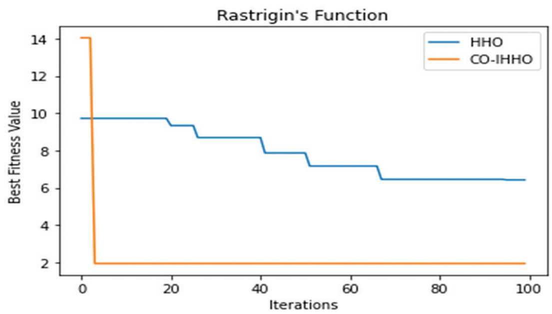

Fig. 5. Convergence curve for CEC F4

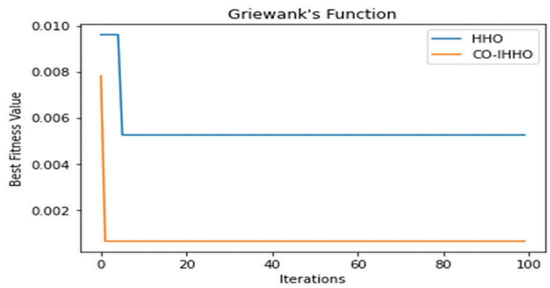

Fig. 6. Convergence curve for CEC F5

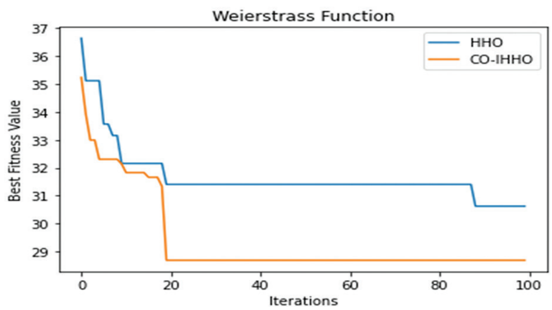

Fig. 7. Convergence curve for CEC F6

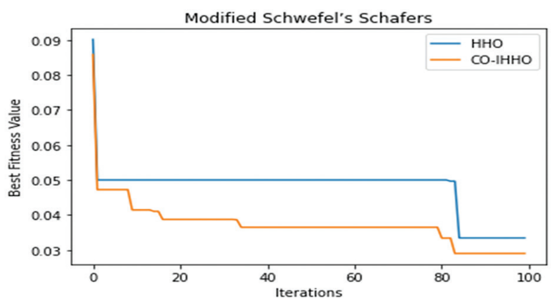

Fig. 8. Convergence curve for CEC F7

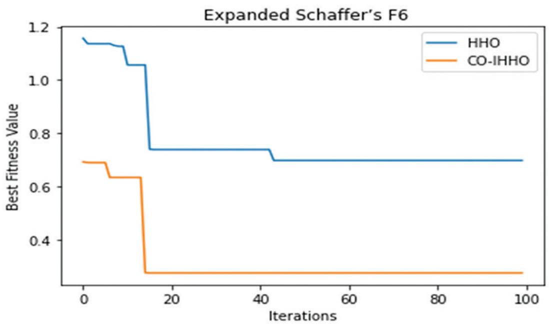

Fig. 9. Convergence curve for CEC F8

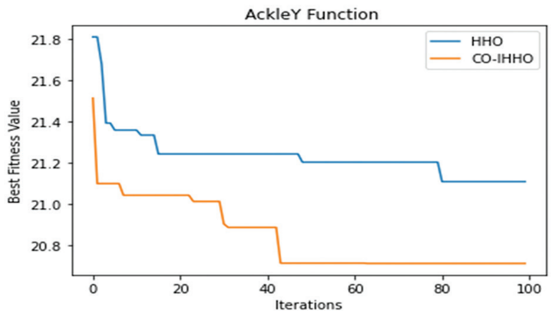

Fig. 11. Convergence curve for CEC F10

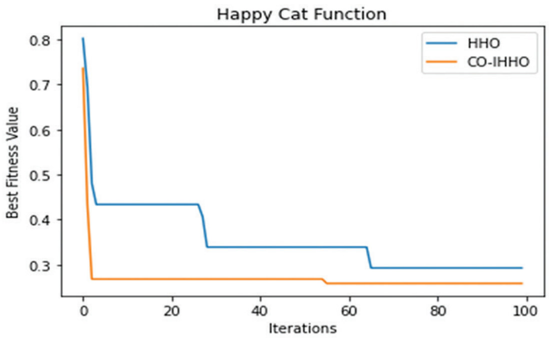

Fig. 10. Convergence curve for CEC F9

Table 2. CEC-06 2019 Benchmark Functions

S. No.	Function Name	Range
F1.	Storn's Chebyshev Polynomial Fitting Problem	[–8192,8192]
F2.	Inverse Hilbert Matrix Problem	[–16384,16384]
F3.	Lennard–Jones Minimum Energy Cluster	[–4,4]
F4.	Rastrigin's Function	[–100,100]
F5.	Griewanck's Function	[–100,100]
F6.	Weierstrass Function	[–100,100]
F7.	Modifed Schwefel'Schafers Functions	[–100,100]
F8.	Expanded Schafer's F6 Function	[–100,100]
F9.	Happy Cat Function	[–100,100]
F10.	Ackley Function	[–100,100]

Table 3. Evaluation Result for CEC-06 2019 Benchmark Functions.

Function	Metric	HHO	CO-IHHO	SSA	GWO	WOA	PSO
F1	Bt.	5.6458408963636614e+57	4.0503471761952476e+57	6.180403739291002e+64	4.4050299978216904e+57	9.425512550977296e+64	5.553789458284711e+57
	Avg.	1.8001192737876405e+59	1.4496940389680123e+58	2.669038785340499e+65	4.405049361695653e+57	2.433135768798515e+65	5.553794197713616e+57
	Sd.	4.829127865299456e+59	1.3535620954277987e+57	9.801780692383188e+64	1.6797038635079378e+58	9.085970285252852e+64	6.703617798945432e+57
F2	Bt.	3.991667151716069	3.9973917809429644	3.997375340600083	3.9951018016288677	3.0854374139651153	3.2763628543348684
	Avg.	3.9995245508433546	3.99979700315296	3.9999312267444482	3.999398176739008	3.9693092439720545	3.768111429602772
	Sd.	0.0015259547174125503	0.0005357237019455018	0.0008885917717980132	0.0009688254637632288	0.16413144511627908	1.4020140157900978
F3	Bt.	-1.0625840664408844	-0.5581271752712231	-2.3814881067413767	-0.8097890269036659	-5.9758752683271024e-18	-3.9915288115300274
	Avg.	-0.021219745050436466	-0.55812 71752712231	-1.8475054329449694	-0.7290514278242319	-9.032367865749103e-08	-2.6374015332542218
	Sd.	0.6594785017613516	0.0	0.2580190544014521	0.050755782735039646	3.922145945550951e-07	0.8153980301270428
F4	Bt.	4.426821733805227	1.0097429773793607	7.957355181876517e+55	3387003.906655918	82.90815749102207	3.9195737433495026e-08
	Avg.	4.480084756471913	1.2561787419150254	1.1565204077536015e+56	3387003.9066559565	160.52086235529387	3.960639551880973e-08
	Sd.	0.03837515684925129	0.04593711910053741	2.811800251441804e+55	1.9999777335956407e-08	77.40570403960551	1.8230480101262743e-10
F5	Bt.	0.7918726025294613	0.08753646705113927	6.455600250692994	2.0095036745715333e-14	1.3211269724866526e-05	0.6175348701316968
	Avg.	0.7918726032381472	0.527456164202598	9.163005176576055	3.8091196863376806e-13	0.06835713316697926	0.6175577735425246
	Sd.	1.337329484646872e-10	0.2868547368291001	1.4816800113561526	6.141940838294567e-13	0.08538731723710603	1.5748562332045633e-05

F6	Bt.	33.150370660918725	19.999980926513693	28.69511052244359	20.519876260083844	19.999980926513675	19.999980926513746
	Avg.	39.33966281894489	19.99998092651373	39.62164984271977	27.87854387037633	27.942487589997018	19.999980926513743
	Sd.	2.559311914314841	1.486206760386614	3.3426729300780225	5.453364367130319	11.793876127713025	3.552713678800501e-15
F7	Bt.	1266.8341381373614	9.950794487333901	31142.428794015377	10636.425913333696	9.49818576031255	72.5894285819002
	Avg.	1267.1162811961126	9.962486072328463	68873.14557159516	10636.4259133337	16112.375314667242	73.00358299789353
	Sd.	0.1725894510405593	0.0023219303880354495	19268.51653842171	3.637978807091713e-12	22475.706053732516	0.6543264666468622
F8	Bt.	7.169410877512084	2.2699551600740326	6.723493674627376	15.493013232370153	12.678902550412865	3.9108997237343455
	Avg.	7.169410877515147	4.577454211793856	8.32002615763271	26.963196056684094	24.673701286726512	6.291320842737323
	Sd.	9.83375082019743212	1.6065586525065239	1.8309652794532914	5.895551206415807	6.382927960600941	1.7357563057153931
F9	Bt.	-1.1699394334559265e+66	-4.334776244689166e+69	-2.5e+76	-2.5e+76	-5.770430310355887e+72	-2.5e+76
	Avg.	-9.330167953480409e+64	-4.334833326484094e+68	-5.5153021870255146e+75	-1.998534561138153e+76	-5.0265922528784734e+73	-2.5e+76
	Sd.	2.862540782266106e+65	1.3004309707285165e+69	9.135608886381215e+75	3.078090653543935e+75	1.9352465134230854e+74	0.0
F10	Bt.	20.52698445657453	19.99993579171894	19.999999993888967	21.423167174440493	20.05074257169523	19.999999993888967
	Avg.	21.060908317329346	19.999996789276956	19.99999999388897	21.453085896275244	21.184379783145335	19.99999999388897
	Sd.	0.22800868237094374	0.01531973776709719	3.552713678800501	0.2596558779276892	0.32581475455351727	3.552713678800501

*Sd=Standard Deviation (minimum), Bt. = Best value (minimum), and Avg. = Average Value (minimum).

5.3. DATASET DESCRIPTION

The proposed IDS performance is evaluated using the BoT-IoT dataset [31]. This realistic dataset was developed in Cyber Range Lab of UNSW in 2018, and published in 2019 for the IoT environment [34]. It includes both intrusive traffic with different attack categories and normal traffic. The intrusive traffic dataset comprises four primary categories: data exfiltration, DoS, reconnaissance, and DDoS. A summary of the dataset in Table 4 indicates that it is predominantly composed of over 99% intrusive traffic instances, with less than 1% representing normal traffic instances. Moreover, to improve the performance of ML classifiers additional attributes are also added. The BoT-IoT realistic testbed includes a network platform, which includes attacking and normal virtual machines, simulated IoT services, which include five IoT devices simulated using the Red-Node tool, feature extraction using the Agrus tool, and forensic analytics using ML algorithms. The five IoT devices used for simulation include a smart thermostat, smart door, smart fridge, smart lights, and weather station. This dataset has about 72 million labeled records in 74 .csv files with 46 features, out of which 14 are additionally generated from the original feature set. In the process of assessing the performance of the proposed IDS model, a subset amounting to 5% of the entire dataset is taken into account, which corresponds to four .csv files.

Table 4. Dataset Instances.

S.No.	Category	Instances
1.	DDoS	1926624
2.	Normal	477
3.	Information Theft	79
4.	Reconnaissance	91082
5.	DoS	1650260

5.4. EVALUATION METRIC

The evaluation of performance utilizes the following metrics.

Fitness function: The FF is determined using following equation:

$$FF = \propto \times er + \beta_2 \times \left(\frac{Sel\_Fea}{Max\_Fea}\right) \quad (24)$$

where α=0.99 and β_2=1-α

Max_Fea = maximum number of features, Sel_{Fea} = selected features length, and er = 1-Accuracy

Accuracy: This metric defines the identification of data instances from complete traffic data correctly. It is mathematically defined as:

$$Accuracy = \frac{TpS+TnS}{TpS+TnS+FpS+FnS} \quad (25)$$

Precision (P): This metric defines the correctly identifies data instances as positive. It is mathematically defined as:

$$Precision = \frac{TpS}{TpS+FpS} \quad (26)$$

Recall (R): This metric defines the correctly identifies data traffic instances. It is defined mathematically as:

$$Recall = \frac{TpS}{TpS+FnS} \quad (27)$$

F-Score: This metric is calculated as the harmonic mean of recall and precision. Mathematically, it is defined as:

$$F - Score = \left(\frac{R \times P}{R+P}\right) \times 2 \quad (28)$$

Time: The time defines the overall time taken by the algorithm for identifying intrusion.

Features Selected: This indicates the length of features selected by MHA from overall features.

where,

- True Positive (TpS): Data traffic instances correctly classified as positive
- False Positive (FpS): Data traffic instances misclassified as positive
- False Negative (FnS): Number of data traffic instances misclassified as negative
- True Negative (TnS): Data traffic instances correctly classified as negative

5.5. RESULT DISCUSSION AND PERFORMANCE ANALYSIS

Comparison with Other MHA: The result obtained by the proposed work is compared against other wrapper-based MHAs such as ISSA [37], ISCA [38], TMGWO [39], SSA [40], GWO [41], HHO [20], and WOA [42] for FS of the intrusive network traffic for the IoT system. Furthermore, the performance of two ML classifiers: DT, and KNN with the FS methods are compared for identifying intrusive traffic.

Binary Classification: Fig. 12 depicts that CO-IHHO achieves the highest accuracy of 100% using the DT classifier, while ISCA and GWO achieve an accuracy of 99.98% for the BoT-IoT dataset. With KNN as a classifier, CO-IHHO achieves an accuracy of 99.97% while ISSA and SSA achieve an accuracy of 99.95%. Furthermore, Fig. 13 shows that CO-IHHO, ISCA, GWO, and HHO select the lowest number of features i.e. 3 with the DT classifier while ISCA and GWO select the minimum feature length i.e. 2 with KNN classifier for the BoT-IoT dataset.

Fig. 14 depicts that the computation time of CO-IHHO is lowest with both classifiers DT, and KNN in contrast to all other MHA used for FS task. Moreover, TMGWO takes the highest computation time with DT, and KNN classifiers compared to all other MHA used for FS tasks. The convergence curve of CO-IHHO-DT and HHO-DT is shown in Fig. 21 for the BoT-IoT dataset. While the convergence curve of CO-IHHO-KNN and HHO-KNN is shown in Fig. 23. It has been observed that CO-IHHO converges better than HHO for both classifiers.

The overall performance of CO-IHHO-DT is better compared to CO-IHHO-KNN for the accuracy, features selected, and computation time. Furthermore, for binary classification, the performance of CO-IHHO is better among all other MHA used for FS task.

Multiclass Classification: CO-IHHO achieves the highest accuracy of 99.65%, and 98.1% for DT, and KNN classifiers, respectively as depicted in Fig.15. Similarly, Fig. 17, Fig. 18, and Fig. 19. depict that CO-IHHO achieves the highest precision, recall, and F-score each of 100% and 98% with DT and KNN classifier, respectively for the BoT-IoT dataset. As seen in Fig. 16, CO-IHHO with DT classifier selects the minimum number of features i.e. 8. While SSA with DT classifier selects the maximum length of features i.e. 15. Moreover, CO-IHHO with KNN classifier selects the minimum length of features i.e. 5. While HHO selects the maximum length of the feature i.e. 22.

Furthermore, Fig. 20 depicts the CO-IHHO taking the lowest computation time i.e. 31.34 sec. and 42.87 sec. using DT, and KNN classifiers, respectively for the BoT-IoT dataset. TMGWO takes the maximum computation time among all other MHA with DT, and KNN classifier. Convergence curve of CO-IHHO-DT and HHO-DT is shown in Fig. 22. Convergence curve of CO-IHHO-KNN and HHO-KNN for the BoT-IoT dataset is shown in Fig. 24. It has been observed that CO-IHHO converges better than HHO for both classifiers.

The overall performance of CO-IHHO-DT is better compared to CO-IHHO-KNN in terms of number of features selected, accuracy, F-score, precision, computation time, and recall. Furthermore, for multiclass classification, the performance of CO-IHHO is better among all other MHA used for FS task.

Comparison with other recent work: The presented research is also benchmarked against other recent studies that share similarities. These recent investigations employ the BoT-IoT dataset as the basis for evaluating their performance.

Binary Classification: Table 5 depicts the accuracy comparison of CO-IHHO-DT with other recent work for the binary classification. It has been observed that the accuracy of the proposed CO-IHHO-DT is higher compared to the other similar approaches such as BD-PSO-V [43], DNN [44], BGWO-NB [45], AQUa [46], and RSA [47].

Multiclass Classification: Table 6 shows the accuracy comparison of CO-IHHO-DT with other similar approaches for the multiclass classification. The proposed CO-IHHO-DT attains the maximum accuracy of 99.65% compared to other approaches such as GbFS [48], AQUa [44], and RSA [47].

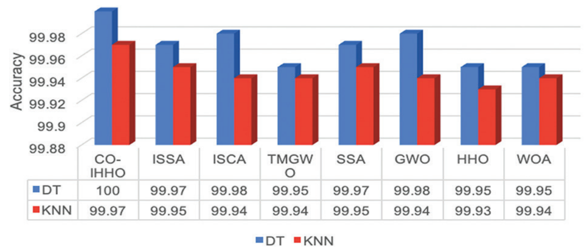

	CO-IHHO	ISSA	ISCA	TMGWO	SSA	GWO	HHO	WOA
DT	100	99.97	99.98	99.95	99.97	99.98	99.95	99.95
KNN	99.97	99.95	99.94	99.94	99.95	99.94	99.93	99.94

Fig. 12. Binary classification accuracy for BoT-IoT dataset

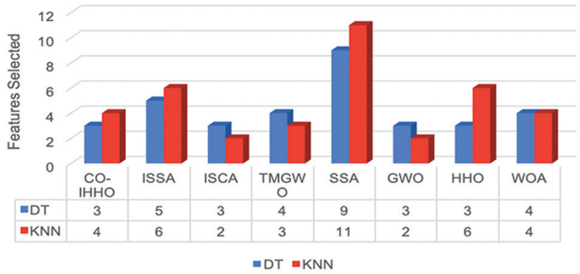

	CO-IHHO	ISSA	ISCA	TMGWO	SSA	GWO	HHO	WOA
DT	3	5	3	4	9	3	3	4
KNN	4	6	2	3	11	2	6	4

Fig. 13. Binary classification features selected for BoT-IoT dataset

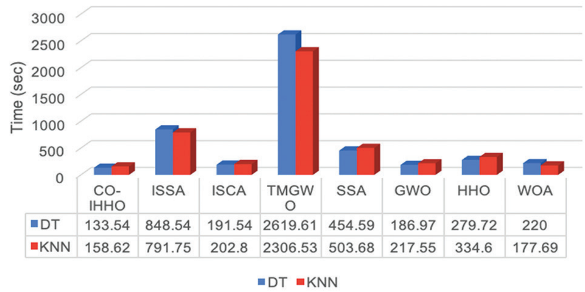

	CO-IHHO	ISSA	ISCA	TMGWO	SSA	GWO	HHO	WOA
DT	133.54	848.54	191.54	2619.61	454.59	186.97	279.72	220
KNN	158.62	791.75	202.8	2306.53	503.68	217.55	334.6	177.69

Fig. 14. Binary classification computation time for BoT-IoT dataset

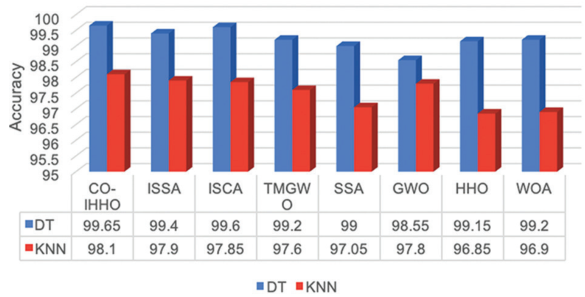

	CO-IHHO	ISSA	ISCA	TMGWO	SSA	GWO	HHO	WOA
DT	99.65	99.4	99.6	99.2	99	98.55	99.15	99.2
KNN	98.1	97.9	97.85	97.6	97.05	97.8	96.85	96.9

Fig. 15. Multiclass classification accuracy for BoT-IoT dataset

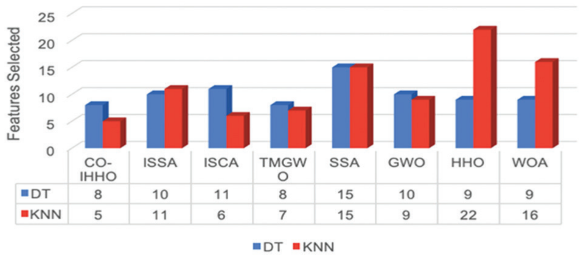

	CO-IHHO	ISSA	ISCA	TMGWO	SSA	GWO	HHO	WOA
DT	8	10	11	8	15	10	9	9
KNN	5	11	6	7	15	9	22	16

Fig. 16. Multiclass classification features selected for BoT-IoT dataset

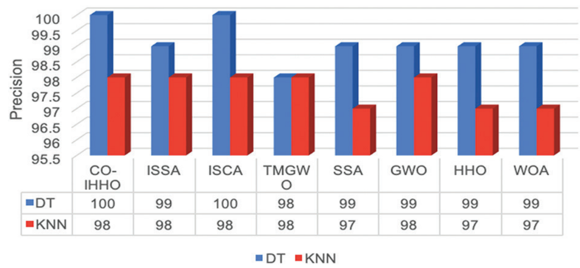

	CO-IHHO	ISSA	ISCA	TMGWO	SSA	GWO	HHO	WOA
DT	100	99	100	98	99	99	99	99
KNN	98	98	98	98	97	98	97	97

Fig. 17. Multiclass classification precision for BoT-IoT dataset

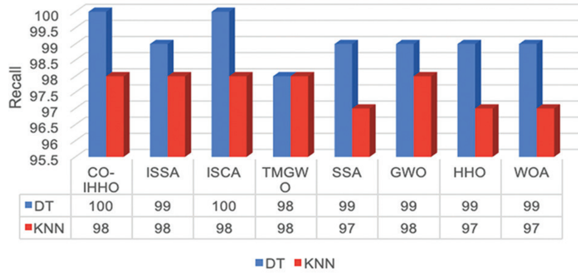

	CO-IHHO	ISSA	ISCA	TMGWO	SSA	GWO	HHO	WOA
DT	100	99	100	98	99	99	99	99
KNN	98	98	98	98	97	98	97	97

Fig. 18. Multiclass classification recall for BoT-IoT dataset

	CO-IHHO	ISSA	ISCA	TMGWO	SSA	GWO	HHO	WOA
DT	100	99	100	98	99	99	99	99
KNN	98	98	98	98	97	98	97	97

Fig. 19. Multiclass classification F-Score for BoT-IoT dataset

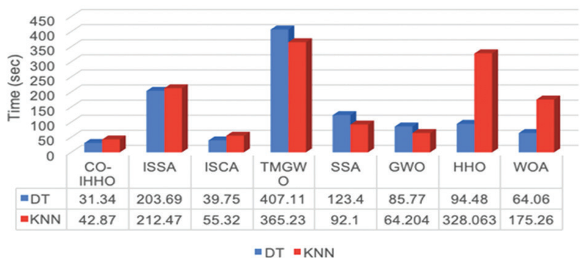

	CO-IHHO	ISSA	ISCA	TMGWO	SSA	GWO	HHO	WOA
DT	31.34	203.69	39.75	407.11	123.4	85.77	94.48	64.06
KNN	42.87	212.47	55.32	365.23	92.1	64.204	328.063	175.26

Fig. 20. Multiclass classification computation time for BoT-IoT dataset

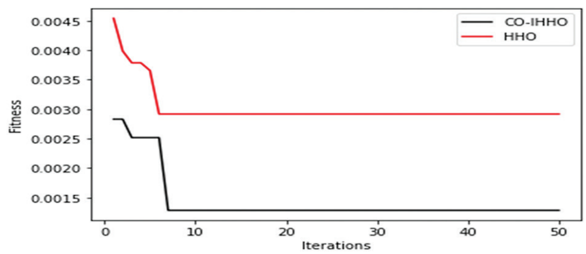

Fig. 21. Binary convergence curve with DT for BoT-IoT dataset

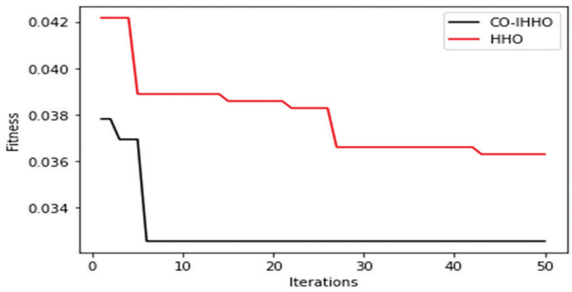

Fig. 22. Multiclass convergence curve with DT for BoT-IoT dataset

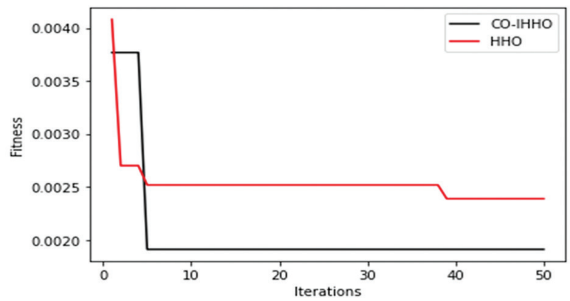

Fig. 23. Binary convergence curve with KNN for BoT-IoT dataset

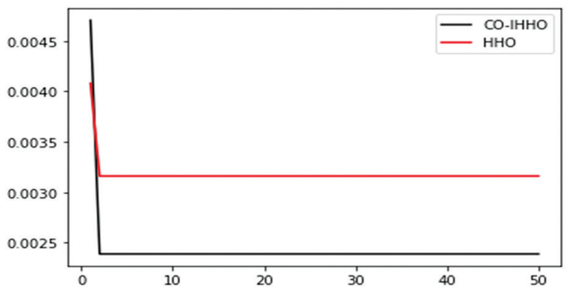

Fig. 24. Multiclass convergence curve with KNN for BoT-IoT dataset

Table 5. Binary classification

S.No.	Method	Accuracy
1.	BD-PSO-V [46]	99.91%
2.	DNN [47]	99.01%
3.	BGWO-NB [48]	99.15%
4.	CO-IHHO-DT (Proposed)	100%
5.	AQUa [44]	99.99%
6.	RSA [45]	99.99%

Table 6. Multiclass classification

S. No.	Method	Accuracy
1.	GbFS [48]	98.90%
2.	CO-IHHO-DT (Proposed)	99.65%
3.	AQUa [46]	98.90%
4.	RSA [47]	98.92%

5.6. REAL WORLD APPLICATIONS

The feature selection using CO-IHHO for IoT based IDS finds application in many real world scenarios, such as:

Smart Homes: Enhancing the security of smart homes by selecting relevant features for intrusion detection in IoT devices such as smart cameras, door sensors, and environmental sensors.

Industrial IoT (IIoT): Securing industrial processes and critical infrastructure by optimizing feature sets for intrusion detection in sensors, controllers, and communication networks.

Healthcare IoT: Protecting patient data and medical devices by employing MHA to select features for intrusion detection in healthcare IoT systems.

Supply Chain Management: Securing IoT-enabled supply chain systems by optimizing features for intrusion detection in RFID tags, sensors, and communication networks.

Energy Management: Improving the security of energy grids and IoT-enabled smart energy systems by selecting features for intrusion detection in smart meters, sensors, and communication networks.

Environmental Monitoring: Securing environmental monitoring systems by optimizing features for intrusion detection in sensors deployed for climate monitoring, pollution detection, and wildlife tracking.

Banking and Finance: Protecting IoT-enabled financial services and ATMs by optimizing intrusion detection features in devices connected to banking networks.

Telecommunications: Protecting IoT devices and networks within the telecommunications sector by optimizing intrusion detection features in routers, switches, and communication equipment.

Military and Defence: Securing military IoT systems by optimizing features for intrusion detection in surveillance equipment, communication networks, and unmanned aerial vehicles (UAVs).

6. CONCLUSION

With the advancement in IoT technology, the everyday utilization of smart IoT devices is increasing briskly. These smart IoT equipment are connected to the internet usually via a wireless network, which makes them vulnerable to several attacks. Hence, security is one of the major issues with the IoT framework. As a result, this paper introduces a metaheuristic-based Intrusion Detection System (IDS) designed for the IoT framework. The feature selection process for network traffic data is accomplished using CO-IHHO, which is an enriched version of the metaheuristic harris hawk optimization algorithm. CO-IHHO achieves a better convergence rate compared to HHO. Furthermore, the result of CO-IHHO is classified using two ML classifiers: DT and KNN. The experimental result shows that CO-IHHO-DT achieves better accuracy compared to CO-IHHO-KNN. The performance of the proposed system is assessed by conducting a comparative analysis with various MHAs used as FS methods. These MHAs include ISSA, ISCA, TMGWO, SSA, GWO, HHO, and WOA. The result shows that the performance of CO-IHHO-DT attains maximum accuracy of 100%, and minimal computation time for binary classification. CO-IHHO-DT attains the highest accuracy of 99.65% among all other MHA used for FS task of multiclass classification of intrusive traffic. The proposed IDS model is further subjected to comparison with other contemporary approaches. The outcomes indicate that CO-IHHO-DT consistently achieves superior accuracy in both binary and multiclass classification scenarios when compared to these alternatives. The performance of CO-IHHO is further evaluated using CEC-06 2019 benchmark function. In the future, we can utilize deep learning techniques to achieve more refined classification results while addressing real-world applications.

7. REFERENCES

[1] O. Novo, N. Beijar, M. Ocak, J. Kjällman, M. Komu, T. Kauppinen, "Capillary networks - bridging the cellular and IoT worlds", Proceedings of the IEEE 2nd World Forum on Internet of Things, Milan, Italy, 14-16 December 2015.

[2] A. Duraisamy, S. Muthusamy, C. R. R. Robin, "An Optimized Deep Learning Based Security Enhancement and Attack Detection on IoT Using IDS and KH-AES for Smart Cities", Studies in Informatics and Control, Vol. 30, No. 2, 2021, pp. 121-131.

[3] M. F. Elrawy, A. I. Awad, H. F. A. Hamed, "Intrusion detection systems for IoT-based smart environments: a survey", Journal of Cloud Computing: Advances, Systems and Applications, Vol. 7, No. 21, 2018, pp. 1-20.

[4] A. Thakkar, R. Lohiya, "A Review on Machine Learning and Deep Learning Perspectives of IDS for IoT: Recent Updates, Security Issues, and Challenges", Archives of Computational Methods in Engineering, Vol. 28, 2021, pp. 3211–3243.

[5] S. Maza, M. Touahria, "Feature Selection Algorithms in Intrusion Detection System: A Survey", KSII Transactions on Internet and Information Systems, Vol. 12, No. 10, 2018, pp. 5079-5099.

[6] V. R. Balasaraswathi, M. Sugumaran, Y. Hamid, "Feature selection techniques for intrusion detection using non-bio-inspired and bio-inspired optimization algorithms", Journal of Communications and Information Networks, Vol. 2, No. 4, 2017, pp. 107-119.

[7] B. Venkatesh, J. Anuradha, "A review of feature selection and its methods", Cybernetics and Information Technologies, Vol. 19, No. 1, 2019, pp. 3-26.

[8] J. D. Ser, E. Osaba, D. Molina, X.-S. Yang, S. Salcedo-Sanzf, D. Camacho, S. Das, P. N. Suganthan, C. A. C. Coello, F. Herrera, "Bio-inspired Computation: Where We Stand and What's Next", Swarm and Evolutionary Computation, Vol. 48, 2019, pp. 220-250.

[9] Y. Otoum, D. Liu, A. Nayak, "DL-IDS: a deep learning–based intrusion detection framework for securing IoT", Transactions on Emerging Telecommunications Technologies, Vol. 33, No. 3, 2022, p. e3803.

[10] P. K. Keserwani, M. C. Govil, E. S. Pilli, P. Govil, "A smart anomaly based intrusion detection system for the Internet of Things (IoT) network using GWO–PSO–RF model", Journal of Reliable Intelligent Environments, Vol. 7, No. 1, 2021, pp. 3-21.

[11] S. S. Kareem, R. R. Mostafa, F. A. Hashim, H. M. El-Bakry, "An Effective Feature Selection Model Using Hybrid Metaheuristic Algorithms for IoT Intrusion Detection", Sensors, Vol. 22, No. 4, 2022, p. 1396.

[12] R. A. Khurma, I. Almomani, I. Aljarah, "IoT Botnet Detection Using Salp Swarm and Ant Lion Hybrid Optimization Model", Symmetry, Vol. 13, No. 8, 2021, p. 1377.

[13] A. Davahli, M. Shamsi, G. Abaei, "Hybridizing genetic algorithm and grey wolf optimizer to advance an intelligent and lightweight intrusion detection system for IoT wireless networks", Journal of Ambient Intelligence and Humanized Computing, Vol. 11, No. 11, 2020, pp. 5581-5609.

[14] M. Alweshah, S. Alkhalaileh, M. Beseiso, M. Almiani, S. Abdullah, "Intrusion detection for IoT based on a hybrid shuffled shepherd optimization algorithm", The Journal of Supercomputing, Vol. 78, No. 10, 2022, p. 12278-12309.

[15] H. Haddadpajouh, A. Mohtadi, A. Dehghantanaha, H. Karimipour, X. Lin, K.-K. R. Choo, "A Multikernel and Metaheuristic Feature Selection Approach for IoT Malware Threat Hunting in the Edge Layer", IEEE Internet of Things Journal, Vol. 8, No. 6, 2020, pp. 4540-4547.

[16] Z. Ahmad, A. S. Khan, K. Nisar, I. Haider, R. Hassan, M. R. Haque, S. Tarmizi, J. J. P. C. Rodrigues, "Anomaly Detection Using Deep Neural Network for IoT Architecture", Applied Sciences, Vol. 11, No. 15, 2021, p. 7050.

[17] R. A. Ramadan, K. Yadav, "A novel hybrid intrusion detection system (IDS) for the detection of internet of things (IoT) network attacks", Annals of Emerging Technologies in Computing, Vol. 4, No. 5, 2020, pp. 61-74.

[18] Y. Li, S. Ghoreishi, A. Issakhov, "Improving the Accuracy of Network Intrusion Detection System in Medical IoT Systems through Butterfy Optimization Algorithm", Wireless Personal Communications, Vol. 126, 2022, pp. 1999-2017.

[19] J. O. Onah, S. M. Abdulhamid, M. Abdullahi, I. H. Hassan, A. Al-Ghusham, "Genetic Algorithm based feature selection and Naïve Bayes for anomaly detection in fog computing environment", Machine Learning with Applications, Vol. 6, 2021, p. 100156.

[20] A. A. Heidari, S. Mirjalili, H. Faris, I. Aljarah, M. Mafarja, H. Chen, "Harris hawks optimization: Algorithm and applications", Future Generation Computer Systems, Vol. 97, 2019, pp. 849-872.

[21] H. M. Alaboo, D. Alarabiat, L. Abualigah, A. A. Heidari, "Harris hawks optimization: a comprehensive review of recent variants and applications", Neural Computing and Applications, Vol. 33, No. 15, 2021, p. 8939-8980.

[22] A. A. Dehkordi, A. S. Sadiq, S. Mirjalili, K. Z. Ghafoor, "Nonlinear-based Chaotic Harris Hawks Optimizer: Algorithm and Internet of Vehicles application", Applied Soft Computing, Vol. 109, 2021, p. 107574.

[23] A. A. Ewees, M. A. Elaziz, "Performance analysis of Chaotic Multi-Verse Harris Hawks Optimization: A case study on solving engineering problems", Engineering Applications of Artificial Intelligence, Vol. 88, 2020, pp. 1-16.

[24] P. Chossat, M. Golubitsky, "Iterates of maps with symmetry", SIAM Journal on Mathematical Analysis, Vol. 19, No. 6, 1988, pp. 1259-1270.

[25] H. R. Tizhoosh, "Opposition-Based Learning: A New Scheme for Machine Intelligence", Proceedings of the International conference on computational intelligence for modelling, control and automation and international conference on intelligent agents, web technologies and internet commerce, Vienna, Austria, 28-30 November2005.

[26] R. Hans, H. Kaur, N. Kaur, "Opposition-based Harris Hawks optimization algorithm for feature selection in breast mass classification", Journal of Interdisciplinary Mathematics, Vol. 23, No. 1, 2020, pp. 97-106.

[27] M. Tubishat, N. Idris, L. Shuib, M. A. Abushariah, "Improved Salp Swarm Algorithm based on opposition based learning and novel local search algorithm for feature selection", Expert Systems with Applications, Vol. 145, 2020, p. 113122.

[28] Z. Wang, H. Ding, Z. Yang, B. Li, Z. Guan, L. Bao, "Rank-driven salp swarm algorithm with orthogonal opposition-based learning for global optimization", Applied Intelligence, Vol. 52, 2022, p. 7922–7964.

[29] X. Zhao, F. Yang, Y. Han, Y. Cui, "An Opposition-Based Chaotic Salp Swarm Algorithm for Global Optimization", IEEE Access, Vol. 8, 2020, pp. 36485-36501.

[30] S. Rahnamayan, H. R. Tizhoosh, M. M. Salama, "Opposition versus randomness in soft computing techniques", Applied Soft Computing, Vol. 8, No. 2, 2008, pp. 906-918.

[31] N. Koroniotis, N. Moustafa, E. Sitnikova, B. Turnbull, "Towards the development of realistic botnet dataset in the Internet of Things for network forensic analytics: Bot-IoT dataset", Future Generation Computer Systems, Vol. 100, 2019, pp. 779-796.

[32] P. Agrawal, A. F. Hattan, G. Talari, M. W. Ali, "Metaheuristic Algorithms on Feature Selection: A Survey of One Decade of Research (2009-2019)", IEEE Access, Vol. 9, 2021, pp. 26766-26791.

[33] H. Jia, C. Lang, D. Oliva, W. Song, X. Peng, "Dynamic Harris Hawks Optimization with Mutation Mechanism for Satellite Image Segmentation", Remote Sensing, Vol. 11, No. 12, 2019, p. 1421.

[34] J. M. Abdullah, T. A. Rashid, "Fitness Dependent Optimizer: Inspired by the Bee Swarming Reproductive Process", IEEE Access, Vol. 7, 2019, pp. 43473-43486.

[35] J. C. Bansal, "Particle Swarm Optimization", Evolutionary and swarm intelligence algorithms, Springer, Berlin, 2019, pp. 11-23.

[36] J. M. Peterson, J. L. Leevy, T. M. Khoshgoftaar, "A Review and Analysis of the Bot-IoT Dataset", Proceedings of the IEEE International Conference on Service-Oriented System Engineering, Oxford, UK, 23-26 August2021.

[37] M. Tubishat, N. Idris, L. Shuib, M. A. Abushariah, S. Mirjalili, "Improved Salp Swarm Algorithm based on opposition based learning and novel local search algorithm for feature selection", Expert Systems with Applications, Vol. 145, 2020, p. 113122.

[38] R. Sindhu, R. Ngadiran, Y. M. Yacob, N. A. H. Zahri, M. Hariharan, "Sine–cosine algorithm for feature selection with elitism strategy and new updating mechanism", Neural Computing and Applications, Vol. 28, 2017, p. 2947-2958.

[39] M. Abdel-Basset, D. El-Shahat, I. El-henawy, V. H. C. Albuquerque, "A new fusion of grey wolf optimizer algorithm with a two-phase mutation for feature selection", Expert Systems with Applications, Vol. 139, 2020, p. 112824.

[40] S. Mirjalili, A. H. Gandomi, S. Z. Mirjalili, S. Saremi, H. Faris, S. M. Mirjalili, "Salp Swarm Algorithm: A bio-inspired optimizer for engineering design problems", Advances in Engineering Software, Vol. 114, 2017, pp. 163-191.

[41] S. Mirjalili, S. M. Mirjalili, A. Lewis, "Grey Wolf Optimizer", Advances in Engineering Software, Vol. 69, 2014, pp. 46-61.

[42] S. Mirjalili, A. Lewis, "The Whale Optimization Algorithm", Advances in Engineering Software, Vol. 95, 2016, pp. 51-67.

[43] M. Asadi, M. A. J. Jamal, S. Parsa, M. Vahid, "Detecting Botnet by Using Particle Swarm Optimization Algorithm Based on Voting System", Future Generation Computer Systems, Vol. 107, 2020, pp. 95-111.

[44] Z. Ahmad, A. S. Khan, K. Nisar, I. Haider, R. Hassan, M. R. Haque, S. Tarmizi, J. J. P. C. Rodrigues, "Anomaly Detection Using Deep Neural Network for IoT Architecture", Applied Sciences, Vol. 11, No. 15, 2021, p. 7050.

[45] I. M. Nur, E. Ulker, "A Novel Hybrid IoT Based IDS Using Binary Grey Wolf Optimizer (BGWO) and Naive Bayes (NB)", European Journal of Science and Technology, No. 2020, 2020, pp. 279-286.

[46] F. Abdulaziz, A. Dahou, M. A. A. Al-qaness, S. Lu, M. A. Elaziz, "Advanced Feature Extraction and Selection Approach Using Deep Learning and Aquila Optimizer for IoT Intrusion Detection System", Sensors, Vol. 22, No. 1, 2021, p. 140.

[47] A. Dahou, M. A. Elaziz, S. A. Chelloug, M. A. Awadallah, M. A. Al-Betar, M. A. A. Al-qaness, "Intrusion Detection System for IoT Based on Deep Learning and Modified Reptile Search Algorithm", Computational Intelligence and Neuroscience, Vol. 2022, 2022.

[48] Z. Halim, M. N. Yousaf, M. Waqas, M. Sulaiman, G. Abbas, M. Hussain, I. Ahmad, M. Hanif, "An effective genetic algorithm-based feature selection method for intrusion detection systems", Computers & Security, Vol. 110, 2021, p. 102448.

An Effective Technique to Detect WIFI Unauthorized Access using Deep Belief Network

Original Scientific Paper

Rajakumar S.
Professor, Department of Electronics & Communication Engineering,
Panimalar Engineering College, Chennai, 600123
India
rajakumar109@outlook.com

Subraja Rajaretnam
Assistant professor, Department of Electronics and Communication Engineering, Sathyabama Institute of Science and Technology, Jeppiaar Nagar,
Chennai 600 119 India
subraja654@gmail.com

William P.
Assistant Professor & Dean,
Research and Development,
Department of Information Technology,
Sanjivani College of Engineering, SPPU, Pune
william.wp09@gmail.com

Azhagu Jaisudhan Pazhani A.
Associate professor, Department of Electronics & Communication Engineering,
Ramco Institute of Technology, Rajapalayam,
Tamil Nadu 626117 India
pazhani876@gmail.com

Mabel Rose R. A.
Assistant Professor,
Computer Science and Engineering,
S.A. Engineering College, Poonamallee, Thiruverkadu,
Tamil Nadu 600077 India.
rose.RA87@gmail.com

Ahilan A
Associate Professor, Department of Electronics and Communication Engineering,
PSN College of Engineering and Technology,
India
listentoahil098@gmail.com

Abstract *– Network security has grown to be a major concern in recent years due to the popularity and development of Wi-Fi networks. However, the use of Wi-Fi networks is expanding quickly, and so is the number of attacks on Wi-Fi networks. In this paper, a novel WiFi Unauthorized Access Detection System (WUADS) technique has been proposed to detect unauthorized access in the WiFi network. Initially, the Wi-Fi frames are collected from the AWID dataset. The features of the Wi-Fi frame are extracted by using Principal Component Analysis (PCA). Finally, the Deep Belief Network (DBN) is employed for classification into authorized access and unauthorized access. The efficiency of the proposed WUADS technique was evaluated based on the parameters like accuracy, F1score, detection rate, precision, and recall. The performance analysis of the proposed WUADS technique achieves an overall accuracy range of 99.52%. The proposed WUADS method has a high success rate and the quickest attack detection time compared to deep learning techniques like CNN, RNN, and ANN. The proposed WUADS improves the overall accuracy better than 1.12%, 0.1%, and 14.22% comparative analysis of the SAE (Stacked AutoEncoder), WNIDS (wireless Network Intrusion Detection System), and 3D-ID (3 Dimensional-Identification) respectively.*

Keywords: *Wi-Fi networks, unauthorized access detection system, Principal Component Analysis, Deep Belief Network.*

1. INTRODUCTION

A Wi-Fi network comprises a wireless gateway facilitating internet access for various devices, with the router acting as a central hub connected to the internet modem [1]. Globally, wireless networks face increasing cyber threats, marked by sophisticated and persistent attacks that can bypass traditional security measures. The ubiquity of WiFi in diverse settings, such as businesses, coffee shops, and educational institutions, makes it challenging to verify users, leading to potential vulnerabilities [2, 3]. Wireless Local Area Networks (WLANs) utilize access points and wireless media, expanding rapidly as a wired technology alternative [4]. Found in numerous sectors like finance, telecommunications, healthcare, education, and public agencies, WLANs establish an invisible pathway between devices and the internet [5]. The growing popularity of WiFi can be attributed to its high data rate, flexibility, affordability, efficiency, mobility, and universal accessibility [6].

Data is transmitted and received by WiFi (sometimes referred to as a transceiver). A WLAN and fixed wire network can be connected by an access point, which also creates links between users on the network [7]. WiFi data usage and communication are growing and are now considered necessities of an ever-expanding modern society; they are present in almost all homes, businesses, and public places [8, 9]. The Wi-Fi-Protected-Access/Preshared-Key (WPA2-PSK) does not guarantee 100% security and is still vulnerable to some types of attacks, including de-authentication, downgrade, and network security can be compromised by Denial-of-Service (DoS) attacks [10]. The challenge is coming up with a proactive and efficient method for quickly identifying illicit WiFi access. Current intrusion detection systems frequently fail to provide alerts in real time or may produce false positives, which negatively affects user experience and network performance. Furthermore, a solution that can detect unwanted access across a variety of devices and network configurations and react to developing threats is required due to the growth of IoT devices and diverse network designs. To overcome the above problem, a novel WUADS technique has been proposed to detect unauthorized access in the WiFi network. The main contributions are as follows:

- Initially, all Wifi frames are collected from the network traffic and from that data, a dataset has been constructed.
- After that, the features of the WiFi frames are extracted using Principal Component Analysis (PCA) to reduce the dimensionality of Wi-Fi frames and capture the most significant variations in the data.
- Then , the extracted features are given as input to the Deep Belief Network (DBN) for the classification of Wi-Fi frames into authorized access and unauthorized access.
- If Wi-Fi frames signal unauthorized access, the subsequent steps may include generating alerts and blocking the unauthorized device.
- The criteria F1 score, recall, precision, specificity, and accuracy are used to analyse the proposed technique's performance.

The remainder of the analysis is divided into the following sections: The literature review is thoroughly described in Section II. The recommended WUADS method is described in Section III. Section IV presents the findings, while section V summarizes the results.

2. LITERATURE SURVEY

Wi-Fi attacks fall into two main groups: those targeting network security and those affecting network deployment strategies. Here's an overview of recent advancements in security management for Wi-Fi networks.

Ref. [11] had analysed various wireless network assaults and performed network attack classification using stacked autoencoder (SAE) and deep neural networks (DNN). The experimental result shows that the classification accuracies achieved a 98.4%, 98.3% and 73.12%, respectively. The paper lacks discussion on model interpretability, essential for practical deployment in real-world scenarios.

Ref. [12] had analysed various risks to users' personal activities in light of growing business interest in tracking openly broadcast wireless data. Additionally, it demonstrates how an utterly inert eavesdropper can identify the data being transferred over the network. The lack of workable remedies for dangers to user privacy that have been outlined in the study leaves users in the dark about how to reduce the risks.

A Wireless Network Intrusion Detection system (WNIDS) [13] was developed to effectively detect attacks. In order to order the network data as normal or belonging attack. With a smaller set of features, WNIDS gets a multi-class classification accuracy of 99.42%. Drawback of the proposed WNIDS is that it has identified some flooding assault events in the test dataset as regular records.

A 3D-ID, a WiFi vision-based person re-ID system [14] was proposed in three dimensions. WiFi can picture a person in their actual surroundings thanks to WiFi equipment and a 2D AoA (Angle of Arrival) assessment of the signal reflections. The precision of the 3D-ID system is 85.3%. A disadvantage is that it has trouble with limited user evaluation, sensing range, and crowded areas.

CSI-based localization [15] was proposed, using an active device in place of a jamming harmful signals and disrupting communications, which serves as a relay and passes the received frames with a random delay. Promising initial results and a prototype show efficient location obfuscatio. The drawback is that it faces limitations and complexities, particularly in MIMO systems and real-world deployment challenges.

An automatic feature selection system and two-phase hybrid ensemble learning NIDS based on machine learning [16] was proposed Using four distinct machine learning classifiers. With a detection rate of 0.9314 and a false alarm rate of 0.0144, the THE-AFS-RF model outperformed the others for the wireless application. Drawback is the Proposed NIDS struggles with data volume, lacks external validation.

A method for training artificial neurons to identify intrusions on WiFi networks using a bio-inspired optimization algorithm (BOA) [17] was proposed. The WiFi intrusion detection framework works better than any other method, therefore it might be considered a backup plan for protecting WiFi networks. Proposed WiFi intrusion detection faces challenges handling complex features, potential convergence issues in real-world scenarios.

A high-performing, low-complexity machine learning-based WiFi intrusion detection system (WiFi IDS) [18] was proposed. According to the results, it performs better than other classifiers and offers enhanced accuracy with 20% fewer test runs and 26 times shorter training times than XGBoost. One disadvantage of WiFi Intrusion Detection Systems (IDSs) is that they are susceptible to difficulties with outdated models and processing costs.

Although these techniques function better than those previously created, they have significant disadvantages, including data loss, privacy infringement, high service costs, hosting, and server issues. In this research, a unique proposed approach called WUADS has been offered to address the aforementioned shortcomings.

3. PROPOSED SYSTEM

In this section, a novel WUADS technique has been proposed to detect unauthorized access in the WiFi network. Initially, the Wi-Fi frames are collected from the AWID (Aegean Wi-Fi Intrusion Dataset) dataset. The features of Wi-Fi frame are extracted by using Principal Component Analysis (PCA). Finally, the Deep Belief Network (DBN) is employed for classified into authorized access and unauthorized access. WUADS is an anomaly-based Wi-Fi network detection system. By searching for the state machine, which encapsulates the normal behavior of the protocol through its state transitions, one can keep an eye on state transitions in the Wi-Fi protocol. WUADS mimics the WiFi protocol's typical behavior. The results of network experiments can vary depending on the protocol that is utilized. Each protocol may have quite different communication protocols, and there is a chance that the experiment's channel and bandwidth will not work as intended. 802.11n is the most widely used wireless communication standard in the real world. Figure 1 shows the overview of proposed WUADS methodology.

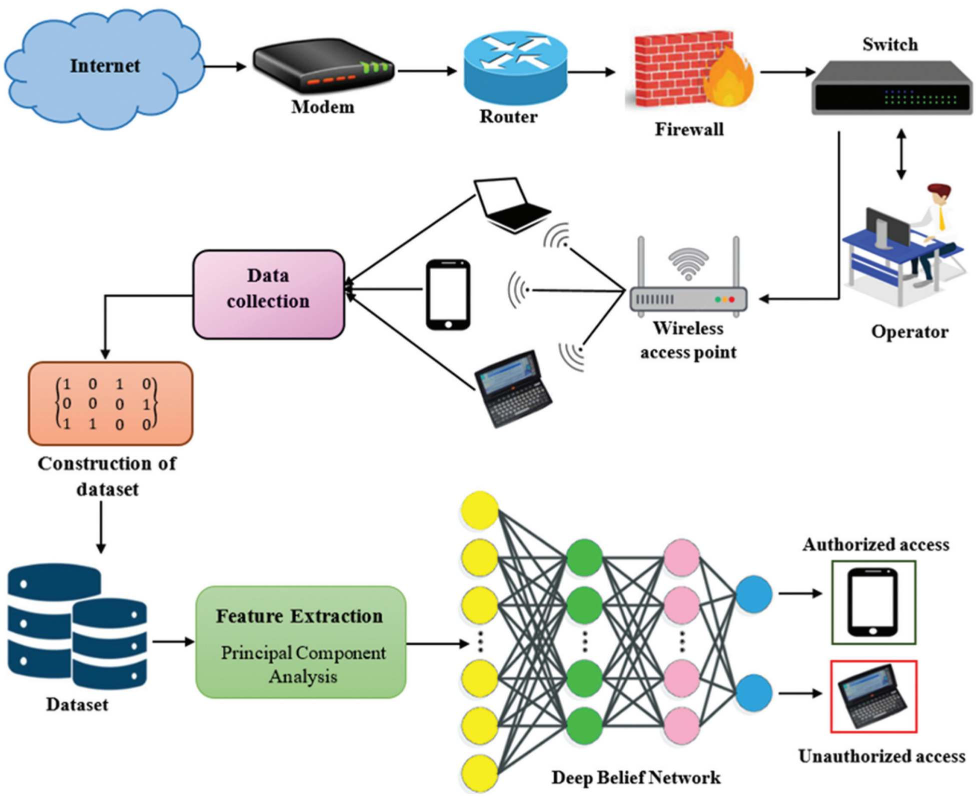

Fig. 1. An overview of proposed WUADS methodology

3.1. WORK FLOW OF WUADS METHODOLOGY

The proposed method's overview consists of a procedure for gathering and analyzing data. A variety of technologies, including computers, smartphones, tablets, the internet, modems, routers, firewalls, and switches, are used to gather data. After gathering the data, a dataset has been constructed. Principal component analysis is used to extract features from the dataset that the deep belief network can analyze. The authorization or unauthorizedness of data access is determined by the deep belief network. Either permitted or unauthorized access is the process's outcome.

3.2. DATASET COLLECTION

The dataset contains Wi-Fi activity that was captured over around five days and simulates a WUADS scenario. It has a desktop in monitor mode collecting frames, an access point, and Wi-Fi stations. One gadget invades the other. The dataset has four identified classes—three attack classes and one normal class—and provides multiple variations, including attack-specific and attack-class variants. The three types of assault are impersonation, flooding, and injection. 17 different Wi-Fi assaults are assigned to traffic records by the attack-specific version. We use the condensed attack-class form of the dataset, which is available in both big and smaller variants to accommodate varying processing capacities.

3.3. PRINCIPAL COMPONENT ANALYSIS (PCA)

In this section, describe the WiFi frames can be feature extraction process by using PCA [19]. It is a widely used technique to reduce the dimensions of features. When the feature space is complex, conventional PCA cannot produce effective results since it linearly lowers the dimensions. To enhance the feature reduction process generalizes standard PCA to nonlinear dimension reduction. A useful feature dimension reduction approach is PCA, which is applied after the features have been normalised. To lower the dimensionality of huge datasets, eigenvectors of the covariance matrix with the greatest eigenvalues are identified using dimensionality reduction techniques like PCA. PCA algebraic definition is as follows:

Calculate the mean of B for data framework B as follows:

$$\mu = E(B) \tag{1}$$

Determine B's covariance as follows:

$$CU = C_{ov}(B) = E[(B-\mu)(B-\mu)^T \tag{2}$$

Count the eigenvalue λ_j, and eigenvector $a_1, a_2, \ldots a_N$, j= 1, 2…N of the covariance CV. The equation is solved for the Covariance CV;

$$W_k = \frac{\sum_{j=1}^{K} \lambda_n}{\sum_{j=1}^{M} \lambda_n} \tag{4}$$

The mutual range should be 83% greater than the size of the major segments, therefore choose the first K eigenvalue that did this, information about a more compact measurement subspace,

$$P = W^t - Y \tag{5}$$

Where Y is the original data that was knotted, and t denotes the transfer matrix. Operating the main K eigenvector independently from n to K ($K \ll n$).) increases the number of variables or measurements. The Wi-Fi network packets contain the attributes listed in Table 1.

$$|\lambda l - CV| = 0 \tag{6}$$

Whereas, l give the identity matrix credit for having dimensions that resembles CV. Decide on the λ_n Eigenvalues of the component K by counting the proportion of the data that the first component accounts for. The weight matrix W_k, whose columns are $B_T B$ eigenvalues, is established as follows:

Table 1. Initial feature set from dataset

Sl.No	Features	Description
1.	frame_epoch_time	Epoch time
2.	IP Add 1	Mac add 1
3.	IP Add 2	Mac add 2
4.	frame_type	Frame type
5.	frame_subtype	Framesubtype

To extract the frame epoch time from an unprocessed Wi-Fi frame, which represents the moment that the network device first noticed the frame, 1 and 2 addresses. The address frame type and frame variation can be found in two different places in a Wi-Fi frame. Using a set of frame source and frame destination addresses, we divide the Wi-Fi data into flows or sessions with a time interval of "t seconds". Depending on the type of Wi-Fi frame and how the Wi-Fi protocol is implemented, we can use the first four Wi-Fi addresses to determine the source and target Wi-Fi addresses.

3.4. DEEP BELIEF NETWORK (DBN)

WiFi frames may be divided between authorized and unauthorised access using the Deep Belief network. This network is referred from [20-22]. The DBN, which is able to extract the deep characteristics of the original data, is created by superimposing Boltzmann finite devices on a number of layers. The DBN's goal is to raise the likelihood of training data. Architecture of DBM shown in Fig. 2.

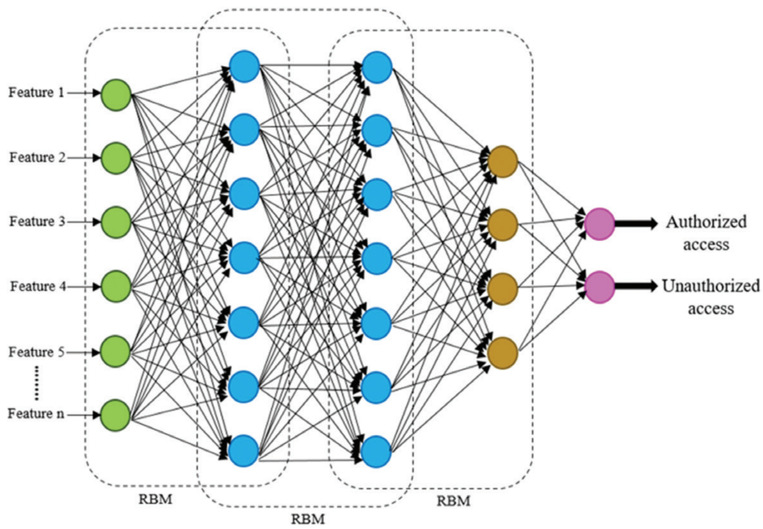

Fig. 2. Architecture of DBN

The DBN inputs are first sent to a low-level Restricted Boltzmann machine (RBM), which then begins the training process. After training the DBN outputs-containing top level RBM, the training process proceeds gradually up the hierarchy. Application of the energy function comprises:

$$\rho(L_x, L_y) = F_p^{-1} * e^{-F(L_x, L_y)} \quad (6)$$

Where L_{xj} and L_{xk} stand for the binary states of the hidden unit k and the visible unit j, respectively, and F_p designates the partition function created by combining probable pairings of exposed and hidden units,

$$F_p = \sum_{L_x, L_y} e^{-F(L_x, L_y)} \quad (7)$$

The following formula is used to get the energy of the entire hidden and visible unit configuration.

$$F(L_x, L_y) = -\sum_{j=1} b_j L_{xj} - \sum_{k=1} c_k L_{yk} - \sum_{j,k} L_{xj} L_{yk} Z_{jk} \quad (8)$$

Where Z_{jk} stands for the ratio of visible to hidden units, and b_j and c_k refer to the overt and covert unit biases, respectively. Updating the RBM weight requires:

$$\Delta Z_{j,k} = F_t\left(L_{xj} L_{yk}\right) - F_m\left(L_{xj} L_{yk}\right) \quad (9)$$

Where $F_t\,(L_{xj}\,L_{yk})$ and F_m=$(L_{xj}\,L_{yk})$ represent the expectations of the model and the training set, respectively. Ultimately, WiFi frames are categorized into allowed and unauthorized access using a DBN.

4. RESULT AND DISCUSSION

In this section, the experimental arrangement of the suggested WUADS was implemented using MATLAB to detect authorized and unauthorized access. Accuracy, precision, recall and specificity, are the different metrics used to evaluate it.

4.1. PERFORMANCE ANALYSIS

The following statistical metrics, including precision, specificity, F1 score, recall, and accuracy, are used to evaluate the success of the classification technique.

$$Accuracy = \frac{TP+TN}{TP+TN+FP+FN} \quad (10)$$

$$Precision = \frac{TP}{TP+FP} \quad (11)$$

$$Recall = \frac{TP}{TP+TN} \quad (12)$$

$$Specificity = \frac{TN}{TN+FP} \quad (13)$$

$$F1\ score = 2\left(\frac{Precision*Recall}{Precision+Recall}\right) \quad (14)$$

Where *TP, FP* stands for the true and false of the sample and *TN, FN* stands for the true and false negatives.

Table 2 displays the classification of various WiFi security classes in relation to specific factors. the suggested WUADS's average accuracy, F1score, precision, recall, and specificity with the given parameters. The suggested WUADS have an average accuracy of 99.49% and 99.56%, respectively. Presentation scrutiny of the proposed model shown in Fig. 3.

Table 2. Performance Analysis of the proposed model

Class	Accuracy	Specificity	Precision	Recall	F1 Score
Authorized	99.49	95.56	89.25	85.97	88.89
Unauthorize	99.56	96.25	90.31	86.69	88.75

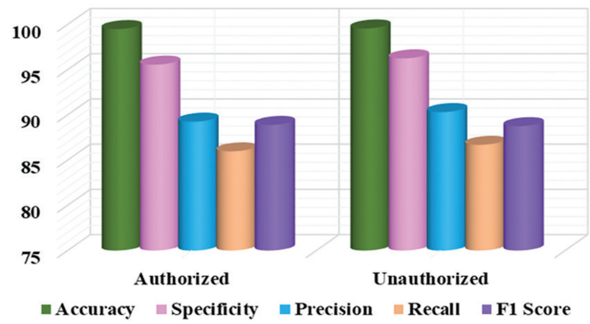

Fig. 3. Performance analysis of the proposed model

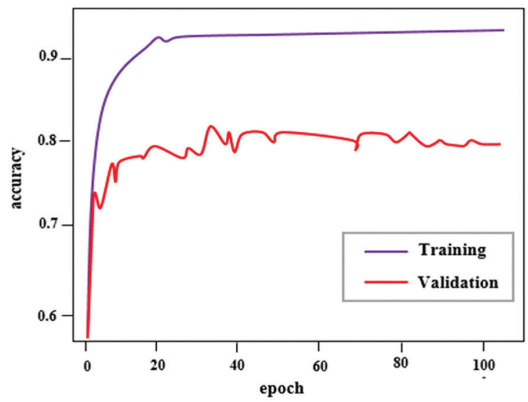

Fig. 4. Accuracy of proposed approach training and testing

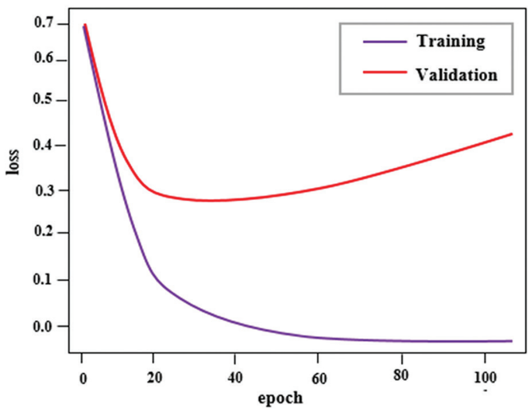

Fig. 5. Loss of proposed approach in training and testing

Figures 4 and 5 show how the recommended method has produced excellent accuracy throughout both training and testing. Performance is determined by accuracy, specificity, precision, recall, and the F1 score, and the proposed model's accuracy is 99.52%.

4.2. COMPARISON ANALYSIS

The proposed model and the current deep learning models are compared and analysed in this section. Precision, specificity, recall, accuracy, and F1 score were castoff to assess the presentation of current approaches in order to prove that the recommended strategy's outcome is more successful. Table. 3 compares the proposed model to CNN, RNN, ANN, and DBN, four types of machines learning neural networks.

Table 3. comparison between the suggested model to current deep learning networks.

Network	Success Rate (%)	Detection Time (sn)
CNN	70.5	710
RNN	74.8	736
ANN	85.4	787
Proposed(DBN)	92.9	863

From Table 3 compares the various algorithms such as CNN, RNN, ANN, DBN and it determined the unauthorized access at the highest rate and in the shortest time. It would be instructive to also list in Table 4 the corresponding optimal scores by the other deep learning algorithms. And it clearly indicates that the proposed DBN achieved better result than other algorithms. Successive rate of prevailing deep learning networks and the proposed model shown in Fig. 6.

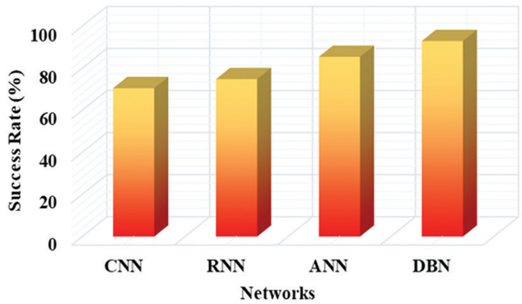

Fig. 6. Successive rate of existing deep learning networks and the proposed model

Fig. 6 illustrate, the successive rate of existing deep learning networks and the suggested technique. It clearly shows the proposed WUADS method has high success rate compare to deep learning techniques like CNN, RNN, and ANN.

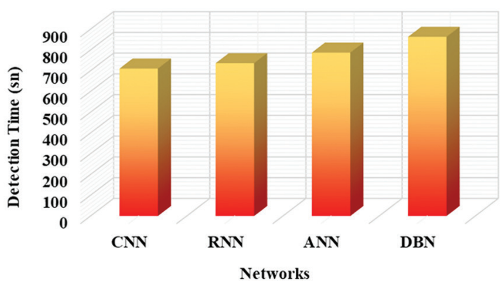

Fig. 7. Detection time of existing deep learning networks and the proposed model

The typical time required to spot one assault is shown in Fig. 7. The proposed WUADS outperforms CNN, RNN, and ANN by roughly 75% and has the shortest attack detection time when compared to existing methods.

Table 4. Comparison of the current and suggested models

Authors	Methods	Accuracy
Wang et al. [11]	SAE	98.4%
Reyes et al. [13]	WNIDS	99.42%
Ren et al. [14]	3D-ID	85.3%
Proposed	WUADS	99.52%

From Table 4 the proposed WUADS progresses the inclusive accurateness better than 1.12%, 0.1%, 14.22% Wang et al. [11], Reyes et al. [13], and Ren et al. [14]. The various recommended techniques are contrasted in Table 4. The data clearly demonstrates that the average accuracy value is 99.52%, meaning that the classifier used in the feature extraction and classification approach provides a higher accuracy number.

An extensive comparison of accuracy amongst extensive approaches is shown in Fig. 8, Sharp differences demonstrate proposed WUADS better performance and demonstrate how well it works to produce accurate results when compared to other models. The proposed WUADS improves the overall accuracy of 1.12%, 0.1%, 14.22% than existing SAE, WNIDS, 3D-ID correspondingly.

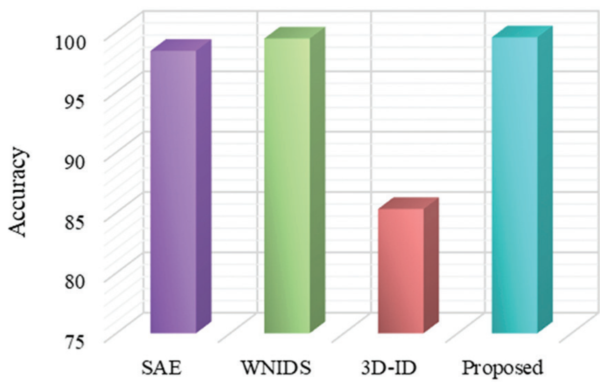

Fig. 8. Comparison in terms of Accuracy

5. CONCLUSION

In this paper, a novel WiFi Unauthorized Access Detection System (WUADS) technique has been proposed to detect unauthorized access in the WiFi network.The AWID dataset is where the Wi-Fi frames are first gathered. PCA is used to extract the Wi-Fi frame's features. Lastly, approved and illegal access are classified using the DBN. The efficacy of the suggested WUADS technique was evaluated based on variables such as detection rate, F1score, precision, accuracy, and recall. The suggested WUADS technique's performance analysis yields an overall accuracy range of 99.52%. Comparing the suggested WUADS method against deep learning techniques such as CNN, RNN, and ANN, it has the fastest attack detection time and a high success rate.

Comparative examination of the SAE, WNIDS, and 3D-ID shows that the proposed WUADS improves overall accuracy by 1.12%, 0.1%, and 14.22%, respectively. Although proposed WUADS provides a solid solution, it has several drawbacks, such as dataset dependence and possible noise in the feature extraction process the future work will be to integrate user authentication procedures to DBN-based detection, resulting in a multi-layered security strategy that blends machine learning and conventional techniques.

6. REFERENCES

[1] W. A. Jabbar, T. K. Kian, R. M. Ramli, S. N. Zubir, N. S. Zamrizaman, M. Balfaqih, V. Shepelev, S. Alharbi, "Design and fabrication of smart home with internet of things enabled automation system", IEEE Access, Vol. 7, 2019, pp. 144059-144074.

[2] J. B. Sequeiros, F. T. Chimuco, M. G. Samaila, M. M. Freire, P. R. Inácio, "Attack and system modeling applied to IoT, cloud, and mobile ecosystems: Embedding security by design," ACM Computing Surveys, Vol. 53, No. 2, 2020, pp.1-32.

[3] A. E. Omolara, A. Alabdulatif, O. I. Abiodun, M. Alawida, A. Alabdulatif, H. Arshad, "The internet of things security: A survey encompassing unexplored areas and new insights", Computers & Security, Vol. 112, 2022, p. 102494.

[4] S. Das, E. Mao, "The global energy footprint of information and communication technology electronics in connected Internet-of-Things devices", Sustainable Energy, Grids and Networks, Vol. 24, 2020, p. 100408.

[5] N. Sidek, N. A. Ali, G. Alkawsi, "An Integrated Success Model of Internet of Things (IoT)-Based Services in Facilities Management for Public Sector", Sensors, Vol. 22, No. 9, 2022, p. 3207.

[6] X. Fu, G. Fortino, W. Li, P. Pace, Y. Yang, "WSNs-assisted opportunistic network for low-latency message forwarding in sparse settings", Future Generation Computer Systems, Vol. 91, 2019, pp. 223-237.

[7] J. Hua, N. Shunwuritu, "Research on term extraction technology in computer field based on wireless network technology", Microprocessors and Microsystems, Vol. 80, 2021, p. 103336.

[8] T. De Schepper, J. Famaey, S. Latré, "Multi-technology management of heterogeneous wireless networks", Proceedings of the IEEE/IFIP Network Operations and Management Symposium, Budapest, Hungary, 20-24 April 2020, pp. 1-6.

[9] M. Tao, Z. A. Bhuiyan, A. Rahman, G. Wang, T. Wang, M. Ahmed, J. Li, "Economic perspective analysis of protecting big data security and privacy", Future Generation Computer Systems, Vol. 98, 2019, pp. 660-671.

[10] Q. Jiang, X. Huang, N. Zhang, K. Zhang, X. Ma, J. Ma, "Shake to communicate: Secure handshake acceleration-based pairing mechanism for wrist worn devices", IEEE Internet of Things Journal, Vol. 6, No. 3, 2019, pp. 5618-5630.

[11] S. Wang, B. Li, M. Yang, Z. Yan, "Intrusion detection for WiFi network: A deep learning approach", Proceedings of Wireless Internet: 11th EAI International Conference, Taipei, Taiwan, 15-16 October 2018, pp. 95-104.

[12] P. Shrivastava, P. Agarwal, "WiFi Data Leakage Detection", IOP Conference Series: Materials Science and Engineering, Vol. 804, No. 1, 2020, p. 12042.

[13] A. Reyes, D. F. Vaca, G. A. Castro Aguayo, Q. Niyaz, V. Devabhaktuni, "A machine learning based two-stage Wi-Fi network intrusion detection system," Electronics, Vol. 9, No. 10, 2020, p. 1689.

[14] Y. Ren, J. Yang, "Robust Person Identification: A WiFi Vision-based Approach", arXiv:2210.00127, 2022.

[15] M. Cominelli, F. Gringoli, R. L. Cigno, "AntiSense: Standard-compliant CSI obfuscation against unauthorized Wi-Fi sensing", Computer Communications, Vol. 185, 2022, pp. 92-103.

[16] A. K. Mananayaka, S. S. Chung, "Network Intrusion Detection with Two-Phased Hybrid Ensemble Learning and Automatic Feature Selection", IEEE Access, Vol. 11, 2023, pp. 45154-45167.

[17] L. Narengbam, S. Dey, "WiFi Intrusion Detection using Artificial Neurons with Bio-inspired Optimization Algorithm", Procedia Computer Science, Vol. 218, 2023, pp. 1238-1246.

[18] A. A. Bhutta, A. N. Mian, "Lightweight real-time WiFi-based intrusion detection system using LightGBM", Wireless Networks, 2023, pp. 1-13.

[19] S. Ayesha, M. K. Hanif, R. Talib, "Overview and comparative study of dimensionality reduction techniques for high dimensional data", Information Fusion, Vol. 59, 2020, pp. 44-58.

[20] Agasthian, R. Pamula, Kumaraswamidhas, "Integration of monitoring and security based deep learning network for wind turbine system", International Journal of System Design and Computing, Vol. 1, No. 1, 2023, pp. 11-17.

[21] X. Sun, G. Wang, L. Xu, H. Yuan, N. Yousefi, "Optimal estimation of the PEM fuel cells applying deep belief network optimized by improved archimedes optimization algorithm", Energy, Vol. 237, 2021, p. 121532.

[22] P. G. Sreelekshmi, M. B. Priya, V. Vishu, "Deep Forgery Detect: Enhancing Social Media Security Through Deep Learning-based Forgery Detection", International Journal of Data Science and Artificial Intelligence, Vol. 1, No. 1, 2023, pp. 9-19.

Increasing Efficiency and Reliability in Multicast Routing based V2V Communication for Direction-Aware Cooperative Collision Avoidance

Original Scientific Paper

Lekshmi V.
Department of Computer Science and Engineering,
Noorul Islam, Centre for Higher Education,
Thackalay, Tamil Nadu, India
lekshmi123v@outlook.com

Suji Pramila. R
Department of Computer Science and Engineering,
Mar Baselios Institute of Technology and Science,
Kerala, India
sujipramila88r@gmail.com

Abstract – *Mobile ad hoc networks (MANETs), which are a promising method for the intelligent transportation system, include vehicular ad hoc networks (VANETs) (ITS). Developing reliable and strong cooperative collision avoidance (CCA) strategy to mitigate the growing number of road fatalities each year is one of the main difficulties facing vehicular ad hoc networks (VANETs).A proper and successful routing method aids in the successful expansion of vehicular ad hoc networks. This study explains the architecture, interface layers, safety features, and implementation of a novel priority-based direction-aware collision avoidance system (P-DVCA). It distinguishes our study in the collision area of VANETs by accounting for realistic bi-directional traffic. The scheme begins with the development of dynamic clusters, which is difficult because of the bi-directional diverse traffic and the need to avoid collisions within and between clusters. The target node is sent an early warning message that includes the safe speed and the likelihood of a collision in order to notify it of an impending danger. To determine the least expensive, shortest one with the fewest hops between the source and the endpoint. A crucial problem with VANETs is the transmission of data from a source node to the base station. Cross-layer issues must be solved for a robust and stable collision avoidance programme to function properly in a VANET communication architecture. The results of the simulation show that the suggested scheme significantly outperforms CCM and C-RACCA in terms of cluster stability, fewer collisions, low latency, and low communication overhead. According to the findings, P-DVCA offers stable clustering, minimises network congestion, and lowers communication overhead and latency.*

***Keywords**:* *Vehicular ad hoc networks, Intelligent transportation system, Collision avoidance, Direction-Aware Vehicular Collision Avoidance*

1. INTRODUCTION

The term "vehicular ad hoc network" (VANET) refers to a subclass of mobile ad hoc networks made up of mobile nodes made up of automobiles with wireless transceivers known as OBUs (On Board Units) that may collect, compute, receive, and broadcast data to other nodes [1]. In VANETs, each vehicle has the capacity to transmit data either directly to an external base station known as a Road Side Unit (RSU) through vehicle to infrastructure communication or between vehicles via vehicle-vehicle communication (V2V) (V2I) [2, 3]. It is necessary to deal with diverse information, such as traffic, roads, automobiles, and so on, in order to realise intelligent transportation [4]. Sharing information is crucial for preventing accidents, reducing traffic, and enhancing driving. In order to reduce traffic accidents, cooperative collision avoidance (CCA) methods assess impact rates between nodes on occasion and include the results in alert texts along with the appropriate preventive measures [5]. But in order to achieve effective collision avoidance in a CCA application, several issues need to be resolved at every level of the VANET communication architecture [6]. As a result, application layer collision probability computations are erroneous [7]. Furthermore, the performance of the current application layer protocols is negatively impacted by their reliance on preset decelerations as preventive measures [8]. Due to their large computational and communication overheads and unencrypted transmission of warning messages, the current security services layer architectures jeopardise message confidentiality [9]. Furthermore, it is discovered that the current VANET architectures are unable to handle the regular topological changes on bi-directional roads while routing warning messages [10]. One further significant drawback of the current VANET architectures is the unprioritized sending of warning messages at the MAC layer.

Problem Statement

It is found that existing VANET communication designs do not have a specific direction-aware communication architecture designed to reduce collisions on bi-directional roads. Furthermore, the collision prediction procedure is negatively impacted by the current architectures' failure to account for the direction component.

Contribution

The following contributions are made by the priority-based direction-aware collision avoidance (P-DVCA) protocol that we suggest:

- Priority-based direction-aware Collision avoidance, a novel CCA method (P-DVCA). The project uses a clustered environment and a V2V communication mechanism in a pure ad hoc architecture.
- As far as we are aware, P-DVCA is the first of its type to handle the more difficult and realistic highly dynamic heterogeneous bi-directional traffic scenarios in the collision avoidance domain of VANETs.
- Existing techniques, such as the collision computation model (CCM) in a unidirectional scenario and the cluster-based risk-aware CCA (C-RACCA). The existing technologies lack the ability to provide real-time bidirectional collision avoidance. However, we have proposed the priority-based direction-aware collision avoidance system (P-DVCA), which provides real-time bidirectional collision avoidance. The existing methods, CCM and C-RACCA, reduce the efficacy of CCA and delay in clock synchronization. The suggested P-DVCA results in a more dependable and efficient CCA by reducing network congestion when compared to the existing Methods.
- Results in quick clock synchronisation with a security service layer protocol protects the confidentiality of nodes, authenticates messages, and offers security for the delivery of secure alert notifications.
- A network layer protocol that, through greater channel utilisation, reduced communication overhead, and consideration of the orientations and relative positions of nodes, guarantees the timely and precise exchange of warning messages.
- The DCM suggested calculating the separation between the vehicles.

The remainder of the paper is structured as follows. Section 3 introduces the proposed method Experimental results and discussions are given in Section 4. Performance measures are in Section 5. Finally, conclusion and future work are presented in Section 6.

2. RELATED WORK

The performance and efficiency of VANET applications are major problems for transport systems these days, but these are usually related to the way messages are sent between the nodes. One of the primary issues is coming up with a better routing protocol for dynamic VANET systems [1].

Automobile clustering is a practical way to increase the network's scalability and connection stability. VANET features also impact the clustering's performance [2]. In addition to being impacted by the outside world, VANETs' communication efficiency is also more susceptible to malevolent attacks [3]. Message passing between neighboring base stations (BSs) and other multicast network functionalities are concentrated into the layer-2 of the BSs protocol stack in the proposed approach [4].

To determine the course from the Modified Zone Multicasting Routing Protocol (MZMRP) technique has been used in this study work to route data from the source node to the destination node. In this multicasting strategy, the network's root nodes are selected for data routing [11].

In order to achieve energy-efficient communication, a metaheuristic algorithm, such as the Enhanced Dragonfly Algorithm (EDA), which optimizes the parameter as minimum energy consumption in VANET, is used to identify efficient nodes from each cluster [5]. Future research can go in a number of different areas. Situations involving particular assaults (Sybil, Blackhole) on the hybrid trust model and look into how different groups communicate with one another and how different hops interact after the revocation process [6]. The CCAV-OLC strategy enabled the AVs to cooperate with one another, significantly reducing the danger of collision. The investigation of the network's capacity and communication range demonstrated the effectiveness of 6GV2X connectivity [12]. Based on contrasts of calculation cost and clash probable under various conditions, the proposed CCAV-OLC technique has an accuracy of 94.12% and reduces collisions by 87.23 percent [7].

Fuzzy logic has been used to enhance inter-vehicle geo cast routing. The suggested protocol used LET and PAD parameters as fuzzy system inputs to choose the most reliable link and prevent packets from being rebroadcast throughout the geographical region [9]. The overhead of the network, repeating packets, and link failure between two cars are reduced by using a dependable link [13].

The framework consists of three levels: the simulation of the VANET network is the first, followed by the reliability- and geometry-based routing criteria at the second level, and the routing algorithm at the third [14]. In VANET, a unique distributed tree generation distributed multicast routing technique was presented. The multicast route developed a dependable tree structure [15]. First, we create a vehicle mobility model at the crossings to forecast the connection time between vehicles. Then, in order to determine the physical layer transmission rate, we create a theoretical model of V2V communication [8]. The proposed method takes the nodes' mobility and bandwidth when creating an overlay tree [10].

The fuzzy-based cooperative MAC and prioritized message distribution protocol (FPMDC-MAC) is created [16]. It includes a priority assignment technique that takes into account the message type, severity level, and movement direction to improve the delivery of emergency warning signals. An Emergency Message Broadcast Protocol (EMBP) is suggesting [17]. By using a suboptimal relay node selection technique, we may ensure broadcast reliability while still choosing the best relay node based on factors like channel fading, mobility, and directionality [18].

Suggest a method for fusion location [19]. This method uses a hierarchical optimization strategy to incorporate light intensity measurements, inertial navigation data, and geomagnetic data [20]. Numerous routing protocols, such as unicast, multicast, broadcast, etc., have been proposed in the literature that takes advantage of the topology of the network.

3. PROPOSED METHOD

The delivery of warning signals must be prioritised under CCA schemes since they are time-sensitive. Giving warning messages a higher priority than non-warning communications is a promising strategy in this regard. This has a negative impact on the transmission of collision-prone warning messages, especially in congested networks.

3.1. PRIORITY-BASED DIRECTION-AWARE COLLISION AVOIDANCE (P-DVCA)

This section outlines our suggested P-DVCA protocol for transmitting V2V warning messages on dual lanes. The P-DVCA methodology begins with clustering the nodes in order to improve node manageability and to limit the broadcast areas. The node clock synchronisation that is necessary for time slot reservation comes next. Here, we present a method for synchronising local clocks that consists of two phases: synchronizations between and within clusters of clusters. P-DVCA structure is shown in Fig. 1.

P-DVCA is a protocol family with application, security, network, MAC, and physical layer components. Layer-by-layer characteristics of the suggested P-DVCA architecture. Using our variation of the dragonfly-based clustering technique, which was first presented in, application layer P-DVCA begins with nodes' clustering. The security services layer is in charge of securely transmitting warning signals in order to handle such urgent situations. Since nodes often enter and exit each other's communication range, frequent path rebuilding processes are required. Our three-tier priority assignment approach is used to send vital warning signals at a higher priority when MAC layer warning messages are time-sensitive.

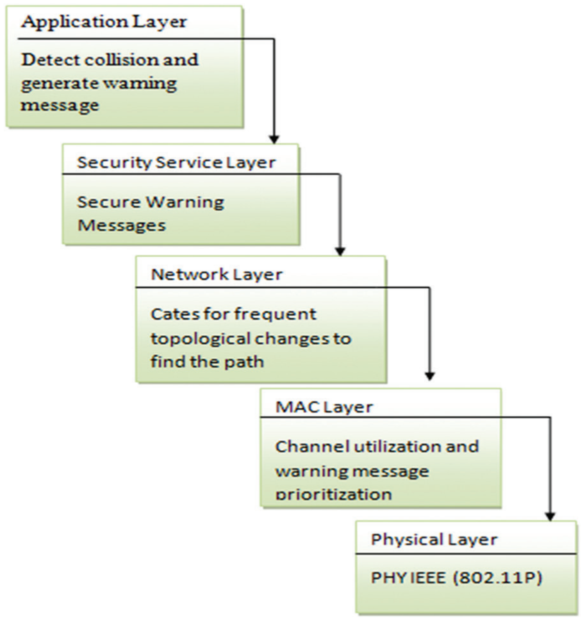

Fig. 1. P-DVCA structure

3.1.1. Application Layer

Our direction-aware CCA application is put into use by the P-DVCA application layer to specify preventive actions and identify potential collisions between nodes on bi-directional roads. The first metric, the Manhattan distance, determines the distance that exists between each neighbouring CH and an ideal node.

$$\eta = |X_1 - X_2| + |Y_1 - Y_2| \quad (1)$$

Where η Manhattan distance between the candidate node's coordinates (X_1-X_2) and (Y_1-Y_2), and the CHs is represented by the symbol. After calculating the Manhattan distance, the Hamming distance-which accounts for traffic flow in both directions is the second clustering metric.

$$k = \begin{cases} 1, & if\ \varphi = same \\ 0, & if\ \varphi = opposite \end{cases} \quad (2)$$

The importance of relying on the two indicators indicated above for node affiliation with clusters cannot be overstated. Assume that Node A is located 2 m from C2:CH and 3 m from C3: CH.

$$\delta = \frac{\eta}{K} \quad (3)$$

Where the separation (δ) between two neighbouring nodes is given. Eq. computes the distance to all surrounding CHs since P-DACCA only establishes an eligible node's link to a cluster when it is closest to the relevant CH. Where the separation (δ) between two neighbouring nodes is given. Eq. computes the distance to all surrounding CHs since P-DACCA only establishes an eligible node's link to a cluster when it is closest to the relevant CH.

3.1.2. Security service layer

When a malicious node intercepts a warning message meant to notify the target node to slow down in order to avoid a potential collision, it has the ability to either disregard the message or alter it in a way that will result in that collision. The security services layer is in charge of ensuring that warning signals are transmitted securely in order to overcome such dire circumstances.The security services layer is in charge of securely transmitting warning signals in order to handle such urgent situations. To do this, DVCA offers improved message authentication and node privacy preservation.

CH^i:

$$\beta_{CH^i} \leftarrow P_k \odot SID_{CH^i}$$

$$CH^i \ sends \ (\beta_{CH^i}||\tau) \ ton^i$$

n^i:

$$\beta_{n^i} \leftarrow P_k \odot SID_{n^i}$$

$$n^i \ sends \ (\beta_{n^i}||\tau) to \ CH^{\ i}$$

$CH^{\ i}$

$$CH^i \ generates \ key$$

$$key_i \leftarrow \beta_{n^i} \odot SID_{CH^i}$$

n^i:

$$n^i \ generates \ key$$

$$key_i \leftarrow \beta_{CH^i} \odot SID_{n^i}$$

Here, P_k stands for the public key, SID for a node's covert identity. The encrypted warning messages look like this.

Random generation of 1×4 matrix, Y

```
    For j=1 To 4
        Switch(Y(j))
Case 1:
            For x=1 To size(w) -1
            W(x)←w(x)⊕w(x+1)
            End For
            W←W⊕ Key_i
Case 2:
    W←Circular shift(W,C_s)
Case 3:
    Generate the random vector, rv
            w←w⊕rv
Case 4:
            Byte wise substitution operation
        End Switch
    End for
```

The warning message (W) that was obtained during the previously stated encryption process is then updated using the verification process hash that P-DVCA has generated.

$$\sigma_s = PID_s \odot PID_d \odot w \odot \tau \odot Key_i \quad (5)$$

In this case, PID stands for a node's public identification, which it uses to communicate with other nodes, and σ_s stands for the authentication hash created at the source node. To prevent blackhole attacks, a predetermined threshold is maintained that specifies how long warning messages should be retransmitted if the source nodes don't get any acknowledgements.

3.1.3. Network layer

Facilitating the prompt and dependable transmission of alert messages is the duty of the network layer. Due to high-speed nodes on bi-directional highways, VANETs frequently undergo topological modifications. Due to the frequent entry and exit of nodes inside each other's communication range, this causes frequent path rebuilding procedures. In addition to the distance parameter, P-DVCA adds two further parameters to account for these modifications. These parameters, which assist in determining the best appropriate path from the available set of paths, include the direction component and the relative positions of the source and destination nodes.VANETs frequently encounter topological changes. In order to deal with these changes, DVCA adds two more parameters in addition to the distance parameter. For a rear source node (S) with destination (D) having (S,) =1, the distance Δ between D and the subsequent hop (H) is calculated as

$$\Delta\ (D, H) = \frac{|H_x - D_x| + |H_y - D_y|}{k(S,H)} \quad (6)$$

In a case, where D remains rear to S, Δ is computed as

$$\Delta\ (D, H) = |H_x - D_x| + |H_y - D_y| k(S, H) \quad (7)$$

When S and D are travelling in opposing directions, D can be found using equation (6), and when they are travelling in the same direction, D can be found using formula (7). This type of direction-aware routing improves network performance. To ensure that warning messages are delivered on time, a direction-aware routing strategy optimizes network throughput by lowering packet drop rates and end-to-end delays. After that, the MAC layer receives the warning message from the network layer.

3.1.4. MAC Layer

P-DVCA synchronises clocks between and within clusters at the MAC layer. The effective completion of node clustering is followed by clock synchronisation. Nodes' familiar clocks are synchronised to a communal clock during the next two phases.

A. Syncing Clocks Across Clusters

The node's timer is regarded as synced and valid if $validate\_timer$ = 1. Conversely, if $validate\_timer$ = 0, no clock synchronisation is possible and the timer is still considered invalid by all other nodes in the network. Every node's admission to the highway requires clock synchronisation, which is why P-DVCA maintains the *validate_timer* default choice at 0.

The term "CH" refers to the collection of all CHs in the network that were chosen using the k-medoids algorithm. A CH is randomly selected from $\overline{CH}$ for this inter-cluster clock synchronisation, and is designated as "CH_B". The remaining CHs then follow the steps below to synchronise their local clocks with the CH_B shared clock. All reachable CHs respond to the clock synchronisation message (SyncCH) issued by CH_B.

B. Intra-Cluster Clock Synchronization

The method for synchronising clocks between and within clusters that has been proposed. Nodes can perform prioritised message dissemination after clock synchronisation; the process is described in more detail in the section below.

C. Prioritized Warning Message Dissemination

As illustrated in Table 1, there are three levels of warning messages: SL_0, SL_1, and SL_2. Here, SL_0 denotes the warning message with the lowest likelihood of collision, and SL_2 denotes the message with the highest likelihood of collision. When a warning message falls within the $SL0$ category, S waits for an $\daleth_s$ available, maintaining this warning message type's lowest priority. By raising the priority level, SL_1 allows S to request the release of a space that was previously filled by $\daleth_s$ warning message with a lower priority or a non-warning message. This guarantees the timely and accurate delivery of extremely important warning signals.

Table 1. Security level of warning message

Security level (SL)	SL Range	Limit of Probability of Impact (p_c)
SL_0	00	$0.00 < p_c \leq 0.33$
SL_1	01	$0.34 < p_c \leq 0.66$
SL_2	10	$0.67 < p_c \leq 1.00$
NW	11	$p_c = 0.00$

The algorithm requires the following inputs: S, D, R, $\propto_f$, -and W. R denotes the set of intermediary relay nodes$\propto_f$ denotes the set of free $\daleth_s$, and W denotes a alert message. The algorithm's output consists of the choice of B_f and the reserve of s to transmit W.

Algorithm 1:
Prioritized warning message dissemination

Input: S, D, R, $\propto_f$, and W
Output: B_f selection and time slot reservation for warning message dissemination
Begin:
Repeat
If $D \epsilon R$ Then
$S >> D$
Else
For i=1 **To** |size of(R)
$\mu_i \leftarrow |D_x - R_{i_x}| + |D_y - R_{iy}|$
$k_i \leftarrow H(R_i, D)$
If $H(S, D)$=1 Then
If S=Rear & D=Front node Then
$\delta_i \leftarrow \mu_i / k_i$
Else
$\delta_i \leftarrow \mu_i k_i$
End If
Else
IF S, D move towards each other **Then**
$\delta_i \leftarrow \mu_i / k_i$
Else
$\delta_i \leftarrow \mu_i k_i$
End If
End for
$B_f \leftarrow$Min(δ)
If $\propto_f = \emptyset$ Then
If $W[SN\_bit]$ = 1
$\ell \leftarrow W[severity\text{-}bits]$
Switch(ℓ)
Case:00
S waits for a free $\daleth_s$
Case: 01
S requests to release a $\daleth_s$
Case: 10
S releases $\daleth_s$ already reserved by
A warning message that is not a warning or of lesser priority.
End Switch
Else
S waits for a free $\daleth_s$
End If
Else
***S* reserver a** $\daleth_s$ from$\propto_f$
End if
Until B_f=D
End

3.2. DISTANCE CALCULATION METHOD (DCM)

To calculate the distance between two vehicles, the DCM applies the distance formula. The DCM assumes that every car in the network has a GPS facility. The distance equation found in Eq.

Using Eq. 8, determine the distance D between A and B.

$$D_{ij} = \sqrt{(X_2 - X_1)^2 + (Y_2 - Y_1)^2} \quad (8)$$

The distance between two cars is represented by the D_{ij}. Equation 9 illustrates D_{ij}'s structure.

$$D_{ij} = D(i, j), edge(i, j) \in R \quad (9)$$

where D_{ij} is the measure of the separation between the cars. A route between cars is represented by R. The '*i*' and '*j*'stand for edges on route R. A route is a grouping of edges. Vehicle B uses Eq. 8 to determine the precise distance between two vehicles whenever it gets a beacon message from vehicle A. The distance computation method used to determine how far apart two cars are is shown in Fig. 2. In order to respond to the beacon messages, both vehicles operated in a promiscuous manner. The beacon is created and broadcast by First A. Upon receiving a beacon, every vehicle changes its corresponding routing table. The receiver vehicle routing tables contain computed D's.

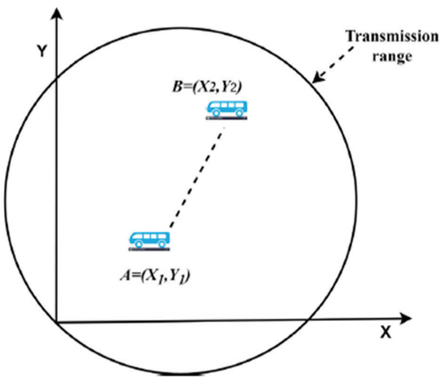

Fig. 2. Determining the separation between two cars

4. PERFORMANCE MEASURE

Comparing the performance of the suggested framework to the current plan allows for performance evaluation. The proposed approach is assessed in the simulator using the following performance metrics.

Packet Delivery Ratio (PDR):

This parameter shows the proportion between the total number of data packets generated during simulation and the total number of data packets received at the destination. The following Equation 3 can be used to calculate the Packet Delivery Ratio (PDR):

$$PDR = \frac{\sum_{ies} npacketReceived\ (i.d)}{\sum_{ies} npacketSent\ (i.s)} \quad (10)$$

Packet loss rate:

Calculated is the message loss rate (P_r).

$$P_r = \sum_{i=1}^{P_l} \frac{P_{l_i}}{P_t} \quad (11)$$

where P_{l_i} stands for a single message that is dropped and P_t stands for the total number of messages that were sent through the network. Choosing B_{fis} an important choice when transmitting warning messages.

End to End Delay:

The amount of time needed to transfer a packet from its source to its destination is known as the end-to-end delay (E2ED), and it may be calculated using Equation 10.

$$E2ED = 1/R \sum_{i=1...n} \sum_{j=1...ki} \left(r(Pij) - t(Pij)\right) \quad (12)$$

Throughput:

Routing protocols ought ideally to increase network performance since more data would be successfully routed via the network if they did.

$$\text{Throughput}=\frac{Number\ of\ received\ packets}{Total\ simulation\ time} * packet\ size \quad (13)$$

Routing overhead:

In order to make the message less stable for the recipient, extra bits are added to the packet containing the actual message at the MAC and physical layers. More data bits can be conveyed in a packet if the overhead is low since fewer bits are needed for information other than the actual data.

$$Overhead = \frac{totalPhybytes - totalAppBytes}{totalPhyBytes} \quad (14)$$

5. RESULT AND DISCUSSION

The simulation results are obtained using Python. Performance evaluation metrics include cluster stability, collision probability, packet destruction rate, packet delivery rate, complete delay, and throughput.

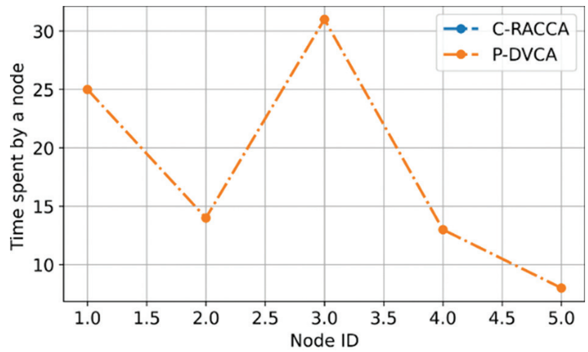

Fig. 3. Using C-RACCA and P-DVCA, node association to a cluster

Fig. 3. demonstrates the outcomes of P-DVCA and C-RACCA. Node 1 can be observed to spend the most of its time in C1. C-cluster RACCA's stability is hampered by this pointless cluster switch. In P-DACCA, the direction-aware clustering effectively corrects the aforementioned C-RACCA flaw. By maintaining constant relative speed, the effect of relative distance on collision is shown in Fig. 4.

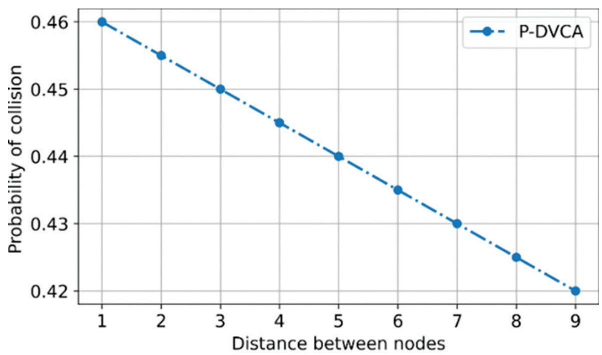

Fig. 4. By maintaining constant relative speed, the effect of relative distance on collision

Fig. 5 demonstrate a decrease in the likelihood of a collision as the distance between nodes grows, indicating that nodes are becoming safer at each stage.

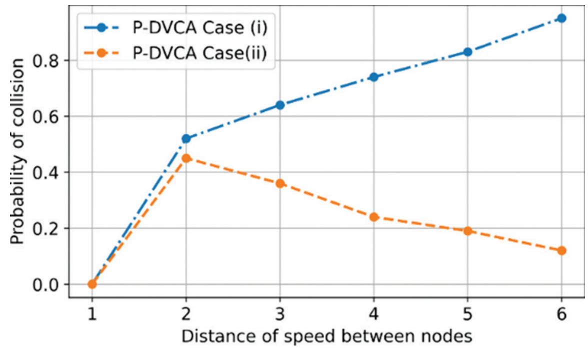

Fig. 5. Effect of relative speed on the likelihood of a collision given the expected state of the nodes and a constant relative distance

In scenario I the front node accelerates to a speed of 42 m/s and is followed by the rear node at a speed of 42 m/s. According to the results, the likelihood of a collision increases uniformly as the relative speed changes in relation to the front node's speed. This demonstrates the P-effectiveness DACCA's in estimating collision probabilities. When real-time nodes move along a highway, the distance also changes as the front node slows down. Although it is assumed that all of the individual occurrences occurring at various intervals are independent of one another, the relative distance is treated as constant in this simulation. Consequently, it shouldn't be mistaken for the front node's ongoing slowing. Similar to example I the rear node slows down by 4 m/s every time. The likelihood of a collision decreases when the rear node decelerates, in contrast to the front node. Each independent interval's estimated collision probability exhibits a linear decline. As a result, case (ii) also supports the usefulness of the suggested plan. Warning message generation is shown in Fig. 6.

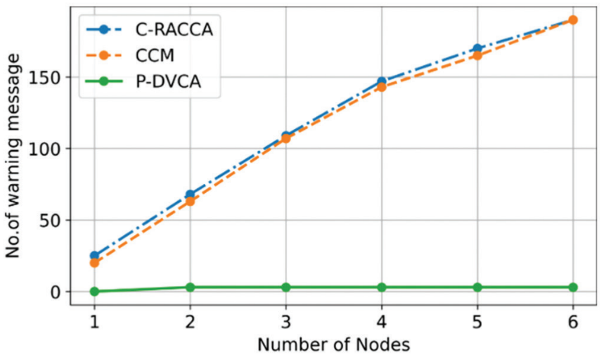

Fig. 6. warning message generation

P-DACCA, on the other hand, maintains the production rate constant regardless of the number of nodes. The extra communication overhead from these unnecessary warning messages contributes to network congestion, which reduces the effectiveness of CCA. P-DACCA creates a more reliable and efficient CCA by reducing network congestion.

In Fig. 7. it is quite clear that P-DVCA doesn't provide any pointless warning messages. For C-RACCA and CCM, on the other hand, the generation rate of pointless warning messages continues to be very high and grows exponentially as the number of nodes rises.

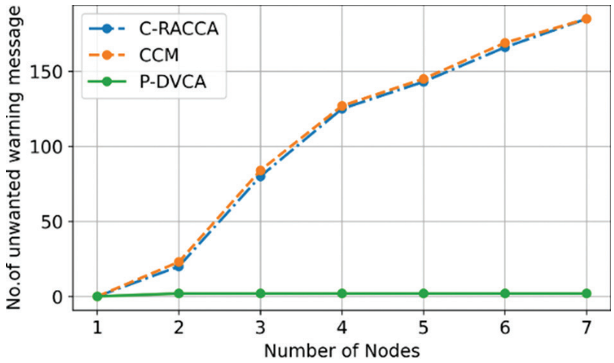

Fig. 7. creation of unwanted warning messages

The findings in Fig. 8 demonstrate the impact of an increase in hop count on warning message transmission latency. Due to the reduction in reaction time to implement preventative actions caused by the warning message transmission delay, the likelihood of accident increases.

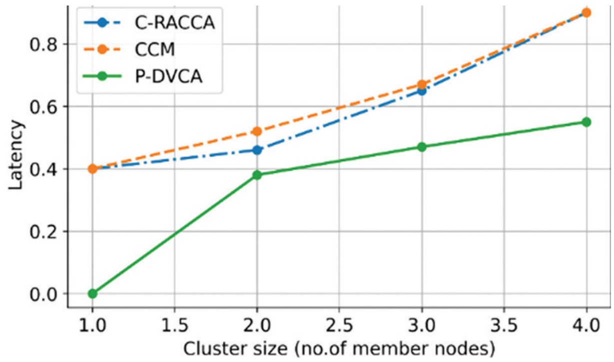

Fig. 8. Effect of hop count on warning message transmission latency

The number of $\daleth_s$ on the frame continues to be inversely correlated with the quantity of messages. As a result, each $\daleth_s$'s duration also changes or lengthens in accordance. This suggests that a higher network traffic load reduces the frame's $\daleth_s$ duration in P-DVCA, which increases end-to-end delay. Due to these factors, P-DVCA performs better than C-RACCA and CCM, as evidenced by the findings in Fig. 9 a. The findings in support the higher throughput achieved by P-DVCA when compared to C-RACCA and CCM thanks to our ground-breaking three-tier priority assignment method. In the outcomes reported in Fig. 9 b, P-DVCA also maintained its superiority over C-RACCA and CCM. When a relay node faces away from the destination node, the likelihood of a network partition rises, which ultimately leads to a higher rate of message loss. The findings shown in Fig. 9 c support this assertion. Fig. 9 d's findings reveal that P-DVCA has the least amount of communication overhead when compared to C-RACCA and CCM.

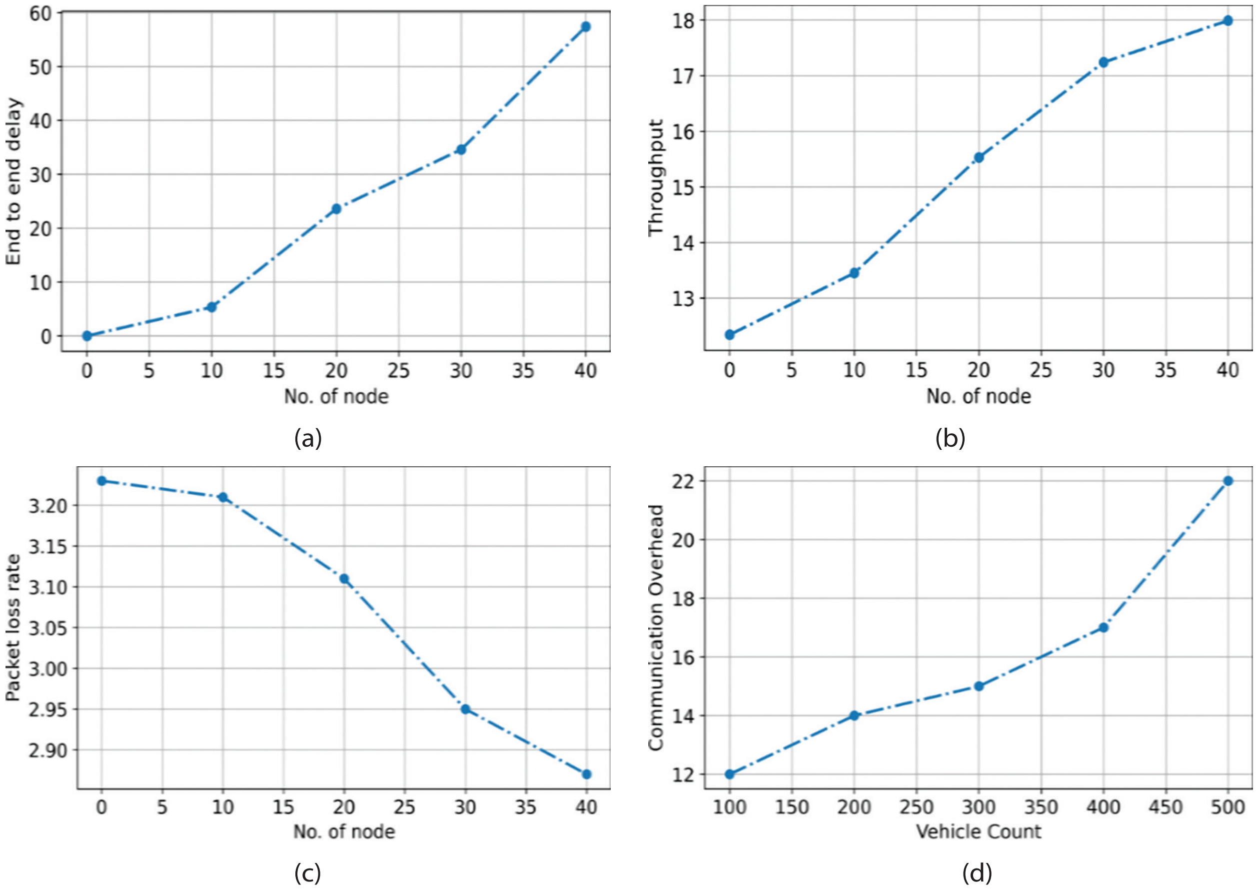

Fig. 9. Performance parameter of (a) End-to-End Delay, (b)Throughput, (c) Packet loss rate, (d) Communication overhead

6. CONCLUSION

P-DVCA offers a CCA scheme for bi-directional highways in an effort to close this gap. In an effort to provide a safe driving environment, it offers an effective method for reducing traffic accidents. P-DVCA is a clustered V2V technique that handles both intra- and inter-cluster collision avoidance utilising a pure ad hoc VANET architecture. To the best of our knowledge, bi-directional traffic has never before been present in the crash-avoidance region of the VANET. In order to guarantee the prompt and accurate delivery of alert texts, top billing allocation in P-DVCA in the message type, severity level, and direction component of nodes. the formation of steady clumps. After clustering, the nodes' anticipated states are calculated. Some projected states are used to determine the probability of a collision between every pair of connected units. In addition to threshold-based message distribution, the communication overhead is decreased by avoiding unnecessary warning messages. The findings demonstrate that P-DVCA offers reliable clustering, little network slack, decreased latency, and reduced communication overhead.

7. REFERENCES:

[1] E. Khoza, C. Tu, P. A. Owolawi, “An Ant Colony Hybrid Routing Protocol for VANET”, Proceedings of the International Conference on Intelligent and Innovative Computing Applications, Mon Tresor, Mauritius, 6-7 December 2018, pp. 1-6.

[2] M. K. Jabbar, H. Trabelsi, “Clustering Review in Vehicular Ad hoc Networks: Algorithms, Comparisons”, Challenges and Solutions. International Journal of Interactive Mobile Technologies, Vol. 16, No. 10, 2022.

[3] H. Xia, Z. San-shun, L. Ben-Xia, L. Li, C. Xiang-Guo, “Towards a Novel Trust-Based Multicast Routing for VANETs”, Security and Communication Networks, Vol. 2018, 2018.

[4] S. Roger, D. Martín-Sacristán, D. Garcia-Roger, J. F. Monserrat, P. Spapis, A. Kousaridas, A. Kaloxylos, “Low-latency layer-2-based multicast scheme for localized V2X communications”, IEEE Transactions on Intelligent Transportation Systems, Vol. 20, No. 8, 2018, pp. 2962-2975.

[5] M. Elhoseny, K. Shankar, “Energy efficient optimal routing for communication in VANETs via clustering model”, Emerging Technologies for Connected Internet of Vehicles and Intelligent Transportation System Networks, Vol. 242, Springer, 2020, pp. 1-14.

[6] H. Hasrouny, A. E. Samhat, C. Bassil, A. Laouiti, “A security solution for V2V communication within VANETs”, Proceedings of Wireless Days, Dubai, United Arab Emirates, 3-5 April 2018, pp. 181-183.

[7] A. Malathi, N. Sreenath, “Multicast routing selection for VANET using hybrid scatter search ABC algorithm”, Proceedings of the IEEE International Conference on Power, Control, Signals and Instrumentation Engineering, Chennai, India, 21-22 September 2017, pp. 441-446.

[8] X. Fan, Y. Lu, B. Liu, D. Liu, S. Wen, B. Fu, “High-integrity based cooperative file transmission at urban intersections using pure V2V communication”, Ad Hoc Networks, Vol. 122, 2021, p. 102612.

[9] A. Malathi, N. Sreenath, “Improved Shuffled Frog-Leaping Algorithm Based QoS Constrained Multicast Routing for Vanets”, Wireless Personal Communications, Vol. 103, 2018, pp. 2891-2907.

[10] P. K. Swetha, “An Improved Cluster based Multicasting Technique on Vehicular Adhoc Network”, Proceedings of the Second International Conference on Green Computing and Internet of Things, Bangalore, India, 16-18 August 2018, pp. 263-267.

[11] S. Ali, A. Chaudhary, H. Pasricha, “A novel modified zone multicasting routing protocol for path establishment in VANET”, International Journal of Computer Science and Network, Vol. 9, 2020, pp. 38-45.

[12] S. B. Prathiba, G. Raja, N. Kumar, “Intelligent cooperative collision avoidance at overtaking and lane changing maneuver in 6G-V2X communications”, IEEE Transactions on Vehicular Technology, Vol. 71, No. 1, 2021, pp. 112-122.

[13] E. Moridi, H. Barati, “Increasing efficiency and reliability in multicasting geographical routing based on Fuzzy Logic in VANETs”, Journal of Soft Computing and Information Technology, Vol. 12, No. 39, 2020, pp. 11-19.

[14] S. A. Rashid, M. Alhartomi, L. Audah, M. M. Hamdi, “Reliability-Aware Multi-Objective Optimization-Based Routing Protocol for VANETs Using Enhanced Gaussian Mutation Harmony Searching”, IEEE Access, Vol. 10, 2022, pp. 26613-26627.

[15] S. Babu, A. R. K. Parthiban, “DTMR: An adaptive distributed tree-based multicast routing protocol for vehicular networks”, Computer Standards & Interfaces, Vol. 79, 2022, p. 103551.

[16] M. Manoj, A. Ch Sudhir, “Fuzzy Based Prioritized Message Dissemination and Cooperative MAC Protocol for VANET", Wireless Personal Communications, Vol. 133, 2023, pp. 1175-1198.

[17] Z. Xiang, Y. Zhang, Y. Chen, Y. Ma, H. Cao, L. Tian, "Emergency message broadcasting scheme based on V2V and V2I", ITU Journal on Future and Evolving Technologies, Vol. 4, No. 4, 2023, pp. 549-561.

[18] M. Bilal, E. U. Munir, A. Ullah, "BEMD: Beacon-oriented Emergency Message Dissemination scheme for highways", Ad Hoc Networks, Vol. 142, 2023, p. 103095.

[19] Y. Han, X. Yu, P. Zhu, X. Xiao, M. Wei, S. Xie, "A Fusion Positioning Method for Indoor Geomagnetic/Light Intensity/Pedestrian Dead Reckoning Based on Dual-Layer Tent–Atom Search Optimization–Back Propagation", Sensors, Vol. 23, No. 18, 2023, p. 7929.

[20] M. Sohail, Z. Latif, S. Javed, S. Biswas, S. Ajmal, U. Iqbal, M. Raza, "Routing protocols in Vehicular Adhoc Networks (VANETs): A comprehensive survey", Internet of Things, Vol. 23, 2023, p. 100837.

PrioriNet: An Energy-Efficient Emergency Priority Protocol for Sustainable Communication in Disaster Scenarios

Original Scientific Paper

Krishnapriya M.
Department of Computer Science,
AJK College of Arts and Sciences,
Coimbatore, Tamil Nadu, India.
Krishnapriya.M12@outlook.com

Angeline Prasanna G.
Department of Computer Science,
AJK College of Arts and Sciences,
Coimbatore, Tamil Nadu, India.
angelineprasanna156g@gmail.com

Abstract *– During disaster scenarios, effective communication systems are essential for coordinating emergency response efforts and ensuring the safety of affected individuals. However, existing communication protocols often face challenges in providing reliable and efficient communication in these highly dynamic and resource-constrained environments. To overcome these challenges a novel energy-efficient emergency priority protocol namely PrioriNet technique which specifically tailored for urban earthquake scenarios. The protocol focuses on prioritizing the transmission of emergency data packets to ensure their prompt and reliable delivery, while appropriately managing normal data packets. The PrioriNet prioritizes the emergency messages as high and low priority messages and allocate them to energy efficient nodes efficiently. The experimental results indicates that the suggested protocol performs better than the existing LEACH technique in terms of energy consumption, network coverage, packet delivery ratio, and throughput. In emergency data scenarios, the LEACH protocol demonstrates throughputs between 0.3 Mbps and 1.2 Mbps, whereas the proposed method consistently outperforms the LEACH protocol with throughputs ranging from 0.7 Mbps to 1.8 Mbps respectively.*

Keywords*:* *PrioriNet, LEACH, earthquake, emergency priority protocol, energy, MATLAB*

1. INTRODUCTION

A natural disaster is an unforeseen and catastrophic event that can strike anywhere in the world, disrupting societies and causing significant loss of life, rationality, and economic impact [1]. In such dire situations, disaster management plays a crucial role in providing support to those at risk and managing emergencies efficiently [2]. To recover and improve communications in post-disaster scenarios, various technologies have been proposed to facilitate faster and more reliable communication [3]. Earthquakes, tsunamis, and storms are among the disasters that necessitate low-power operating systems and devices for the people in disaster places to communicate with the outside world for help. Rescue efforts by the rescue teams are prioritized using rescue urgency degrees (RUDs), which are based on the seismic intensity measured by the seismographs from the impacted locations [4]. RUD will demonstrate the reverse effects caused by the earthquake and the urgency level for rescuing the persons affected in the disaster zone. Therefore, for sharing emergency-related information among first responders and their supervisors, a robust, reactive, and energy-efficient routing protocol is crucial. Prioritizing limited resources becomes critical to saving lives and minimizing further damage [5-8]. Existing protocols, such as LEACH, partially address these limitations but fail to fully meet the specific requirements of disaster scenarios [9-10]. They lack efficient prioritization of emergency messages, leading to potential delays and compromised situational awareness. Additionally, energy resources are often inefficiently utilized, resulting in premature depletion of node energy and reduced network lifetime [11]. To overcome these limitations, a novel emergency priority protocol is proposed. The research contribution of this study has been outlined as follows:

- The proposed PrioriNet protocol effectively differentiates emergency and non-emergency data and ensures the prompt transmission of critical information. Priorities are assigned according to predefined criteria.
- The generated emergency calls are then received and processed by the PrioriNet, based on urgency levels, ensuring swift attention to critical information.
- The effectiveness of the proposed PrioriNet protocol has been assessed on the basis of network coverage, packet delivery ratio, energy consumption and throughput.

The remaining sections of the paper are organised as follows: The literature review is described in Section II. The proposed technique is described in Section III. The experimental results are described in Section IV, and the study concludes including some suggestions for further investigation in Section V.

2. LITERATURE REVIEW

To address the seamless mobilization of rescue teams for providing emergency services during disasters, various strategies have been explored in the existing literature. Among those, some of the literature has been reviewed in this section.

Araghipour and Mostafavi [11] proposed a new emergency routing protocol based on ERGID. To accomplish these objectives, a mechanism for prioritizing urgent data was created. Shreyas et al [12] proposed the Energy Efficient Emergency Response System (EEER). During emergencies, the suggested EEER efficiently and quickly distributes crucial data. Abdellatif et al. [13] suggested using IoT devices and LTE device-to-device ProSe (D2D ProSe) technology to create an effective emergency communication network during a disaster.

Campioni et al. [14] proposed a novel Aceso - Proof-of-Concept smart city middleware technique. It offers location- and context-aware services to completely support Humanitarian Assistance and Disaster Relief (HADR) operations. Zhao et al. [15] presented a directional-area-forwarding-based energy-efficient opportunistic routing (DEOR) approach for the post-disaster MioT. Mohammadiounotikandi et al. [16] proposed a hybrid nature-inspired optimization approach, Emperor Penguin Colony, and Particle Swarm Optimization (EPC-PSO). Tang et al. [17] proposed an optimal solution according to observable workloads and communication channel connectivity.

Olatinwo et al. [18] proposed a coordinated superframe duty cycle hybrid MAC (SDC-HYMAC) protocol to enhance energy efficiency and to prolong the devices' lifetime. Al-Hady et al. [19] proposed an IoT-based automated emergency response website that leverages IoT technology to gather real-time data from various sensors installed in the site and uses machine learning algorithms to predict and prevent potential fire incidents.

The reviewed literature has various advantages in prioritizing emergency messages during disasters, however, they possess some drawbacks which is given in Table 1.

Table 1. Comparison of existing techniques

Reference	Method	Result	Advantage	Disadvantage
Araghipour and Mostafavi [11]	emergency routing protocol based on ERGID	performs better than ERGID by 60% and 35%, for end-to-end time and packet loss rate respectively.	speeds up the transmission of emergency data	high complexity
J Shreyas et al. [12]	EEER	improvements in power consumption, packet delivery speed, and end-to-end latency of 5%, 6%, and 7%, respectively.	the suggested EEER efficiently and quickly distributes crucial data.	did not consider resource allocation
Abdellatif et al. [13]	D2D ProSe technology	significantly outperforms others suggested in the literature	effective communication during disaster	Very low throughput
Campioni et al. [14]	novel Aceso - Proof-of-Concept smart city middleware technique	Aceso's value in prioritizing the processing and routing of crucial information.	offers location- and context-aware services to support HADR operations	Less efficiency
Zhao et al. [15]	DEOR approach	outperforms existing methods in terms of energy consumption, and network lifetime	Less energy consumption	Limited capacity
Mohammadiounotikandi, et al. [16]	EPC-PSO	decreased the execution time and cost by 10.41% and 25% compared to other algorithms.	achieve a sustainable system and less energy consumption	Low scalability
Tang et al. [17]	cooperative learning-based solution	superior in terms of service quality and energy conservation in diverse environments	optimal solution according to observable communication channel connectivity	Higher delay
Olatinwoet al. [18]	SDC-HYMAC protocol	performed better convergence speed, energy efficiency, and devices' lifetime.	enhance energy efficiency and prolong the devices' lifetime	Deployment Cost is high
Al-Hady, S.M.Z., et al [19]	IoT-based automated emergency response website	reduce the impact of fire disasters by providing accurate and timely information.	machine learning algorithm for preventing potential fire incidents	Lower throughput

3. PRIORINET TECHNIQUE FOR URBAN EARTHQUAKE SCENARIOS

We have considered a scenario in a densely populated urban area, a devastating earthquake strikes, causing widespread destruction and chaos. For reliable communication, the energy-efficient PrioriNet protocol in emergency disaster situations is implemented in this section. These nodes can be wireless devices, such as sensors or communication devices, strategically placed to provide coverage and enable communication within the disaster-affected region. The overall block diagram of the proposed PrioriNet protocol is given in Fig. 1.

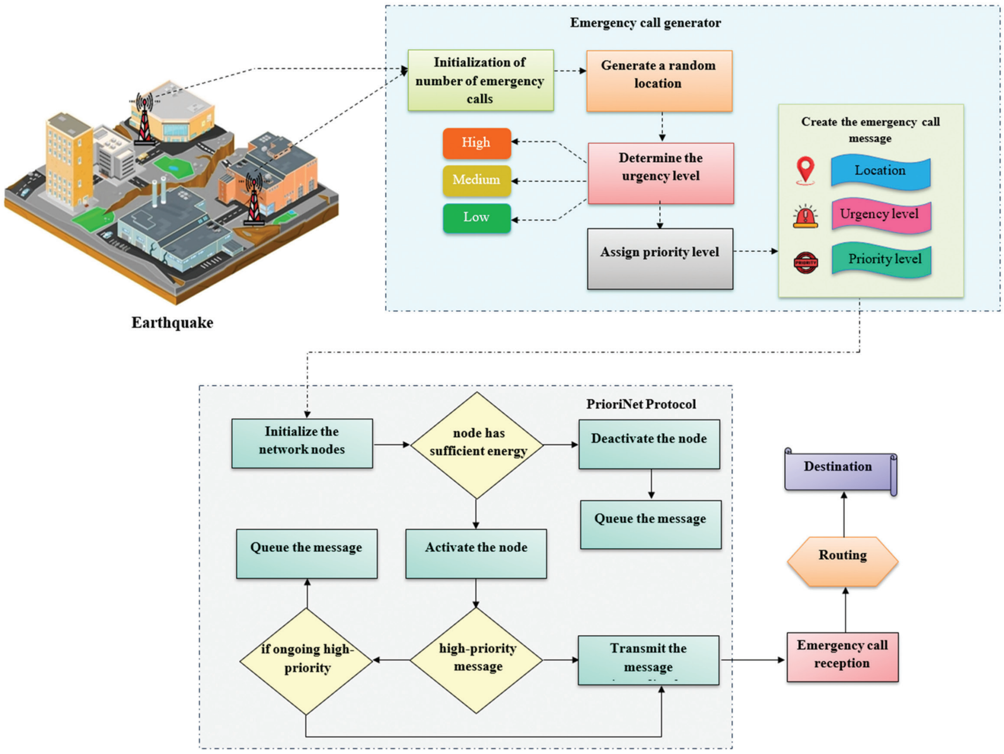

Fig. 1. Proposed PrioriNet technique

3.1. EMERGENCY CALL GENERATION

The process initiates with the generation of emergency calls, simulating distress signals from affected individuals or devices reflecting the urgent need for assistance, while the emergency call generator module simulates the generation of calls with varying urgency levels and assigns priorities based on predefined criteria vital signs of a person, the battery level, or the location. The algorithm 1 uses a loop to generate multiple emergency calls based on the specified number of calls (numCalls). Each call is assigned a random location, urgency level, and priority level. The generated emergency call messages are then queued for transmission based on higher priority calls that are given precedence.

Algorithm.1: On emergency call generation

1. Initialize the number of emergency calls to be generated (numCalls).
2. Set the loop counter (i) to 1.
3. Start the loop to generate emergency calls:
   a. Generate a random location within the affected area for the emergency call.
   b. Determine the urgency level for the emergency call (e.g., high, medium, low).
   c. Assign a priority level to the emergency call based on its urgency.
   d. Create the emergency call message with the location, urgency level, and priority level.
   e. Queue the emergency call message for transmission based on its priority.
   f. Increment the loop counter (i) by 1 and check if the loop counter (i) ≤ the number of emergency calls (numCalls).
   g. If true, repeat steps a-f.
4. End the loop.

3.2. ASSIGN PRIORITY LEVEL

The proposed protocol uses scheduling algorithm which considers both the priority of the data packet and the remaining level of energy of the sensor node, which can be formulated using the following equation:

$$S(i) = P(i) * E(i) \quad (1)$$

where $S(i)$ represents the scheduling score for data packet i, $P(i)$ and $E(i)$ denotes the priority assigned, remaining energy level to the packet i. In this equation, a higher $P(i)$ signifies the urgency and criticality of the data packet, while a higher $E(i)$ indicates the available energy resources of the transmitting node.

3.2.1. PrioriNet protocol

In PrioriNet, data packets providing critical details are all assigned to the higher priority queue, whereas packets containing regular sensed data are placed in the lower priority queue.

Algorithm.2: PrioriNet Protocol

1. Initialize the network nodes and their parameters.
2. Set simulation parameters, such as simulation time and message generation rate.
3. Start the simulation loop:
   a. Generate messages based on the specified rate.
   b. Determine the priority of each message based on its type and urgency.
   c. Check the network nodes for available energy:
      i. **if** a node has sufficient energy {
         // **Activate the node**
         Check the priority of the message:
            if it is a high-priority message {
               // **Handle high-priority message**
Transmit the message immediately.
Update energy consumption for the transmitted message.
            }
            else {
               // **Handle low-priority message**
Check if there is ongoing high-priority communication:
If yes, queue the message for later transmission.
If no, transmit the message immediately.
Update energy consumption for the transmitted message.
            }
         }
      ii. **if** a node has low energy or is unable to transmit {
         // **Deactivate the node to conserve energy**
         Queue the message for later transmission.
         }
   d. Update the energy levels of active nodes based on their transmission and reception activities.
   e. Repeat steps a-d until the simulation time is reached.
4. Calculate and display the performance metrics (e.g., energy consumption, message delivery ratio).

End

3.3. EMERGENCY CALL RECEPTION

During a disaster scenario, timely response to emergency calls is critical for effective disaster management and saving lives. Algorithm 3 optimizes resource allocation and energy consumption by activating nodes with sufficient energy and considering the urgency and priority levels of each call. By considering population density and building types, the protocol prioritizes areas with a higher concentration of people and critical infrastructure, ensuring a more targeted response. The features of PrioriNet are flexibility, adaptability, interagency collaboration and clear communication of prioritization. An effective emergency call protocol for earthquake scenarios integrates technology, prioritization criteria, and community engagement to ensure a rapid, targeted, and coordinated response.

Algorithm.3: On receiving an emergency call:

if (node's energy >= threshold_energy):
   Activate the node for emergency call processing.
   Determine the priority level of the emergency call.
   if (priority level is high):
      Allocate necessary resources for high-priority emergency call processing.
      Transmit an acknowledgement message to the sender.
   else if (priority level is medium or low):
      Check ongoing high-priority emergency calls.
      if (no ongoing high-priority calls):
         Allocate resources for medium or low-priority emergency call processing.
Queue the emergency call for processing.
      else:
Delay the processing of the emergency call until ongoing high-priority calls are completed.
      else:
Deactivate the node due to insufficient energy.
End

4. PERFORMANCE AND EVALUATION

To assess the efficiency of the developed emergency priority protocol a comprehensive simulation has been conducted in contrast to the well-known existing protocol, LEACH. LEACH has been chosen for comparison in the context of emergency priority protocols due to its widespread use and recognition. By comparing new protocols against LEACH, researchers and practitioners can assess the efficacy of proposed in the context of energy efficiency, scalability, and adaptability, providing valuable insights into the advancements made in addressing the challenges posed by emergency scenarios in these highly dynamic and resource-constrained environments.

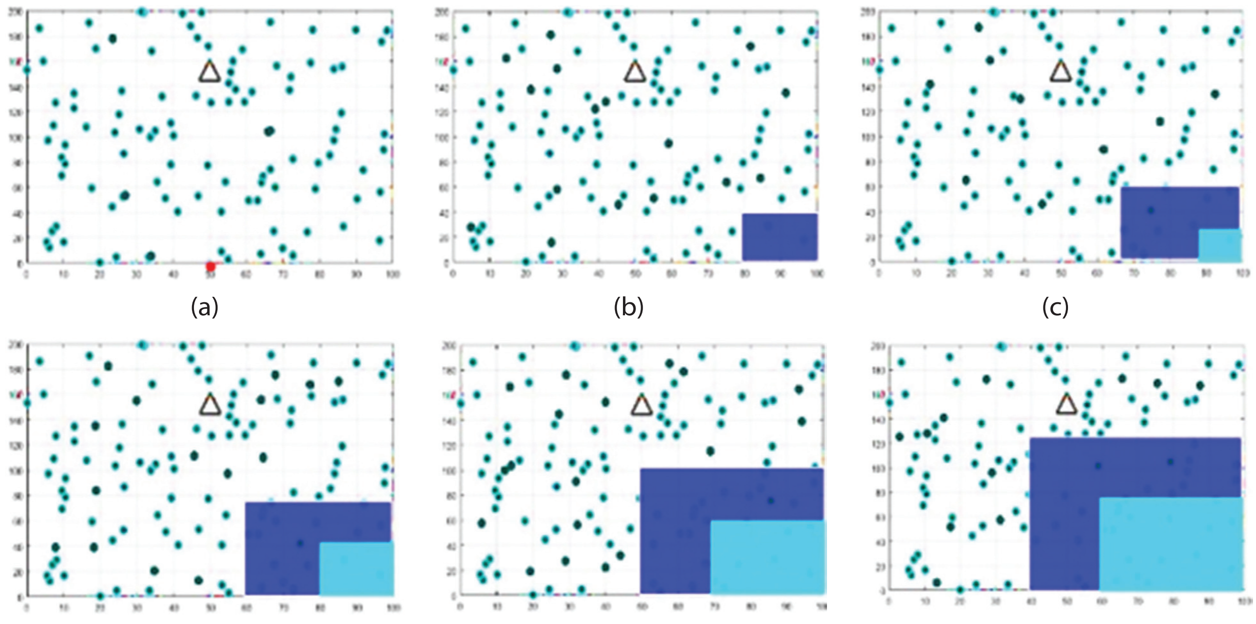

Fig. 2. Simulation scenarios: (**a**) with a certain number of nodes, representing the initial phase of the communication network. (**b**) As the disaster intensifies, resulting in potential damage and communication disruptions. (**c**) the escalation of the disaster's intensity and impact on communication. (**d**) the situation worsens, depicting the growing challenges in establishing effective communication. (**e**) the communication system faces critical failures and disruptions. (**f**) the disaster reaches its peak impact, resulting in a significant number of non-functional nodes and communication dead zones throughout the urban area.

4.1. SIMULATION SETUP

The simulation was conducted using MATLAB 2017a on a computer system with Windows 10 Enterprise-64bit as the operating system, an Intel Core i7 processor, and 8 GB of memory. Node movement is modeled using the Random Waypoint model, simulating realistic mobility patterns in situations of disaster. Table 2 presents the simulation parameters.

Table 2. Parameters for simulation

Parameter	Value
Size of Network	100
Size of Area	1000m * 1000m
Node Density	0.1 nodes/m^2
Mobility pattern	realistic mobility patterns
Communication Range	100m
Transmission Power	0.5 Watts
Initial Energy	1 Joule
Emergency Packet Size	1000 bytes
Normal Packet Size	500 bytes
Normal Transmission Rate	10 Kbps
Residual Energy Threshold	0.3 Joules
Simulation Time	3600 seconds
Traffic Pattern	Dynamic
Node Movement Model	Random Waypoint

To ensure the practicality and realism of our research, it is crucial that the simulation environment closely reflects the real-world situation.

Fig. 2 shows the simulation scenario that unfolds in different stages: (a) with a certain number of nodes, representing the initial phase of the communication network. (b) As the disaster intensifies, resulting in potential damage and communication disruptions. (c) the escalation of the disaster's intensity and impact on communication (d) the situation worsens, depicting the growing challenges in establishing effective communication; (e) the communication system faces critical failures and disruptions; (f) the disaster reaches its peak impact, resulting in a significant number of non-functional nodes and communication dead zones throughout the urban area.

4.2. PERFORMANCE METRICS

We concentrate on analyzing and contrasting a number of performance metrics in this phase of our research to determine the PrioriNet performs in disaster scenarios. The criteria for comparison and analysis include the following variables:

Energy Consumption

The amount of energy utilized by all of the network's sensor nodes during the simulation is measured as energy consumption which is given in equation 2.

$$EC=N\times (ET_{active} * P_{active} + ET_{sleep} * P\_sleep) \quad (2)$$

Where, N is the network's total number of nodes, ET_{active}, P_{active} is the energy consumed per unit time, percentage of time nodes spend in active mode, ET_{sleep}, P_{sleep} is the energy consumed and the percentage of time nodes spend in sleep mode.

Network Lifetime: A crucial metric to evaluate the sustainability and longevity of the network during the disaster scenario is Network lifetime.

Packet Delivery Ratio (PDR): The measure of proportion of packets that are successfully delivered to all of the packets that a source node has sent is known as PDR.

Network Throughput: Throughput refers to the amount of data successfully transmitted within a given time frame.

Network Coverage: Network coverage measures the extent of the network's geographical area that is effectively covered by sensor nodes.

4.3. COMPARISON ANALYSIS

A comparative evaluation is performed between the proposed model and the existing LEACH method to assess the performance of the proposed method.

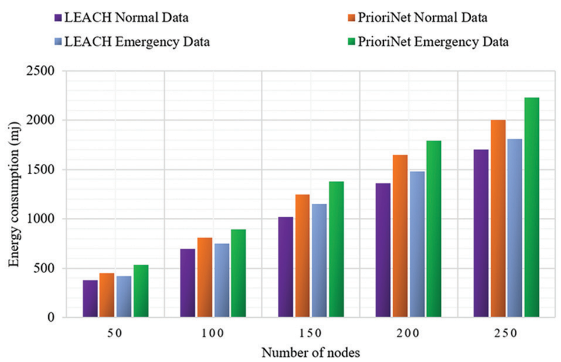

Fig. 3. Energy consumption vs Number of Nodes

Fig. 3 represents the energy consumption of the proposed PrioriNet protocol in comparison with the existing LEACH technique. In normal data scenarios, with increase in number of nodes, the LEACH protocol displays energy consumption ranging from 520 units to 2230 units, while the proposed method demonstrates lower energy consumption, ranging from 420 units to 1810 units. Similarly, for emergency data, the LEACH protocol's energy consumption varies between 450 units and 2000 units, whereas the proposed method consistently achieves reduced energy consumption, ranging from 380 units to 1700 units, even with increasing numbers of nodes.

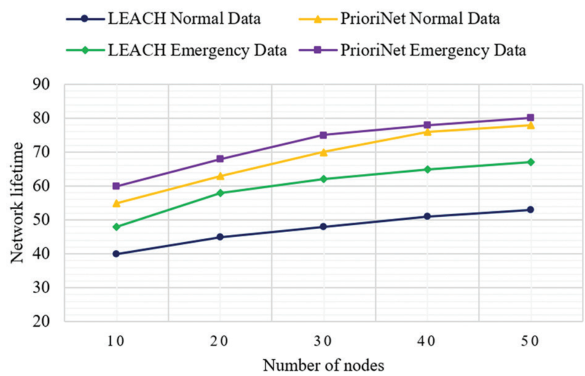

Fig. 4. Network Lifetime vs Energy Threshold

Fig. 4 represents the network lifetime of the proposed PrioriNet protocol in comparison with the existing LEACH technique. From fig. 4, it is observed that the proposed method consistently achieves longer network lifetimes compared to the LEACH protocol for both normal and emergency data scenarios. The proposed method outperforms the LEACH protocol in terms of network lifetimes, with durations ranging from 55 to 78 hours compared to LEACH's range of 40 to 53 hours. In emergency data scenarios, the PrioriNet consistently surpasses the efficiency of the LEACH protocol, exhibiting network lifetimes ranging from 60 to 80 hours.

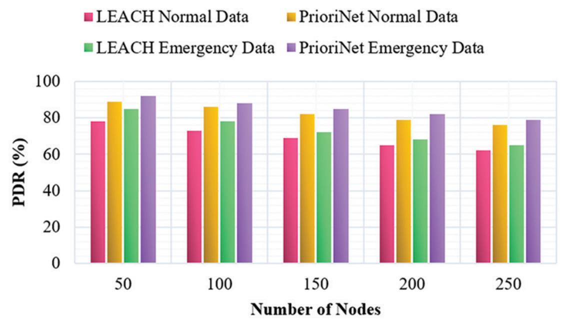

Fig. 5. PDR vs Number of Nodes

Fig. 5 represents the PDR of the proposed PrioriNet protocol in comparison with the existing LEACH technique. According to fig. 5, the proposed method consistently outperforms the LEACH protocol, achieving higher packet delivery ratios in both normal and emergency data scenarios. By assigning priorities to emergency messages and optimizing resource utilization, the proposed method ensures that critical information is given precedence, resulting in improved message delivery and overall system performance. Fig. 6 represents the Network throughput of the proposed PrioriNet protocol in comparison with the existing LEACH technique. In normal data scenarios, the LEACH protocol achieves throughputs ranging from 0.2 Mbps to 0.9 Mbps with increase in nodes, while the proposed method consistently attains higher throughputs, ranging from 0.5 Mbps to 1.6 Mbps, with an increasing number of nodes. Similarly, in emergency data scenarios, the LEACH protocol demonstrates throughputs between 0.3 Mbps and 1.2 Mbps, whereas the proposed method consistently outperforms the LEACH protocol with throughputs ranging from 0.7 Mbps to 1.8 Mbps.

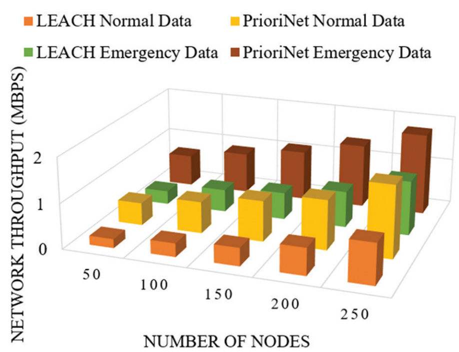

Fig. 6. Network throughput vs number of nodes

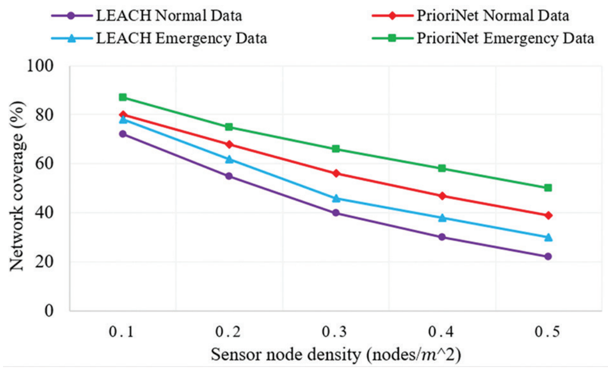

Fig. 7. Network Coverage vs Node Density

Fig. 7 represents the Network Coverage of the proposed PrioriNet protocol in comparison with the existing LEACH technique in terms of spatial area. From fig. 7, it is evident that the proposed method consistently achieves higher network coverage compared to the LEACH protocol for both normal and emergency data scenarios. The proposed method achieves a higher network coverage of 30.8% than existing LEACH technique.

5. CONCLUSION

In this paper, a novel PrioriNet protocol was developed to enhance communication efficiency, and improve emergency response coordination. The experimental results indicates that the suggested protocol performs better than the existing LEACH technique in terms of energy consumption, network coverage, packet delivery ratio, and throughput. In emergency data scenarios, the LEACH protocol demonstrates throughputs between 0.3 Mbps and 1.2 Mbps, whereas the proposed method consistently outperforms the LEACH protocol with throughputs ranging from 0.7 Mbps to 1.8 Mbps. The proposed method achieves a higher network coverage of 30.8% than existing LEACH technique. The future development of the proposed work will focus on enhancing the security of sustainable devices to ensure uninterrupted services.

6. REFERENCES

[1] Y. Lu, J. Xu, "The progress of emergency response and rescue in China: a comparative analysis of Wenchuan and Lushan earthquakes", Natural Hazards, Vol. 74, 2014, pp. 421-444.

[2] M. A. Soomro, M. I. Channa, Z. Hussain, M. Ahmed, "EPLAODV: Energy Priority and Link Aware Ad-hoc On-demand Distance Vector Routing Protocol for Post-disaster Communication Networks", Engineering, Technology & Applied Science Research, Vol. 10, 2020, p. 5148.

[3] G. Zussman, A. Segall, "Energy efficient routing in ad hoc disaster recovery networks", Proceedings of the Twenty-second Annual Joint Conference of the IEEE Computer and Communications Societies, San Francisco, CA, USA, 2003, pp. 682-691.

[4] M. S. Al-kahtani, L. Karim, N. Khan, "Efficient Opportunistic Routing Protocol for Sensor Network in Emergency Applications", Electronics, Vol. 9, No. 3, 2020, p. 455.

[5] F. Luqman, F. T. Sun, H. T. Cheng, S. Buthpitiya, M. Griss, "Prioritizing data in emergency response based on context, message content and role", Proceedings of the 1st International Conference on Wireless Technologies for Humanitarian Relief, December 2011, pp. 63-69.

[6] I. Joe, S.-B. Kim, "A Message Priority Routing Protocol for Delay Tolerant Networks (DTN) in Disaster Areas", Proceedings of the International Conference on Future Generation Information Technology: Future Generation Information Technology, Jeju Island, Korea, 13-15 December 2010.

[7] F. Peña-Mora, A. Y. Chen, Z. Aziz, L. Soibelman, L. Y. Liu, K. El-Rayes, C. A. Arboleda, T. S. Lantz, A. P. Plans, S. Lakhera, "Mobile Ad Hoc Network-Enabled Collaboration Framework Supporting Civil Engineering Emergency Response Operations", Journal of Computing in Civil Engineering, Vol. 3, 2010, pp. 302-312.

[8] V. G. Menon, J. P. Pathrose, J. Priya, "Ensuring Reliable Communication in Disaster Recovery Operations with Reliable Routing Technique", Mobile Information Systems, Vol. 2016, 2016.

[9] H. Suzuki, Y. Kaneko, K. Mase, S. Yamazaki, H. Makino, "An ad hoc network in the sky, skymesh, for large-scale disaster recovery", Proceedings of the IEEE Vehicular Technology Conference, Melbourne, QC, Australia, 25-28 September 2006, pp. 1-5.

[10] T. Sakano, S. Kotabe, T. Komukai, T. Kumagai, Y. Shimizu, A. Takahara, T. Ngo, Z. M. Fadlullah, H. Nishiyama, N. Kato, "Bringing movable and deployable networks to disaster areas: development and field test of MDRU", IEEE Network, Vol. 30, No. 1, 2016, pp. 86-91.

[11] A. Araghipour, S. Mostafavi, "An Improved Emergency Response Routing Protocol for Internet of Things", Wireless Personal Communications, Vol. 2022, 2022, pp. 1-24.

[12] J. Shreyas, S. Shilpa, P. K. Udayaprasad, N. N. Srinidhi, S. M. D. Kumar, “An Energy Efficient Routing for Emergency Rescue in IoT-Based WSN”, Futuristic Trends in Networks and Computing Technologies: Select Proceedings of Fourth International Conference on FTNCT 2021, Springer, 2022, pp. 331-338.

[13] S. Abdellatif, O. Tibermacine, W. Bechkit, A. Bachir, “Heterogeneous IoT/LTE ProSe virtual infrastructure for disaster situations”, Journal of Network and Computer Applications, Vol. 213, 2023, p. 103602.

[14] L. Campioni, F. Poltronieri, C. Stefanelli, N. Suri, M. Tortonesi, K. Wrona, “Enabling civil–military collaboration for disaster relief operations in smart city environments”, Future Generation Computer Systems, Vol. 139, 2023, pp. 181-195.

[15] Q. Zhao, W. Yang, L. Zhang, “Energy-Efficient Opportunistic Routing Algorithm for Post-Disaster Mine Internet of Things Networks”, Sensors, Vol. 23, No. 16, 2023, p. 7213.

[16] A. Mohammadiounotikandi, H. F. Fakhruldeen, M. N. Meqdad, B. F. Ibrahim, N. Jafari Navimipour, M. Unal, “A Fire Evacuation and Control System in Smart Buildings Based on the Internet of Things and a Hybrid Intelligent Algorithm”, Fire, Vol. 6, No. 4, 2023, p. 171.

[17] X. Tang, F. Chen, F. Wang, Z. Jia, “Disaster Resilient Emergency Communication with Intelligent Air-Ground Cooperation”, IEEE Internet of Things Journal, 2023. (in press)

[18] D. D. Olatinwo, A. M. Abu-Mahfouz, G. P. Hancke, H. C. Myburgh, “Energy Efficient Priority-Based Hybrid MAC Protocol for IoT Enabled WBAN Systems”, IEEE Sensors Journal, Vol. 23, No. 12, 2023, pp. 13524-13538.

[19] S. M. Z. Al-Hady, M. R. Islam, M. M. Rashid, “Development of IoT-Based Automated Dynamic Emergency Response System Against Fire Incidents in Academic Building”, International Journal of Engineering Materials and Manufacture, Vol. 8, No. 3, 2023, pp. 75-87.

Classification and Segmentation of MRI Images of Brain Tumors Using Deep Learning and Hybrid Approach

Original Scientific Paper

Sugandha Singh
Department of Computer Science
Babasaheb Bhimrao Ambedkar University
Vidya Vihar, Rae Bareli Road, Lucknow (U.P.) 226025, INDIA
singhsugandha3@gmail.com

Vipin Saxena
Department of Computer Science
Babasaheb Bhimrao Ambedkar University
Vidya Vihar, Rae Bareli Road, Lucknow (U.P.) 226025, INDIA
vsax1@rediffmail.com

Abstract – *Manual prediction of brain tumors is a time-consuming and subjective task, reliant on radiologists' expertise, leading to potential inaccuracies. In response, this study proposes an automated solution utilizing a Convolutional Neural Network (CNN) for brain tumor classification, achieving an impressive accuracy of 98.89%. Following classification, a hybrid approach, integrating graph-based and threshold segmentation techniques, accurately locates the tumor region in magnetic resonance (MR) brain images across sagittal, coronal, and axial views. Comparative analysis with existing research papers validates the effectiveness of the proposed method, and similarity coefficients, including a Bfscore of 1 and a Jaccard similarity of 93.86%, attest to the high concordance between segmented images and ground truth.*

Keywords: *tumor images, graph-based approach, threshold segmentation, CNN, tumor identification, meningioma*

1. INTRODUCTION

Glioma, atypical meningioma, and schwannoma disease are among the most severe forms of brain tumor that pose a significant threat to human life. The primary brain tumor is estimated to affect 24,810 people by 2023 in the United States. In the early stage of a medical condition, patients may experience headaches. However, as time passes, the condition may progress, potentially leading to visual impairments [1]. Glioma is the most common primary brain tumor and the symptoms depend on the tumor's location, growth, and infiltration of tumors. Glioma symptoms can be quite severe. On the other hand, meningiomas are typically benign tumors that occur in adults. They are commonly found attached to the dura and arise from the meningothelial cell of the arachnoid. These tumors are rounded in shape with a well-defined dural base, which can lead to the compression of the underlying brain tissue. Meningiomas have two stages: atypical and anaplastic. Atypical meningiomas often exhibit a high rate of recurrence and more aggressive local growth. Atypical meningioma may require radiotherapy along with surgery. While most schwannomas within the cranial vault primarily occur at the cerebellopontine angle, where they are typically attached to the vestibular branch of the eight cranial nerves, the symptoms experienced by patients often include tinnitus and hearing loss. Early detection of these brain tumors is crucial for preventing further complications. Therefore, both classification and segmentation are critical factors in identifying brain tumors at an early stage [2].

Due to the abnormal and rapid growth of tumor tissues within the brain, it becomes imperative to accurately locate the position of the tumor that affects the brain cells. Worldwide, medical practitioners and radiologists are continually striving to diagnose brain tumors effectively. This is where MRI modalities play a crucial role in enhancing the accuracy of brain tumor diagnosis and identifying the affected areas. MRI is the dedicated imaging modality, a non-invasive technique widely used for detailed visualization of the brain's internal structures. The integration of artificial intelligence (AI) in MRI analysis has become imperative due to the complex and voluminous nature of medical imaging data.

MRI generates high-dimensional and intricate datasets that pose challenges for efficient interpretation by human observers alone. The application of AI, particularly deep learning models like convolutional neural networks (CNNs), has shown promise in automating the analysis of MRI images. These models excel at discerning intricate patterns and features within the images, enabling more accurate and rapid identification of abnormalities, such as brain tumors.

Referring to existing literature, studies by Deb and Roy [3], and Ranjbarzadeh et al. [4] have explored the application of artificial intelligence (AI), specifically neural networks, for MRI image analysis. They emphasize the need for advanced computational techniques to handle the complexity of MRI data and enhance diagnostic accuracy. The introduction thus establishes the context of MRI as the chosen imaging modality and justifies the integration of AI to address the inherent challenges in its analysis, drawing on insights from relevant studies in the field. Noteworthy among these advancements is the work of Rehman et al. [5], which introduces a compelling strategy using an enhanced encoder-decoder network. 'BrainSeg-Net,' their novel approach, merits careful consideration in the broader landscape of medical image analysis.

To enhance the computational complexity and accuracy of brain tumor detection, a novel CNN based classification and segmentation method is employed. Samples of normal brain images and brain tumor images with glioma, atypical meningioma, and schwannoma, were collected from various hospitals as illustrated in Fig. 1 representing the transverse plane of both contrast and non-contrast MR images.

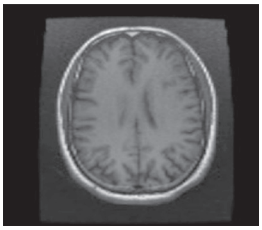

(a) Normal brain image

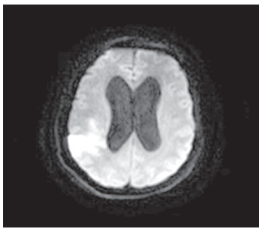

(b) Schwannoma brain tumor image

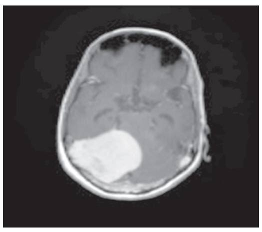

(c) Atypical meningioma brain tumor image

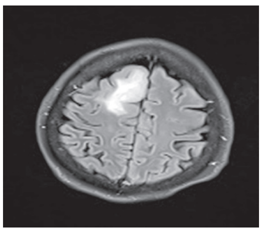

(d) Glioma brain tumor image

Fig. 1. Sample of (a) normal brain image and brain tumor images with (b) schwannoma, (c) atypical meningioma and (d) glioma

2. RELATED WORKS

In the references provided, the imaging modality used was primarily MRI (Magnetic Resonance Imaging). Specifically, Karayegen and Aksahin [6] utilized MRI for semantic segmentation to detect brain tumors using 3D imaging They compared ground truth with the segmented result. However, the classification error rate was not successfully minimized. Saleem et al. [7] utilized the MRI Brats 2018 dataset for 3D brain tumor segmentation and analyzed the segmentation model by applying interpretability technique to different tumor regions, including non-enhancing tumors, edema, and enhancing tumors. Khosravanian et al. [8] introduced a superpixels fuzzy clustering method with a multiscale morphological gradient reconstruction operation. They evaluated the method's performance on both synthetic data and the MR Brats 2017 dataset. However, a limitation of this paper is the use of single-modality MRI image fluid-attenuated inversion recovery (FLAIR) for tumor segmentation. Zhang et al. [9] introduced a multi-scale mesh aggregation network for MRI brain tumor image segmentation. One limitation of their approach is that the 2D network cannot fully leverage the details within the three spatial dimensions in 3D volume images. Lei et al. [10] employed a sparse constrained level set method to analyse brain tumor segmentation, implementing it using the MR Brats 2017 dataset. Their approach achieved higher accuracy compared to other methods. Shree and Kumar [11], utilized MR data extracted features using a grey-level co-occurrence matrix (GLCM) and applied discrete wavelet transform (DWT) with a region-growing segmentation method, achieving an accuracy of 98.02%. Mamatha et al. [12], introduced a graph theory based segmentation method in which a weighted directed graph is constructed. Each pixel in the image is represented as a nodes, and paths are obtained for the detection of MR brain tumors before the segmentation process. They applied pre-processing steps to enhance image quality and achieved favorable results. Balamurugan and Gnanamanoharan [13], present a novel approach employing a hybrid deep convolutional neural network (DCNN) with an enhanced LuNet classifier has been proposed. The primary goal is to precisely locate and classify MRI brain tumors as glioma or meningioma. The preprocessing stage involves the utilization of a laplacian gaussian filter (LOG), while a fuzzy c means with gaussian mixture model (FCM-GMM) algorithm is introduced for segmentation. The extended LuNet algorithm is then applied for data division, and VGG16 feature extraction yields thirteen categorical features. Hossain et al. [14], proposed method leverages lightweight deep learning models, namely MicrowaveSegNet, to achieve precise brain tumor segmentation, and BrainImageNet, for accurate image classification. The research integrates advanced computational techniques for efficient brain tumor analysis. The utilization of a portable sensor-based microwave imaging system adds a dimension of flexibility to the diagnostic process, showcasing the potential impact of this innovative methodology in the field of medical imaging and brain tumor research. The proposed approach [15] combines adam sewing training based optimization with UNet++ (AdamSTBO+UNet++) for MRI brain tumor segmentation and adam salp water wave optimisation with the deep convolutional neural network (AdamSWO-DCNN) for classification. The introduction of AdamSTBO, an adaptation of the Adam optimizer integrated with the upgrade function of the sewing training based optimization (STBO) algorithm, signifies a distinctive advancement in optimization strategies. Ansari's [16], explores automated support systems for brain tumor detection using MRI, leveraging soft computing and machine learning algorithms. The study proposes a strategy utilizing a fuzzy clustering algorithm and a neural network system to identify brain tumor cells in their early stages. Ullah et al. [17] applied a statistical approach to enhance the image quality, to improve classification performance. For classification, they utilized discrete wavelet transform to extract features from MRI images and categorized them into malignant and benign tumor classes in deep neural networks. However, the limitations of this approach include its incompatibility with larger datasets and the longer execution time required. Amin et al. [18] applied a fusion technique using discrete wavelet transform (DWT) on MRI images. They employed a partial differential diffusion filter to remove noise and performed tumor segmentation using a global thresholding method. The segmented image was then passed to a proposed CNN model for classification into tumor and non-tumor regions. Their analysis revealed that fusion images provide superior results, and this method was extended to PET and CT images. However, a drawback was noted as the fusion images sometimes produced distorted images, which had an impact on the classification process.

While these studies do not directly resolve all the highlighted problems, each contributes valuable insights that could be leveraged to address the identified challenges. Techniques such as improved segmentation methods, utilization of multiple modalities, network enhancements, and preprocessing stages are all potential avenues to explore in minimizing classification errors and leveraging multi-modality imaging for more accurate tumor segmentation.

3. PROBLEM STATEMENT

The critical stage of brain tumor identification is a vital task to avoid severe brain issues. Several techniques have been developed to discover brain abnormalities through brain images in a precise manner. However, image classification and segmentation are the most challenging and essential tasks for medical images. Various segmentation techniques are applied to locating brain tumors, but they come with certain drawbacks and challenges. Which are listed below.

- The classification error rate in brain tumor segmentation needs to be minimized.
- The limitation of using single-modality MRI images for tumor segmentation.

These are the major challenges of different methods that motivate us to research on segmentation and classification. The paper addresses a suitable method to detect brain tumors more accurately and effectively.

4. MATERIAL AND METHOD

The aim of the research is to analyze radiologist's diagnoses using a deep learning model for classification and a hybrid approach for segmentation. The primary goal of the proposed method is to locate tumor-affected tissues in a more precise and efficient manner. The CNN approach is applied for the classification of tumor and no-tumor classes. The segmentation process partitions the tumor-affected tissues from healthy brain tissues, with practitioners performing this crucial step for clinical aids. The designed deep learning model, based on radiologist's assumptions, undergoes thorough analysis to achieve effective performance and accuracy surpassing existing approaches. The techniques are implemented and experimented with real MRI images collected from reputable hospitals are shown in Fig. 2.

1. In the pre-processing step, 2D MRI images are normalized to a scale of 1.0/255.0 using normalization techniques and resized to 224*224 to reduce computational complexity.
2. The 2D CNN model is applied to the trained images, and to perform classification into tumor and no-tumor.
3. After classification, the tumor region is located using a hybrid approach for tumor segmentation.
4. Evaluate the classification accuracy and segmentation similarity coefficients.

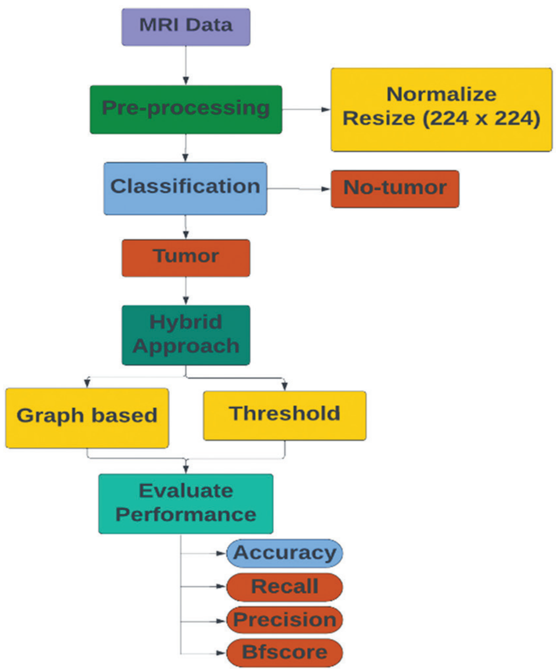

Fig. 2. Schematic representation of proposed system

4.1. DATASET SPECIFICATION

The dataset was obtained from distinct hospitals and encompasses three categories of brain tumor cases, namely atypical meningioma, glioma, and schwannoma, alongside normal brain images. Initially stored in the DICOM format, these images underwent preprocessing, during which they were converted into the JPG format. The collected dataset consists of various MRI sequences for further pre-processing. Following preprocessing, the images were categorized into two groups: with tumors and no-tumor, and facilitating further analysis. The dataset comprises a total of 884 MRI brain images categorized into two classes: 624 images with tumors and 260 images of normal brains. The brain MRI dataset is divided into training and test sets, with 707 images for training and 77 for testing. Each image has been resized to 224 x 224 pixels. A summary of the dataset specifications is provided in Table 1.

Table 1. Dataset specification

Data	Specification
Dataset source	Safdarjung, Medanta and SGPGI Hospitals
Image Format	DICOM
Size of Images	224 x 224
No. of Classes	Two
Name of Classes	Tumor, No-tumor
Name of Sequence	T1, T2, FLAIR, T1+C
Train	80%
Test	20%

In Table 2 the demographic details of patients with three brain tumor categories including atypical meningioma, glioma, and schwannoma, along with normal brain MRI images. The patient data has been collected from radiologists, accompanied by authorized reports and the consent of both patients and, their attendants.

Table 2. Demographic details of patients

Patient	Hospital	Age	Gender	Category
Patient#1	Medanta	58	Female	Glioma
Patient#2	SGPGI	54	Male	Schwannoma
Patient#3	Safdarjung	62	Female	Atypical Meningioma
Patient#4	SGPGI	45	Female	Normal brain

4.2. MRI IMAGING SEQUENCES

All MRI sequences exhibit diverse properties characteristics, and distinct appearances, which play a crucial role in the analysis and grading of tumors. These MR sequences rely on the application of radiofrequency pulses and gradients to capture detailed tissue information and intensity variations. For instance, FLAIR images are valuable for assessing lesions near the ventricles and distinguishing them from cerebral spinal fluid (CSF).

In the T2 sequence, which is often used in the evaluation of inflammatory processes, many diseases manifest an increase in tissue fluid content. Consequently, these lesions appear brighter and are employed, much like T1-weighted imaging, to assess anatomical structures and most lesions throughout the body. However, it is important to note that T2-weighted imaging may not be the optimal choice for evaluating lesions around the brain ventricles, as both lesions and CSF can have a similar appearance in this sequence.

On the other hand, T1-weighted images with contrast enhancement (T1+C), achieved by injecting contrast material like gadolinium, serve to increase the T1 signal from moving blood. These MRI sequences will be discussed in more detail in the context of the specific images used.

4.2.1. Fluid-Attenuated Inversion Recovery (FLAIR) image

The FLAIR image in MRI is notable for its similarities to T2-weighted imaging regarding brain tissue intensities, with the key distinction being the appearance of cerebrospinal fluid (CSF) as dark rather than bright. It achieves this by selectively suppressing the signals from fluids through the use of long echo (TE) and repetition (TR) times.

In FLAIR images, grey matter appears brighter than white matter, and CSF stands out as dark. This particular characteristic makes FLAIR sequences a valuable tool for the assessment of various brain disorders, including infarction, hemorrhage, and head traumas. Additionally, FLAIR imaging has the added benefit of reducing cerebrospinal fluid production. An illustrative example of the axial view of a FLAIR image is depicted in Fig. 3.

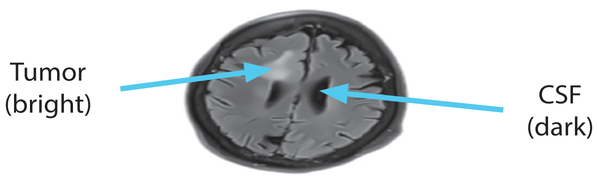

Fig. 3. Axial view of FLAIR sequence

4.2.2. T1 image

In the T1 sequence, tissue intensities reflect T1, which is the long relaxation time. On T1 scans, fatty tissue appears bright, but CSF with no fat appears dark. The T1 sequence produces short TE and TR times, which darkens the CSF. The axial view of the T1 image is represented in Fig. 4.

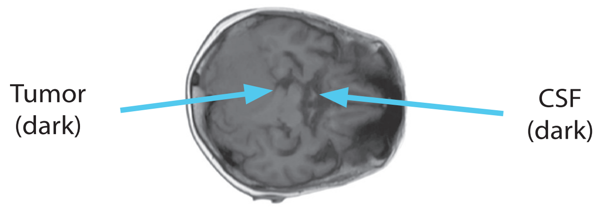

Fig. 4. Axial view of T1 sequence

4.2.3. T2 image

The T2-weighted sequences generate long TE and TR times, making CSF appear very bright. In the T2 sequence, fluid, bone, and air appear dark. As a part of the inflammatory process, most diseases exhibit increased fluid content, causing lesions to appear bright. The sagittal view of the T2 image is shown in Fig. 5.

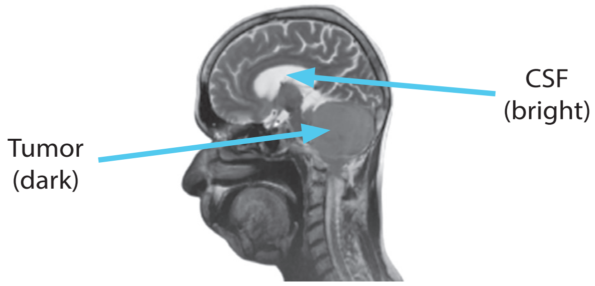

Fig. 5. Sagittal view of T2 sequence

4.2.4. T1+C image

In the T1+C sequence, contrast material is injected, which increases the T1 signal from moving blood and thus allows the detection of highly vascular lesions. Tissues have the same intensities as in T1, except that the moving blood is bright. It is useful in determining hypervascular lesions in haemangiomas and lymphangiomas. The axial view of the T1+C image is shown below in Fig. 6.

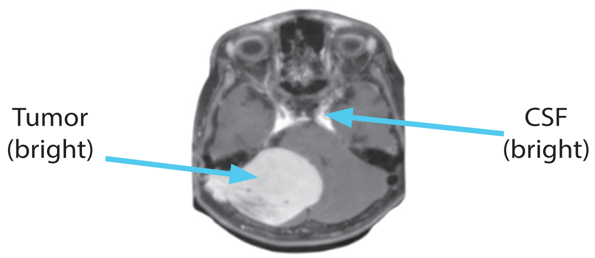

Fig. 6. Axial view of T1+C sequence

The properties of the MRI sequences are compared and represented in Table 3.

Table 3. Comparison between MRI sequences

MRI Sequence	CSF	White Matter	Grey Matter	TE/TR
T1	Hypointense	White	Grey	Short/Short
T2	Hyperintense	Grey	White	Long/Long
FLAIR	Hypointense	Grey	White	Very Long/ Very Long
T1+C	Hyperintense	White	White	Long/Long

The MRI scans can be viewed in three dimensions, namely Sagittal, Axial, and Coronal, allowing medical professionals to study the morphology of tumors as shown in Fig. 7.

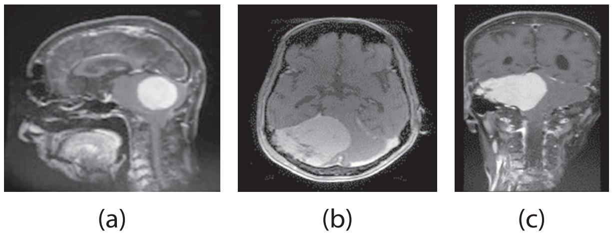

Fig. 7. (a) Sagittal (b) Axial, and (c) Coronal plane

4.3. CONVOLUTIONAL NEURAL NETWORK

The architecture of the CNN model is shown in Fig. 8. The deep learning process consists of 2D convolution and max-pooling layers.

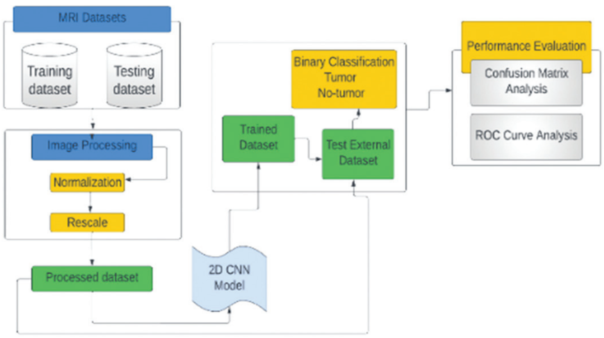

Fig. 8. Representation of 2D CNN Model

MRI datasets are utilized, encompassing training and validation approaches. The images undergo normalization and augmentation processes, and the processed dataset is then fed into the 2D model. Finally, the model produces binary classification results, which are used to categorize MRI brain images into tumor and no-tumor categories.

To improve the performance of the CNN model, the dataset has been normalized for feature scaling. The process begins with image pre-processing, which includes the augmentation of images. After that, data generators are created, and random patches extracted from MR images are inserted as input. The model has a total of 11 layers with varying numbers of neurons and dense layers such as convolution layers, batch normalization layers, max-pooling layers, and LeakyReLU layers. The process of convolution deep learning is processed with the SoftMax, and pixel classification layers. The architecture of CNN network layers is shown in Fig. 9.

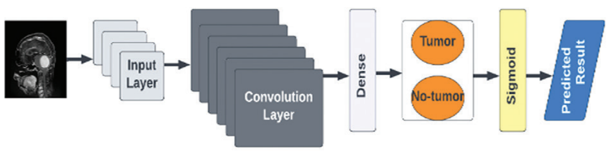

Fig. 9. Architecture of 2D CNN layers

The total number of layers can be counted as follows:

Input Layer: The model takes grayscale images with dimensions (150, 150, 1) as input.

Convolutional Blocks:

First Block: Applies Convolutional operation with 8 filters, kernel size (5, 5), and LeakyReLU activation. Followed by MaxPooling2D layer (2, 2).

Second Block: Applies Convolutional operation with 8 filters, kernel size (3, 3), and LeakyReLU activation. Followed by MaxPooling2D layer (2, 2).

Third Block: Applies Convolutional operation with 16 filters, kernel size (3, 3), and LeakyReLU activation.

Fourth Block: Applies Convolutional operation with 16 filters, kernel size (3, 3), and LeakyReLU activation. Followed by BatchNormalization for normalization and MaxPooling2D layer (2, 2).

Flatten Layer: Converts the 2D feature maps into a 1D vector.

Fully Connected Layers: Dense Layer (Hidden): Consists of 10 neurons with LeakyReLU activation.

Dense Layer (Output): Consists of 2 neurons with Softmax activation, representing the output classes for binary classification.

Optimizer and Compilation: Uses the Adam optimizer with a learning rate of 0.001, beta_1 of 0.9, and beta_2 of 0.999. Compiles the model with categorical crossentropy loss and accuracy as the metric.

Data Augmentation: Utilizes the ImageDataGenerator for real-time data augmentation during training.

Training Configuration: Specifies 100 epochs and a batch size of 40 for training. The architecture is shown in Fig. 10.

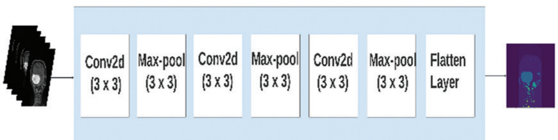

Fig. 10. CNN neural network layers

4.4. HYBRID APPROACH FOR SEGMENTATION

To locate tumors, a hybrid approach is applied. Firstly, graph-based segmentation is used, and thereafter, the threshold method is applied to the segmented MRI brain images.

4.4.1. Graph-based

Graph-based [19] method was originally introduced for a greedy approach to image segmentation based on predicates and has been utilized in various fields of image processing. The predicate P concludes in case there is an edge for segmentation. The fast minimum tree-based clustering on the image grid that produces a multichannel image is one of the concepts of graph-based segmentation concepts used in the proposed method and can be defined as:

$$P(a_1, a_2) = \begin{cases} \text{true} & \text{if } \mathrm{Diff}(a_1, a_2) > \mathrm{Dint}(a_1, a_2) \\ \text{false} & \text{otherwise} \end{cases}, \quad (1)$$

$P(a1, a2)$ is a binary indicator function in Eq. (1) that outputs true if the variation between modules $a1$ and $a2$, denoted by Diff($a1$, $a2$), is greater than the internal variation within $a1$ and $a2$, represented by Dint($a1$, $a2$). Otherwise, it outputs false.

$$\mathrm{Diff}(a_1, a_2) = \min_{v_i \in a_1, v_j \in a_2, (v_i, v_j) \in E} w(v_i, v_j), \quad (2)$$

Diff($a1$, $a2$) in Eq. (2) represents the variation between two modules. It calculates the minimum weight edge connecting a node v_i in module $a1$ to a node v_j in $a2$.

The term $w(v_i, v_j)$ represents the weight associated with the edge connecting node v_i in module $a1$ to node v_j in module $a2$.

$$\mathrm{Max}(a) = \max_{e \in MST(a,E)} w(e), \quad (3)$$

Max(a) in Eq (3), calculates the maximum weight edge in the Minimum Spanning Tree (MST) of the module a. $w(e)$ is a function that assigns a weight to the edge e in the graph.

$$\mathrm{Dint}\,(a1, a2) = \min(\max(a1 + \tau(a1)), \max(a2) + \tau(a2)), \quad (4)$$

Dint ($a1$, $a2$) in Eq. (4) calculates the internal variation within modules a1 and a2. It involves the minimum of the maximum weights of nodes in the modules with a threshold factor $\tau(a)$.

$$\tau(a) = \frac{k}{|a|}. \quad (5)$$

In eq. (5), k is a constant or parameter, and $|a|$ denotes the cardinality (number of elements) in the set a.

4.4.2. Threshold

The threshold method is a very simple technique used to select threshold value T. The RGB image is converted into a grayscale image, and further, it is converted into a binary image for a segment of the tumor region. The threshold value, T, is obtained from the grayscale image and is classified within the range of 0 to 255. The formula for the threshold can be given as in Eq. (6):

$$m(i,j) = \begin{cases} 0 & if\ k(i,\ j) < T \\ 1 & if\ k(i,j) \geq T \end{cases}, \quad (6)$$

where, $k(i, j)$ is an image and m (i, j) is grey conversion.

In Fig. 11, the proposed method has been combined to locate the tumor region. Further, the selected RGB image is scaled and segmented to partition affected tissue from MR brain images. In the final stage, morphological operation is applied.

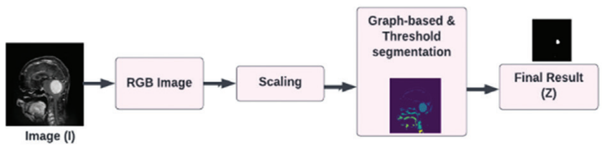

Fig. 11. Graph-based and threshold segmentation method

The hybrid approach algorithm is formed which is given as:

Start

[Step 1] Input MRI brain image (I) from datasets

[Step 2] Check for the presence of a tumor (Classification)

[Tumor Present]

[Step 3] Partition Image ($I1$, $I2$, ..., In)

[Step 4] Determine the number of partitions (n) using felzenswalb()

[Step 5] Cluster the Partition Images based on Image grid (k) [300 <= k <= 1000]

[Step 6] Set Parameters (S):

- Image (Height, Width), Scale: 350
- Sigma: 0.2, *Min_Size*: 20
- Threshold T >= 80

[Step 7] Compute the approximate distance (D_T) of Pixels of Tumors Image

[Step 8] Return the final segmentation result

[No Tumor]

[Step 9] Return the result "No Tumor Detected"

End

In the algorithm, select MRI brain images as input from the dataset for tumor segmentation. The input image is partitioned into 'n' numbers of segments using the Felzenszwalb() module. The partitioned image is clustered based on the image grid (k) with a range of 300 >= k <= 1000 and set parameters (S) for image (I) such as to scale indicate the largeness of clusters, sigma for smoothening of the image, *min_size* defines the size of the output image and set threshold T >= 80 for segmentation. After setting parameters, compute the approximate distance (D_T) of pixels of the tumor image. Finally, the result of Z is computed.

The observation result of testing images is shown in Fig. 12 column-wise.

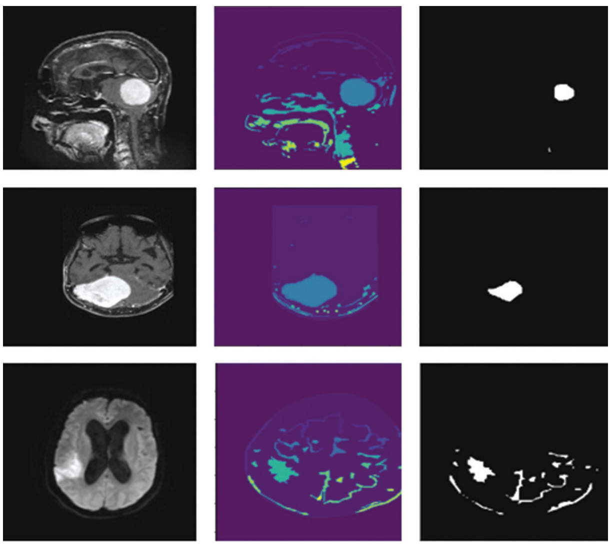

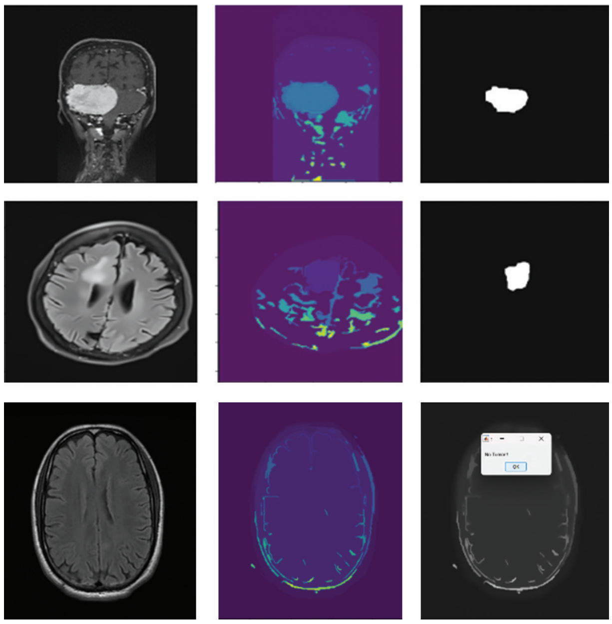

(a) (b) (c)

Fig. 12. Brain tumor segmentation using a hybrid approach: (a) Original images, (b) Graph-based segmentation, (c) Hybrid approach

5. EVALUATION METRICS AND RESULTS

The proposed method of classification and segmentation is implemented on a computer with an intel core i5 11[th] generation processor unit with 8GB RAM, operating at a frequency of 2.40 GHz, and NVIDIA GEFORCE GTX, using Python programming language. The results in the research work are discussed.

To calculate accuracy, a confusion matrix is created for classifying models and evaluating the segmentation outcomes of the proposed method.

$$\text{Accuracy} = \frac{(TP+TN)}{(TP+TN+FN+FP)}, \tag{7}$$

$$\text{Recall (r)} = \frac{TP}{(TP+FP)}, \tag{8}$$

$$\text{Precision (p)} = \frac{TP}{(TP+FP)}, \tag{9}$$

The confusion matrix includes True Positive (TP), True Negative (TN), False Positive (FP), and False Negative (FN), which are essential for assessing classification accuracy, recall, and precision. Additionally, BF (Boundary F1) score and Jaccard are employed to assess segmentation performance, as outlined in Eq. (7)-(11).

The BF score, a contour matching score, is utilized to evaluate image segmentation techniques. In this scenario, the two groups considered are the binary mask of objects and the segmentation result obtained from the hybrid approach.

$$\text{Bfscore (S (x, y), G (x, y)} = 2*\frac{p*r}{(r+p)}, \tag{10}$$

In the provided context, $S(x, y)$ represents the input image, and $G(x, y)$ is the binary mask depicting the segmentation result. The variables r denote recall, and p signifies precision.

$$Jaccard(A, B) = |intersection(A, B)| / |union(A, B)|, \quad (11)$$

where A is the input image and B is the ground truth image.

5.1. RESULTS

5.1.1. Performance of classification

By examining the study depicted in Fig. 13 (a, b, c). It can be observed that the training accuracy acquired at 98.01% and the validation accuracy at 98%. The data was split into 80 % for training and 20% for validation.

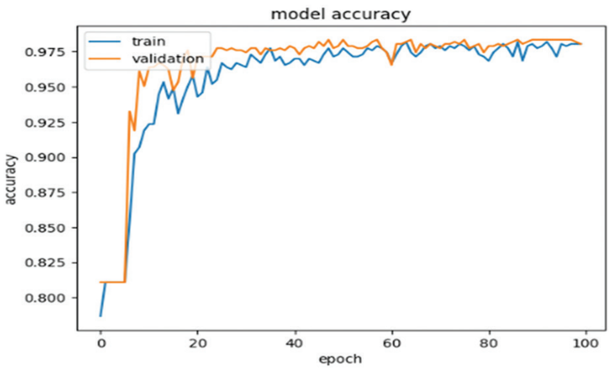

Fig. 13. (a) Training and validation accuracy

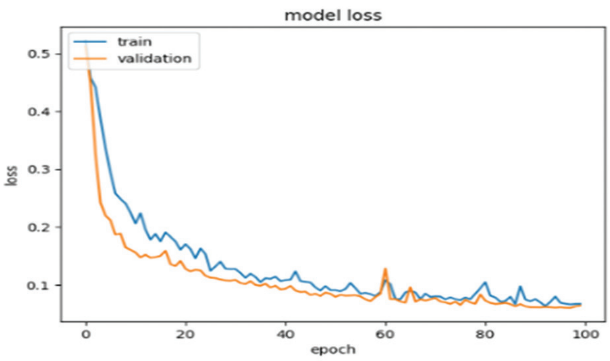

Fig. 13. (b) Training and validation loss

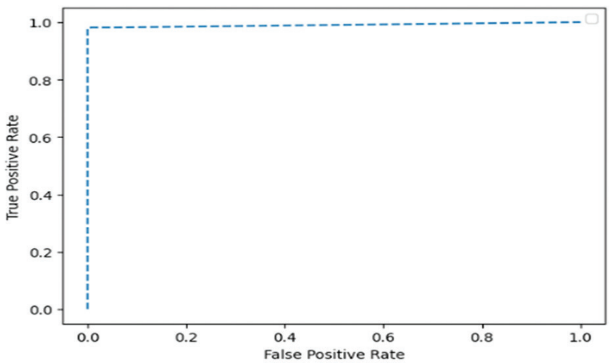

Fig. 13. (c) True Positive and False Positive Rate

The classification results of tumor and no-tumor are represented in Fig. 14.

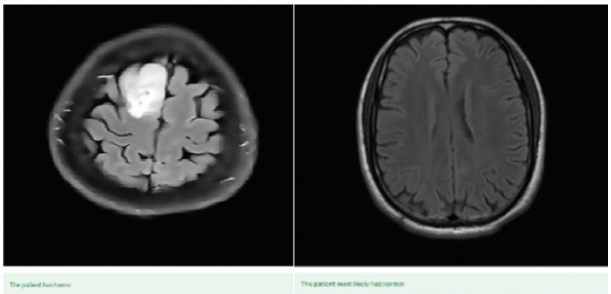

Fig. 14. Tumor and no-tumor classification results

5.1.2. Performance measure of segmentation

To assess and scrutinize the performance of the proposed hybrid method for tumor segmentation, a comparison is made with the ground truth image. Five images obtained are utilized as test images.

Table 4 shows results with Bfscore, and Jaccard, indicating the similarity coefficients and segmentation outcomes. The results for each test image demonstrate satisfactory performance.

Table 4. Results based on similarity coefficients (a) Original image, (b) Ground truth image, (c) Segmentation using a hybrid approach, (d) Bfscore, and (e) Jaccard

Input	Ground Truth	Hybrid approach	Bfscore	Jaccard
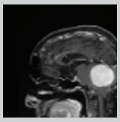			0.92236	0.88438
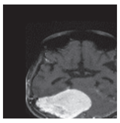			0.88353	0.88912
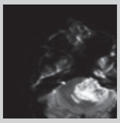			0.56858	0.6722
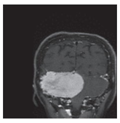			1	0.93862
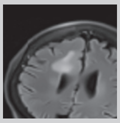			0.87662	0.72371
(a)	(b)	(c)	(d)	(e)

6. DISCUSSION

The successful performance of the proposed system and comparative results are summarized in Table 5.

According to Table 5, Zhang et al. [20] employed back propagation neural network (BPNN) classification following the enhancement of image quality using 2D DWT Decomposition. They achieved a classification accuracy of 98.10% but were limited to consist of T2-

weighted MR brain images, with only 66 images for training and testing. Notably, they did not incorporate any segmentation technique to locate tumor regions. Selvaraj et al. [21] achieved an accuracy of 96%, but they used a support vector machine classifier as a validation technique. Al Kadi et al. [22] focused on extracting histopathological features, without applying any segmentation method, and achieved an accuracy of 92% accuracy using a fuzzy clustering machine for classification. In contrast, Muezzinoglu et al. [23] proposed the ResNet50 transfer learning technique, classifying multiple types of brain tumors with a 98% accuracy. Georgiardis et al. [24] attained an accuracy of 93%, though segmentation was not part of their study. Considering the studies outlined in Table 5 it is evident that the proposed method in this paper boasts minimum computational complexity and demonstrates commendable segmentation accuracy.

The essential stages of the research are as follows:

- The utilization of multimodal MRI sequence images is considered for the classification model.
- Implementation of 2D CNN to showcase high classification proficiency.
- Achievement of 98.89% accuracy in the proposed classification.
- Application of a hybrid approach for comparing test image results.
- Evaluation of similarity coefficients to yield robust segmentation results, with Bfscore registering a high value of 1 and Jaccard with 93.86%.
- However, some drawbacks of our proposed method include:
- The need for more cases of brain tumor for comprehensive validation.
- Suboptimal performance of the segmentation method when applied to non-contrast MRI brain images.

Table 5. Performance comparison between the proposed method and previous work

Author	Total images	Classification method	Classifier	Segmentation	Accuracy	F1 Score	Recall	Precision
Zhang et al. [20]	66	2D-DWT level 3 decomposition, DWT	BPNN	NA	98.02%	x	X	x
Selvaraj et al. [21]	1100	GLCM-4	LS-SVM KNN	NA	96%	x	X	x
Al Kadi et al. [22]	320	Histopathological features	FCM	NA	92%	x	X	x
Muezzinoglu et al. [23]	3264	ResNet50	Multi feature selector and KNN	NA	98.10%	98.01%	98.15%	97.91
Georgiardis et al. [24]	67	Histogram 4, LCM-22, GRLM-10	LSFT-PNN	NA	93%, 83.33%	75.65%	79%	88%
Proposed Method	884	CNN	Binary	Graph-based and Threshold	98.89%	-	98.14%	98.43%

7. CONCLUSION AND FUTURE WORK

The proposed segmentation technique, the hybrid approach, aims to more accurately locate tumor regions while achieving high classification accuracy. The presented work utilized an MRI brain tumor dataset, achieving a notable 98.89% accuracy using a 2D CNN model. Segmentation similarity coefficients, including a Bfscore of 1 and a Jaccard coefficient of 93.86%, underscore the effectiveness of our approach in tumor detection and segmentation. This method offers a promising avenue for future research, with plans to expand the dataset, incorporate more samples, and explore additional techniques for enhancing brain tumor location and diagnosis.

8. REFERENCES

[1] S. Chang, “Brain Tumor: Introduction”, www.cancer.net/cancer-types/brain-tumor (accessed: 2023)

[2] U. Asim, E. Iqbal, A. Joshi, F. Akram, K. N. Choi, "Active Contour Model for Image Segmentation with Dilated Convolution Filter", IEEE Access, Vol. 9, 2021, pp. 168703-168714.

[3] D. Deb, S. Roy, “Brain tumor detection based on hybrid deep neural network in MRI by adaptive squirrel search optimization”, Multimedia Tools and Applications, Vol. 80, 2021, pp. 2621-2645.

[4] R. Ranjbarzadeh, K. A. Bagherian, G. S. Jafarzadeh et al. “Brain tumor segmentation based on deep learning and an attention mechanism using MRI multi-modalities brain images”, Scientific Reports, Vol. 11, 2021, p. 10930.

[5] M. U. Rehman, S. Cho, J. Kim, K. T. Chong. “BrainSeg-Net: Brain Tumor MR Image Segmentation via Enhanced Encoder-Decoder Network”, Diagnostics, Vol. 11, 2021, p. 169.

[6] G. Karayegen, M. F. Aksahin, “Brain Tumor Prediction on MR Images with Semantic Segmentation by using Deep Learning Network and 3D Imaging

of Tumor Region", Biomedical Signal Processing and Control, Vol. 66, 2021, p. 102458.

[7] H. Saleem, A. R. Shahid, B. Raza, "Visual Interpretability in 3D Brain Tumor Segmentation Network", Computers in Biology and Medicine, Vol. 133, 2021, p. 104410.

[8] A. Khosravanian, M. Rahmanimanesh, P. Keshavarzi, S. Mozaffari, "Fast Level Set Method for Glioma Brain Tumor Segmentation based on Superpixel Fuzzy Clustering and lattice Boltzmann Method", Computer Methods, and Programs in Biomedicine, Vol. 198, 2021, p. 105809.

[9] Y. Zhang, Y. Lu, W. Chen, Y. Chang, H. Gu, B. Yu, "MSMANet: A Multi-scale Mesh Aggregation Network for Brain Tumor Segmentation", Applied Soft Computing, Vol. 110, 2021, pp. 1568-4946.

[10] X. Lei, X. Yu, J. Chi, Y. Wang, J. Zhang, C. Wu, "Brain Tumor Segmentation in MR Images using a Sparse Constrained Level Set Algorithm", Expert Systems with Applications, Vol. 168, 2020, p. 114262.

[11] N. V. Shree, T. N. R. Kumar, "Identification, and Classification of Brain Tumor MRI Images with Feature Extraction using DWT and Probabilistic Neural Network", Brain Informatics, Vol. 5, 2018, pp. 23-30.

[12] S. K. Mamatha, H. K. Krishnappa, N. Shalini, "Graph Theory Based Segmentation of Magnetic Resonance Images for Brain Tumor Detection", Pattern Recognition and Image Analysis, Vol. 32, 2022, pp. 153-161.

[13] T. Balamurugan, E. Gnanamanoharan, "Brain tumor segmentation, and classification using hybrid deep CNN with LuNetClassifier", Neural Computing and Applications, Vol. 35, 2023, pp. 4739-4753.

[14] A. Hossain, M. T. Islam, T. Rahman, M. E. H. Chowdhury, A. Tahir, S. Kiranyaz, K. Mat, G. K. Beng, M. S. Soliman, "Brain Tumor Segmentation and Classification from Sensor-Based Portable Microwave Brain Imaging System Using Lightweight Deep Learning Models", Biosensors, Vol. 13, No. 3, 2023, p. 302.

[15] P. S. Bidkar, R. Kumar, A. Ghosh, "Hybrid Adam Sewing Training Optimization Enabled Deep Learning for Brain Tumor Segmentation and Classification using MRI Images", Computer Methods in Biomechanics and Biomedical Engineering: Imaging & Visualization, Vol. 11, No. 5, 2023, pp. 1921-1936.

[16] A. S. Ansari, "Numerical Simulation and Development of Brain Tumor Segmentation and Classification of Brain Tumor Using Improved Support Vector Machine", International Journal of Intelligent Systems and Applications in Engineering, Vol. 11, No. 2s, 2023, pp. 35-44.

[17] Z. Ullah, M. U. Farooq, S. H. Lee, D. An, "A hybrid image enhancement based brain MRI images classification technique", Medical Hypotheses, Vol. 143, 2020, p. 109922.

[18] J. Amin, M. Sharif, N. Gul, M. Yasmin, S. A. Shad, "Brain tumor classification based on DWT fusion of MRI sequences using convolutional neural network", Pattern Recognition Letters, Vol. 129, 2020, pp. 115-122.

[19] P. F. Felzenszwalb, D. P. Huttenlocher, "Efficient Graph-Based Image Segmentation", International Journal of Computer Vision, Vol. 59, 2004, pp. 167-181.

[20] Y. Zhang, D. Zhengchao, W. Lenan, W. Shuihua, "A Hybrid Method for MRI Brain Image Classification", Expert Systems with Applications, Vol. 38, No. 8, 2011, pp. 10049-10053.

[21] H. Selvaraj, S. T. Selvi, D. Selvathi, L. Gewali, "Brain MRI Slices classification using Least Squares Support Vector Machine", International Journal of Intelligent Computing in Medical Sciences and Image Processing, Vol. 1, No. 1, 2007, pp. 21-33.

[22] O. Al-Kadi, "A Multiresolution Clinical Decision Support System based on Fractal Model Design for Classification of Histological Brain tumours", Comput Med Imaging Graph, Vol. 41, 2015, pp. 67-79.

[23] T. Muezzinoglu et al. "PatchResNet: Multiple Patch Division-Based Deep Feature Fusion Framework for Brain Tumor Classification Using MRI Images", Journal of Digital Imaging, Vol. 36, 2023, pp. 973-987.

[24] G. Pantelis, C. Dionisis, K. Ioannis, D. Antonis, K. C. George, S. Koralia, M. Menelaos, N. George, S. Ekaterini, "Improving Brain Tumor Characterization on MRI by Probabilistic Neural Networks and Non-Linear Transformation of Textural Features", Computer Methods and Programs in Biomedicine, Vol. 89, No. 1, 2008, pp. 24-32.

Intelligent Classifiers for Football Player Performance Based on Machine Learning Models

Original Scientific Paper

Baydaa M. Merzah
Department of Computer Science,
College of Computer Science and Information Technology,
University of Anbar, Ramadi, Iraq
Al-Nahrain University, Baghdad, Iraq
bai21c1007@uoanbar.edu.iq

Muayad S. Croock
Department of Control and Systems
University of Technology,
Baghdad, Iraq
muayad.s.croock@uotechnology.edu.iq

Ahmed N. Rashid
Department of Computer Networks Systems,
College of Computer Science and Information Technology,
University of Anbar, Ramadi, Iraq
rashidisgr@uoanbar.edu.iq

Abstract *– The remarkable effectiveness of Machine Learning (ML) methodologies has led to a significant increase in their application across various academic domains, particularly in diverse sports sectors. Over the past decade, scholars have utilized Machine Learning (ML) algorithms in football for varied objectives, encompassing the analysis of football players' performances, injury prediction, market value forecasting, and action recognition. Nevertheless, there has been a scarcity of research addressing the evaluation of football players' performance, which is a noteworthy concern for coaches. Hence, the objective of this work is to categorize the performance of football players into active, normal, or weak based on activity features. This will be achieved through the utilization of the Performance Evaluation Machine Learning Model (PEMLM), employing two novel datasets that cover both training and match sessions. To attain this goal, seven machine learning methods are applied, namely Random Forest, Decision Tree, Logistic Regression, Support Vector Machine, Gaussian Naïve Bayes, Multi-Layer Perceptron, and K-Nearest Neighbor. The findings indicate that in the dataset corresponding to match sessions, the Decision Tree classifier attains the highest accuracy (100%) and the shortest test time. In contrast, the K-Nearest Neighbor demonstrates the best accuracy (96%) and a reasonable test time for the training dataset. These reported metrics underscore the reliability and validity of the proposed assessment approach in evaluating the performance of football players in online games. The results are verified and the models are assessed for overfitting through a k-fold cross-validation process.*

Keywords*: Dataset structuring, Football, Machine learning, Player performance*

1. INTRODUCTION

Machine Learning (ML) has emerged as a powerful catalyst, transforming various fields by effectively extracting valuable insights from extensive and complex datasets. Its significance goes beyond technological limitations, profoundly impacting a wide range of industries, including healthcare [1-3], wireless sensor networks [4, 5], sports [6-9], and various other domains [10-12]. In the realm of football, the applications of ML can be categorized into distinct groups, as depicted in Fig. 1.

The prevention and anticipation of injuries are extremely important in the sports industry, significantly affecting the financial stability of sports clubs and team performance. The absence of essential players from games and training sessions due to injury has a significant financial impact, costing the team a total of EUR 188 million annually. The financial burden incorporates various factors, encompassing expenses associated with player recuperation, efforts in rehabilitation, and the salaries of players [13]. Recent empirical studies have emphasized the effectiveness of ML techniques in the injury prediction domain. Additionally, these techniques have demonstrated excellent outcomes for predicting injuries in adult handball and football players [14].

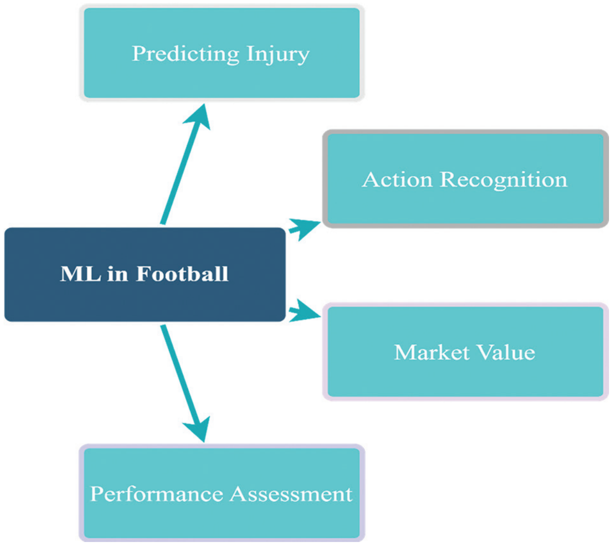

Fig. 1. ML applications in football

Furthermore, ML has proven to be more sensitive in forecasting injuries among young football players who are at an elite level [15].

Furthermore, the game analysis data plays a pivotal role as an essential indicator in action recognition. This data empowers sports physiologists and coaches to enhance the monitoring, evaluation, and design of training plans [16]. As a result, sports analytics has received significant attention in the field of artificial intelligence (AI). Several sources demonstrate how the field of action recognition has significantly advanced due to the amount of precise data [17,18].

Conversely, a player's market value represents an estimation of the sum that a team could be able to get for the sale of their contract to another team. It bears substantial significance in the negotiations between football clubs and the agents representing players. The method used in [19] can provide an objective and quantitative way to estimate the transfer fees and salaries of players, which are usually determined by subjective and non-transparent expert judgments. The paper also analyzes the most important factors that affect the market value of players, such as age, position, skills, and potential. Consequently, in appraising players' market worth, it becomes imperative to take into account their specific skills contingent upon their positional role on the field. The work by [20] introduces an effective approach to forecast the market values of football players by leveraging the FIFA 20 dataset. After implementing the clustering according to the playing area, the model was trained and evaluated each cluster using the regression technique. This method is highly effective in identifying relevant characteristics and simplifies the determination of the market value for the player.

In addition, assessing individual and team performances helps to understand the strategic and successful approach of team sports and is consistent with a fundamental objective of sports science [21]. As a result, ML has become imperative to build professional teams [18, 22, 23].

This work aims to assess the physical performance of football players in training and real match sessions and to introduce intelligent classification methods using ML algorithms. The utilized algorithms are the state of art algorithms used in the sports field and they are commonly used in previous studies. The algorithms are Random Forest (RF) [24], Gaussian Naïve Bayes (GNB) [25], Decision Tree (DT) [26], Logistic Regression (LR) [27], Support Vector Machine (SVM) with linear and radial base function kernels [28], Multi-Layer Perceptron (MLP) [29], and the K-Nearest Neighbor (KNN) [30]. The model implementation used Anaconda 2022.10, Jupyter Notebook 1.0, Scikit-learn library 1.0.2, and Python 3.11. Two separate datasets were constructed: the initial set comprised activity features extracted from player footage during actual match sessions, and the second set employed sensor data to replicate player activity features during training sessions. These datasets were employed for model testing to identify the most effective one for assessing player performance and validating categorization choices. The classifiers demonstrated high accuracies, utilizing important measurable activity features.

The contributions of this work are:

- The proposed method uses ML techniques along with specialized datasets to classify the physical performance of football players during the training and match sessions.
- The proposed models present new datasets one for players metrics during the match session and the second for training session.
- The efficacy of the proposed approach has been evaluated based on specific parameters, including accuracy, precision, recall, and F1-score.

The remainder of the paper is structured as follows: Section 2 provides an overview of the literature, Section 3 outlines the methodology employed in this work, and Sections 4 and 5 present the findings and conclusions, respectively.

2. RELATED WORK

Football is now acknowledged to encompass a wealth of statistical information on seasons, games, clubs, and players. While traditionally considered the domain of specialists and analysts, sports organizations are increasingly recognizing the scientific insights concealed within their data. Accordingly, these organizations have adopted ML technologies to unlock this knowledge and maximize strategic advantages. ML demonstrates the diversity in handling various types of sports data, including match statistics, players' metrics, videos, and time series. The outcomes derived from these technologies contribute significantly to the capabilities of trainers and coaches, aiding in the prediction of match results and player injuries, performance assessment of players, identification of sports talents, recognition of match actions, and estimation of players' market value.

Several studies employing ML techniques to assess player performance have been identified in the domain of football. Notably, Tindaro et al. [31] conducted a study aiming to forecast the physical performance of elite football players, utilizing their anthropometric characteristics. To achieve this, the researchers developed a regression model that incorporated both upper and lower body features to forecast the physical prowess of these players. The investigation involved enrolling sixteen male soccer players under the age of 15, all belonging to the elite group, the study administered the Yo-Yo test to gather the requisite data for the proposed model. The study's findings underscored the significance of the selected characteristics as pivotal indicators of both sprint efficiency and aerobic fitness. It is worth noting, however, that the model's predictive capability exhibited a subpar level. This suggests that factors beyond anthropometric characteristics may play a role in predicting variations in performance among these athletes.

The primary objective of the PlayeRank data-driven framework, as developed and implemented by Luca et al. [32], is to assess and rank soccer players' performances using an extensive dataset of match events. The paper delves into the PlayeRank assessments, revealing significant patterns that illuminate the attributes of exceptional performances and the factors that differentiate elite players. The dataset employed in this study includes millions of match events for 18 major football leagues. Despite the numerous advantages of the paper, it acknowledges certain inherent limitations of the PlayeRank framework. Notably, factors such as tactical arrangements, opponent strength, match results, and other contextual aspects are conspicuously overlooked.

The objective outlined by Ahmet et al. [33] is to employ a ML model for utilizing football players' attributes and performance data to determine their market value. The study employs a dataset encompassing 18,000 players sourced from the Football Manager 2018 game, coupled with their corresponding values from transfermarkt.com. The researchers undertake various preprocessing techniques to appropriately condition the data for modeling purposes. Subsequently, they conduct a comparative analysis of different ML algorithms, including linear regression, decision tree, random forest, and artificial neural networks, to identify the most suitable one for the task at hand. The results indicate that the random forest algorithm surpasses its counterparts, demonstrating superior performance in both mean absolute error (MAE) and coefficient of determination (R2) metrics.

Bartosz et al. [22] explored the use of ML techniques to predict the success of player transfers in professional football. The study defines various parameters for player evaluation, including age, position, goals, assists, passes, and tackles. Three definitions of a successful transfer are proposed, based on player, team, and transfer fee performance. Employing Random Forest, Naive Bayes, and AdaBoost algorithms on data from Transfermarkt, the authors report promising results, suggesting ML's potential in team building and player transfer planning. They propose further development for application as a tool of professional utility for scouts specializing in football talent. However, the study's limitation lies in its reliance on data solely from the English Premier League 2018/2019 season, potentially restricting the generalizability of findings to other contexts and periods.

The primary objective of Mikael et al. [34] was to implement and compare various ML algorithms for the classification of professional goalkeepers' performance levels based on their technical data. The researchers utilize a dataset comprising 14,671 player-match observations from the elite divisions of England, Spain, Germany, and France. Three ML algorithms, namely Logistic Regression, Random Forest Classifier, and Gradient Boosting Classifier are applied in the study. Recursive feature elimination is employed to identify the most crucial features for the classification task. The results suggest that the ability of goalkeepers with their feet is more important than their ability with their hands to distinguish elite and sub-elite performance. In addition, the essential features for predicting goalkeepers' performance levels encompass factors such as passes received, successful passes, short distribution, and clean sheets. However, the lack of information on physical and psychological parameters was the main limitation of this work.

In her study, Didem [35] employs seven distinct ML algorithms to identify the optimal player combination for the U13 team at Altınordu Football Academy. The article integrates data derived from player training sessions and coach evaluations, supplementing the analysis with synthetically generated data to enhance classification accuracy. The findings of the study highlight the utility of ML algorithms in the player selection and team formation processes. Notably, the random forest algorithm emerges as particularly effective, achieving a 93.93% reliability in player selections. Furthermore, the lineup suggestions generated by these algorithms exhibit a remarkable 97.16% similarity to the coach's ideal team. These findings underscore the precision of ML algorithms in addressing player classification challenges. Incorporating additional input data, such as coach assessments and quantitative measurements detailing player talents and position-specific capabilities, could enhance the overall reliability of these results.

These studies offer valuable insights into possible areas for development and propose future avenues for sports-related research, making a crucial contribution to the field of football analytics. Table 1 presents a summary of the preceding research.

Table 1. Preceding research summary

Author	Aim	Limitations
Tindaro et al. [31],2021	To predict elite football players' physical performance	Required specific tests and requirements. It is not suitable for use during training or match sessions. Limited data samples
Luca et al. [32], 2019	To rank the players	The (ball-touches) represent one part of football match actions
Ahmet et al. [33], 2020	To assess the value of football player	-
Bartosz et al. [22], 2021	To predict the transfer success of the players	Data only concerned the male players/leagues.
Mikael et al. [34], 2021	To classify the performance levels	Absent data on physical/ psychological parameters
Didem [35], 2021	To find the best combination of players.	Quantitative data to represent players' skills was missed

3. METHOD: PERFORMANCE EVALUATION ML MODEL (PEMLM)

The assessment of players' performance holds paramount importance, whether during training to optimize future workloads or in matches to empower coaches in strategic decision-making and substitutions. Consequently, this work incorporates both training and match session datasets in the Performance Evaluation Machine Learning Model (PEMLM). Unlike prior works limited by the number of tested samples, this research overcomes such constraints by providing a sufficiently ample sample size, ensuring the generalizability of ML results. Notably, the datasets employed both male and female samples and incorporated quantitative metrics reflective of players' physical skills. An additional aspect often overlooked in previous studies is the consideration of the time necessary for conducting ML tests. In online applications, time emerges as a crucial factor, prompting this work to incorporate it as a key evaluation metric.

3. 1. GENERAL BLOCK DIAGRAM

Various supervised ML models are employed to evaluate the physical performance of football players utilizing recorded features extracted from both match and training sessions. The PEMLM system employs three classes: weak, normal, and active performance for both training and match datasets. The recorded datasets undergo clustering and labeling before the pre-processing step, responsible for dataset reformation to prepare it for training and testing. Subsequently, the datasets are partitioned into training and testing groups, with an 80% and 20% ratio, respectively. The test samples are then fed into the trained ML models to be classified into the three designated classes. Figure 2 provides the complete system as a block diagram.

3. 2. DATASETS STRUCTURING

The dataset in this work comprises two sources: the match session dataset (MSDS) and the training session dataset (TSDS), each containing 2040 samples. The records within these datasets represent the characteristics of an individual player. They serve as inputs to the proposed (ML) model to determine the performance level of the player. This classification is considered a guide for making decisions related to player replacements or game strategy adjustments during matches and for optimizing the training workload.

The datasets utilized in this work undergo various pre-processing techniques to make them suitable for use in the ML models, as illustrated in Figure 3. The two datasets are sourced from different origins, as detailed in the subsequent subsections. Initially, area-based clustering is employed for dataset labeling, utilizing K-Nearest Neighbors (KNN) where n=3 to group players occupying the same field areas (midfielders, forwarders, defenders). Each instance in the group is then associated with one performance level (active or normal or weak). The subsequent step involves removing outliers to identify and eliminate extreme values, reducing the match dataset to 1949 samples, while the number of samples in the training dataset remains unchanged. The normalization phase follows, employing quantile normalization, which proves effective in transforming features into a normal distribution format. Subsequently, stratified sampling ensures the representation of each subgroup in the final sample, enhancing precision and reliability in analyzing the entire population.

3.2.1. MSDS

The data for this work is sourced from actual match videos captured by tactical cameras. Six features are extracted from the adopted videos: ID, Gender, Area, CD, Sp, and AC, along with the Class. The methodology for obtaining the dataset is illustrated in Figure 4 [36]. The definitions of these features are as follows:

ID: Every player in the dataset has a distinctive code, which functions as an identifying record.

G: Using a binary gender classification approach, which assigns a value of 1 to male teams and a value of 0 to female teams.

Area: There are three main categories of playing positions on the field, denoted by numbers: forwards (1), defenders (2), and midfielders (3).

CD: This measure represents the estimated cross-distance traveled by every player while playing.

Sp: This feature gives information about each player's speed and agility.

AC: The activity count metric is represented by a numerical value, it reflects the player's level of engagement in ball touches during the match and interactions with other players.

The CSRT tracker was used in this work to implement the tracking module, utilizing the OpenCV Python library [37]. The KNN unsupervised learning algorithm accomplishes the dataset labeling process where k is set to 3. Accordingly, three discrete classes were generated: active performance denoted by Class 0; weak performance indicating Class 1; and normal performance signifying Class 2. Table 2 views the head from the total of 2040 collected samples of the MSDS. Additionally, the general statistics of the collected dataset are presented in Table 3, while position-based statistical metrics are illustrated in Table 4, where Max and Min represent the maximum and minimum values, respectively, Mean is the mean value for each feature, and STD is the standard deviation.

Table 2. MSDS samples

ID	G	Area	CD	Sp	AC	Class
1	0	2	0.855	5.263	23	2
2	0	2	0.85	5.232	26	0
3	0	2	0.794	4.891	32	0
4	0	2	0.711	4.377	4	1
5	0	3	0.631	3.888	0	1
6	0	3	0.678	4.177	0	1
7	0	3	0.627	3.86	28	0
8	0	3	0.52	3.206	0	1
9	0	1	0.623	3.835	16	2
10	0	1	0.75	4.619	18	2

Table 3. Original MSDS statistics

Statistics	CD	Sp	AC
Max	1.16	7.144	33
Min	0.032	0.2	0
Mean	0.556	3.425	17.62
STD	0.209	1.285	12.28

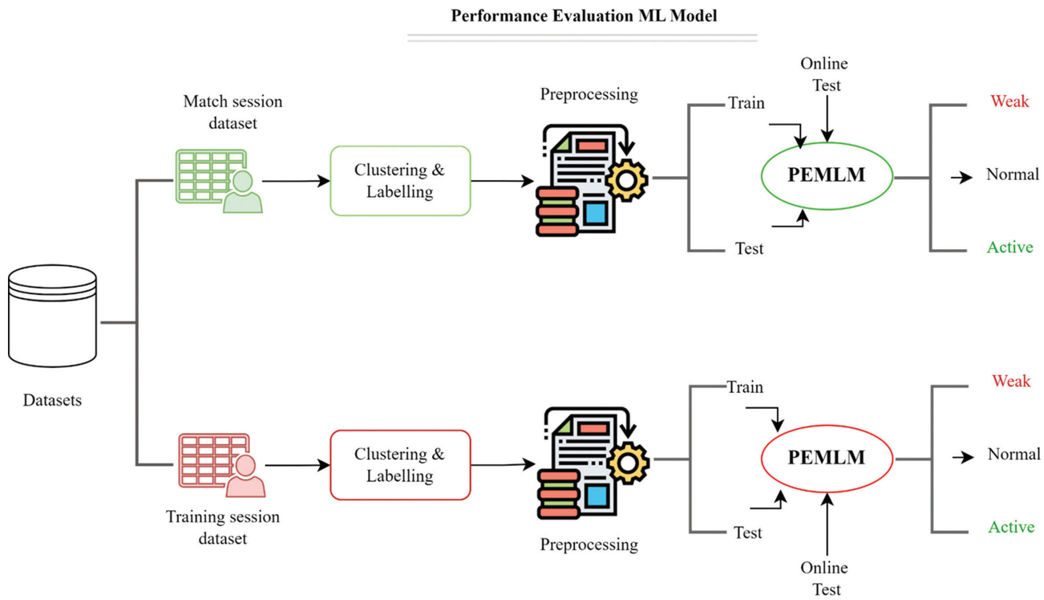

Fig. 2. General block diagram

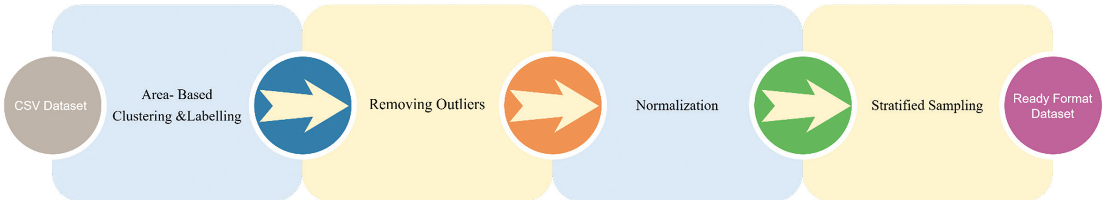

Fig. 3. Dataset pre-processing workflow

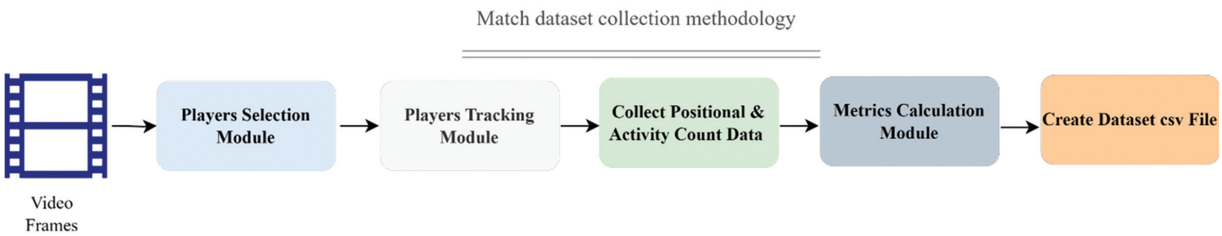

Fig. 4. MSDS collection methodology

Table 4. Area-based statistics

Statistics	CD	Sp	AC
Area 1 = forwarders			
Max	1.16	7.144	33
Min	0.081	0.5	0
Mean	0.556	3.426	16.824
STD	0.208	1.283	12.147
Area 2 = defenders			
Max	1.155	7.114	33
Min	0.032	0.2	0
Mean	0.553	3.409	19.614
STD	0.212	1.308	11.816
Area 3 = midfielders			
Max	1.159	7.135	33
Min	0.032	0.2	0
Mean	0.559	3.442	16.017
STD	0.205	1.261	12.52

3.2.2. TSDS

Precision in gathering data concerning the physiological attributes of soccer athletes holds paramount importance for coaches and trainers, enabling them to make well-informed decisions regarding team selection and the formulation of effective training strategies. Due to the high privacy of football players' data and the unavailability of the necessary data in the literature, synthetic data for 2040 samples are generated to simulate the real values. Tables 5, 6, and 7 showcase examples from the dataset, overall statistics, and playing region statistics, respectively. The MSDS included features such as ID, Gender, and Area, with additional features being incorporated, namely:

Heart Rate (HR): The heart rate is measured by bpm, which indicates the number of beats per minute. Football players' heart rates vary depending on fitness level, age, and playing position. In general, the resting heart rate is 40-60 (bpm), maximum heart rate is about 193.85 ± 5.2 [38], [39].

Oxygen Level (O2): Oxygen level is usually measured by %SpO2, which represents a percentage of oxygen-bound hemoglobin in the blood. Hemoglobin is a blood protein responsible for transporting oxygen to the body's tissues. The standard SpO2 range indicated by pulse oximeters is 95% to 100% [40].

Steps: The tactical effectiveness, work rate, and durability assessment of football players during the match is usually measured by their step count. This feature is used by the coaches to gain insights into the positioning, physical condition, and overall contribution to the game. Continuous monitoring enables the patterns' identification, helping optimize training strategies and playing. Maintaining an optimal step count indicates sustained performance and efficient field coverage. The count increases gradually from zero every ten seconds.

Energy: The vitality of football players significantly influences the team's on-field performance. Adequate energy levels are imperative for optimal running, decision-making, and passing, concurrently mitigating the risk of injuries. Coaches meticulously observe and manage players' energy expenditure, develop a customized training plan, and emphasize appropriate hydration and nutrition to optimize performance. Energy-effective management is essential to reach optimum performance in professional matches. It is important to note that each athlete's energy needs mainly depend on physical activity [41].

Table 5. TSDS sample

ID	G	Area	HR	O2	Steps	Energy	Class
1	0	2	76	92	3	90	1
2	0	2	78	90	14	96	1
3	0	2	76	93	10	92	1
4	0	2	74	92	8	93	1
5	0	3	80	94	8	93	0
6	0	3	74	91	12	91	0
7	0	3	85	80	28	75	2
8	0	3	78	91	18	91	0
9	0	1	96	84	38	84	2
10	0	1	102	80	70	61	0

Table 6. TSDS statistics

Statistics	HR	O2	Steps	Energy
Max	113	94	106	98
Min	73	80	2	48
Mean	88.335	85.313	39.63	79.162
STD	8.919	4.605	22.658	11.327

Table 7. Area-based statistics

Statistics	HR	O2	Steps	Energy
Area 1 = forwarders				
Max	109	94	106	98
Min	74	80	4	50
Mean	88.863	85.196	42.637	79.302
STD	8.76	4.559	23.346	11.368
Area 2 = defenders				
Max	110	94	106	98
Min	73	80	2	48
Mean	87.110	85.191	36.933	79.244
STD	8.677	4.582	22.443	11.16
Area 3 = midfielders				
Max	113	94	100	98
Min	74	80	4	48
Mean	89.295	85.494	40.824	79.011
STD	9.093	4.645	22.226	11.469

3.3. PEMLM ALGORITHM

The PEMLM algorithm provides a comprehensive procedural overview of the proposed models, with a detailed breakdown of the steps elucidated below:

1. Data Pre-processing: The utilized datasets undergo pre-processing, as detailed in Section 3.2.
2. Testing Module: This step involves determining the training or match module.
3. Dataset Selection Module: The type (Training or Match) of the dataset is selected based on the cho-

sen testing module, contingent on the evaluation period.

4. ML Model Training: The ML models are trained on the mentioned datasets to identify the right model for each scenario.
5. Model Testing: All employed algorithms undergo testing using the test sets and validation through a 5-fold validation.
6. Output: Three performance levels are the output of the model (active, normal, and weak).

Recommendations are then adopted based on the session state. For weak performance during a training session, it is suggested to intensify the training workload for the evaluated player. Conversely, in a match session, replacement is recommended. Normal results suggest maintaining or altering the workload, depending on whether it is a training or match session, respectively. Active players are advised to continue playing and training at the existing level.

PEMLM algorithm: Pseudo Code

1. Data Pre-processing
2. Testing module (Training or Match) session
3. Dataset selection module
4. Model Training
5. Model Testing
6. Output

IF (MSDS): THEN
    IF (Weak Performance): THEN Replacement Recommended
    ELSE IF (Normal Performance):
        THEN Playing Strategy Change Recommended
    ELSE (Active Performance): THEN Continue
IF (TSDS) THEN
    IF (Weak Performance):
        THEN Enhance Workload Recommended
    ELSE IF (Normal Performance):
        THEN Training Workload Justification Recommended
    ELSE (Active Performance): THEN Continue

7. END

4. RESULTS

In the preceding section, we applied the PEMLM models to assess the performance of football players using both MSDS and TSDS datasets. The obtained results are categorized into two primary groups based on the dataset type. We employed five metrics to assess the outcomes: accuracy, precision, recall, F1-score, and test time. These metrics are defined by equations (1-4), wherein TP denotes true positives, FP signifies false positives, TN represents true negatives, and FN stands for false negatives. The time denotes the total seconds required to evaluate the model's performance on the test set.

$$accuracy = \frac{TP + TN}{TP + TN + FP + FN} \quad (1)$$

$$precesion = \frac{TP}{TP + FP} \quad (2)$$

$$recall = \frac{TP}{TP + FN} \quad (3)$$

$$F1 - score = 2.\frac{precision\,.recall}{precision + recall} \quad (4)$$

4.1. MSDS RESULTS

The analysis of various ML models applied to MSDS reveals noteworthy performance metrics. The DT model in Table. 8 stands out with impeccable scores of 100% in accuracy, precision, recall, and F1-score, indicating precise and accurate predictions, coupled with an efficient classification time of 0.0032 seconds.

Table 8. MSDS results

Model	Acc	Pre	Rec	F1	Time
DT	100	100	100	100	0.0032 s
RF	99	99	99	99	0.0167 s
LR	97	97	97	97	0.0016 s
GNB	87	89	87	86	0.0022 s
SVM (Linear)	97	97	97	97	0.0022 s
SVM (RBF)	97	97	97	97	0.0019 s
KNN	95	95	95	95	0.0046s
MLP	99	99	99	99	0.0026 s

The RF model exhibits robust performance, securing a commendable 99% across all metrics, albeit with a slightly longer classification time of 0.0167 seconds due to its ensemble approach. LR delivers solid performance with a 97% score across all metrics, accompanied by a swift classification time of 0.0016 seconds. GNB shows respectable performance, although it falls short in comparison, particularly in accuracy and recall, achieving 86%- 89% in these metrics, respectively, with a classification time of 0.0022 seconds. The linear and (RBF) SVM both achieve an impressive 97% in all measures; the linear SVM takes 0.0022 seconds, while the RBF SVM takes 0.0019 seconds, which is a little faster. KNN performs admirably, scoring 95% on every metric, however, it takes 0.0046 seconds longer to classify data than other algorithms. The MLP model has a reasonable classification time of 0.0026 seconds and scores 99% on accuracy, precision, recall, and F1-score, matching the top-performing models across all criteria. Finally, the models exhibit varied levels of performance, with DT, RF, LR, and MLP emerging as top performers, stressing the significance of evaluating both accuracy and time based on online application needs. The confusion matrix for the highest accuracy model is shown in Fig. 5.

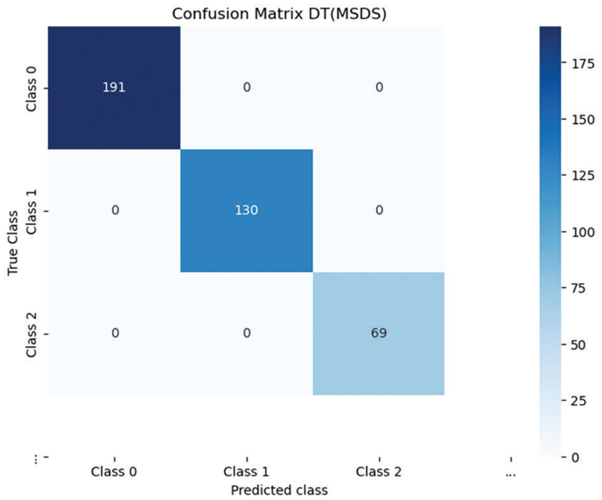

Fig. 5. Confusion matrix for DT model

4.2. TSDS RESULTS

The examination of the performance metrics for diverse ML models applied to the training session dataset reveals distinctive outcomes. DT, RF, GNB, and MLP demonstrate a relatively consistent accuracy range of 68-71%, reflecting balanced performance across metrics such as precision, recall, and F1-score. These models exhibit a comparable processing time, with DT and RF requiring 0.0029 seconds and 0.0272 seconds, respectively, showcasing efficiency in their computations. In contrast, LR and (SVM) (both Linear and RBF) display lower accuracy ranging from 50-58%, suggesting less optimal performance in classification tasks. KNN, however, stands out with an impressive accuracy of 96%, indicating strong predictive capabilities. KNN is good when the basic patterns in the data are clearly represented by the distances between samples. These results underscore the importance of considering both accuracy and computational time, with certain models showcasing more balanced performance across the evaluated metrics. The KNN and MLP are preferred for online applications. The classification performance metrics for the proposed models are listed in Table 9 and the confusion matrix for the best-fit model is presented in Fig. 6.

Table 9. TSDS results

Model	Acc	Pre	Rec	F1	Time
DT	68	68	68	68	0.0029 s
RF	68	68	68	68	0.0272 s
LR	50	47	50	48	0.0011 s
GNB	70	69	70	70	0.0025 s
SVM (Linear)	58	55	58	54	0.00167 s
SVM (RBF)	50	47	50	41	0.0015 s
KNN	96	96	96	96	0.0033 s
MLP	71	70	71	70	0.0037 s

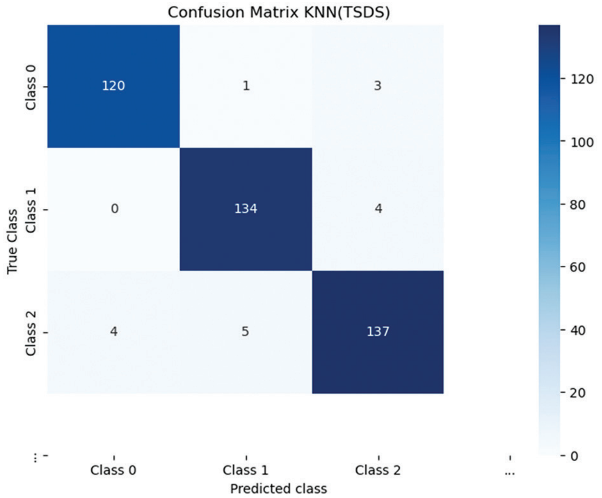

Fig. 6. Confusion matrix for KNN model

4.3. VALIDATION AND COMPARISONS WITH PREVIOUS WORK

The k-fold cross-validation process is used to validate the results and ensure that the models don't have an overfitting problem. The outcomes as presented in Table 10 for both datasets, reveal consistent accuracy, precision, recall, and F1-score across different models. Specifically, for the MSDS, both DT and MLP exhibit identical accuracy levels. Conversely, when assessed on the testing data within the training dataset, KNN demonstrates the best performance in correct classification compared to the other models. The overfitting problem is not observed in all models. The 5-fold performance for all models is illustrated in Figures 7 and 8 for the MSDS, while Figures 9,10, and 11 presented the models' performance validation of the training dataset.

The proposed models operate on both training and match sessions, providing a comprehensive assessment and classification of football player performance. Focusing on match session data, we scrutinized four crucial physical activity metrics: playing position, total distance covered during play, speed during play, and a novel metric gauging player activities during a match. In the case of the training session dataset, synthetic data was employed to simulate the authentic metrics due to the unavailability of an actual dataset, driven by privacy concerns. The selected features have been substantiated in the existing literature as reliable indicators for gauging the physical performance of players. These datasets are utilized in supervised ML models to evaluate players' physical performance.

Table 10. 5-fold cross-validation results

	Model	Avg Acc	Avg Pre	Avg Rec	Avg F1	Avg Time
Match session dataset	DT	100	100	100	100	0.0032 s
	MLP	100	100	100	100	0.0026 s
	GNB	68	66	68	67	0.0024 s
Training session dataset	MLP	71	70	71	71	0.0037 s
	KNN	94	94	94	94	0.0033 s

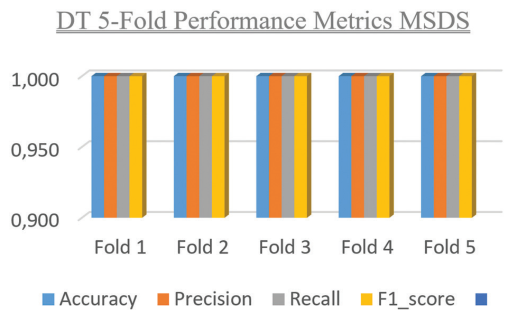

Fig. 7. DT 5-fold cross-validation (MSDS)

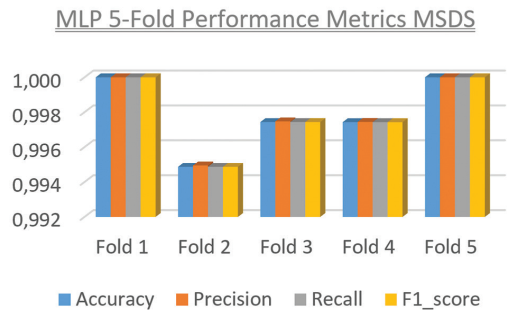

Fig. 8. MLP 5-fold cross-validation (MSDS)

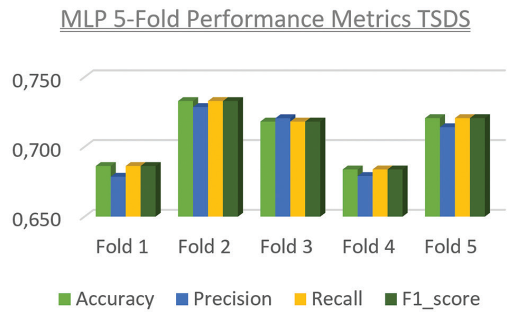

Fig. 9. MLP 5-fold cross-validation (TSDS)

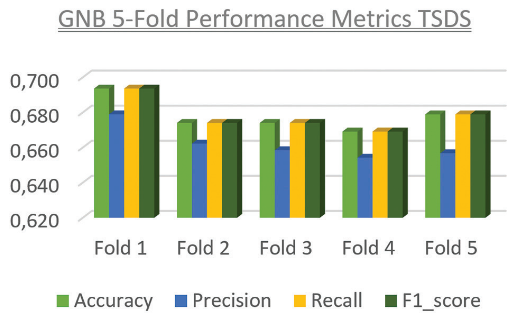

Fig. 10. GNB 5-fold cross-validation (TSDS)

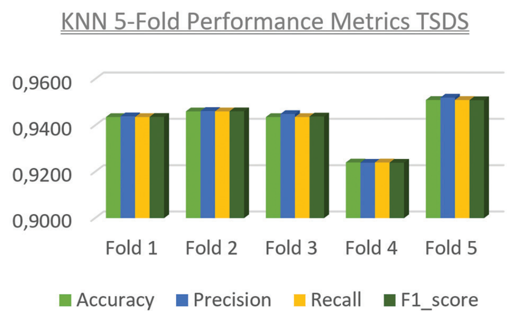

Fig. 11. KNN 5-fold cross-validation (TSDS)

The findings underscore the resilience and effectiveness of the proposed methodology in terms of time efficiency, accuracy, and suitability for integration into online applications. In contrast to the studies presented by [22], [24-27], the PEMLM handles substantial datasets derived from both training and match sessions. The inclusivity of a diverse set of studied features ensures a robust evaluation of players, distinguishing it from the approach in [25], where the prediction of physical performance relies on ball-touch descriptions. Notably, the introduced ML models account for dataset samples from both male and female players, offering a more comprehensive perspective compared to prior studies that exclusively analyzed male samples. Additionally, the considered features in PEMLM encompass the physical skills of players, addressing a gap apparent in the works of [26] and [27].

5. CONCLUSION

In this paper, we present an innovative approach to constructing datasets for the evaluation of football player performance in training and match sessions. The method leverages various ML models and features to train these models effectively. The proposed methodology undergoes a comprehensive evaluation, considering key metrics such as accuracy, precision, recall, and F1 score. Additionally, the validation process employs a robust 5-fold cross-validation technique. Our experimental results reveal that the proposed DT model attains an exceptional classification accuracy of 100% when applied to match session datasets. Conversely, the KNN model demonstrates superior performance when applied to training session datasets. We are confident that the implementation of these techniques will prove invaluable to coaches and trainers, streamlining the task of evaluating physical player performance. This, in turn, will enhance strategic decision-making during matches and optimize training session workloads. Consequently, both models exhibit potential for integration into online systems. We advocate exploring the feasibility of implementing the proposed PEMLM for real-time predictions during live matches. It is crucial to acknowledge and address the challenges associated with real-time data processing and model deployment, paving the way for future research endeavors. Additionally, a more nuanced analysis of gender-based performance patterns could reveal potential differences in play styles or strategies between them.

6. REFERENCES:

[1] L. Abdullah, A. Mazin, N. Ahmed, K. Seifedine, H. Karrar, N. Jan, M. Radek, R. Imran, “Restricted Boltzmann machine assisted secure serverless edge system for internet of medical things”, IEEE Journal of Biomedical and Health Informatics, Vol. 27, No. 2, 2022, pp. 673-683.

[2] A. M. Abdulrahman, A. Belal, A.M. Mazin, “Breast cancer images Classification using a new transfer

learning technique", Iraqi Journal for Computer Science and Mathematics, Vol. 4, No. 1, 2023, pp. 167-180.

[3] A. M. Mazin, L. Abdullah, A. Z. Dilovan, Karrar A. Hameed, N. Jan, M. Radek, T. Usman, A. Majed, T. Prayag, "Adaptive secure malware efficient machine learning algorithm for healthcare data", CAAI Transactions on Intelligence Technology, 2023. (in press)

[4] H. S. Sama, S. C. Muayad, "Increasing WSN Lifetime using Clustering and Fault Tolerance Methods", Iraqi Journal for Electrical and Electronic Engineering, Vol. 17, No. 1, 2021, pp. 94-99.

[5] H. A. Sahar, N. Ahmed, "Prediction of Single Object Tracking Based on Learning Approach in Wireless Sensor Networks", Proceedings of the 14th International Conference on Developments in eSystems Engineering, Sharjah, United Arab Emirates, 7-10 December 2021, pp. 352-357.

[6] J. Rong, "Research on Basketball Shooting Action Based on Image Feature Extraction and Machine Learning", IEEE Access, Vol. 8, 2020, pp. 138743-138751.

[7] G. Brandon, P. Peter, K. Stephanie, R. Machar, "Differentiating movement styles in professional tennis: A machine learning and hierarchical clustering approach", European Journal of Sport Science, Vol. 23, No.1, 2021, pp. 44-53.

[8] O. Musa, T. Cevdet, S. Boran, A. Caner, U. Y. Hasan, "Performance Prediction and Evaluation in Female Handball Players Using Machine Learning Models", IEEE Access, Vol 8, 2020, pp. 116321-116335.

[9] B. Daniel, L. Phillippe, D. Werner, "Incorporating domain knowledge in machine learning for soccer outcome prediction", Machine Learning, Vol. 108, No. 1, 2019, pp. 97-126.

[10] T. A. Saja, A. Rafah, S. C. Muayad, "Enhancement of student performance prediction using modified K-nearest neighbor", TELKOMNIKA, Vol. 18, No. 4, 2020, pp. 1777-1783.

[11] A. U. Masar, S. C. Muayad, "Multiclassification of license plate based on deep convolution neural networks", International Journal of Electrical and Computer Engineering, Vol. 11, No. 6, 2021, pp. 5266-5276.

[12] K. S. Abrar, N. R. Ahmed, "Applications of machine learning for earthquake prediction: A review", Proceedings of the Al-Kadhum 2nd International Conference on Modern Applications of Information and Communication Technology, Baghdad, Iraq, 8-9 December 2021.

[13] R. Alessio, P. Luca, "A Narrative Review for a Machine Learning Application in Sports: An Example Based on Injury Forecasting in Soccer", Sports, Vol. 10(1), No. 5, 2022, pp. 1-16.

[14] L. O. Jon, A. Francisco, D. S. C. Mark, L. S. Rhodri, D. M. Greg, J. R. Paul, "Using machine learning to improve our understanding of injury risk and prediction in elite male youth football players", Journal of Science and Medicine in Sport, Vol. 23, No. 11, 2020, pp. 1044-1048.

[15] V. Emmanuel, S. Nicolas, I. Abdelhak, M. Jacky, P. Stephane, "Combining Internal- and External-Training-Loads to Predict Non-Contact Injuries in Soccer", Applied Sciences, Vol. 10, No. 15, 2020, p. 5261.

[16] G. Abraham, M. Moisés, C. Javier, R. Asier, L. Sergio, "In-game behavior analysis of football players using machine learning techniques based on player statistics", International Journal of Sports Science & Coaching, Vol. 16, No. 1, 2021, pp. 148-157.

[17] G. Yaparla, S. T. Allaparthi, K. M. Sai, R. M. Garimella, "A Novel Framework for Fine-Grained Action Recognition in Soccer", Proceedings of the International Work-Conference on Artificial Neural Networks, Gran Canaria, Spain, 12-14 June 2019, pp. 137-150.

[18] L. Guiliang, L. Yudong, S. Oliver, K. Tarak, "Deep soccer analytics: learning an action-value function for evaluating soccer players", Data Mining and Knowledge Discovery, Vol. 34, 2020, pp. 1531-1559.

[19] A. A. Mustafa, T. Sakir, "Predict the Value of Football Players Using FIFA Video Game Data and Machine Learning Techniques", IEEE Access, Vol. 10, 2022, pp. 22631-22645.

[20] B. Iman, M. R. Seyed, "A novel machine learning method for estimating football players' value in the transfer market", Soft Computing, Vol. 3, No. 1, 2020, pp. 2499-2511.

[21] K. Shitanshu, S. Sergiy, Y. Zhu, G. Paul, A. Maya, "Machine Learning Enabled Team Performance

Analysis in the Dynamical Environment of Soccer", IEEE Access, Vol. 8, 2020, pp. 90266-90279.

[22] Ć. Bartosz, G. Agata, C. Michal, "Who Will Score? A Machine Learning Approach to Supporting Football Team Building and Transfers", Entropy, Vol. 23, No. 1, 2021, p. 90.

[23] L. G. B. Tom, G. P. F. Wouter, M. N. A. Susan, R. M. Rob, J. R. Ruud, "How soccer scouts identify talented players", European Journal of Sport Science, Vol. 22, No. 7, 2022, pp. 994-1004.

[24] K. H. Tin, "Random Decision Forests", Proceedings of the 3rd International Conference on Document Analysis and Recognition, Montreal, QC, Canada, 14-16 August 1995, pp. 278-282.

[25] B. Thomas, "An Essay Towards solving problem in the doctrine of chances", Royal. Society, Vol. 53, 1997, pp. 370-418.

[26] R. Q. John, "Induction of Decision Trees", Machine Learning, Vol. 1, 1986, pp. 81-106.

[27] A. Žilinskas, "Reviewed Work(s): Practical Mathematical Optimization: An Introduction to Basic Optimization Theory and Classical and New Gradient-Based Algorithms", INFORMS, Vol. 36, No. 6, 2006, pp. 613-615.

[28] C. Corinna, V. Vladimir, "Support-Vector Networks", Machine Learning, Vol. 297, 1995, pp. 273-297.

[29] M. T. Hagan, "Neural network design, Second Edition", 2nd Edition, PWS Publishing Co., 2003.

[30] G. Jacob, E. H. Geoffrey, R. Sam, R. S. Russ, "Neighborhood Components Analysis", Proceedings of the 17th International Conference on Neural Information Processing Systems, Vancouver, BC, Canada, 1 December 2004, pp. 513-520.

[31] B. Tindaro, T. Athos, C. Luca, R. Alessio, P. Enrico, P. Giulio, F. M. Laia, A. Giampietro, "Importance of anthropometric features to predict physical performance in elite youth soccer: a machine learning approach", Research in Sports Medicine, Vol. 29, No. 3, 2021, pp. 213-224.

[32] P. Luca, C. Paolo, F. Paolo, M. Emanuele, P. Dino, G. Fosca, "PageRank: Data-driven Performance Evaluation and Player Ranking in Soccer via a Machine Learning Approach", ACM Transactions on Intelligent Systems and Technology, Vol. 10, No. 5, 2019, pp. 1-27.

[33] T. Y. Ahmet, S. Barış, K. Tolga, "Football Player Value Assessment Using Machine Learning Techniques", Proceedings of the Intelligent and Fuzzy Techniques in Big Data Analytics and Decision Making: Proceedings of the INFUS 2019 Conference, Istanbul, Turkey, 23-25 July 2020, pp. 289–297.

[34] J. Mikael, P. Ashwin, M. Saumya, B. Marco, M. Daniel, C. Mark, "Using multiple machine learning algorithms to classify elite and sub - elite goalkeepers in professional men' s football", Scientific Reports, Vol. 11, 2021, p. 22703.

[35] A. Didem, "A case study on player selection and team formation in football with machine learning", Turkish Journal of Electrical Engineering and Computer Sciences, Vol. 29, No. 3, 2021, pp. 1672-1691.

[36] M. M. Baydaa, S. C. Muayad, N.R. Ahmed, "Football player tracking and performance analysis using the OpenCV library", Mathematical Modelling of Engineering Problems, Vol.11, No. 1, 2024, pp. 123-132.

[37] L. Alan, V. Tomas, C. Z. Luca, M. Jiri, K. Matej, "Discriminative Correlation Filter Tracker with Channel and Spatial Reliability", Proceedings of the IEEE Conference on Computer Vision and Pattern Recognition, Honolulu, HI, USA, 21-26 July 2017, pp. 671-688.

[38] R. Vincenzo, K. Peter, M. Rafael, R. Antonio, M. Magni, "Training load and submaximal heart rate testing throughout a competitive period in a top-level male football team", Journal of Sports Sciences, Vol. 38, No. 11-12, 2020.

[39] A. Aşçı, "Heart Rate Responses during Small Sided Games and Official Match-Play in Soccer", Sports, Vol. 4(2), No. 31, 2016, pp. 11-14.

[40] G. Chiara, C. Emanuele, C. Andrea, N. Stefano, B. Carmine, C. Carlo, G. Michele, "COVID-19 disease in professional football players: symptoms and impact on pulmonary function and metabolic power during matches", Physiological Reports, Vol. 10, No. 11, 2022, pp. 1-11.

[41] D. Hubert, K. Aleksandra, W. Dariusz, "Nutrition for Female Soccer Players Recommendations", Medicina, Vol. 56, No. 1, 2020, pp. 28-44.

Quantum Computing in The Cloud – A Systematic Literature Review

Review Paper

Amirul Asyraf Zhahir
Universiti Sains Islam Malaysia,
Faculty of Science and Technology,
Bandar Baru Nilai, Negeri Sembilan, Malaysia
asyrafzhahir@gmail.com

Siti Munirah Mohd
Universiti Sains Islam Malaysia,
Kolej PERMATA Insan,
Bandar Baru Nilai, Negeri Sembilan, Malaysia
smunirahm@usim.edu.my

Mohd Ilias M Shuhud
Universiti Sains Islam Malaysia,
Faculty of Science and Technology,
Bandar Baru Nilai, Negeri Sembilan, Malaysia
ilias@usim.edu.my

Bahari Idrus
Universiti Kebangsaan Malaysia,
Center for Artificial Intelligence Technology (CAIT),
Faculty of Information Science and Technology
Bangi, Selangor, Malaysia
bahari@ukm.edu.my

Hishamuddin Zainuddin
Xiamen University Malaysia,
Department of Physics,
School of Mathematics and Physics,
Sepang, Selangor, Malaysia
hishamuddinz@gmail.com

Nurhidaya Mohamad Jan
Universiti Sains Islam Malaysia,
Kolej PERMATA Insan,
Bandar Baru Nilai, Negeri Sembilan, Malaysia
nurhidaya.mj@usim.edu.my

Mohamed Ridza Wahiddin
Universiti Sains Islam Malaysia,
Tahmidi Centre,
Bandar Baru Nilai, Negeri Sembilan, Malaysia
mridza@usim.edu.my

***Abstract** – Quantum computing was proposed to simulate processes that surpass the capabilities of its counterpart, classical computing. Utilizing the principles of quantum mechanics, it improves the computing power of quantum computing. Top developers namely IBM, Rigetti, D-Wave, Qutech and Google have invested greatly in the technology. Nowadays, users can access the quantum computing system publicly over the network in a cloud environment, this system architecture is known as cloud-based quantum computing. However, different developers deliver different architecture and functionality of the system on their platforms. This has indirectly spawned a question of which cloud-based quantum computing platform is a better option based on certain specific requirements by an individual or group. The main objective of this study is to provide a proposed framework using the existing cloud-based service of quantum computing based on previous studies for users with their specific demands.*

***Keywords**: cloud-based quantum computing, quantum processors, quantum software development kits, quantum simulators*

1. INTRODUCTION

Quantum computing was initially intended to simulate processes surpassing the capabilities of its counterpart [1-7]. The core concept of quantum computing was principally harnessed from quantum mechanics [8, 9]. The main difference between quantum and classical mechanics is that quantum mechanics observes objects microscopically while classical mechanics observes objects macroscopically.

Same train but different coaches, quantum mechanics and classical mechanics are both extremely important in physics. In quantum computation, it harvested these main elements from quantum mechanics namely quantum entanglement, qubit (quantum bit) and superposition [10-13]. Substantially, combining these elements would definitely elevates the computing power in quantum computer.

Quantum entanglement is one of the most explored features in quantum mechanics, which is a critical element in areas, especially quantum computing. This feature is a catalyst in demonstrating the advantage of quantum computing over its adversary, classical computing. Qubit (quantum bit) is the basic unit of information carried in quantum information.

To put it into perspective, classical computing uses bit (0s or 1s) to carry its information while qubit (0s and 1s) is used in quantum computing [14-16]. A qubit vector state unit can be presented as $|0\rangle = \begin{bmatrix} 1 \\ 0 \end{bmatrix}$ and $|1\rangle = \begin{bmatrix} 0 \\ 1 \end{bmatrix}$.

Superposition may be described as a quantum system that is in multiple states at a given time until it is interrupted, usually by measurement [17, 18]. Created by entangled quantum subsystem, superposition exists when two or more quantum states are overlapped, it produces another valid quantum state. Mathematically, it can be denoted as $|\psi\rangle=\alpha|0\rangle+\beta|1\rangle$.

The attention towards quantum computing, a subdivision of quantum information theory has been growing over the past years not only in scientific research domain but also the industrial technology [19]. Some leading companies namely IBM, Google, Rigetti, D-Wave and Intel are investing greatly in developing the technology [20, 21]. Aside from private sector players, some countries are also joining the race for quantum technologies, including the United States, China, Britain and others [22]. It is not surprising as quantum technologies could be a significant asset, or even a threat for some.

Harnessing the principles of quantum mechanics, the quantum computing power has been growing over the years, demonstrating its capabilities over classical computing in solving complex problems in remarkable amount of time [23, 24]. Experts refer this as achieving the quantum supremacy or quantum advantage [25]. Quantum computing may definitely revolutionize various areas such as cryptography, chemistry, finance and machine learning [26-37].

Preskill [38] coined the term NISQ era, which stands for Noisy Intermediate-Scale Quantum, referred the phrase "Noisy" to be the inability to perfectly control the qubits [39, 40]. While the phrase "intermediate-scale" to be the size of quantum processors, suggested the range to be between 50 to a few hundred qubits is the milestone. This has been proven by top developers such as IBM and Google as they have developed quantum computing devices in the range asserted [41, 42].

Even though a considerably massive progress has been achieved in quantum computing, it is still a long way to go for quantum computer to be a reliable and fault-tolerant device. That said, the vigorously expanding technology should be regarded as a step towards developing a more powerful quantum computing in the future [25].

The goal to provide access of the functional quantum device to research community, clients and public users has yielded a new computer system architecture; cloud-based quantum computing [43, 44]. It serves as a connection medium between users and the quantum systems through the network via classical devices, which allows users to access the technology through the quantum cloud without even the need to have a physical quantum device.

Furthermore, these cloud-based quantum computing platforms came with software packages namely IBM's Qiskit, Google's Cirq and Rigetti's Forest which enable users to create and execute quantum algorithms on the platforms [45]. These providers also provide a manual as a guideline to use their respective quantum computing platforms.

Different developers deliver a different architecture design and functionality of their cloud-based quantum computing platforms [20, 46]. For instance, IBM's quantum computing platform enables users to do visual programming as well as code programming, while Qutech's quantum computing platform only allows users to do code programming. These indirectly prompted a dispute on which cloud-based quantum computing platforms are the most suitable for one, according to one's objective and specification on solving a complex computational problem or even exploring the technology.

In this context, this study aims to provide a general overview on the quantum computing technology, identify several existing cloud-based quantum computing platforms as well as providing a proposed framework of using the existing service of quantum computers for potential users; physicists, computer scientist, researchers, and beginners based on their specific needs, leveraging the existing cloud-based quantum computing platforms.

Contemplating from previous studies, a comprehensive analysis of various cloud-based quantum computing platforms and their functionalities is presented. By considering the specific needs, demands and skills of individual users or groups, the proposed framework aims to assist in selecting the optimal cloud-based quantum computing platform.

The significance of this review lies in its potential to layout a guide map for users in deciding the best possible options of the available platforms. By offering a systematic evaluation and comparison of the platforms' architectures and functionalities, aligned with the specific requirements set, this review is set to enhance the accessibility and usability experience of cloud-based quantum computing systems.

This paper is organized as follows. Section 2 describes the research methodology in detail. Section 3 discusses the foundations of quantum computing with the proposed conceptual framework and section 4 concludes the study.

2. MATERIALS AND METHODS

Publication standards implemented in this study will be discussed in this section which include items; (1) review protocol, (2) research question formulation, (3) systematic searching strategy, (4) quality appraisal, and (5) data extraction and analysis. Preferred Reporting Items for Systematic Review and Meta-analysis (PRISMA) were used as the review protocol.

2.1. PRISMA REVIEW PROTOCOL

PRISMA review protocol was used in the study [47]. The systematic literature review was conducted on the guidance of the review protocol by formulating the research questions, systematic searching strategy, the appraisal of quality and the extraction and analysis of data. The scope of research determined was cloud-based quantum computing.

2.2. RESEARCH QUESTION FORMULATION

Research questions formulated in preliminary phase serve as a guidance in conducting the systematic literature review. In accordance with the research objectives which are to provide a general overview on the quantum computing technology, identify several existing cloud-based quantum computing platforms as well as providing a proposed framework of using the existing service of quantum computers for potential users based on their specifications. The research questions formulated are: (1) What is quantum computing? (2) What are the existing quantum computing platforms for users to use or explore? (3) Which quantum computing platforms are best for users based on their specific needs?

2.3. SYSTEMATIC SEARCHING STRATEGY

The systematic searching strategy used in the study is based on these elements: identification, screening and eligibility.

2.3.1. Identification

Relevant published indexed articles and other additional sources for the review was determined at this level. Indexed articles were primarily selected from the two of the most powerful multidisciplinary search engines, Scopus and Web of Science (WOS), as well as Google Scholar as an additional database. As part of a thorough search, field tags "TITLE-ABS-KEY" (title, abstract, keyword) was used in Scopus search engine, while "TS" (topic) was used in WOS. Search strings were generated with specific keywords mainly cloud-based quantum computing, quantum cloud and cloud quantum computing divided from a complex sentence into parts to frame the subject matter more precisely in searching (see Table 1).

The search process was conducted in June 2022. Related articles derived from the same keywords were handpicked manually from Google Scholar database. A total of 1636 potential related articles were identified in the process from Scopus and WOS database through systematic searching and 178 articles were downloaded for further analysis. Moreover, an additional 3 articles were added from Google Scholar database in the process. Fig. 1 depicted the search results of systematic searching in Scopus and WOS database.

Table 1. Systematic literature review search string

Database	Search strings
Scopus	TITLE-ABS-KEY ((quantum) AND (software OR platform OR emulator* OR simulator* OR processor*))
	TITLE-ABS-KEY ((quantum*) AND (cloud* OR "cloud computing" OR "computing simulator*" OR "computing software*" OR "software platform*" OR "virtual machine" OR "computer simulator*" OR " cloud service" OR "cloud computing platform" OR "cloud-based computing"))
	TITLE-ABS-KEY ((quantum*) AND (cloud* OR "cloud computing" OR "computing simulator*" OR "computing software*" OR "software platform*" OR "virtual machine" OR "computer simulator*" OR " cloud service" OR "cloud computing platform" OR "cloud-based computing")) AND (LIMIT-TO (PUBYEAR,2022) OR LIMIT-TO (PUBYEAR,2021) OR LIMIT-TO (PUBYEAR,2020))
WOS	TS=((quantum) AND (software OR platform OR emulator* OR simulator* OR processor*))
	TS = ((quantum*) AND (cloud* OR "cloud computing" OR "computing simulator*" OR "computing software*" OR "software platform*" OR "virtual machine" OR "computer simulator*" OR " cloud service" OR "cloud computing platform" OR "cloud-based computing"))
	TS = ((quantum*) AND (cloud* OR "cloud computing" OR "computing simulator*" OR "computing software*" OR "software platform*" OR "virtual machine" OR "computer simulator*" OR " cloud service" OR "cloud computing platform" OR "cloud-based computing")) – 2020-2022

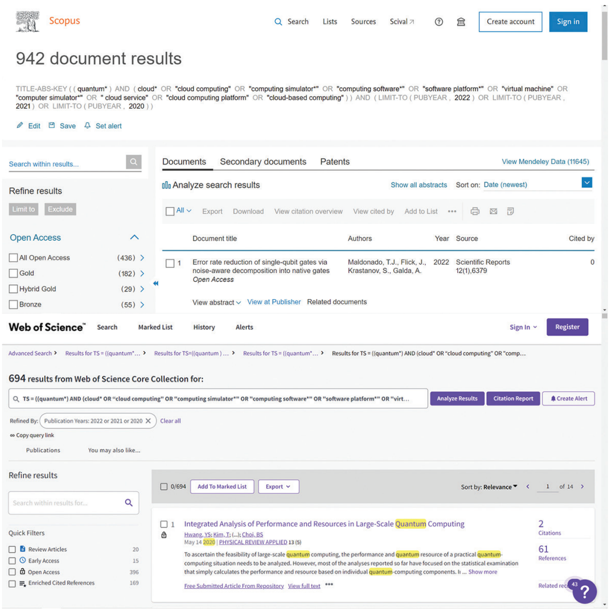

Fig. 1. Search results in Scopus and WOS databases

2.3.2. Screening

In this study, the indexed articles on the subject matter reviewed were selected based on articles published between 2015 to 2022. The maturity of the subject influenced the chosen 7-year period [48]. A total of 87 from 181 downloaded articles were excluded due to duplication of articles in both Scopus and WOS databases. The remaining articles were examined thoroughly to ensure they all meet the inclusion and exclusion criteria set in the preliminary phase. The criteria of both inclusion and exclusion were the subject matter, the type of articles, publication year and the language of articles (see Table 2).

2.3.2. Eligibility

The remaining 94 articles from screening level were then reviewed again for the suitability of the study in this level. A thorough observation was done, removing 16 articles based on their research theme which did not suit the direction of this study, cloud-based quantum computing. The remaining 78 articles were then prepared for quality appraisal (see Fig. 2).

Table 2. Inclusion and exclusion criteria

Inclusion criteria	Exclusion criteria
Articles related to the keywords "cloud-based quantum computing", "quantum cloud" and "cloud quantum computing"	Articles written in language other than English
Indexed journal articles	Articles published before 2015

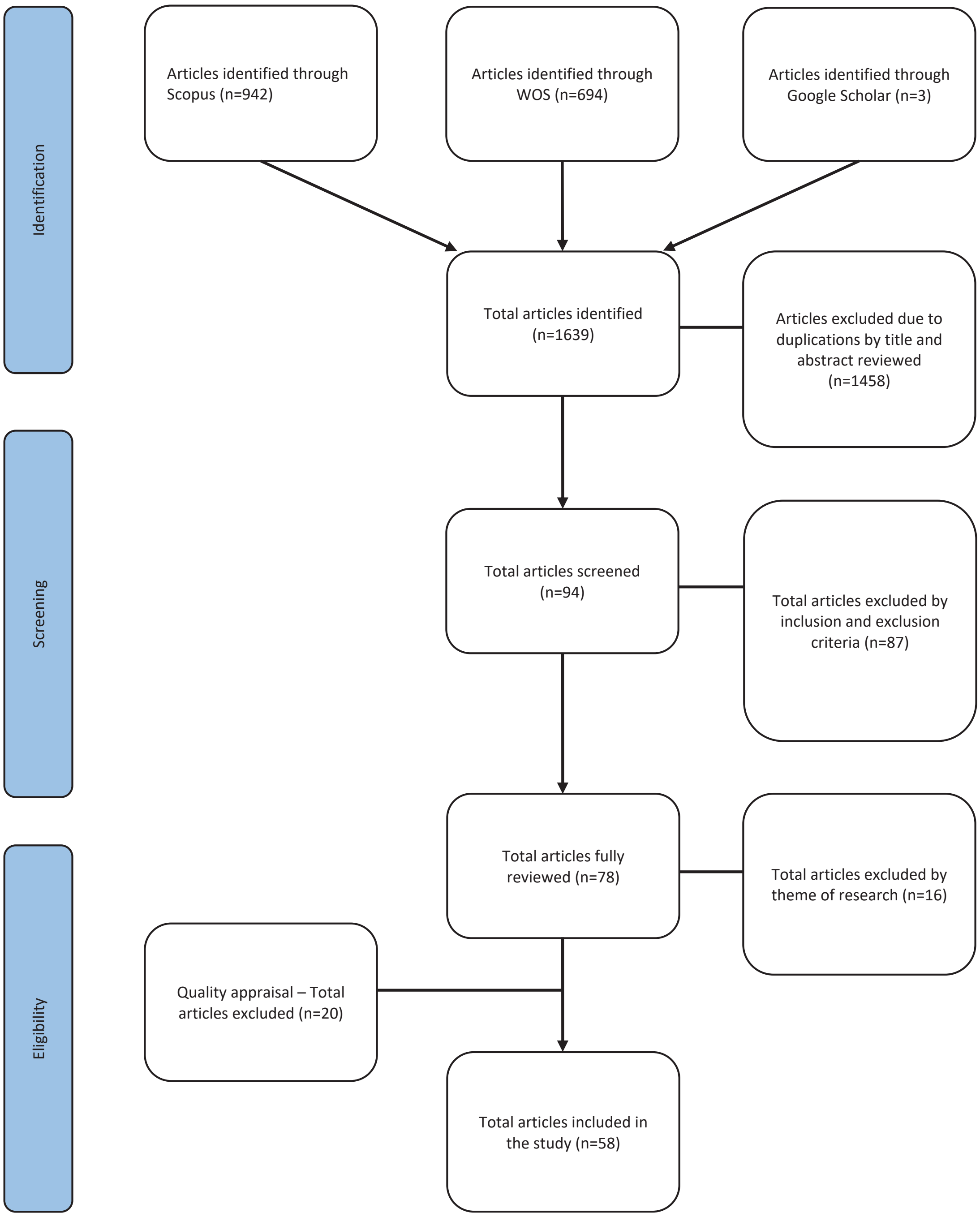

Fig. 2. Articles selection process

2.4. QUALITY APPRAISAL

In the quality appraisal phase, the remaining 78 articles selected were presented to an expert to make certain of the standard of articles used in the study. According to Petticrew & Roberts [49], the remaining articles obtained after a thorough filtering process should be ranked as high, moderate or low quality, with only high and moderate ranked standard quality articles should be included in the study.

Specific elements, namely theme, objective and results of the articles were focused by the expert to meet the standard. As a result, a total of 20 articles were excluded and the remaining 58 articles were determined suitable for the study.

2.5. DATA EXTRACTION AND ANALYSIS

In depth analysis was observed to extract relevant data from the articles. This process undergone several steps namely analysing the abstract, discussion and conclusion section, then finally the body of the articles.

The extracted data were then tabulated in Microsoft Word software in a local device for further analysis. The articles selected can be divided into groups based on the published year (see Fig. 3). There was an article published in both 2015 and 2016, 2 articles in 2018, 6 articles in 2019, 17 articles in 2020, 23 articles in 2021 and finally, 8 articles in 2022. The main theme determined of the extracted data is cloud-based quantum computing platforms. The theme will be discussed in the next section.

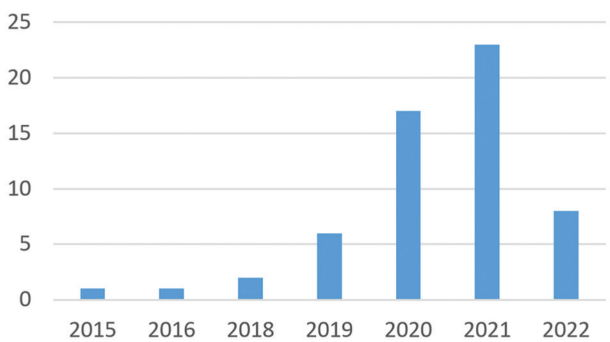

Fig. 3. Articles group by published year

3. RESULTS AND DISCUSSION

This section discusses the theme determined, the foundations of quantum computing technology comprising of the cloud-based quantum computing, quantum computing processors, quantum software development kits, quantum computing simulators and proposed conceptual framework.

3.1. CLOUD-BASED QUANTUM COMPUTING

Cloud-based quantum computing provides a quantum computing platform that can be accessed by anyone in a cloud environment which allows users to perform quantum processing tasks. Fig. 4 depicts the connection between users and quantum systems through quantum cloud.

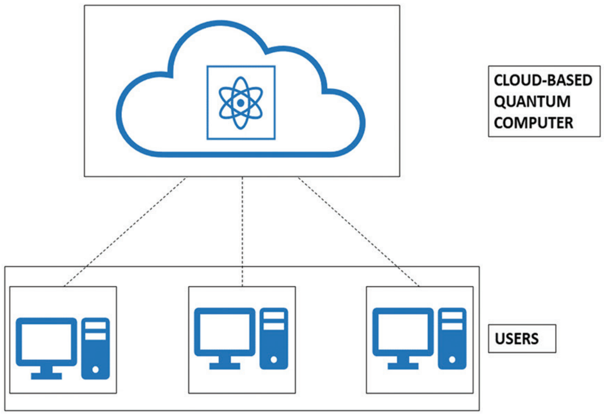

Fig. 4. Connection between users and quantum systems through quantum cloud

Leading developers of the technology have been adapting the quantum cloud concept and making it accessible for the public. Table 3 shows several existing cloud-based quantum computing platforms.

Among all available cloud-based quantum computers, it was determined that based on 58 articles accepted after quality appraisal, the used cloud-based quantum computer was summarized in Table 4. Additionally, it was determined that several articles had addressed numbers of cloud-based quantum computing platforms in its articles [20, 46, 50-59].

As shown in Fig. 5, it has been determined that the most used cloud-based quantum computing platforms from previous studies were by IBM, followed by Rigetti, D-wave, Honeywell, Qutech, Intel, IonQ, Google and Amazon.

In accordance with the pillar of this study, it can be concluded that the platform provided by IBM is the most highly acceptable platform among users. This could immensely influence the existing or potential users in the future and could also possibly shape the future of cloud-based quantum computing platforms architectures. Table 4 shows the cloud-based quantum computing platforms used in previous studies.

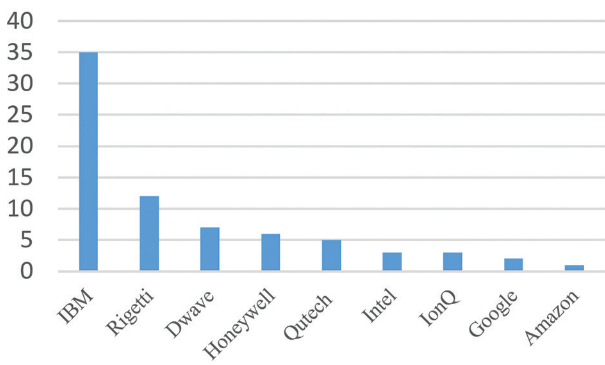

Fig. 5. The most used cloud-based quantum computing platforms from previous studies

Table 3. Existing cloud-based quantum computing platforms

Developer	Quantum cloud	Source	Descriptions
IBM	IBM Q Experience	https://quantum-computing.ibm.com/	A quantum system and simulator
D-Wave Systems	The Leap	https://www.dwavesys.com/	Provide access to a portfolio of hybrid solvers
Google	Google Quantum AI	https://quantumai.google/	A quantum system and simulator
Rigetti Computing	Forest	https://www.rigetti.com/	AI and machine learning infused quantum system
Qutech	Quantum Inspire	https://www.quantum-inspire.com/	A quantum computing platform provides a fully programmable 2-qubit electron spin quantum processor and a 5-qubit transmon processor on QX simulator
Xanadu	Xanadu Quantum Cloud	https://www.xanadu.ai/	A photonic quantum computing platform
Microsoft	Azure Quantum	https://azure.microsoft.com/en-us/	A quantum system
Amazon	Amazon Braket	https://aws.amazon.com/braket/	A quantum simulator that can be run on different quantum hardware technologies
QC Ware	Forge	https://forge.qcware.com/	Built for turn-key algorithm implementations for experts
Alpine Quantum Technologies	Pine System	https://www.aqt.eu/	Trapped ion quantum computer technology
Oxford Quantum Circuit	Quantum Computing as-a-Service (QCaaS)	https://oxfordquantumcircuits.com/	Private cloud built for strategic partners and customers
IonQ	IonQ Quantum Cloud	https://ionq.com/	Trapped ion quantum computer technology
Honeywell	Honeywell System	https://www.honeywell.com/	Trapped ion quantum computer technology

Table 4. Cloud-based quantum computing platforms used in previous studies

No.	Source	Title	Platform service
1.	[60]	Deterministic one-way logic gates on a cloud quantum computer	IBM
2.	[61]	A Novel Approach to the Implementation of Cloud-Based Quantum Programming Platforms in VR Environment	IBM
3.	[62]	Adaptive job and resource management for the growing quantum cloud	IBM
4.	[63]	Challenges and Opportunities of Near-Term Quantum Computing Systems	IBM
5.	[64]	Quantum computing: A measurement and analysis review	IBM
6.	[46]	Cloud Quantum Computing Concept and Development: A Systematic Literature Review	IBM
7.	[65]	Experimental cryptographic verification for near-term quantum cloud computing	IBM
8.	[66]	Quantum Algorithm Implementations for Beginners	IBM
9.	[58]	Measurement Crosstalk Errors in Cloud-Based Quantum Computing	IBM
10.	[67]	Error-Robust Quantum Logic Optimization Using a Cloud Quantum Computer Interface	IBM
11.	[68]	Quantum Algorithms and Experiment Implementations Based on IBM Q	IBM
12.	[69]	Quantum Pulse Coding for Rabi and Ramsey Evolution on IBM Armonk	IBM
13.	[70]	Grover algorithm-based quantum homomorphic encryption ciphertext retrieval scheme in quantum cloud computing	IBM
14.	[71]	Quantum k-means algorithm based on trusted server in quantum cloud computing	IBM
15.	[72]	Design of a quantum repeater using quantum circuits and benchmarking its performance on an IBM quantum computer	IBM
16.	[73]	Demonstration of entanglement purification and swapping protocol to design quantum repeater in IBM quantum computer	IBM
17.	[74]	Simulating molecules on a cloud-based 5-qubit IBM-Q universal quantum computer	IBM
18.	[50]	Comparison of cloud-based ion trap and superconducting quantum computer architectures	IBM
19.	[55]	Parallel quantum trajectories via forking for sampling without redundancy	IBM
20.	[53]	Quantum amplitude-amplification operators	IBM
21.	[54]	Quantum chemistry as a benchmark for near-term quantum computers	IBM
22.	[56]	Demonstration of Fidelity Improvement Using Dynamical Decoupling with Superconducting Qubits	IBM
23.	[52]	Benchmarking quantum state transfer on quantum devices	IBM
24.	[51]	Spectral quantum tomography	IBM
25.	[75]	Application of quantum machine learning using the quantum variational classifier method to high energy physics analysis at the LHC on IBM quantum computer simulator and hardware with 10 qubits	IBM
26.	[76]	Implementing efficient selective quantum process tomography of superconducting quantum gates on IBM quantum experience	IBM

27.	[77]	A verifiable (t, n) threshold quantum state sharing scheme on IBM quantum cloud platform	IBM
28.	[78]	Comparison the performance of five-qubit IBM quantum computers in terms of Bell states preparation	IBM
29.	[20]	Realizing Quantum Algorithms on Real Quantum Computing Devices	IBM
30.	[79]	Performance Analysis of the IBM Cloud Quantum Computing Lab against MacBook Pro 2019	IBM
31.	[57]	MISTIQS: An open-source software for performing quantum dynamics simulations on quantum computers	IBM
32.	[80]	Qiskit pulse: programming quantum computers through the cloud with pulses	IBM
33.	[81]	Cryptography in Quantum Computing	IBM
34.	[59]	Playing quantum nonlocal games with six noisy qubits on the cloud	IBM
35.	[82]	Integrated Analysis of Performance and Resource of Large-Scale Quantum Computing	IBM
36.	[43]	A quantum-classical cloud platform optimized for variational hybrid algorithms	Rigetti
37.	[58]	Measurement Crosstalk Errors in Cloud-Based Quantum Computing	Rigetti
38.	[83]	Measurement-Based Adaptation Protocol with Quantum Reinforcement Learning in a Rigetti Quantum Computer	Rigetti
39.	[50]	Comparison of cloud-based ion trap and superconducting quantum computer architectures	Rigetti
40.	[84]	Variational quantum algorithm for nonequilibrium steady states	Rigetti
41.	[55]	Parallel quantum trajectories via forking for sampling without redundancy	Rigetti
42.	[59]	Playing quantum nonlocal games with six noisy qubits on the cloud	Rigetti
43.	[57]	MISTIQS: An open-source software for performing quantum dynamics simulations on quantum computers	Rigetti
44.	[85]	Experimental Implementation of a Quantum Autoencoder via Quantum Adders	Rigetti
45.	[56]	Demonstration of Fidelity Improvement Using Dynamical Decoupling with Superconducting Qubits	Rigetti
46.	[54]	Quantum chemistry as a benchmark for near-term quantum computers	Rigetti
47.	[86]	Robust implementation of generative modeling with parametrized quantum circuits	Rigetti
48.	[87]	Intel Quantum Simulator: a cloud-ready high-performance simulator of quantum circuits	Intel
49.	[88]	Practical error modeling toward realistic NISQ simulation	Intel
50.	[89]	qHiPSTER: The Quantum High Performance Software Testing Environment	Intel
51.	[46]	Cloud Quantum Computing Concept and Development: A Systematic Literature Review	Qutech
52.	[90]	Quantum Inspire: QuTech's platform for co-development and collaboration in quantum computing	Qutech
53.	[20]	Realizing Quantum Algorithms on Real Quantum Computing Devices	Qutech
54.	[51]	Spectral quantum tomography	Qutech
55.	[52]	Benchmarking quantum state transfer on quantum devices	Qutech
56.	[91]	Performance Optimization of Quantum Computing Applications using D Wave Two Quantum Computer	D-Wave
57.	[92]	Early Warning of Heat/Cold Waves as a Smart City Subsystem: A Retrospective Case Study of Non-anticipative Analog Methodology	D-Wave
58.	[93]	Thermodynamics of a quantum annealer	D-Wave
59.	[94]	Solving the Minimum Spanning Tree Problem with a Quantum Annealer	D-Wave
60.	[95]	Solving the sparse QUBO on multiple GPUs for Simulating a Quantum Annealer	D-Wave
61.	[96]	Comparison between a quantum annealer and a classical approximation algorithm for computing the ground state of an Ising spin glass	D-Wave
62.	[97]	Optimizing the Selection of Recommendation Carousels with Quantum Computing	D-Wave
63.	[50]	Comparison of cloud-based ion trap and superconducting quantum computer architectures	IONQ
64.	[53]	Quantum amplitude-amplification operators	IONQ
65.	[59]	Playing quantum nonlocal games with six noisy qubits on the cloud	IONQ
66.	[59]	Playing quantum nonlocal games with six noisy qubits on the cloud	Honeywell
67.	[98]	Entanglement from Tensor Networks on a Trapped-Ion Quantum Computer	Honeywell
68.	[99]	Filtering variational quantum algorithms for combinatorial optimization	Honeywell
69.	[100]	Suppression of midcircuit measurement crosstalk errors with micromotion	Honeywell
70.	[101]	The efficient preparation of normal distribution in quantum registers	Honeywell
71.	[102]	Qubit efficient entanglement spectroscopy using qubit resets	Honeywell
72.	[103]	Large scale multi-node simulations of Z2 gauge theory quantum circuits using Google Cloud Platform	Google
73.	[57]	MISTIQS: An open-source software for performing quantum dynamics simulations on quantum computers	Google
74.	[104]	Quantum Software as a Service Through a Quantum API Gateway	Amazon

3.2. QUANTUM COMPUTING PROCESSORS

One of the core components of a quantum computer, quantum computing processors also referred as quantum processing unit (QPUs) or quantum chip is a set of physically built electronic circuit, housing numbers of interconnected qubits [43]. The most known quantum processing unit (QPUs) types in quantum computing are circuit-based quantum processors and annealing quantum processors [8, 62, 105, 106]. Table 5 briefly describes the differences between circuit-based quantum processors and annealing quantum processors.

Based on Table 5, the circuit-based quantum processors use gate model, which means that it requires the problems to be expressed in quantum gates [107]. While in annealing quantum processors, mainly solves optimization problems but it requires the problems to be expressed in the operations language [105]. Furthermore, due to high sensitivity to noise, the circuit-based quantum processors find it difficult to produce a stable qubits state compared to annealing quantum processors. Moreover, the annealing quantum processors are less user-friendly compared to circuit-based quantum processors in term of operation due to the operations language used especially to beginners of quantum computing. Some circuit-based and annealing quantum processors devices were listed in Table 6 and Table 7 respectively.

Table 5. The differences between Circuit-based quantum processors and Annealing quantum processors

Circuit-based quantum processors	Annealing quantum processors
Gate model	Quantum annealing
Drag-and-drop tools and codes	Operations language codes
Poor qubits stability	Good qubits stability
Extremely sensitive to noise	Less affected by noise
User friendly	Less user-friendly

Table 6. Circuit-based quantum processors devices

Developer	Name	Architecture	Qubit(s)	Release year
Google	Bristlecone	Superconducting transmon	72	2018
	Sycamore	Superconducting transmon	53	2019
IBM	Eagle	Superconducting	127	2021
	Hummingbird	Superconducting	65	2020
	Falcon	Superconducting	27	2019
	Canary family	Superconducting	5-16	2017
Intel	Tangle Lake	Superconducting	49	2018
IonQ	Aria	Trapped Ion	32	2020
QuTech	Starmon-5	Superconducting	5	2020
	Spin-2	Semiconductor spin qubits	2	2020
Rigetti	Aspen-M-1	Superconducting	80	2022
	Aspen-11	Superconducting	80	2021
Xanadu	Borealis	Photonics	216	2022
	X12	Photonics	12	2020
	X8	Photonics	8	2020

Table 7. Annealing quantum processors devices

Developer	Name	Architecture	Qubit(s)	Release year
D-Wave	D-Wave 2X	Superconducting	1152	2015
	D-Wave 2000Q	Superconducting	2048	2017
	D-Wave Advantage	Superconducting	5760	2020

For one to claim which quantum processors are better than the other may not be wise as it depends on one's objectives and experiences. As listed in Table 6 and Table 7, superconducting is the most preferred by developers as an architecture of a quantum computing system. This is due to its advantages which are, high designability, scalability, easy to couple and easy to control [60, 108].

Furthermore, developers seem to prefer the circuit-based over annealing quantum processors. This may have been influenced by the complexity of annealing quantum processors language of operations. In addition, towards the end of 2021, D-Wave Systems announced in a conference that its organization are keen to adopt the circuit-based quantum processors into their next-generation quantum computing platform which includes both annealing and circuit-based model [109].

Top developers such as IBM and D-Wave Systems are working in full swing towards developing reliable, fault-tolerance, NISQ quantum devices. In accordance, both developers among others have produced a development roadmap of their quantum computer technology for the coming years. IBM's near-term goals is to achieve an astonishing over 1000 qubits by the end of 2023 [110, 111]. While D-Wave Systems aiming with its next-generation Advantage 2 quantum system which contains over 7000 qubits in the coming years [109].

These quantum race on the road to quantum advantage has paved the way for a promising future of quantum computing. As stated by Preskill [38], even though it is still a long way to achieve the promising future of quantum computing, quantum computers will be a useful tool to solve complex problems and to explore more on other areas of the technology. Experts believe it will definitely benefit various fields namely security, material science and pharmaceuticals. In addition, the creation of quantum software development kits has been beneficial for potential users of quantum computers.

3.3. QUANTUM SOFTWARE DEVELOPMENT KITS

Quantum software development kits are a tool for users to develop quantum algorithms to be executed in a quantum computer. Some developers namely IBM, Rigetti and Google developed an open-source quantum software development kit. These developed kits allow users to utilize classical programming language such as Python or even quantum programming language such as Q#. By using these kits provided, users can run and solve problems through the cloud accessing the available quantum computer platforms available. Table 8 shows several known developers' quantum software development kits and brief descriptions.

3.4. QUANTUM COMPUTING SIMULATORS

Quantum computing simulator is a device allowing users to solve computational problems in a programming environment adhering to the principles of quantum mechanics. It performs quantum gates operation by the use of classical gates. Presently, various existing quantum computing simulators developed are considerably hospitable as it serves users to access with classical programming languages, catering their needs. This occasion will likely draw more potential users to explore quantum computing technology. Several quantum computing simulators were tabulated in Table 9.

3.5. CONCEPTUAL FRAMEWORK OF USING CLOUD-BASED QUANTUM COMPUTING SERVICE

As part of the main objective of this study, which to provide a conceptual framework of using cloud-based quantum computing service, the conceptual framework was developed on the basis of the cloud-based quantum computing platforms used in previous studies with quantum simulators, software development kits and language. The proposed conceptual framework will only cover several quantum computing platforms of circuit-based quantum processors, not the annealing quantum processors quantum computers. Fig. 6 illustrates the proposed conceptual framework of using cloud-based quantum computing service.

Table 8. Quantum software development kits

Developer	Name	Language
IBM (https://www.ibm.com/quantum)	Qiskit	Open QASM/Python
D-Wave (https://www.dwavesys.com/)	Ocean	Qbsolv/QMASM/Python
Rigetti (https://www.rigetti.com/)	Forest	Quil
Xanadu (https://www.xanadu.ai/)	PennyLane	Blackbird/ Python/C++/Java/C#/JavaScript
Google (https://quantumai.google/)	Cirq	Python
Microsoft (https://azure.microsoft.com/en-us/)	Quantum Development Kit	Q#/Python/C#/F#
Amazon (https://aws.amazon.com/braket/)	Braket	Python
Intel (https://www.intel.com/content/www/us/en/research/quantum-computing.html)	N/A	C/C++
Qutech (https://qutech.nl/)	Quantum Inspire	cQASM/Python
Cambridge Quantum Computing (https://cambridgequantum.com/)	Tket	Python

Table 9. Quantum computing simulators

Source	Developer	Software Development Kit	Simulator
https://quantum-computing.ibm.com/lab/docs/iql/manage/simulator/	IBM	Qiskit	QASM, Statevector, stabilizer, extended stabilizer, Matrix Product State (MPS)
https://pyquil-docs.rigetti.com/en/1.9/qvm.html	Rigetti	Forest	Quantum Virtual Machine (QVM)
https://www.xanadu.ai/products/lightning/ https://www.xanadu.ai/products/jet/	Xanadu	PennyLane Strawberry Fields	Lightning and Jet
https://quantumai.google/cirq	Google	Cirq	cirq.Simulator (pure state) and cirq.DensityMatrixSimulator (mixed state)
https://visualstudio.microsoft.com/	Microsoft	Quantum Development Kit	Visual Studio
https://github.com/iqusoft/intel-qs https://intel-qs.readthedocs.io/en/docs/getting-started.html	Intel	N/A	Intel Parallel Studio Compiler/Intel-Quantum Simulator (IQS)
http://quantum-studio.net/ https://github.com/QuTech-Delft/qx-simulator	Qutech	Quantum Inspire	QX Simulator

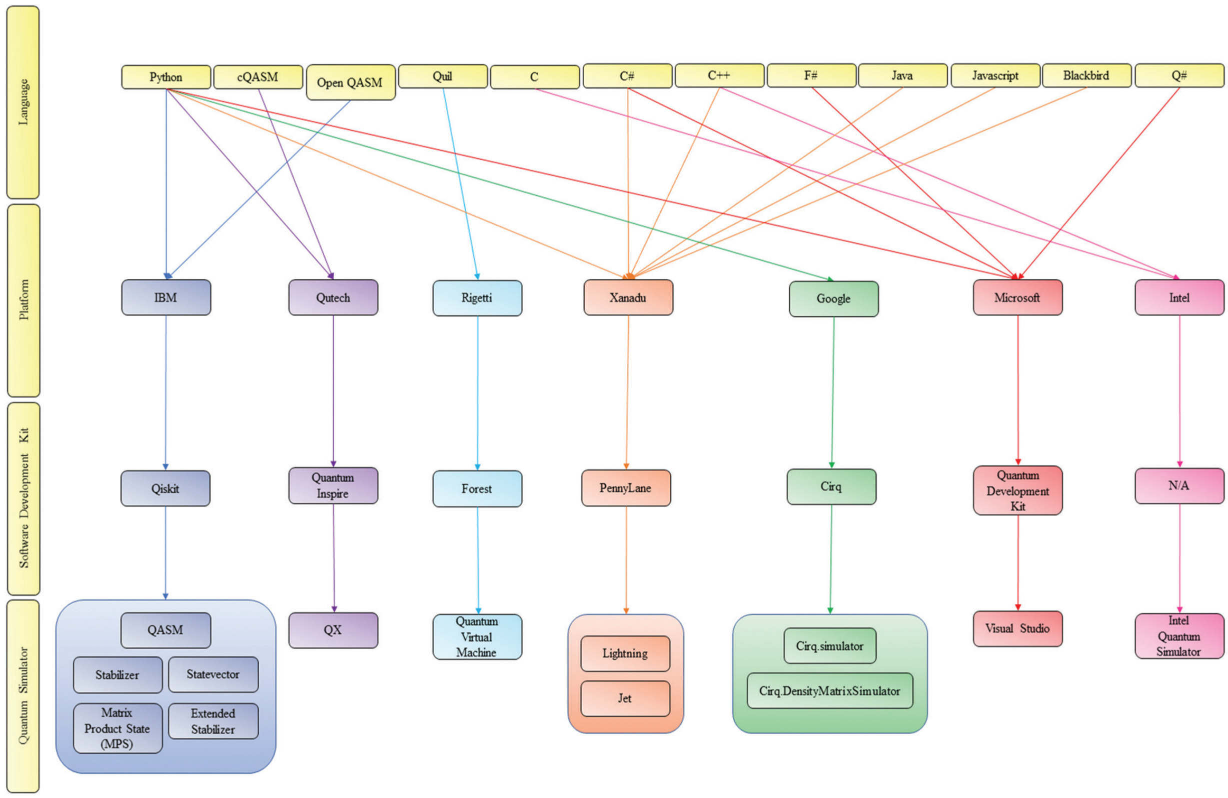

Fig. 6. Proposed conceptual framework

4. CONCLUSION

Utilizing developed cloud-based quantum computing platforms poses challenges for potential individual users or groups as different developers deliver different architecture and functionality of the existing platforms. This disparity sparks a dispute on which cloud-based quantum computing platforms are the most suitable based on one's specific requirements and needs.

This study presents a comprehensive overview of the fundamentals of quantum computing with several existing numbers of cloud-based quantum computing platforms used in earlier studies. Additionally, it has discussed quantum computing processors, quantum software development kits and quantum computing simulators. Furthermore, a conceptual framework of using cloud-based quantum computing services as a guidance and reference for future work is delivered, enabling users to navigate cloud-based quantum computing services by particular requirements and needs by an individual or groups.

The understanding and development of quantum computing technology is progressing rapidly. However, developed cloud-based quantum computing platforms are still not considerably inclusive to existing and potential users. Future research efforts should be built upon the proposed conceptual framework to develop a universal cloud-based quantum computer that addresses the diverse needs of users.

In conclusion, this study aids as a valuable resource for individuals and groups interested in getting a first-hand experience on quantum computing. By offering insights into the complexities of quantum computing platforms and providing a framework for choosing the best options available, this review aims to enhance the accessibility and usability of these systems. Future advancements aligned with the proposed framework will contribute to the realization of more universal cloud-based quantum computing platforms.

5. ACKNOWLEDGEMENT

This research is part of a research project supported by the Malaysian Ministry of Higher Education Fundamental Research Grant Nos. FRGS/1/2021/ICT04/USIM/01/1 (USIM/FRGS/KGI/KPT/50121).

6. REFERENCES

[1] S. M. Ardelean, M. Udrescu, "Graph coloring using the reduced quantum genetic algorithm", PeerJ Computer Science, Vol. 8, 2022, p. e836.

[2] D. Maslov, J.-S. Kim, S. Bravyi, T. J. Yoder, S. Sheldon, "Quantum advantage for computations with limited space", Nature Physics, Vol. 17, No. 8, 2021, pp. 894-897.

[3] G. Nannicini, L. S. Bishop, O. Günlük, P. Jurcevic, "Optimal qubit assignment and routing via integer programming", ACM Transactions on Quantum Computing Vol. 4, No. 1, 2022, pp. 1-31.

[4] K. Seyhan, S. Akleylek, "Indistinguishability under adaptive chosen-ciphertext attack secure double-NTRU-based key encapsulation mechanism", PeerJ Computer Science, Vol. 9, 2023, p. e1391.

[5] A. Singh, H. Singh, K. Dorai, "Experimental classification of entanglement in arbitrary three-qubit pure states on an NMR quantum information processor", Physical Review A, Vol. 98, No. 3, 2018, p. 032301.

[6] R. Wille, S. Hillmich, L. Burgholzer, "Tools for Quantum Computing Based on Decision Diagrams", ACM Transactions on Quantum Computing, Vol. 3, No. 3, 2022, pp. 1-17.

[7] X. Wu, "Introduction to the Special issue on the Techniques of Programming Languages, Logic, and Formal Methods in Quantum Computing", ACM Transactions on Quantum Computing, Vol. 2, No. 4, 2021, pp. 1-3.

[8] D. Chen, "Intelligent Retrieval Platform for University Digital Resources Based on Quantum Cloud Computing", Proceedings of the Fifth International Conference on I-SMAC (IoT in Social, Mobile, Analytics and Cloud), Palladam, India, 11-13 November 2021, pp. 633-636.

[9] Y. Xu et al. "Automatic Qubit Characterization and Gate Optimization with QubiC", ACM Transactions on Quantum Computing Vol. 4, No. 1, 2022, pp. 1-12.

[10] Y. Y. Ghadi, T. AlShloul, Z. I. Nezami, H. Ali, M. Asif, H. Aljuaid, S. Ahmad, "An efficient optimizer for the 0/1 knapsack problem using group counseling", PeerJ Computer Science, Vol. 9, 2023, p. e1315.

[11] Abhijith J. et al. "Quantum Algorithm Implementations for Beginners", ACM Transactions on Quantum Computing, Vol. 3, No. 4, 2022, pp. 1-92.

[12] A. Li, S. Stein, S. Krishnamoorthy, J. Ang, "QASMBench: A Low-Level Quantum Benchmark Suite for NISQ Evaluation and Simulation", ACM Transactions on Quantum Computing, Vol. 4, No. 2, 2023, pp. 1-26.

[13] Y. Shingu, Y. Takeuchi, S. Endo, S. Kawabata, S. Watabe, T. Nikuni, H. Hakoshima, Y. Matsuzaki, "Variational secure cloud quantum computing", Physical Review A, Vol. 105, No. 2, 2022, p. 022603.

[14] H. F. Fakhruldeen, R. A. Alkaabi, I. Jabbar, I. Al-Kharsan, S. Shoja, "Post-quantum Techniques in Wireless Network Security: An Overview", Malaysian Journal of Fundamental and Applied Sciences, Vol. 19, 2023, pp. 337-344.

[15] P. Fremantle, P. Scott, "A survey of secure middleware for the Internet of Things", PeerJ Computer Science, Vol. 3, 2017, p. e114.

[16] K. K. Soni, A. Rasool, "Quantum-effective exact multiple patterns matching algorithms for biological sequences", PeerJ Computer Science, Vol. 8, No., 2022, p. e957.

[17] X.-J. Huang et al. "Entanglement-interference complementarity and experimental demonstration in a superconducting circuit", Quantum Information, Vol. 9, No. 1, 2023, p. 43.

[18] A. Ivashkin, D. Abdurashitov, A. Baranov, F. Guber, S. Morozov, S. Musin, A. Strizhak, I. Tkachev, "Testing entanglement of annihilation photons", Scientific Reports, Vol. 13, No. 1, 2023, p. 7559.

[19] A. Suau, G. Staffelbach, H. Calandra, "Practical Quantum Computing: Solving the Wave Equation Using a Quantum Approach", ACM Transactions on Quantum Computing, Vol. 2, No. 1, 2021, pp. 1-35.

[20] C. G. Almudever, L. Lao, R. Wille, G. G. Guerreschi, "Realizing Quantum Algorithms on Real Quantum Computing Devices", arXiv:2007.01000, 2020.

[21] S. Hillmich, A. Zulehner, R. Kueng, I. L. Markov, R. Wille, "Approximating Decision Diagrams for Quantum Circuit Simulation", ACM Transactions on Quantum Computing, Vol. 3, No. 4, 2022, pp. 1-21.

[22] M. Messmer, J. Shires, A. V. Rij, "Quantum technology competition must not become an arms race", https://www.chathamhouse.org/publications/the-world-today/2023-10/quantum-technology-competition-must-not-become-arms-race (accessed: 2023)

[23] X. Wang, J. Huang, Z. Duan, Y. Xu, Y. Yao, "Randomness analysis of end-to-end delay in random forwarding networks", PeerJ Computer Science, Vol. 8, 2022, p. e942.

[24] A. A. Zhahir, S. M. Mohd, M. I. M. Shuhud, B. Idrus, H. Zainuddin, N. M. Jan, M. R. Wahiddin, "Quantum Computing and Its Application", International

Journal of Advanced Research in Technology and Innovation, Vol. 4, No. 1, 2022, pp. 55-65.

[25] J. Preskill, "Quantum computing 40 years later", arXiv:2106.10522, 2021.

[26] A. M. Aboussalah, C. Chi, C.-G. Lee, "Quantum computing reduces systemic risk in financial networks", Scientific Reports, Vol. 13, No. 1, 2023, p. 3990.

[27] P. Díez-Valle et al. "Multiobjective variational quantum optimization for constrained problems: an application to cash handling", Quantum Science and Technology, Vol. 8, No. 4, 2023, p. 045009.

[28] D. Herman, C. Googin, X. Liu, Y. Sun, A. Galda, I. Safro, M. Pistoia, Y. Alexeev, "Quantum computing for finance", Nature Reviews Physics, Vol. 5, No. 8, 2023, pp. 450-465.

[29] Z. Udvarnoki, G. Fáth, N. Fogarasi, "Quantum advantage of Monte Carlo option pricing", Journal of Physics Communications, Vol. 7, No. 5, 2023, p. 055001.

[30] R. K. Ahalya, F. M. Almutairi, U. Snekhalatha, V. Dhanraj, S. M. Aslam, "RANet: a custom CNN model and quanvolutional neural network for the automated detection of rheumatoid arthritis in hand thermal images", Scientific Reports, Vol. 13, No. 1, 2023, p. 15638.

[31] B. Fliszkiewicz, M. Sajdak, "Fragments quantum descriptors in classification of bio-accumulative compounds", Journal of Molecular Graphics and Modelling, Vol. 125, 2023, p. 108584.

[32] A. Ajagekar, F. You, "Molecular design with automated quantum computing-based deep learning and optimization", Computational Materials, Vol. 9, No. 1, 2023, p. 143.

[33] J. Kim, J. Huh, D. K. Park, "Classical-to-quantum convolutional neural network transfer learning", Neurocomputing, Vol. 555, 2023, p. 126643.

[34] C. Feniou, M. Hassan, D. Traoré, E. Giner, Y. Maday, J.-P. Piquemal, "Overlap-ADAPT-VQE: practical quantum chemistry on quantum computers via overlap-guided compact Ansätze", Communications Physics, Vol. 6, No. 1, 2023, p. 192.

[35] C. Cao, J. Sun, X. Yuan, H.-S. Hu, H. Q. Pham, D. Lv, "Ab initio quantum simulation of strongly correlated materials with quantum embedding", Computational Materials, Vol. 9, No. 1, 2023, p. 78.

[36] N. S. Kirsanov, V. A. Pastushenko, A. D. Kodukhov, M. V. Yarovikov, A. B. Sagingalieva, D. A. Kronberg, M. Pflitsch, V. M. Vinokur, "Forty thousand kilometers under quantum protection", Scientific Reports, Vol. 13, No. 1, 2023.

[37] H. C. Ukwuoma, G. Arome, A. Thompson, B. K. Alese, "Post-quantum cryptography-driven security framework for cloud computing", Open Computer Science, Vol. 12, No. 1, 2022, pp. 142-153.

[38] J. Preskill, "Quantum computing in the NISQ era and beyond", Quantum, Vol. 2, 2018, p. 79.

[39] C.-C. Chen, M. Watabe, K. Shiba, M. Sogabe, K. Sakamoto, T. Sogabe, "On the Expressibility and Overfitting of Quantum Circuit Learning", ACM Transactions on Quantum Computing, Vol. 2, No. 2, 2021, pp. 1-24.

[40] X. Fu et al. "Quingo: A Programming Framework for Heterogeneous Quantum-Classical Computing with NISQ Features", ACM Transactions on Quantum Computing, Vol. 2, No. 4, 2021, pp. 1-37.

[41] P. Ball, "First quantum computer to pack 100 qubits enters crowded race", Vol. 599, 2021, p. 542.

[42] M. Günes, H. Majumdar, P. Muratore-Ginanneschi, J. Pekola, "InstituteQ: The Finnish National Quantum Institute", Arkhimedes, 2022.

[43] P. J. Karalekas, N. A. Tezak, E. C. Peterson, C. A. Ryan, M. P. da Silva, R. S. Smith, "A quantum-classical cloud platform optimized for variational hybrid algorithms", Quantum Science and Technology, Vol. 5, No. 2, 2020, p. 024003.

[44] A. Mccaskey, T. Nguyen, A. Santana, D. Claudino, T. Kharazi, H. Finkel, "Extending C++ for Heterogeneous Quantum-Classical Computing", ACM Transactions on Quantum Computing, Vol. 2, No. 2, 2021, pp. 1-36.

[45] A. A. Saki, M. Alam, K. Phalak, A. Suresh, R. O. Topaloglu, S. Ghosh, "A survey and tutorial on security and resilience of quantum computing", Proceedings of the IEEE European Test Symposium, Bruges, Belgium, 24-28 May 2021, pp. 1-10.

[46] H. Soeparno, A. S. Perbangsa, "Cloud Quantum Computing Concept and Development: A Sys-

tematic Literature Review", Procedia Computer Science, Vol. 179, 2021, pp. 944-954.

[47] M. J. Page et al. "The PRISMA 2020 statement: an updated guideline for reporting systematic reviews", BMJ, Vol. 372, 2021, p. 71.

[48] S. Kraus, M. Breier, S. Dasí-Rodríguez, "The art of crafting a systematic literature review in entrepreneurship research", International Entrepreneurship and Management Journal, Vol. 16, No. 3, 2020, pp. 1023-1042.

[49] M. Petticrew, H. Roberts, "Systematic Reviews in the Social Sciences: A Practical Guide", Wiley, 2006.

[50] S. Blinov, B. Wu, C. Monroe, "Comparison of cloud-based ion trap and superconducting quantum computer architectures", AVS Quantum Science, Vol. 3, No. 3, 2021, p. 033801.

[51] J. Helsen, F. Battistel, B. M. Terhal, "Spectral quantum tomography", npj Quantum Information, Vol. 5, No. 1, 2019, p. 74.

[52] Y.-T. Huang, J.-D. Lin, H.-Y. Ku, Y.-N. Chen, "Benchmarking quantum state transfer on quantum devices", Physical Review Research, Vol. 3, No. 2, 2021, p. 023038.

[53] H. Kwon, J. Bae, "Quantum amplitude-amplification operators", Physical Review A, Vol. 104, No. 6, 2021, p. 062438.

[54] A. J. McCaskey, Z. P. Parks, J. Jakowski, S. V. Moore, T. D. Morris, T. S. Humble, R. C. Pooser, "Quantum chemistry as a benchmark for near-term quantum computers", Quantum Information, Vol. 5, No. 1, 2019, p. 99.

[55] D. K. Park, I. Sinayskiy, M. Fingerhuth, F. Petruccione, J.-K. K. Rhee, "Parallel quantum trajectories via forking for sampling without redundancy", New Journal of Physics, Vol. 21, No. 8, 2019, pp. 083024.

[56] B. Pokharel, N. Anand, B. Fortman, D. A. Lidar, "Demonstration of fidelity improvement using dynamical decoupling with superconducting qubits", Physical review letters, Vol. 121, No. 22, 2018, p. 220502.

[57] C. Powers, L. Bassman, T. M. Linker, K.-i. Nomura, S. Gulania, R. K. Kalia, A. Nakano, P. Vashishta, "MISTIQS: An open-source software for performing quantum dynamics simulations on quantum computers", SoftwareX, Vol. 14, 2021, p. 100696.

[58] S. Seo, J. Bae, "Measurement Crosstalk Errors in Cloud-Based Quantum Computing", IEEE Internet Computing, Vol. 26, No. 1, 2021, pp. 26-33.

[59] M. Sheffer, D. Azses, E. G. D. Torre, "Playing Quantum Nonlocal Games with Six Noisy Qubits on the Cloud", Advanced Quantum Technologies, Vol. 5, No. 3, 2022, p. 2100081.

[60] Z.-P. Yang et al. "Deterministic one-way logic gates on a cloud quantum computer", Physical Review A, Vol. 105, No. 4, 2022, p. 042610.

[61] H. H. Genç, S. Aydın, H. Erdal, "A Novel Approach to the Implementation of Cloud-Based Quantum Programming Platforms in VR Environment", Proceedings of the Innovations in Intelligent Systems and Applications Conference, Istanbul, Turkey, 15-17 October 2020, pp. 1-6.

[62] G. S. Ravi, K. N. Smith, P. Murali, F. T. Chong, "Adaptive job and resource management for the growing quantum cloud", Proceedings of the IEEE International Conference on Quantum Computing and Engineering, Broomfield, CO, USA, 17-22 October 2021, pp. 301-312.

[63] A. D. Córcoles et al. "Challenges and opportunities of near-term quantum computing systems", arXiv:1910.02894, 2019.

[64] M. Gupta, M. J. Nene, "Quantum computing: A measurement and analysis review", Concurrency and Computation: Practice and Experience, Vol. 33, No. 20, 2021, p. e6344.

[65] Chen, X., B. Cheng, Z. Li, X. Nie, N. Yu, M.-H. Yung, X. Peng, "Experimental cryptographic verification for near-term quantum cloud computing", Science Bulletin, Vol. 66, No. 1, 2021, pp. 23-28.

[66] A. Adedoyin et al. "Quantum algorithm implementations for beginners", arXiv:1804.03719, 2018.

[67] A. R. R. Carvalho, H. Ball, M. J. Biercuk, M. R. Hush, F. Thomsen, "Error-Robust Quantum Logic Optimization Using a Cloud Quantum Computer Interface", Physical Review Applied, Vol. 15, No. 6, 2021, p. 064054.

[68] W. Liu, J. Chen, Y. Xu, J. Tang, L. Tong, X. Song, "Quantum Algorithms and Experiment Implementations Based on IBM Q", Computers, Materials & Continua, Vol. 65, No. 2, 2020, pp. 1671-1689.

[69] M. A. Ullah, A. Farooq, Y. Jeong, H. Shin, "Quantum Pulse Coding for Rabi And Ramsey Evolution on IBM Armonk", Proceedings of the International Conference on Information and Communication Technology Convergence, Jeju Island, Korea, 20-22 October 2021, pp. 848-850.

[70] C. Gong, J. Du, Z. Dong, Z. Guo, A. Gani, L. Zhao, H. Qi, "Grover algorithm-based quantum homomorphic encryption ciphertext retrieval scheme in quantum cloud computing", Quantum Information Processing, Vol. 19, No. 3, 2020, pp. 105.

[71] C. Gong, Z. Dong, A. Gani, H. Qi, "Quantum k-means algorithm based on trusted server in quantum cloud computing", Quantum Information Processing, Vol. 20, No. 4, 2021, p. 130.

[72] S. Das, M. S. Rahman, M. Majumdar, "Design of a quantum repeater using quantum circuits and benchmarking its performance on an IBM quantum computer", Quantum Information Processing, Vol. 20, No. 7, 2021, p. 245.

[73] B. K. Behera, S. Seth, A. Das, P. K. Panigrahi, "Demonstration of entanglement purification and swapping protocol to design quantum repeater in IBM quantum computer", Quantum Information Processing, Vol. 18, No. 4, 2019, p. 108.

[74] S. Leontica, F. Tennie, T. Farrow, "Simulating molecules on a cloud-based 5-qubit IBM-Q universal quantum computer", Communications Physics, Vol. 4, No. 1, 2021, p. 112.

[75] S. L. Wu et al. "Application of quantum machine learning using the quantum variational classifier method to high energy physics analysis at the LHC on IBM quantum computer simulator and hardware with 10 qubits", Journal of Physics G: Nuclear and Particle Physics, Vol. 48, No. 12, 2021, pp. 125003.

[76] A. Gaikwad, K. Shende, Arvind, K. Dorai, "Implementing efficient selective quantum process tomography of superconducting quantum gates on IBM quantum experience", Scientific Reports, Vol. 12, No. 1, 2022, p. 3688.

[77] X. Song, Y. Liu, M. Xiao, H. Deng, S. Yang, "A verifiable (t, n) threshold quantum state sharing scheme on IBM quantum cloud platform", Quantum Information Processing, Vol. 19, No. 9, 2020, p. 337.

[78] M. Sisodia, "Comparison the performance of five-qubit IBM quantum computers in terms of Bell states preparation", Quantum Information Processing, Vol. 19, No. 8, 2020, pp. 215.

[79] A. Martin Grande, R. Ayala, I. Khan, P. Sarkar, T. K. Mohd, "Performance Analysis of the IBM Cloud Quantum Computing Lab Against MacBook Pro 2019", Intelligent Human Computer Interaction, 2022, pp. 449-459.

[80] T. Alexander, N. Kanazawa, D. J. Egger, L. Capelluto, C. J. Wood, A. Javadi-Abhari, D. C. McKay, "Qiskit pulse: Programming quantum computers through the cloud with pulses", Quantum Science and Technology, Vol. 5, No. 4, 2020, p. 044006.

[81] P. Choy, D. Cates, F. Chehwan, C. Rodriguez, A. Leider, C. Tappert, "Cryptography in Quantum Computing", Advances in Intelligent Systems and Computing, 2019.

[82] Y. Hwang, T. Kim, C. Baek, B.-S. Choi, "Integrated Analysis of Performance and Resources in Large-Scale Quantum Computing", Physical Review Applied, Vol. 13, No. 5, 2020, p. 054033.

[83] J. Olivares-Sánchez, J. Casanova, E. Solano, L. Lamata, "Measurement-based adaptation protocol with quantum reinforcement learning in a Rigetti quantum computer", Quantum Reports, Vol. 2, No. 2, 2020, pp. 293-304.

[84] N. Yoshioka, Y. O. Nakagawa, K. Mitarai, K. Fujii, "Variational quantum algorithm for nonequilibrium steady states", Physical Review Research, Vol. 2, No. 4, 2020, p. 043289.

[85] Y. Ding, L. Lamata, M. Sanz, X. Chen, E. Solano, "Experimental implementation of a quantum autoencoder via quantum adders", Advanced Quantum Technologies, Vol. 2, No. 7-8, 2019, p. 1800065.

[86] V. Leyton-Ortega, A. Perdomo-Ortiz, O. Perdomo, "Robust implementation of generative modeling with parametrized quantum circuits", Quantum Machine Intelligence, Vol. 3, No. 1, 2021, p. 17.

[87] G. G. Guerreschi, J. Hogaboam, F. Baruffa, N. Sawaya, "Intel Quantum Simulator: A cloud-ready high-performance simulator of quantum circuits", arXiv:2001.10554, 2020.

[88] T. Tanimoto, S. Matsuo, S. Kawakami, Y. Tabuchi, M. Hirokawa, K. Inoue, "Practical Error Modeling Toward Realistic NISQ Simulation", Proceedings of the IEEE Computer Society Annual Symposium on VLSI, Limassol, Cyprus, 6-8 July 2020, 2020, pp. 291-293.

[89] M. Smelyanskiy, N. P. Sawaya, A. Aspuru-Guzik, "qHiPSTER: The quantum high performance software testing environment", arXiv:1601.07195, 2016.

[90] T. Last et al. "Quantum Inspire: QuTech's platform for co-development and collaboration in quantum computing", SPIE, Vol. 11324, 2020.

[91] G. Sundar, D. Narmadha, "Performance Optimization of Quantum Computing Applications using D Wave Two Quantum Computer", Proceedings of the 5th International Conference on Trends in Electronics and Informatics, Tirunelveli, India, 3-5 June 2021.

[92] Z. Dmytro, "Early Warning of Heat/Cold Waves as a Smart City Subsystem: A Retrospective Case Study of Nonanticipative Analog Methodology", BRAIN. Broad Research in Artificial Intelligence and Neuroscience, Vol. 6, 2015, pp. 44-54.

[93] L. Buffoni, M. Campisi, "Thermodynamics of a quantum annealer", Quantum Science and Technology, Vol. 5, No. 3, 2020, p. 035013.

[94] W. O'Quinn, S. Mao, "Solving the Minimum Spanning Tree Problem with a Quantum Annealer", Proceedings of the IEEE Globecom Workshops, Taipei, Taiwan, 7-11 December 2020, pp. 1-6.

[95] T. Imanaga, K. Nakano, R. Yasudo, Y. Ito, Y. Kawamata, R. Katsuki, S. Ozaki, T. Yazane, K. Hamano, "Solving the sparse QUBO on multiple GPUs for Simulating a Quantum Annealer", Proceedings of the Ninth International Symposium on Computing and Networking, Matsue, Japan, 23-26 November 2021, pp. 19-28.

[96] R. Yaacoby, N. Schaar, L. Kellerhals, O. Raz, D. Hermelin, R. Pugatch, "Comparison between a quantum annealer and a classical approximation algorithm for computing the ground state of an Ising spin glass", Physical Review E, Vol. 105, No. 3, 2022, p. 035305.

[97] M. F. Dacrema, N. Felicioni, P. Cremonesi, "Optimizing the Selection of Recommendation Carousels with Quantum Computing", Proceedings of the 15th ACM Conference on Recommender Systems, September 2021, pp. 691-696.

[98] M. Foss-Feig et al. "Entanglement from Tensor Networks on a Trapped-Ion Quantum Computer", Physical Review Letters, Vol. 128, No. 15, 2022, p. 150504.

[99] D. Amaro, C. Modica, M. Rosenkranz, M. Fiorentini, M. Benedetti, M. Lubasch, "Filtering variational quantum algorithms for combinatorial optimization", Quantum Science and Technology, Vol. 7, No. 1, 2022, p. 015021.

[100] J. P. Gaebler, C. H. Baldwin, S. A. Moses, J. M. Dreiling, C. Figgatt, M. Foss-Feig, D. Hayes, J. M. Pino, "Suppression of midcircuit measurement crosstalk errors with micromotion", Physical Review A, Vol. 104, No. 6, 2021, p. 062440.

[101] A. G. Rattew, Y. Sun, P. Minssen, M. Pistoia, "The efficient preparation of normal distributions in quantum registers", Quantum, Vol. 5, 2021, p. 609.

[102] J. Yirka, Y. Subaşı, "Qubit-efficient entanglement spectroscopy using qubit resets", Quantum, Vol. 5, 2021, p. 535.

[103] E. Gustafson et al. "Large scale multi-node simulations of Z 2 gauge theory quantum circuits using Google Cloud Platform", Proceedings of the IEEE/ACM Second International Workshop on Quantum Computing Software, 2021, pp. 72-79.

[104] J. Garcia-Alonso, J. Rojo, D. Valencia, E. Moguel, J. Berrocal, J. M. Murillo, "Quantum Software as a Service Through a Quantum API Gateway", IEEE Internet Computing, Vol. 26, No. 1, 2022, pp. 34-41.

[105] R. Biswas et al. "A NASA perspective on quantum computing: Opportunities and challenges", Parallel Computing, Vol. 64, 2017, pp. 81-98.

[106] Z. G. Izquierdo, I. Hen, T. Albash, "Testing a Quantum Annealer as a Quantum Thermal Sampler", ACM Transactions on Quantum Computing, Vol. 2, No. 2, 2021, pp. 1-20.

[107] F. Ahmed, P. Mähönen, "Quantum computing for artificial intelligence based mobile network optimization", Proceedings of the IEEE 32nd Annual International Symposium on Personal, Indoor and Mobile Radio Communications, Helsinki, Finland, 13-16 September 2021, pp. 1128-1133.

[108] H.-L. Huang, D. Wu, D. Fan, X. Zhu, "Superconducting quantum computing: a review", Science China Information Sciences, Vol. 63, No. 8, 2020, pp. 1-32.

[109] B. C. Burnaby, "Let's Get Practical*: D-Wave Details Product Expansion & Cross Platform Roadmap", https://www.dwavesys.com/company/newsroom/press-release/let-s-get-practical-d-wave-details-product-expansion-cross-platform-roadmap/ (accessed: 2021)

[110] IBM, https://www.ibm.com/quantum/roadmap (accessed: 2023)

[111] H. Riel, "Quantum Computing Technology", Proceedings of the IEEE International Electron Devices Meeting, San Francisco, CA, USA, 11-16 December 2021.

Exploring the Satisfaction and Continuance Intention to Use E-Learning Systems: An Integration of the Information Systems Success Model and the Technology Acceptance Model

Original Scientific Paper

Ahmad AL-Hawamleh
Department of Electronic Training,
Institute of Public Administration,
Malaz, Riyadh, Saudi Arabia
alhawamleha@ipa.edu.sa

Abstract – *In view of the global crisis that has increased the use of online learning, it is imperative to comprehend the factors that affect users' perceptions and behaviors when utilizing e-learning systems. In order to examine the impact of quality factors on user satisfaction and continuance intention using e-learning systems, this study integrates the Information Systems Success Model (ISSM) with the Technology Acceptance Model (TAM). The aim of this research is to shed light on the relationships between the e-learning systems' quality, perceived usefulness, perceived ease of use, user satisfaction, and intention to continue using them. This research employed partial least squares structural equation modeling (PLS-SEM) to assess the research model. The analysis was grounded in survey data collected from a randomly selected sample of 372 students at Arab Open University in Saudi Arabia. The study's results confirm that information quality for platforms and courses positively influences perceived usefulness, system quality, and perceived ease of use. Additionally, perceived usefulness and ease of use are significantly linked to user satisfaction, supporting the notion that enhancing information quality contributes to higher user satisfaction and encourages continued engagement. The developers of e-learning systems and educational institutions may use these findings to enhance the design, content, and usability of their platforms.*

Keywords: *quality factors, usefulness, ease of use, user satisfaction, continuance intention, e-learning systems*

1. INTRODUCTION

The COVID-19 pandemic has led to a significant transformation in education, prompting universities to adopt innovative approaches like e-learning and mobile learning. These technologies aim to enhance accessibility, meet diverse student needs, improve tracking capabilities, and ensure cost-effectiveness [1]. However, this shift has also highlighted gaps in internet access and technology resources, leading to a digital divide among students [2]. E-learning systems are crucial for their versatility, adaptability, and scalability, allowing students to continue their education despite physical obstacles [3].

In 2022, the global e-learning market reached a substantial size of $288.8 billion, and projections indicate a trajectory towards $840.11 billion by 2030, reflecting a notable compound annual growth rate (CAGR) of 17.5% from 2021 to 2030 [4, 5]. As per SPER Market Research report [6], the Saudi Arabia e-learning market is anticipated to witness substantial growth, with predictions indicating a market size of $8.44 billion by 2032. This projection reflects a Compound Annual Growth Rate (CAGR) of 16.32%, underscoring the significant momentum and expansion expected within the e-learning sector in Saudi Arabia [6]. The data suggests a robust upward trajectory, emphasizing the increasing prominence and investment in e-learning initiatives in the country [6].

Despite substantial financial investments, particularly in Saudi Arabia, certain educational institutions face challenges in realizing the full potential of e-learning [7], leading to a focused scholarly exploration through empirical studies. The sudden shift to remote learning during the global pandemic presented challenges in adapting to new technologies, causing dissatisfaction among learners who prefer traditional, in-person classes [8]. Issues such as a non-conducive home environment, concerns about online education quality, and the absence of social interactions found in traditional classrooms have adversely affected students' e-learning experiences [9]. To address this decline in student interest and improve the e-learning landscape, scholarly efforts are crucial, emphasizing the need to adapt technology, redefine learning environments, and enhance the overall online educational experience.

E-learning system success relies on a thorough examination of course quality, information quality, system quality, services quality, and content usefulness [10, 11]. These factors help create engaging and credible learning experiences, build trust, minimize disruptions, and foster a supportive environment [12]. A well-structured curriculum aligned with learning objectives enhances engagement and comprehension, while accurate and well-organized information builds trust among learners. The technical robustness of the system, coupled with responsive customer support and supplementary resources, contributes to a supportive learning environment and overall learner satisfaction. Intuitive navigation and a user-friendly interface reduce barriers, enhancing accessibility for users. By addressing these quality factors, e-learning providers can tailor their platforms to meet learners' needs and ensure their educational initiatives' success.

The fusion of the Information Systems Success Model (ISSM) and the Technology Acceptance Model (TAM) presents a holistic framework for assessing e-learning systems [13]. Through the integration of these models, researchers gain a comprehensive tool to enhance e-learning systems, focusing on critical factors such as system quality, information quality, and user satisfaction. This thorough examination of elements ensures the sustenance of motivation and facilitates the design of systems aligned with learners' needs. The integrated ISSM and TAM approach enables the identification of strengths and weaknesses, providing insights for initiatives aimed at enhancing system efficiency and overall quality. This method proves instrumental in recognizing both the positive aspects and limitations of e-learning systems, thereby formulating strategies to amplify their effectiveness and quality. Such integration is indispensable for the development of e-learning systems that are not only useful but also of high quality.

This research strives to understand user satisfaction and their intention to continue using e-learning systems by integrating ISSM and TAM models. This will allow for the development of effective techniques for handling issues during crises. The study aims to enhance the learning environment within the e-learning system by identifying factors that contribute to a more satisfying and engaging user experience, ultimately leading to increased retention of learning outcomes. Furthermore, the outcomes of this study provide direction to e-learning system supervisors on how to boost the user experience and facilitate the learning process.

2. LITERATURE REVIEW

2.1. E-LEARNING SYSTEM

E-learning systems are essential for today's society. Because of the rising use of technology and the internet, the e-learning platform has become an essential tool for learners and instructors [14]. According to [15], e-learning is the process of teaching and learning via the use of electronic devices and digital media. It may be delivered through multiple channels, such as online courses, webinars, video conferencing, podcasts, and virtual classrooms. E-learning platforms provide students and teachers with a flexible, convenient, and cost-effective way to study [16].

E-learning systems are described as information systems that provide a secure environment for learning where students can register for online courses [17]. Because platforms enable students to search for online courses and pay the enrollment cost directly, these platforms have been referred to as online training course markets [18]. Similar to this, [19] described an e-learning system as a coordinated collection of interactive services that are available online and are not constrained by time or location. These platforms give educators, students, and individuals who are interested in learning the resources and tools they need to support and improve the educational process [20]. Learners may access courses and take part in a variety of educational activities through an e-learning system. In addition, they provide collaborative environments where students may interact online, share knowledge, and collaborate to solve issues [1].

Moodle is one example of an e-learning platform. Worldwide, educators utilize Moodle, a free and open-source learning management system [21]. According to [22], Moodle offers an environment for developing and delivering online courses that allows students to access course materials, communicate with instructors and other students, and complete assessments. Another example is Blackboard, which is used by numerous universities all around the world. According to [23], Blackboard is a recognized learning management system. Course administration, communication tools, and evaluation tools are only some of its many features and functions. Along with learning management systems, another type of e-learning platform that is growing is massive open online courses (MOOCs). MOOCs are free online courses that are offered by educational institutions and organizations. They usually feature interactive quizzes, discussion boards, and video lectures. MOOCs have limitations, such as poor completion rates and a lack of accreditation, despite the fact that they give many students an opportunity to access high-quality education [24].

Overall, as a result of technological developments and educational reforms, the nature of e-learning platforms is constantly changing. As technology advances, e-learning is anticipated to play a more significant role in how education is delivered. Research on e-learning pros and cons is essential for effective, accessible education.

2.2. BENEFITS AND CHALLENGES

E-learning emerges as a transformative powerhouse in education, fundamentally reshaping learning dynamics beyond conventional boundaries [25]. Its multifaceted advantages redefine how individuals acquire and disseminate knowledge, marking a paradigm shift in educational engagement. Central to its impact is unparalleled flexibility, liberating learners from rigid schedules and allowing them to engage with course materials at their own pace, transcending convenience to foster a culture of lifelong learning [26]. Beyond flexibility, the inherent cost-efficiency of e-learning diverges significantly from traditional models, eliminating physical infrastructure and reducing travel expenses, democratizing education, and breaking socio-economic barriers to access [1]. The global reach of e-learning dismantles geographical constraints, fostering cultural exchange as learners from diverse corners of the world converge in virtual classrooms, highlighting its unifying potential [3]. Additionally, e-learning platforms champion a customizable learning experience through the seamless integration of adaptive technologies, allowing educators to tailor courses to individual needs [27]. This high level of customization ensures an adaptive and responsive journey, accommodating diverse learning styles and preferences [28]. The integration of interactive content further enhances the experience, making multimedia elements integral components that foster engagement, active participation, and improved knowledge retention in online courses [29].

The e-learning landscape, despite its numerous advantages, is intricately entwined with challenges, demanding a nuanced and comprehensive approach for the continual enhancement of online education. Technical barriers pose formidable obstacles to achieving equitable e-learning opportunities, manifested through limited access to reliable internet connections, outdated hardware, and insufficient digital literacy skills [30]. Closing these disparities is crucial for fostering inclusivity in the digital education era, underscoring the urgency of addressing both infrastructural and skill-based gaps. The absence of face-to-face interaction introduces complexity to e-learning as virtual classrooms strive to recreate interpersonal dynamics, yet replicating the immediacy of traditional classroom interactions proves to be inherently intricate [31]. Balancing technological connectivity with the essential human element becomes a persistent challenge in ensuring effective and engaging e-learning experiences, necessitating the ongoing exploration of innovative solutions that cultivate meaningful connections in virtual spaces [32]. Additionally, the e-learning landscape grapples with the critical concern of assessment integrity in the online environment, where the remote nature of evaluations amplifies the risks of cheating and plagiarism [33]. Proactive measures are essential to ensuring the credibility of e-learning programs, emphasizing the implementation of secure and adaptable assessment methods tailored to the nuances of the online medium [34]. Navigating these challenges requires a holistic approach, addressing technical, pedagogical, and socio-economic factors to unlock the transformative potential of e-learning, ushering in an era where education transcends boundaries and becomes universally accessible.

3. THEORETICAL DEVELOPMENT AND FORMATION OF HYPOTHESES

3.1. TECHNOLOGY ACCEPTANCE MODEL (TAM)

The Technology Acceptance Model (TAM) is a theoretical framework rooted in Fishbein & Ajzen's theory of reasoned action, emphasizing that pre-existing attitudes and behavioral intentions shape individual behavior [35]. TAM asserts that a user's attitude toward a new technology, influenced by beliefs such as Perceived Usefulness and Perceived Ease of Use, dictates whether the user will adopt or reject the technology [36]. While TAM has garnered support for its applicability, critics note its limited explanatory and predictive power [37-39], prompting researchers to explore extensions such as substituting learning outcome beliefs for user log data to enhance practicality in the e-learning context [14, 40, 41].

Variables within TAM include Perceived Usefulness, Perceived Ease of Use, attitude, behavioral intentions, and actual use. The model's critical constructs, Perceived Usefulness and Perceived Ease of Use, significantly impact learners' acceptance of e-learning technology and their behavioral intention to use it in future scenarios [41]. Successful technology integration in learning depends on how available technologies are embraced and used, with Perceived Usefulness and Perceived Ease of Use determining learners' acceptance and overall e-learning performance [14]. Additionally, attitude plays a pivotal role in influencing behavioral intention and actual system usage [42]. Studies have consistently highlighted attitude as a crucial factor in acceptance behavior, with Perceived Ease of Use and Perceived Usefulness influencing students' attitudes toward technology [35, 36, 39, 40]. Overall, positive attitudes toward e-learning are fostered when instructors and learners find it valuable and easy to use.

3.2. DELONE AND MCLEAN INFORMATION SYSTEMS SUCCESS MODEL (ISSM)

The DeLone and McLean Information Systems Success Model (ISSM) serves as a comprehensive framework for assessing information systems, including e-learning systems [43]. Originating in 1992 and updated in 2003, the model aims to provide a thorough understanding of factors contributing to information systems' success in organizations [44]. The six ISSM factors encompass system quality, information quality, service quality, user satisfaction, use, and net benefits, offering a comprehensive framework for evaluating the effectiveness of information systems. This model delves into the performance and impact of e-learning systems on learning outcomes, evaluating technological features, educational material accuracy, service quality, system use, and positive outcomes like improved learning performance and efficiency [10, 11, 45].

Within the ISSM, system quality is gauged by technological features such as reliability, accessibility, and usability, while information quality assesses the accuracy, relevance, and completeness of educational material [43, 46]. Service quality measures student assistance and support, influencing user satisfaction, and perceptions of the e-learning system [43, 47]. The model emphasizes system use as a success indicator, with frequency and intensity playing pivotal roles [48]. The net benefits dimension explores positive outcomes, including enhanced learning performance and efficiency [46]. By addressing each factor, educational institutions can enhance their e-learning platforms and optimize their impact on students' learning experiences. This includes actions like improving system quality through seamless integration and enhanced user interfaces, curating relevant educational content for information quality, and providing timely and effective learner support services for improved service quality.

3.3. MODEL DEVELOPMENT

The ISSM and TAM serve as pivotal frameworks for evaluating the effectiveness of e-learning systems, with the ISSM assessing information systems' success across various dimensions and the TAM focusing on user acceptance and behavior. Integrating these models allows for a comprehensive evaluation of e-learning systems, considering not only user acceptance but also their overall impact on education quality. This holistic approach facilitates the identification of areas for improvement, enabling the optimization of e-learning environments. Moreover, the ISSM and TAM offer a nuanced understanding of factors influencing user acceptance of e-learning technology [49]. By merging TAM's user-centric approach with ISSM's broader perspective on system success, institutions can create sustainable e-learning systems that continuously enhance user satisfaction and performance. The study aims to examine multiple factors derived from the ISSM and TAM, such as system quality, information quality (course and platform), perceived usefulness, perceived ease of use, user satisfaction, and intention to continue. Through a thorough literature analysis, the study develops a theoretical model by integrating the ISSM with TAM, providing a visual representation of its innovative approach, and laying the groundwork for future research in this domain.

3.3.1. Information Quality

Information quality refers to the level of information generated by a system, including accuracy, validity, reliability, suitability, and intelligibility [50]. In the digital era, information is crucial for the effectiveness of an e-learning system. This quality includes not only the course content but also the platform on which it is delivered [47]. The perceived usefulness of an e-learning system is significantly influenced by information quality, including course and platform quality [51]. Learners are more likely to regard the system as useful and successful when they have access to high-quality, relevant, accurate, and up-to-date information [43]. Additionally, a user-friendly, visually appealing, and easy-to-use platform increases the likelihood of learners interacting with the information and feeling encouraged to continue their studies [52]. Therefore, the quality of information is essential for the success of e-learning. After analyzing the preceding discussions, the following hypotheses are proposed:

H1: There is a positive relationship between the quality of course information and the perceived usefulness of using e-learning systems.

H2: There is a positive relationship between the quality of platform information and the perceived usefulness of using e-learning systems.

3.3.2. System Quality

System quality refers to a user's perception of a system [50], which is crucial for the success of e-learning. It is measured by the range of software applications and hardware offered [53]. A well-designed system serves as a trustworthy guide, guiding learners smoothly towards their objectives [54]. System quality significantly impacts the ease of use factor, as it directly impacts the user's ability to focus on content and absorb knowledge effectively [12]. A high-quality e-learning system should have reliable hardware, user-friendly interfaces, and an intuitive design. It should also be easily accessible, easy to use, and provide appropriate feedback to learners. User satisfaction is a key factor in the success of an e-learning system, and prioritizing system quality in design and implementation is essential [55]. Thus, the following hypothesis is presented based on the preceding discussions:

H3: There is a positive relationship between the quality of the system and the perceived ease of use of the e-learning systems.

3.3.3. Perceived Usefulness and Perceived Ease of Use

User satisfaction can be influenced by perceived usefulness and perceived ease of use [56]. Perceived usefulness relates to learners' perspectives about how utilizing an e-learning system would improve their performance and help them achieve their learning objectives [17], whereas perceived ease of use refers to learners' perceptions of the system's usability and navigation [57]. Learners are more likely to be satisfied with and engaged in the learning process if they view the system as useful and easy to use. To achieve high levels of user satisfaction, it is critical to develop and execute e-learning systems that are considered useful and easy to use. As a result, the following hypothesis is proposed:

H4: There is a positive relationship between the perceived usefulness of an e-learning system and the user's satisfaction with its usage.

H5: There is a positive relationship between the perceived ease of use of e-learning systems and the user's satisfaction with their usage.

3.3.4. User satisfaction and Continuance Intention

User satisfaction is one of the factors that determines an e-learning system's success [56]. Users who feel satisfied with the system are more likely to stay connected to it as well as participate in future learning activities [47]. Continuance intention is an important component of e-learning systems since it impacts whether or not users will use the system in the future [58]. User satisfaction is crucial in molding users' views toward the system and their willingness to utilize it in the future [59]. Users who are satisfied with the e-learning system are more likely to have favorable feelings regarding it, which impacts their willingness to continue using it [60]. Understanding the influence of user satisfaction on continuance intention is therefore critical for the sustained success of e-learning systems. As a result, the hypothesis that follows is proposed:

H6: There is a positive relationship between the user's satisfaction with an e-learning system and their continuance intention to use it.

4. RESEARCH METHODOLOGY

4.1. RESEARCH DESIGN AND SAMPLING

A questionnaire was employed as a data collection method in this study, using a quantitative approach. Data was collected from 384 students, both online and manually, who were chosen at random from Arab Open University, KSA. The research was explained to the participants before they started filling out the questionnaire, and their participation was completely optional. The survey took about 10 minutes to complete. The participants were chosen from different departments and faculties using a random sampling technique. After taking into consideration the missing data and questionnaires that were incomplete, 12 questionnaires were omitted. According to [61], who claimed the minimal sample size for quantitative research is (N = 200), the sample size of this study (N = 372) is adequate in light of this. The sample size was calculated using the formula below.

$$ss = \frac{z^2(p)(q)}{e^2}$$

where SS = Sample Size; z = 1.96 (95% CI); P = Prevalence Level (0.5 used for sample size required); Q = (1-p); E = Error Term (0.05). By inserting values into the formula, the sample size would be:

$$ss = \frac{1.96^2(0.5)(1-0.5)}{0.05^2}$$

$$ss = 384$$

4.2. INSTRUMENT

Our questionnaire items have been adapted to fit the setting of our study from previous studies, as indicated in Table 1. The constructs considered include Course Information Quality (CIQ) [12, 46], Platform Information Quality (PIQ) [62, 63], System Quality (SQ) [63], Perceived Usefulness (PU) [64, 65], Perceived Ease of Use (PE) [66], User Satisfaction (US) [67], and Continuance Intention (CI) [68, 69]. Except for the items in the demographics section of our study (such as age, gender, specialization, and year of study), all of the items used a five-point Likert scale.

Table 1. Questionnaire

Construct	Item	Measure
Course Information Quality	CIQ.1	The educational materials I require are available through the Arab Open University LMS and SIS.
	CIQ.2	The Arab Open University LMS and SIS provide the latest information about educational materials and their diversity.
	CIQ.3	The courses within the Arab Open University LMS and SIS are well prepared.
	CIQ.4	The information about the courses on the Arab Open University LMS and SIS is accurate.
	CIQ.5	The courses featured on the Arab Open University LMS and SIS are closely related to the learning process.
Platform Information Quality	PIQ.1	The Arab Open University provides the latest information about the LMS and SIS platforms.
	PIQ.2	The information provided by the Arab Open University LMS and SIS is completely easy to understand.
	PIQ.3	The instructions and guidelines for using the Arab Open University LMS and SIS are very precise.
	PIQ.4	The Arab Open University provides sufficient information related to the courses available on the LMS and SIS.
System Quality	SQ.1	The Arab Open University LMS and SIS are always available.
	SQ.2	The Arab Open University LMS and SIS are easy to use.
	SQ.3	The Arab Open University LMS and SIS contain attractive features that are admired by students.
	SQ.4	The Arab Open University LMS and SIS provide quick access to information.
Perceived Usefulness	PU.1	Using the Arab Open University LMS and SIS enhances my learning effectiveness.
	PU.2	Using the Arab Open University LMS and SIS can improve my learning performance.
	PU.3	Using the Arab Open University LMS and SIS gives me greater control over my learning.
	PU.4	I find the Arab Open University LMS and SIS to be useful in my learning.
Perceived Ease of Use	PE.1	Learning to use the Arab Open University LMS and SIS would be easy for me.
	PE.2	I would find it easy to use the Arab Open University LMS and SIS to do my tasks.
	PE.3	My interaction with the Arab Open University LMS and SIS would be clear and understandable.
	PE.4	I find the Arab Open University LMS and SIS require less physical effort.
	PE.5	Using the Arab Open University LMS and SIS gives me greater control over my learning.

User Satisfaction	US.1	The Arab Open University LMS and SIS are effective in their use.
	US.2	I am satisfied with the performance of the Arab Open University LMS and SIS.
	US.3	I am pleased with the experience of using the Arab Open University LMS and SIS.
	US.4	I am happy with the functions provided by the Arab Open University LMS and SIS.
	US.5	My decision to use the Arab Open University LMS and SIS was a wise one.
Continuance Intention	CI.1	I will use the Arab Open University LMS and SIS on a regular basis in the future.
	CI.2	I will frequently use the Arab Open University LMS and SIS in the future.
	CI.3	I will strongly recommend that others use it.

5. DATA ANALYSIS AND RESULTS

For analyzing the data related to satisfaction and continuance intention of e-learning systems, we employed the Smart-PLS version 4 software developed by [70]. This software utilizes Partial Least Squares Structural Equation Modeling (PLS-SEM), which was deemed suitable for our exploratory study. PLS-SEM is particularly advantageous when working with small sample sizes, as it provides high statistical power.

Furthermore, the software allows for the evaluation of both the measurement and structural models, which are the two key stages in PLS-SEM analysis [71, 72]. It is important to note, as highlighted by [73], that SEM is the recommended approach when estimating models involving latent variables.

5.1. EVALUATION OF THE MEASUREMENT MODEL

In the ensuing segments, we embark on a comprehensive examination of the measurement model data in terms of evaluating the measures' reliability and validity. Our analysis encompasses an evaluation of internal consistency reliability and item loadings, as well as convergent and discriminant validity [61].

Item loadings and internal consistency reliability. To scrutinize the item loadings, PLS-SEM was employed. As illustrated in Table 2 and Fig. 1, the findings of this analysis reveal that all item loadings exceeded the recommended threshold value of >0.70 [61]. Moreover, the evaluation of internal consistency reliability for the 30 items included in the analysis was carried out using both Cronbach's alpha (α) and composite reliability (CR) measures, both of which exceeded the recommended cutoff limit of 0.70 [61].

Convergent validity. Assessing convergent validity is a pivotal component in gauging the precision of a statistical model, as it affirms that evaluations of comparable constructs have a favorable correlation. To determine convergent validity, the average variance extracted (AVE) serves as a crucial metric [74]. As demonstrated in Table 2, all AVE values surpass the recommended threshold of 0.50, suggesting that the constructs examined in this study exhibit convergent validity.

Discriminant validity. Three tests, the Heterotrait-Monotrait (HTMT) criterion, Fornell and Larcker's criterion, and cross-loadings, were used to assess the discriminant validity of the research constructs [75]. According to the analysis of the cross-loading values, each item loaded on its construct with a value greater than other constructs' cross-loadings, as seen in Table 3's loadings, which are tabulated in boldface font.

Table 2. Construct Reliability and Validity

Construct	Code	Loadings	VIF	CA	CR	AVE
Course Information Quality	CIQ.1	0.800	2.119	0.863	0.901	0.645
	CIQ.2	0.827	3.165			
	CIQ.3	0.855	3.222			
	CIQ.4	0.769	1.788			
	CIQ.5	0.760	1.539			
Platform Information Quality	PIQ.1	0.704	1.537	0.777	0.858	0.612
	PIQ.2	0.858	3.076			
	PIQ.3	0.862	3.135			
	PIQ.4	0.709	1.576			
System Quality	SQ.1	0.775	1.032	0.703	0.719	0.502
	SQ.2	0.715	1.674			
	SQ.3	0.707	1.840			
	SQ.4	0.738	1.411			
Perceived Usefulness	PU.1	0.715	1.871	0.804	0.856	0.606
	PU.2	0.927	2.790			
	PU.3	0.888	2.487			
	PU.4	0.718	1.952			

Perceived Ease of Use	PE.1	0.868	2.940	0.863	0.901	0.646
	PE.2	0.820	2.153			
	PE.3	0.787	2.116			
	PE.4	0.773	1.993			
	PE.5	0.766	2.258			
User Satisfaction	US.1	0.833	2.094	0.898	0.911	0.672
	US.2	0.745	1.540			
	US.3	0.771	2.004			
	US.4	0.830	2.219			
	US.5	0.909	2.781			
Continuance Intention	CI.1	0.759	2.080	0.776	0.851	0.656
	CI.2	0.790	1.643			
	CI.3	0.877	1.518			

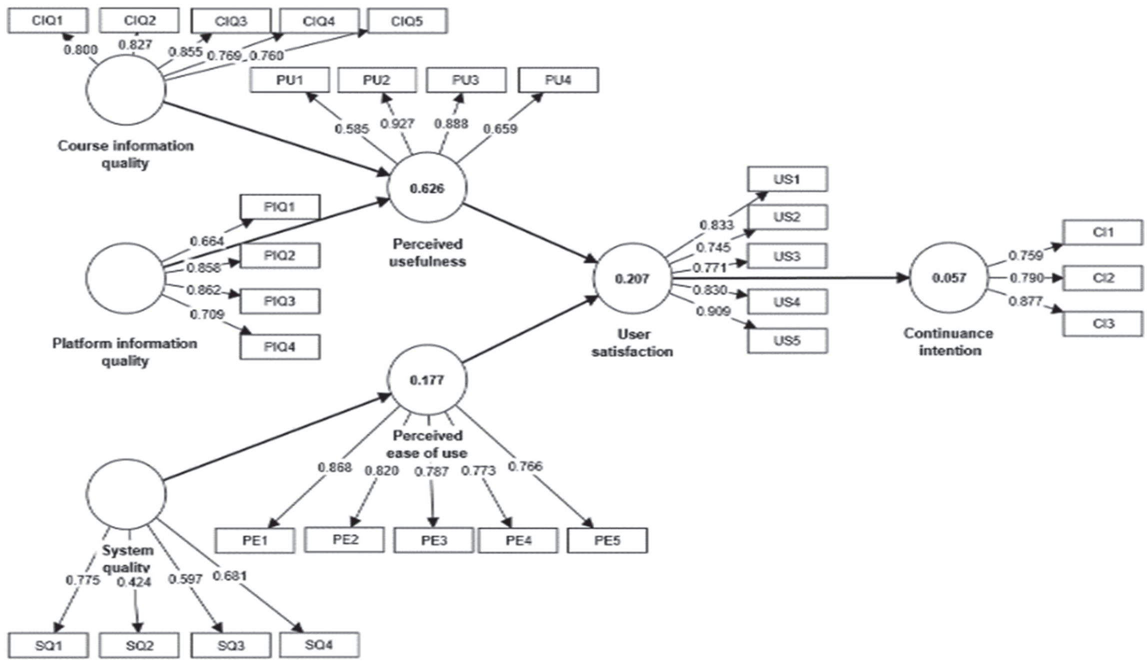

Fig. 1. Item loadings and R^2 values

Table 3. Discriminant validity based on the cross-loadings criterion

Item	CI	CIQ	PE	PU	PIQ	SQ	US
CI1	**0.759**	0.305	0.266	0.126	0.357	0.232	0.036
CI2	**0.790**	0.368	0.406	0.220	0.597	0.352	0.180
CI3	**0.877**	0.131	-0.016	-0.100	0.174	-0.072	0.238
CIQ1	0.383	**0.800**	0.655	0.428	0.645	0.311	0.325
CIQ2	0.160	**0.827**	0.464	0.586	0.503	0.590	0.175
CIQ3	0.250	**0.855**	0.583	0.585	0.499	0.422	0.269
CIQ4	0.311	**0.769**	0.833	0.557	0.695	0.421	0.314
CIQ5	0.118	**0.760**	0.556	0.732	0.617	0.442	0.128
PE1	0.365	0.790	**0.868**	0.530	0.649	0.490	0.250
PE2	-0.097	0.617	**0.820**	0.487	0.529	0.240	0.301
PE3	0.044	0.428	**0.787**	0.566	0.461	0.260	0.243
PE4	0.208	0.572	**0.773**	0.656	0.718	0.322	0.393
PE5	0.219	0.599	**0.766**	0.504	0.636	0.325	0.176
PIQ1	0.385	0.428	0.270	0.461	**0.704**	0.280	0.034
PIQ2	0.317	0.735	0.670	0.651	**0.858**	0.511	0.181
PIQ3	0.386	0.712	0.793	0.555	**0.862**	0.348	0.304
PIQ4	0.264	0.381	0.562	0.587	**0.709**	0.367	0.100
PU1	-0.233	0.266	0.292	**0.715**	0.340	0.375	-0.119
PU2	0.067	0.717	0.632	**0.927**	0.734	0.575	0.050
PU3	0.279	0.769	0.693	**0.888**	0.716	0.546	0.085
PU4	-0.443	0.246	0.331	**0.718**	0.200	0.413	-0.132

SQ1	0.153	0.314	0.366	0.369	0.187	**0.775**	0.288
SQ2	0.066	0.150	-0.043	0.246	0.236	**0.715**	-0.147
SQ3	-0.078	0.404	0.170	0.438	0.359	**0.707**	-0.183
SQ4	0.151	0.487	0.246	0.539	0.590	**0.738**	-0.098
US1	0.368	0.174	0.195	-0.027	0.223	0.081	**0.833**
US2	0.165	0.199	0.324	-0.034	0.107	0.091	**0.745**
US3	0.170	0.240	0.334	0.113	0.192	0.140	**0.771**
US4	0.052	0.262	0.215	-0.010	0.107	0.046	**0.830**
US5	0.176	0.318	0.317	0.051	0.200	0.064	**0.909**

The assessment of discriminant validity was carried out using the [76] criterion. This criterion states that discriminant validity is considered satisfactory when the squared values of the average variance extracted (AVE) surpass the shared variance between the AVE squared values of each construct and those of other constructs. To satisfy the recommendation by [77], a matrix was established, incorporating the correlation coefficient values between the value of each construct and the squared AVE values. As evident from the correlation and squared AVE values in Table 4, the statistical model achieved discriminant validity at the construct level, with higher squared AVE values on the diagonal than off-diagonal values.

Table 4. Discriminant validity assessment using the Fornell-Larcker criterion

Const.	1	2	3	4	5	6	7
CI	0.810						
CIQ	0.287	0.803					
PE	0.209	0.763	0.804				
PU	0.054	0.742	0.686	0.778			
PIQ	0.428	0.736	0.756	0.733	0.778		
SQ	0.145	0.555	0.421	0.621	0.495	0.633	
US	0.239	0.289	0.345	0.021	0.205	0.106	0.820

Table 5. Discriminant validity assessment using the HTMT criterion

Const.	1	2	3	4	5	6	7
CI	-						
CIQ	0.413	--					
PE	0.395	0.843	-				
PU	0.412	0.750	0.740	-			
PIQ	0.590	0.830	0.839	0.785	-		
SQ	0.425	0.637	0.400	0.733	0.672	-	
US	0.256	0.348	0.380	0.152	0.263	0.345	-

The Heterotrait-Monotrait (HTMT) ratio, suggested by [77], is a more recent approach to assessing discriminant validity. A value greater than 0.85 in this method's correlation between two latent variables denotes inadequate discriminant validity [77]. As demonstrated in Table 5, all of our study's HTMT values were below the recommended threshold, indicating sufficient discriminant validity.

5.2. EVALUATION OF THE STRUCTURAL MODEL

The inner Partial Least Squares model was employed throughout the structural model evaluation to assess multiple aspects. These included determining the amount of variance explained by the model, analyzing the magnitude of the relationships between the hypothesized variables, and assessing the significance and contribution of each variable. The coefficient of determination (R^2), effect size (f^2), and predictive relevance (Q^2), three basic metrics proposed by [61], were used to evaluate the structural model. In order to evaluate the model's explanatory power, the strength of the relationships between variables, and the presence of multicollinearity, these metrics were critical.

The findings shown in Table 6 indicate that the proposed model's predictors successfully account for a significant portion of the variance in the relationship between perceived usefulness, platform information quality, and course information quality. The R^2 and adj.R^2 values specifically indicate that the model predictors provide explanations for 62.6% and 62.2%, respectively, of the variation in this relationship. With R^2 and adj.R^2 values of 17.7% and 17.2%, respectively, the proposed model's predictors also account for a significant amount of variation in the relationship between system quality and perceived ease of use.

Additionally, it was found that the relationships between perceived usefulness, perceived ease of use, and user satisfaction were 20.7% and 19.7%, respectively, for R^2 and adj. R^2. On the other hand, user satisfaction and continuance intention had R^2 and adj. R^2 values of 5.7% and 5.1%, respectively. These values indicate that the proposed model predictors explain only a weak proportion of the variance in this relationship.

Nevertheless, it is worth noting that [77] accepts a moderate R2 when the model involves only one or two exogenous latent variables. Determining preferred R^2 values is challenging since they often depend on the level of model complexity and the specific research discipline [61]. Overall, the results indicate that the proposed model effectively explains the relationships between the study factors. However, it is crucial to consider the limitations of the model and the potential impact of other variables not included in the analysis.

A specific exogenous variable's substantive effect on an endogenous variable is measured by f^2, as opposed to R^2, which focuses on each endogenous latent variable. For determining the impact of predictors, this effect size test is employed. The small, medium, and large effects, respectively, are represented by f^2 values of 0.02, 0.15, and 0.35, according to [61], a guideline. Effect size values (f^2) ranging from 0.061 to 0.261 were used in this study to assess how the proposed predictors impacted the variance of the dependent variable. This indicates a medium-level contribution from each predictor in the model. A higher f^2 value suggests a more significant role for the predictor variable.

Furthermore, used to evaluate the PLS model's predictive power was predictive relevance (Q^2). The model is considered valid if the Q^2 value is higher than 0. A blindfolding procedure was used to further assess the accuracy of the model, and the results showed large predictive relevance with Q^2 values of 0.019 and 0.321. Every predictor in the model had a variance inflation factor (VIF) value that was below 3.3.

Table 6. Structural model evaluation

Construct	R2	Adj. R2	f2	Q2
CIQ	-	-	0.240	-
PIQ	-	-	0.203	-
SQ	-	-	0.216	-
PU	0.626	0.622	0.111	0.321
PE	0.177	0.172	0.261	0.103
US	0.207	0.197	0.061	0.128
CI	0.057	0.051	-	0.019

A bootstrapping approach with 5,000 iterations was employed to assess the structural linkages between the study factors. The results revealed several significant positive relationships, confirming the proposed hypotheses, as shown in Table 7.

Table 7. Hypotheses Testing

Structural Path	Coef (β) & T-statistics	P-Values	Bias-corrected 95% CI Lower Upper	Remarks
H1: CIQ→ PU	0.442 (6.108)	0.000	(0.298, 0.576)	Supported
H2: PIQ→ PU	0.407 (5.607)	0.000	(0.270, 0.551)	Supported
H3: SQ→ PE	0.421 (6.468)	0.000	(0.303, 0.559)	Supported
H4: PU→ US	0.408 (4.453)	0.000	(0.577, 0.214)	Supported
H5: PE→ US	0.625 (6.639)	0.000	(0.431, 0.792)	Supported
H6: US→ CI	0.239 (2.852)	0.004	(0.131, 0.384)	Supported

Firstly, results showed that there was a significant positive relationship between course information quality and perceived usefulness (β = 0.442; $p < 0.05$), supporting Hypothesis 1. Similar to the previous finding, Hypothesis 2 was supported by the finding that platform information quality and perceived usefulness had a significant positive relationship (β = 0.407; $p < 0.05$). Additionally, a significant positive relationship between perceived ease of use and system quality was found (β = 0.421; $p < 0.05$), supporting Hypothesis 3.

There was a significant positive relationship between perceived usefulness and user satisfaction (β = 0.408; $p < 0.05$), supporting Hypothesis 4. Additionally, a significant positive relationship between perceived ease of use and user satisfaction was found (β = 0.625; $p < 0.05$), supporting Hypothesis 5. Finally, the findings supported Hypothesis 6 by indicating a significant positive relationship between user satisfaction and continuance intention (β = 0.239; $p < 0.05$). Fig. 2 presents a visual representation of these findings.

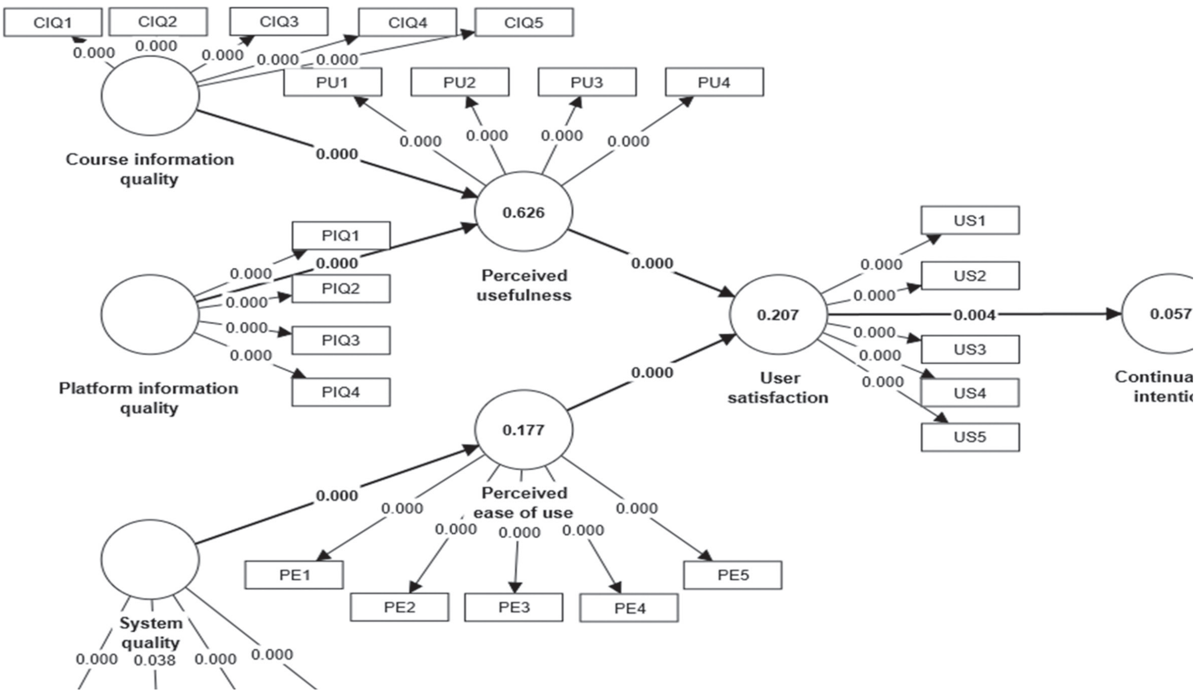

Fig. 2. Coefficient significance test

6. DISCUSSIONS

The study found a positive correlation between the quality of course information and students' perceived usefulness of the course. This suggests that more accurate, comprehensive, and relevant information enhances students' perceptions of the course's usefulness. To improve course information quality, institutions should prioritize it, provide detailed learning outcomes, seek student feedback, offer supplementary resources, and foster communication and transparency. Establishing channels for students to ask questions promotes open dialogue, trust, and a supportive learning environment.

Furthermore, the study found a positive correlation between the quality of platform information and its perceived usefulness, supporting the hypothesis that high-quality information enhances users' perceptions of a platform's usefulness. Institutions and educators should ensure reliable, accurate, and tailored information, communicate features clearly, avoid excessive technical jargon, and regularly solicit user feedback through surveys, interviews, and focus groups. Additionally, providing user support channels like live chat or email can help address user questions and concerns promptly.

To confirm Hypothesis 3, a positive correlation exists between system quality and perceived ease of use. To achieve this, system providers can optimize performance, streamline processes, design an intuitive interface, offer comprehensive user support, conduct regular usability testing, and stay updated with technological advancements and user preferences. This will ensure the system's quality and adaptability to evolving user needs, thereby enhancing the user experience.

To validate Hypothesis 4, system or product providers should align features with user needs through research and feedback, ensure clear functionality, user-friendly interfaces, and comprehensive support channels. Actively gathering user feedback through surveys and testing sessions allows for ongoing improvements and updates. Implementing metrics and analytics to measure perceived usefulness and monitor user engagement provides insights for further enhancements.

The study confirms that perceived ease of use positively influences user satisfaction. To improve satisfaction, system or product providers can simplify the interface, provide clear instructions, streamline workflows, offer responsive support, conduct usability testing, and offer comprehensive training and onboarding resources. Regular usability testing and feedback gathering contribute to continuous improvements. Providing comprehensive training and onboarding resources reduces the learning curve and boosts confidence, further enhancing perceived ease of use and satisfaction.

The study confirms a positive correlation between user satisfaction and e-learning intention to continue, indicating that providers should focus on streamlined interfaces, optimized content delivery, and seamless navigation. Personalizing learning experiences, fostering collaboration, providing timely feedback, updating content and effectively communicating benefits also contribute to satisfaction.

7. CONCLUSION

This study aimed to explore the impact of quality factors on e-learning system user satisfaction and continuance intention by integrating the ISSM with the TAM. The study was motivated by the growing relevance of e-learning systems, particularly in light of the global crisis that has harmed traditional education methods. The study highlights the importance of course information quality, platform information quality, and system quality in enhancing users' perceived usefulness and satisfaction with e-learning systems. Educational institutions and e-learning system providers can use these findings to improve the design, content, and usability of their platforms, leading to higher user satisfaction and increased continuance intention.

However, the study has limitations. Its focus on a specific context or sample may limit its generalizability, and its use of self-reported data is vulnerable to response bias. Additionally, the study did not consider the impact of external factors such as individual characteristics or social factors on user satisfaction and intention to continue. Future research could address these limitations by conducting research in various contexts and using mixed-method techniques.

The study also suggests future research in e-learning systems to understand the impact of individual characteristics, social factors, and new technologies on user satisfaction and continuance intention. Understanding how these factors interact with quality factors can provide insights for personalized e-learning platforms. Longitudinal studies could analyze the long-term impacts of user satisfaction on continuance intention, while new technologies like virtual reality or artificial intelligence could be explored to enhance the effectiveness of e-learning systems in online education.

8. REFERENCES:

[1] S. K. Arumugam, S. Saleem, A. K. Tyagi, "Future Research Directions for Effective E-Learning", Architecture and Technological Advancements of Education 4.0, IGI Global, 2024, pp. 75-105.

[2] A. Ennam, "Assessing Covid-19 pandemic-forced transitioning to distance e-learning in Moroccan universities: an empirical, analytical critical study of implementality and achievability", The Journal of North African Studies, Vol. 29, No. 1, 2024, pp. 153-177.

[3] M. Alenezi, "Digital learning and digital institution in higher education", Education Sciences, Vol. 13, No. 1, 2023, p. 88.

[4] H. Bagdi, S. V. Pothabathula, L. Sharma, H. P. Bulsara, "The global market upsurge in web traffic and revenues during the epidemic: an exploratory research of e-learning companies", International Journal of Development Issues, Vol. 22, No. 3, 2023, pp. 418-444.

[5] P. Dubey, R. L. Pradhan, K. K. Sahu, "Underlying factors of student engagement to E-learning", Journal of Research in Innovative Teaching & Learning, Vol. 16, No. 1, 2023, pp. 17-36.

[6] "Saudi Arabia E-Learning Market Overview", EDUI2306, https://www.sperresearch.com/report-store/saudi-arabia-e-Learning-market.aspx (accessed: 2023)

[7] A. Aldraiweesh, U. Alturki, "Exploring Factors Influencing the Acceptance of E-Learning and Students' Cooperation Skills in Higher Education", Sustainability, Vol. 15, No. 12, 2023, p. 9363.

[8] R. Tulaskar, M. Turunen, "What students want? Experiences, challenges, and engagement during Emergency Remote Learning amidst COVID-19 crisis", Education and information technologies, Vol. 27, No. 1, 2022, pp. 551-587.

[9] L. Soubra, M. A. Al-Ghouti, M. Abu-Dieyeh, S. Crovella, H. Abou-Saleh, "Impacts on student learning and skills and implementation challenges of two student-centered learning methods applied in online education", Sustainability, Vol. 14, No. 15, 2022, p. 9625.

[10] B. A. Y. Al-Nassar, "The influence of service quality in information system success model as an antecedent of mobile learning in education organisations: Case study in Jordan", International Journal of Mobile Learning and Organisation, Vol. 11, No. 1, 2017, pp. 41-62.

[11] M. N. AL-Nuaimi, O. S. Al Sawafi, S. I. Malik, M. Al-Emran, Y. F. Selim, "Evaluating the actual use of learning management systems during the covid-19 pandemic: an integrated theoretical model", Interactive Learning Environments, Vol. 31, No. 10, 2023.

[12] A. Al Mulhem, "Investigating the effects of quality factors and organizational factors on university students' satisfaction of e-learning system quality", Cogent Education, Vol. 7, No. 1, 2020, p. 1787004.

[13] D. Legramante, A. Azevedo, J. M. Azevedo, "Integration of the technology acceptance model and the information systems success model in the analysis of Moodle's satisfaction and continuity of use", The International Journal of Information and Learning Technology, Vol. 40, No. 5, 2023, pp. 467-484.

[14] F. Balaman, M. Baş, "Perception of using e-learning platforms in the scope of the technology acceptance model (TAM): a scale development study", Interactive Learning Environments, Vol. 31, No. 8, 2023, pp. 5395-5419.

[15] R. C. Clark, R. E. Mayer, "E-learning and the science of instruction: Proven guidelines for consumers and designers of multimedia learning", John Wiley & Sons, 2023.

[16] L. Rajab, T. Almarabeh, H. Mohammad, Y. Majdalawi, "Strategic evaluation of e-learning: A case study of the university of Jordan during crisis", International Journal of Data and Network Science, Vol. 8, No. 1, 2024, pp. 109-116.

[17] D. Al-Fraihat, M. Joy, J. Sinclair, "Evaluating E-learning systems success: An empirical study", Computers in Human Behavior, Vol. 102, 2020, pp. 67-86.

[18] L. J. Waks, "Massive Open Online Courses and the Future of Higher Education", Contemporary Technologies in Education: Maximizing Student Engagement, Motivation, and Learning, Palgrave Macmillan Cham, 2019, pp. 183-213.

[19] A. Klašnja-Milićević, B. Vesin, M. Ivanović, Z. Budimac, L. C. Jain, "Introduction to E-learning systems", E-learning systems: Intelligent techniques for personalization, Vol. 112, 2017, pp. 3-17.

[20] A. Haleem, M. Javaid, M. A. Qadri, R. Suman, "Understanding the role of digital technologies in education: A review", Sustainable Operations and Computers, Vol. 3, 2022, pp. 275-285.

[21] O. Guirette-Barbosa, J. G. Vargas-Hernandez, S. Castañeda-Burciaga, M. García-Camacho, J. Reyes-Sánchez, "Moodle: Motivational Element for Pre-

Pandemic Teaching-Learning Processes", in Cases on Economics Education and Tools for Educators, IGI Global, 2024, pp. 205-228.

[22] A. Althunibat et al. "Learning Experience of Students Using the Learning Management System: User's Perspective on the Use of Moodle in the University of Jordan", Advances in Human-Computer Interaction, Vol. 2023, 2023.

[23] F. K. Alzahrani, W. S. Alhalafawy, "Gamification for Learning Sustainability in the Blackboard System: Motivators and Obstacles from Faculty Members' Perspectives", Sustainability, Vol. 15, No. 5, 2023, p. 4613.

[24] S. R. Virani, J. R. Saini, S. Sharma, "Adoption of massive open online courses (MOOCs) for blended learning: The Indian educators' perspective", Interactive Learning Environments, Vol. 31, No. 2, 2023, pp. 1060-1076.

[25] S. J. Marshall, "Shaping the University of the Future: Using Technology to Catalyse Change in University Learning and Teaching", Springer, 2018.

[26] S. He, S. Jiang, R. Zhu, X. Hu, "The influence of educational and emotional support on e-learning acceptance: An integration of social support theory and TAM", Education and Information Technologies, Vol. 28, 2023, pp. 11145-11165.

[27] S.-C. Kong, C.-K. Looi, T.-W. Chan, R. Huang, "Teacher development in Singapore, Hong Kong, Taiwan, and Beijing for e-Learning in school education", Journal of Computers in Education, Vol. 4, 2017, pp. 5-25.

[28] L. G. Palacio et al. "Work in progress: Co-creation as a method for the identification of new functionalities for the customization of students learning styles for virtual learning platforms", Proceedings of the IEEE World Conference on Engineering Education, Bogota, Colombia, 15-18 March 2020, pp. 1-5.

[29] T. Muir, I. Wang, A. Trimble, C. Mainsbridge, T. Douglas, "Using interactive online pedagogical approaches to promote student engagement", Education Sciences, Vol. 12, No. 6, 2022, p. 415.

[30] M. S. Contreras-Ortiz, P. P. Marrugo, J. C. R. Ribón, "E-Learning Ecosystems for People with Autism Spectrum Disorder: A Systematic Review", IEEE Access, Vol. 11, 2023, pp. 49819-49832.

[31] M. T. Costado Dios, J. C. Piñero Charlo, "Face-to-face vs. E-learning models in the covid-19 era: Survey research in a Spanish university", Education Sciences, Vol. 11, No. 6, 2021, p. 293.

[32] I. Gligorea, M. Cioca, R. Oancea, A.-T. Gorski, H. Gorski, P. Tudorache, "Adaptive Learning Using Artificial Intelligence in e-Learning: A Literature Review", Education Sciences, Vol. 13, No. 12, 2023, p. 1216.

[33] M. Sedaghatjou, J. Hughes, M. Liu, F. Ferrara, J. Howard, M. F. Mammana, "Teaching STEM online at the tertiary level during the COVID-19 pandemic", International Journal of Mathematical Education in Science and Technology, Vol. 54, No. 3, 2023, pp. 365-381.

[34] S. A.-L. Akacha, A. I. Awad, "Enhancing Security and Sustainability of e-Learning Software Systems: A Comprehensive Vulnerability Analysis and Recommendations for Stakeholders", Sustainability, Vol. 15, No. 19, 2023, p. 14132.

[35] H. Rafique, Z. Ul Islam, A. Shamim, "Acceptance of e-learning technology by government school teachers: Application of extended technology acceptance model", Interactive Learning Environments, 2023, pp. 1-19. (in press)

[36] G.-Z. Wong, K.-H. Wong, T.-C. Lau, J.-H. Lee, Y.-H. Kok, "Study of intention to use renewable energy technology in Malaysia using TAM and TPB", Renewable Energy, Vol. 221, 2024, p. 119787.

[37] O. Ukoha, H. O. Awa, C. A. Nwuche, I. F. Asiegbu, E. Cohen, "Analysis of Explanatory and Predictive Architectures and the Relevance in Explaining the Adoption of IT in SMEs", Interdisciplinary Journal of Information, Knowledge & Management, Vol. 6, 2011.

[38] F. Munoz-Leiva, S. Climent-Climent, F. Liébana-Cabanillas, "Determinants of intention to use the mobile banking apps: An extension of the classic TAM model", Spanish Journal of Marketing-ESIC, Vol. 21, No. 1, 2017, pp. 25-38.

[39] R. Scherer, F. Siddiq, J. Tondeur, "The technology acceptance model (TAM): A meta-analytic structural equation modeling approach to explaining teachers' adoption of digital technology in education", Computers & Education, Vol. 128, 2019, pp. 13-35.

[40] R. Boateng, A. S. Mbrokoh, L. Boateng, P. K. Senyo, E. Ansong, "Determinants of e-learning adoption among students of developing countries", The International Journal of Information and Learning Technology, Vol. 33, No. 4, 2016, pp. 248-262.

[41] D. R. Bailey, N. Almusharraf, A. Almusharraf, "Video conferencing in the e-learning context: explaining learning outcome with the technology acceptance model", Education and Information Technologies, Vol. 27, No. 6, 2022, pp. 7679-7698.

[42] M. Mailizar, D. Burg, S. Maulina, "Examining university students' behavioural intention to use e-learning during the COVID-19 pandemic: An extended TAM model", Education and Information Technologies, Vol. 26, No. 6, 2021, pp. 7057-7077.

[43] I. Y. Alyoussef, "Acceptance of e-learning in higher education: The role of task-technology fit with the information systems success model", Heliyon, Vol. 9, No. 3, 2023.

[44] W. H. DeLone, E. R. McLean, "The DeLone and McLean model of information systems success: a ten-year update", Journal of management Information Systems, Vol. 19, No. 4, 2003, pp. 9-30.

[45] P. E. Ramirez-Correa, F. J. Rondan-Cataluña, J. Arenas-Gaitán, J. L. Alfaro-Perez, "Moderating effect of learning styles on a learning management system's success", Telematics and Informatics, Vol. 34, No. 1, 2017, pp. 272-286.

[46] A. S. Al-Adwan, N. A. Albelbisi, O. Hujran, W. M. Al-Rahmi, A. Alkhalifah, "Developing a holistic success model for sustainable e-learning: A structural equation modeling approach", Sustainability, Vol. 13, No. 16, 2021, p. 9453.

[47] A. M. Sayaf, "Adoption of E-learning systems: An integration of ISSM and constructivism theories in higher education", Heliyon, Vol. 9, No. 2, 2023.

[48] S. Butt, A. Mahmood, S. Saleem, "The role of institutional factors and cognitive absorption on students' satisfaction and performance in online learning during COVID 19", Plos One, Vol. 17, 2022, No. 6, p. e0269609.

[49] A. A. Yunusa, I. N. Umar, "A scoping review of critical predictive factors (CPFs) of satisfaction and perceived learning outcomes in E-learning environments", Education and Information Technologies, Vol. 26, 2021, pp. 1223-1270.

[50] M. N. Tran, "A holistic success model for sustainable e-learning based on the stakeholder approach: Case of Vietnamese students during the COVID-19 pandemic", Cogent Business & Management, Vol. 10, No. 2, 2023, p. 2236298.

[51] J. Zheng, H. Khalid, "The Adoption of Enterprise Resource Planning and Business Intelligence Systems in Small and Medium Enterprises: A Conceptual Framework", Mathematical Problems in Engineering, Vol. 2022, 2022.

[52] D. N. Tahat et al. "Technology Enhanced Learning in Undergraduate Level Education: A Case Study of Students of Mass Communication", Sustainability, Vol. 15, No. 21, 2023, p. 15280.

[53] R. Weerarathna et al. "Effect of E-learning on Management Undergraduates' Academic Success during COVID-19: A Study at Non-state Universities in Sri Lanka", Heliyon, Vol. 9, No. 9, 2023.

[54] S. Farid, R. Ahmad, M. Alam, A. Akbar, V. Chang, "A sustainable quality assessment model for the information delivery in E-learning systems", Information Discovery and Delivery, Vol. 46, No. 1, 2018, pp. 1-25.

[55] J. S. Mtebe, C. Raphael, "Key factors in learners' satisfaction with the e-learning system at the University of Dar es Salaam, Tanzania", Australasian Journal of Educational Technology, Vol. 34, No. 4, 2018.

[56] R. E. Masadeh, D. Almajali, A. A. Alrowwad, R. Alkhawaldeh, S. Khwaldeh, B. Obeid, "Evaluation of factors affecting university students' satisfaction with e-learning systems used dur-ing Covid-19 crisis: A field study in Jordanian higher education institutions", International Journal of Data and Network Science, Vol. 7, No. 1, 2023, pp. 199-214.

[57] D. Pal, V. Vanijja, "Perceived usability evaluation of Microsoft Teams as an online learning platform during COVID-19 using system usability scale and technology acceptance model in India", Children and Youth Services Review, Vol. 119, 2020, p. 105535.

[58] N. Liu, Q. Pu, "Factors influencing learners' continuance intention toward one-to-one online learning", Interactive Learning Environments, Vol. 31, No. 3, 2023, pp. 1742-1763.

[59] D. M. H. Kee et al. "Post-Pandemic: University Students' Satisfaction on The Use of E-Learning", Asia Pacific Journal of Management and Education, Vol. 6, No. 3, 2023, pp. 1-15.

[60] I. Nedeljković, D. R. Petrović, "Student satisfaction and intention to use e-learning during the Covid-19 pandemic", The International Journal of Information and Learning Technology, Vol. 40, No. 3, 2023, pp. 225-241.

[61] J. F. Hair, J. J. Risher, M. Sarstedt, C. M. Ringle, "When to use and how to report the results of PLS-SEM", European Business Review, Vol. 31, No. 1, 2019, pp. 2-24.

[62] G. Jiang, F. Liu, W. Liu, S. Liu, Y. Chen, D. Xu, "Effects of information quality on information adoption on social media review platforms: Moderating role of perceived risk", Data Science and Management, Vol. 1, No. 1, 2021, pp. 13-22.

[63] N. Gorla, T. M. Somers, B. Wong, "Organizational impact of system quality, information quality, and service quality", The Journal of Strategic Information Systems, Vol. 19, No. 3, 2010, pp. 207-228.

[64] W.-S. Lin, C.-H. Wang, "Antecedences to continued intentions of adopting e-learning system in blended learning instruction: A contingency framework based on models of information system success and task-technology fit", Computers & Education, Vol. 58, No. 1, 2012, pp. 88-99.

[65] Y.-M. Cheng, "Students' satisfaction and continuance intention of the cloud-based e-learning system: roles of interactivity and course quality factors", Education+ Training, Vol. 62, No. 9, 2020, pp. 1037-1059.

[66] T. Humida, M. H. Al Mamun, P. Keikhosrokiani, "Predicting behavioral intention to use e-learning system: A case-study in Begum Rokeya University, Rangpur, Bangladesh", Education and Information Technologies, Vol. 27, No. 2, 2022, pp. 2241-2265.

[67] J. C. Roca, C.-M. Chiu, F. J. Martínez, "Understanding e-learning continuance intention: An extension of the Technology Acceptance Model", International Journal of Human-Computer Studies, Vol. 64, No. 8, 2006, pp. 683-696.

[68] A. Bhattacherjee, "An empirical analysis of the antecedents of electronic commerce service continuance", Decision Support Systems, Vol. 32, No. 2, 2001, pp. 201-214.

[69] M.-C. Lee, "Explaining and predicting users' continuance intention toward e-learning: An extension of the expectation–confirmation model", Computers & Education, Vol. 54, No. 2, 2010, pp. 506-516.

[70] C. Ringle, S. Wende, J. Becker, H. Gmb, "SmartPLS—statistical software for structural equation modeling", Handbook of Market Research, 2017.

[71] M. O. A. Shbail, Z. Jaradat, M. Jbarah, S. O. A. Shbeil, "Factors that influence employees' acceptance of e-accounting: evidences from Jordanian SMEs", International Journal of Business Innovation and Research, Vol. 28, No. 1, 2022, pp. 83-100.

[72] J. Al-Gasawneh, A. AL-Hawamleh, A. Alorfi, G. Al-Rawashde, "Moderating the role of the perceived security and endorsement on the relationship between per-ceived risk and intention to use the artificial intelligence in financial services", International Journal of Data and Network Science, Vol. 6, No. 3, 2022, pp. 743-752.

[73] M. Sarstedt, J. F. Hair Jr, C. Nitzl, C. M. Ringle, M. C. Howard, "Beyond a tandem analysis of SEM and PROCESS: Use of PLS-SEM for mediation analyses!", International Journal of Market Research, Vol. 62, No. 3, 2020, pp. 288-299.

[74] J. Benitez, J. Henseler, A. Castillo, F. Schuberth, "How to perform and report an impactful analysis using partial least squares: Guidelines for confirmatory and explanatory IS research", Information & Management, Vol. 57, No. 2, 2020, p. 103168.

[75] Z. Jaradat, M. A. Shbail, M. B. Baker, "Environmental and organisational factors affecting the adoption of enterprise resource planning systems in the Jordanian banking sector", International Journal of Business Information Systems, Vol. 41, No. 1, 2022, pp. 82-107.

[76] C. Fornell, D. F. Larcker, "Structural equation models with unobservable variables and measurement error: Algebra and statistics", Journal of Marketing Research, Vol. 18, No. 3, 1981, pp. 382-388.

[77] J. Henseler, C. M. Ringle, M. Sarstedt, "A new criterion for assessing discriminant validity in variance-based structural equation modeling", Journal of the Academy of Marketing Science, Vol. 43, 2015, pp. 115-135.

INTERNATIONAL JOURNAL OF ELECTRICAL AND COMPUTER ENGINEERING SYSTEMS

Published by Faculty of Electrical Engineering, Computer Science and Information Technology Osijek, Josip Juraj Strossmayer University of Osijek, Croatia.

About this Journal

The International Journal of Electrical and Computer Engineering Systems publishes original research in the form of full papers, case studies, reviews and surveys. It covers theory and application of electrical and computer engineering, synergy of computer systems and computational methods with electrical and electronic systems, as well as interdisciplinary research.

Topics of interest include, but are not limited to:

- Power systems
- Renewable electricity production
- Power electronics
- Electrical drives
- Industrial electronics
- Communication systems
- Advanced modulation techniques
- RFID devices and systems
- Signal and data processing
- Image processing
- Multimedia systems
- Microelectronics
- Instrumentation and measurement
- Control systems
- Robotics
- Modeling and simulation
- Modern computer architectures
- Computer networks
- Embedded systems
- High-performance computing
- Parallel and distributed computer systems
- Human-computer systems
- Intelligent systems
- Multi-agent and holonic systems
- Real-time systems
- Software engineering
- Internet and web applications and systems
- Applications of computer systems in engineering and related disciplines
- Mathematical models of engineering systems
- Engineering management
- Engineering education

Paper Submission

Authors are invited to submit original, unpublished research papers that are not being considered by another journal or any other publisher. Manuscripts must be submitted in doc, docx, rtf or pdf format, and limited to 30 one-column double-spaced pages. All figures and tables must be cited and placed in the body of the paper. Provide contact information of all authors and designate the corresponding author who should submit the manuscript to https://ijeces.ferit.hr. The corresponding author is responsible for ensuring that the article's publication has been approved by all coauthors and by the institutions of the authors if required. All enquiries concerning the publication of accepted papers should be sent to ijeces@ferit.hr.

The following information should be included in the submission:

- paper title;
- full name of each author;
- full institutional mailing addresses;
- e-mail addresses of each author;
- abstract (should be self-contained and not exceed 150 words). Introduction should have no subheadings;
- manuscript should contain one to five alphabetically ordered keywords;
- all abbreviations used in the manuscript should be explained by first appearance;
- all acknowledgments should be included at the end of the paper:
- authors are responsible for ensuring that the information in each reference is complete and accurate. All references must be numbered consecutively and citations of references in text should be identified using numbers in square brackets. All references should be cited within the text;
- each figure should be integrated in the text and cited in a consecutive order. Upon acceptance of the paper, each figure should be of high quality in one of the following formats: EPS, WMF, BMP and TIFF;
- corrected proofs must be returned to the publisher within 7 days of receipt.

Peer Review

All manuscripts are subject to peer review and must meet academic standards. Submissions will be first considered by an editor-in-chief and if not rejected right away, then they will be reviewed by anonymous reviewers. The submitting author will be asked to provide the names of 5 proposed reviewers including their e-mail addresses. The proposed reviewers should be in the research field of the manuscript. They should not be affiliated to the same institution of the manuscript author(s) and should not have had any collaboration with any of the authors during the last 3 years.

Author Benefits

The corresponding author will be provided with a .pdf file of the article or alternatively one hardcopy of the journal free of charge.

Units of Measurement

Units of measurement should be presented simply and concisely using System International (SI) units.

Bibliographic Information

Commenced in 2010.
ISSN: 1847-6996
e-ISSN: 1847-7003

Published: semiannually

Copyright

Subscription Information

The annual subscription rate is 50€ for individuals, 25€ for students and 150€ for libraries.

Postal Address

Faculty of Electrical Engineering,
Computer Science and Information Technology Osijek,
Josip Juraj Strossmayer University of Osijek, Croatia
Kneza Trpimira 2b
31000 Osijek, Croatia

IJECES Copyright Transfer Form

(Please, read this carefully)

This form is intended for all accepted material submitted to the IJECES journal and must accompany any such material before publication.

TITLE OF ARTICLE (hereinafter referred to as "the Work"):

COMPLETE LIST OF AUTHORS:

The undersigned hereby assigns to the IJECES all rights under copyright that may exist in and to the above Work, and any revised or expanded works submitted to the IJECES by the undersigned based on the Work. The undersigned hereby warrants that the Work is original and that he/she is the author of the complete Work and all incorporated parts of the Work. Otherwise he/she warrants that necessary permissions have been obtained for those parts of works originating from other authors or publishers.

Authors retain all proprietary rights in any process or procedure described in the Work. Authors may reproduce or authorize others to reproduce the Work or derivative works for the author's personal use or for company use, provided that the source and the IJECES copyright notice are indicated, the copies are not used in any way that implies IJECES endorsement of a product or service of any author, and the copies themselves are not offered for sale. In the case of a Work performed under a special government contract or grant, the IJECES recognizes that the government has royalty-free permission to reproduce all or portions of the Work, and to authorize others to do so, for official government purposes only, if the contract/grant so requires. For all uses not covered previously, authors must ask for permission from the IJECES to reproduce or authorize the reproduction of the Work or material extracted from the Work. Although authors are permitted to re-use all or portions of the Work in other works, this excludes granting third-party requests for reprinting, republishing, or other types of re-use. The IJECES must handle all such third-party requests. The IJECES distributes its publication by various means and media. It also abstracts and may translate its publications, and articles contained therein, for inclusion in various collections, databases and other publications. The IJECES publisher requires that the consent of the first-named author be sought as a condition to granting reprint or republication rights to others or for permitting use of a Work for promotion or marketing purposes. If you are employed and prepared the Work on a subject within the scope of your employment, the copyright in the Work belongs to your employer as a work-for-hire. In that case, the IJECES publisher assumes that when you sign this Form, you are authorized to do so by your employer and that your employer has consented to the transfer of copyright, to the representation and warranty of publication rights, and to all other terms and conditions of this Form. If such authorization and consent has not been given to you, an authorized representative of your employer should sign this Form as the Author.

Authors of IJECES journal articles and other material must ensure that their Work meets originality, authorship, author responsibilities and author misconduct requirements. It is the responsibility of the authors, not the IJECES publisher, to determine whether disclosure of their material requires the prior consent of other parties and, if so, to obtain it.

- The undersigned represents that he/she has the authority to make and execute this assignment.
- For jointly authored Works, all joint authors should sign, or one of the authors should sign as authorized agent for the others.
- The undersigned agrees to indemnify and hold harmless the IJECES publisher from any damage or expense that may arise in the event of a breach of any of the warranties set forth above.

________________________ ________________________

Author/Authorized Agent **Date**

CONTACT
International Journal of Electrical and Computer Engineering Systems (IJECES)
Faculty of Electrical Engineering, Computer Science and Information Technology Osijek
Josip Juraj Strossmayer University of Osijek
Kneza Trpimira 2b
31000 Osijek, Croatia
Phone: +38531224600,
Fax: +38531224605,
e-mail: ijeces@ferit.hr